UNIVERSIDAD POLITÉCNICA DE MADRID
Escuela Técnica Superior de Ingeniería Agronómica, Alimentaria y de Biosistemas

Assessing nitrogen transformations, nitrogen fate and mechanisms for nitrous oxide emissions under Mediterranean conditions

DOCTORAL THESIS

Submitted for the degree of Doctor by:

Sandra García Gutiérrez
Graduada en Ciencias Ambientales
Máster en Química Agrícola y Nuevos Alimentos

Madrid, 2025

UNIVERSIDAD POLITÉCNICA DE MADRID
Escuela Técnica Superior de Ingeniería
Agronómica, Alimentaria y de Biosistemas

Doctoral Degree in Agro-environmental Technology for Sustainable Agriculture

Assessing nitrogen transformations, nitrogen fate and mechanisms for nitrous oxide emissions under Mediterranean conditions

DOCTORAL THESIS

Submitted for the degree of Doctor by:

Sandra García Gutiérrez
Graduada en Ciencias Ambientales
Máster en Química Agrícola y Nuevos Alimentos

Under the supervision of:
Dr. Sonia García Marco
Dr. Guillermo Guardia Vázquez

Madrid, 2025

Title: Assessing nitrogen transformations, nitrogen fate and mechanisms for nitrous oxide emissions under Mediterranean conditions

Author: Sandra García Gutiérrez

Doctoral Programme: Agro-environmental Technology for Sustainable Agriculture

Thesis Supervision:

Dr. Sonia García Marco, Profesora Titular, Universidad Politécnica de Madrid (Supervisor)

Dr. Guillermo Guardia Vázquez, Profesor Contratado Doctor, Universidad Politécnica de Madrid

External Reviewers:

Thesis Defense Committee:

Thesis Defense Date:

This thesis has been supported by the FPI grant PRE2019-087594 funded by MCIN/AEI/10.13039/501100011033 and Fondo Social Europeo (FSE) "El FSE invierte en tu futuro".

“Los árboles gritan de dolor al morir,
pero tú no puedes oírlos.”

La princesa Mononoke

A mi abuela Inés

Agradecimientos/Acknowledgements

Sois muchas personas las que merecéis mi gratitud por haberme apoyado durante esta etapa. Estas palabras son sólo una pequeña muestra del agradecimiento que espero haberos sabido mostrar a lo largo de estos años.

Sin duda es necesario comenzar con **Sonia** y **Guillermo**. De todo corazón os digo: qué suerte la mía de haberos tenido como directores. Lo que escriba aquí se va a quedar corto… **Sonia**, eres una guerrera, un ejemplo de lucha, esfuerzo y de pasión por un trabajo bien realizado. Un amor de persona, siempre pendiente de todos, ayudando al resto e intentando mantener un espíritu alegre pese a las complicaciones de la vida. Gracias por soportar todos mis momentos de agobio, por permitir que me desahogara libremente y por ayudarme a mantener unos objetivos fijos. **Guillermo**, mil gracias por estar siempre disponible y por ser tan paciente conmigo. Nunca sabré como sacas tiempo para todo. Eres la personificación de la eficiencia (pese a lo despistado que puedes llegar a ser). La pasión que muestras por tu trabajo, tanto en investigación como en docencia, la transmites a quien está contigo. Ha sido una suerte tener como director a un compañero de trabajo. A ambos: sois maravillosos. Muchas gracias por vuestra confianza, por darme ánimos y por poner en valor lo que una a veces no es capaz de ver. Trabajar con vosotros ha sido una gozada. Más allá de una relación laboral o académica, es un lujo haber podido tener una relación personal con las personas que juegan un papel tan clave durante esta etapa, gracias a la cercanía y confianza que mostráis continuamente. Creo que no me equivoco si digo que este proceso ha sido un aprendizaje mutuo, así que espero que vuestra experiencia dirigiendo vuestra primera tesis doctoral también haya sido, al menos, igual de positiva que la mía como vuestra doctoranda.

Gracias a **Antonio** por haberme dado la oportunidad de realizar esta tesis. Por poner de manifiesto que la carrera investigadora es un continuo aprendizaje, y que poco a poco y con esfuerzo se van alcanzando los objetivos y superando los retos.

Durante estos años he tenido la suerte de trabajar con gente maravillosa. Con buena compañía las horas en el laboratorio pasan volando, y los madrugones para ir a campo en verano se hacen más llevaderos (especialmente si después tienen la recompensa de un desayuno en el Migas). Aparte de los buenos momentos tan necesarios, se agradece muchísimo tener la confianza con tus compañeros como para poder desahogarte con ellos cuando el estrés o la frustración te superan. **Rocío**, ya lo sabes, yo de mayor quiero ser como tú. No se puede negar, eres la mejor (no os enfadéis el resto, hay que tener contenta a La Jefa). En serio, no me imagino estos años sin ti. Infinitas gracias por toda tu ayuda. **Alba**, mi gran confidente de alegrías y penas. Tu compañía durante este tiempo ha sido muy importante. Muchas gracias por los buenos momentos dentro y fuera de la universidad y por la infinidad de veces que has venido a distraerme al despacho. **Rafa**, por supuesto, mil gracias por tu ayuda con los ensayos, pero es más necesario resaltar tu buen carácter, siempre con buena cara, con optimismo. Pese a no saber estarte quieto, qué paz transmites y qué necesario es tener cerca a gente como tú. **Moni**, compañera y mentora desde el inicio, siempre sacando tiempo para ayudar. Toda una luchadora que se nota por donde pisa. Sabes que te echamos mucho de menos los dos años que estuviste fuera. Tu energía y el ruido ambiente que traes contigo crea vida en el departamento. A **Jaime**, **Carmen** y **Juliana** por el buen ambiente que creabais, y a **Jero**, **Susana** y **Raquel** por aguantarme hablando durante bastante tiempo de lo poco que me quedaba para terminar la tesis.

A los profesores del Departamento por ayudarme siempre que lo he necesitado y por vuestras muestras continuas de ánimo: **Alberto**, **Demetrio**, **Augusto**, **Ana**, **Carmen Cartagena**, **Carmen González** y **Fernando**. Se merecen una mención especial **Patricia**, **Laura**, **Lourdes**,

Jesús y de nuevo **Guillermo** por templar mis nervios y darme confianza para afrontar mi reto personal de enfrentarme al mundo de la docencia.

A todos los técnicos que facilitáis día a día el trabajo en el laboratorio: **Pilar**, **Ana**, **Javi**, **Estrella**, **Pilar López** y **Gonzalo**. Sin vosotros todo sería muy distinto, inimaginable. Gracias a las que me han ayudado con los infinitos trámites y gestiones administrativas: **Rosa**, **Mari Carmen, Carmen Diéguez** y **Katerina**.

I also want to thank **Michael**, **Benjamin**, and **Clemens** for giving me the opportunity to work in their research group at IMK-IFU in Garmisch-Partenkirchen. I really appreciate your support. Thanks to **Anja**, **Ulli**, **Allison**, and **Florian** for your patience and technical assistance. Special thanks to **Remi** for letting me be her teacher and for all her support during gas sampling and lab work. Thanks to **Sebastian**, **Lio**, **Jule**, **Lara**, and **Elisabeth** for making it possible to perform my experiment. It would not have been possible without your help, digging the mesocosms in and out, helping me to look for all the material, during the fertilization, and even acting as translators. I am also grateful to the people who made my time in GaPa such a wonderful experience that I wish had lasted longer: **Luna**, **Jana**, **Timo**, **Lio, Sebastian** and **Jule**. And very specials thanks to **Yanick,** for your kindness, for all the pizza and beer evenings, for the exhausting hikes enjoying really nice views, and for all the deep conversations (as deep as my English allowed) that turned you into a good friend.

Gracias a **Javi**. No tienes ni idea de lo necesarias que han sido tus clases de patinaje para liberar estrés, recordarme que los retos se pueden superar, y para conseguir subidones de adrenalina.

Gracias a mis **Matildas** por todo su apoyo. Amigas con las que he crecido, a las que quiero con locura. Causantes de incontables dolores de cabeza, o lo que es lo mismo, momentos de risa, alegría, y evasión. Gracias a mis **ambientólogos** y amigos del lejano Alcorcón. Esto lo celebramos en breve en el L'Europe.

A mi tito **Ferni** por todas las veces que, pacientemente, me ha salvado la vida.

A mis padres **Angelines** y **Rafa** por permitirme elegir mi camino a pesar de lo incierto que pudiera parecer. Siempre respetando mis decisiones y animándome a esforzarme por conseguir mis metas. Sentíos orgullosos de la buena educación que habéis sabido transmitir a vuestros hijos. **Héctor**, tan distintos e iguales. Mi mejor amigo y confidente. Qué poco os digo lo mucho que os quiero a los tres. Sois ejemplo de calma, unión y amor. Mil gracias por todo el apoyo que me habéis dado a lo largo de los años. Y por supuesto, gracias a **Sua**, la princesa de la casa. Sus saludos y su mirada son dosis de felicidad.

A **Hugo**. ¡Qué difícil es agradecerte tanto! Gracias por sacarme día a día sonrisas tan necesarias, por tu infinita paciencia, por aconsejarme una y mil veces, y por seguir haciéndolo con todo tu cariño y buena intención pese al desastre que puedo llegar a ser. En resumen, gracias por acompañarme, ayudarme, animarme y formar parte de esta aventura que has vivido casi en primera persona. Eres mi mejor compañero. Aún nos quedan muchas aventuras por disfrutar.

Abstract

Agriculture is the largest anthropogenic source of nitrous oxide (N_2O), one of the main greenhouse gases and stratospheric ozone depleting substances. Addressing N_2O emission drivers in agricultural systems is essential for implementing cost-effective mitigation strategies. Isotopic ^{15}N tracing techniques provide a robust tool for identifying N_2O emission sources and the fate of applied nitrogen (N).

The main objective of this thesis is to evaluate sustainable agricultural practices that integrate crop residue management and N fertilization strategies in rainfed and irrigated Mediterranean agroecosystems, with the aim of mitigating N_2O emissions without compromising crop yields, focusing on the mechanisms involved in N cycle transformations.

The first experiment to address this objective consisted of a microplot ^{15}N tracing study with winter barley (*Hordeum vulgare* L.) under rainfed conditions. Conventional tillage and no-tillage systems were combined with the application of ^{15}N-labeled ammonium nitrate ($^{15}NH_4NO_3$ or $NH_4{}^{15}NO_3$), with or without the nitrification inhibitor (3,4-dimethyl-1H-pyrazol-1-yl) succinic acid isomeric mixture (DMPSA). The second experiment examined the combined effects of maize (*Zea mays* L.) residue input and cover crops (barley or vetch, *Vicia sativa* L.) compared to bare fallow in an irrigated maize cash crop under integrated soil fertility management. The third experiment consisted of a microplot ^{15}N tracing study with maize preceded by the same cover cropping treatments as in Experiment 2. The microplots were amended with ^{15}N−enriched maize residues or ^{15}N–labeled fertilizer ($^{15}NH_4NO_3$ or $NH_4{}^{15}NO_3$). The fourth experiment consisted of a ^{15}N tracing study conducted in a pre-alpine grassland to quantify N recovery, N_2O and dinitrogen (N_2) fluxes, and to identify key N transformation processes responsible for N_2O emissions.

The results of Experiment 1 showed that DMPSA significantly reduced N_2O emissions derived from both endogenous soil N and fertilizer-derived N during the cropping period. However, most N_2O was emitted during a postharvest rewetting event, where DMPSA had no effect. No tillage enhanced crop N uptake, while DMPSA increased soil N recovery in the upper layer. In Experiment 2, higher maize residue input reduced N_2O emissions before maize fertilization but increased them afterward compared to the low residue input treatment. Cover crops significantly affected N_2O emissions only after their incorporation, with higher emissions in barley compared to bare fallow. Most N_2O was emitted during maize cropping phase, particularly after synthetic N fertilization, favored by high soil moisture and cover crop decomposition. Integrated fertilization reduced maize yield by 7% when preceded by vetch cover crop. Results from Experiments 1 and 3 indicated that ammonium oxidation-based processes were the main sources of N_2O emissions in both rainfed and irrigated Mediterranean croplands. Endogenous soil N was quantitatively relevant for N_2O fluxes, even after synthetic N application, whereas maize residues had a negligible contribution to N_2O emissions (< 7%). Fertilizer N recovery in rainfed barley averaged 23%, whereas N recovery in maize was higher with barley cover crops (42%) compared to bare fallow (26%). In the pre-alpine grassland experiment, N_2 was the dominant gaseous N loss from the soil-plant system. Denitrification accounted for 62% of cumulative N_2O emissions, with higher contribution after fertilization. Of the applied N, 37% was recovered in plants and 54% in soil.

The findings of this thesis may contribute to improve the understanding and quantification of N use efficiency and N_2O emission inventories under contrasting environmental and management conditions. These insights are highly valuable for researchers, as well as for stakeholders and policymakers aiming to develop sustainable, site-specific N_2O mitigation practices based on conservation agriculture and N fertilization practices.

Resumen

La agricultura es la principal fuente antropogénica de óxido nitroso (N_2O), uno de los principales gases de efecto invernadero, precursor de la destrucción de la capa de ozono. Determinar las causas de estas emisiones en sistemas agrícolas es esencial para aplicar estrategias de mitigación rentables. Las técnicas isotópicas de ^{15}N son herramienta clave para identificar las fuentes de emisión de N_2O y el destino del nitrógeno (N) aplicado.

El objetivo principal de esta tesis es evaluar prácticas agrícolas sostenibles combinando manejo de residuos de cultivos y estrategias de fertilización nitrogenada en agroecosistemas mediterráneos de secano y regadío, con el propósito de mitigar las emisiones de N_2O sin afectar a los rendimientos de los cultivos, profundizando en las transformaciones del N.

El primer experimento para alcanzar este objetivo consistió en un ensayo de trazado de ^{15}N en microparcelas con cebada de invierno (*Hordeum vulgare* L.) en secano. Se combinó laboreo convencional y no laboreo con la aplicación de nitrato amónico enriquecido con ^{15}N ($^{15}NH_4NO_3$ o $NH_4{}^{15}NO_3$), con o sin el inhibidor de la nitrificación ácido 2-(N-3,4-dimetil-1H-pirazol-1-il) succínico (DMPSA). El segundo experimento evaluó la incorporación de residuos de maíz (*Zea mays* L.) y cultivos cubierta (cebada y veza, *Vicia sativa* L.), comparados con barbecho) en maíz de regadío con manejo integrado de la fertilización. El tercer experimento consistió en un estudio de trazado de ^{15}N en microparcelas en un cultivo de maíz precedido por los mismos cultivos cubierta del Experimento 2. En las microparcelas se aplicaron residuos de maíz enriquecidos con ^{15}N o fertilizante enriquecido en ^{15}N ($^{15}NH_4NO_3$ o $NH_4{}^{15}NO_3$). El cuarto experimento consistió en un ensayo de trazado de ^{15}N en un pastizal pre alpino para cuantificar la recuperación de N, los flujos de N_2O y nitrógeno molecular (N_2), y los procesos de transformación del N responsables de las emisiones de N_2O.

En el Experimento 1, el DMPSA redujo las emisiones de N_2O derivadas del N endógeno del suelo y del fertilizante durante el período de cultivo de cebada. Sin embargo, la mayor parte del N_2O se emitió en un pico post cosecha, sin efecto del DMPSA. El no laboreo mejoró la absorción de N por el cultivo, y el DMPSA aumentó la retención de N en la capa superficial del suelo. En el Experimento 2, la mayor incorporación de residuos de cosecha redujo las emisiones de N_2O antes de la fertilización del maíz, aumentándolas posteriormente. La incorporación de los cultivos cubierta produjo mayores emisiones de N_2O con cebada que en barbecho. La mayoría de las emisiones ocurrieron durante la fase de cultivo del maíz, especialmente tras la fertilización, favorecidas por la humedad del suelo y la descomposición de los cultivos cubierta. Los resultados de los Experimentos 1 y 3 indican que los procesos derivados de la oxidación del amonio fueron la principal fuente de emisión de N_2O en los sistemas agrícolas mediterráneos. El N del suelo contribuyó significativamente a los flujos de N_2O, mientras que la contribución de los residuos de maíz fue escasa (< 7%). La recuperación media del N del fertilizante fue del 23% en cebada, y del 33% en maíz, con mayor recuperación con cebada como cultivo cubierta, comparado con barbecho. En el pastizal pre alpino, el N_2 fue la principal pérdida de N gaseoso. La desnitrificación representó el 62% de las emisiones de N_2O. El 37% del N del fertilizante fue recuperado por el cultivo, y el 54% permaneció en el suelo.

Los hallazgos de esta tesis pueden contribuir a mejorar la eficiencia del uso del N y los inventarios de emisiones de N_2O en distintos sistemas de cultivo. Estos conocimientos son de gran valor en el ámbito científico, así como en el sector agrícola y para las administraciones públicas de cara al desarrollo de políticas de mitigación de N_2O, promoviendo la agricultura de conservación y estrategias de fertilización sostenibles y adaptadas a las condiciones locales.

Table of contents

List of Figures

List of Tables

Abbreviations and Acronyms

Abbreviations related to the treatments in the different experiments

+R	Higher input of maize residue in the topsoil (Experiment 2)
−R	Lower input of maize residue in the topsoil (Experiment 2)
^{15}AN	$^{15}NH_4{}^{14}NO_3$
^{15}RES	Enriched ^{15}N maize residues (Experiment 3)
AN	NH_4NO_3 without ^{15}N enrichment
A^{15}N	$^{14}NH_4{}^{15}NO_3$
B	Barley cover crop (Experiment 3)
C	Cereal cover crop (Experiment 2)
F	Bare fallow instead of cover crop (Experiments 2 and 3)
N0	Control without N fertilization (Experiment 1)
NT	No tillage (Experiment 1)
L	Legume cover crop (Experiment 2)
T	Conventional tillage (Experiment 1)
V	Vetch cover crop (Experiment 3)

General abbreviations and acronyms

$(NH_4)_2SO_4$	Ammonium sulfate
^{15}NGF	^{15}N gas flux
AGB	Aboveground biomass
AMO	Ammonia monooxygenase
AN	Ammonium nitrate, NH_4NO_3
ANOVA	Analyses of variance
AOA	Ammonia-oxidizing archaea
AOB	Ammonia-oxidizing bacteria
a_p	^{15}N enrichment of the soil NO_3^- pool undergoing denitrification
BGB	Belowground biomass
C	Carbon
CAN	Calcium ammonium nitrate
CENTER	Centro Nacional de Tecnología de Regadíos

CH_4	Methane
CO_2	Carbon dioxide
Comammox	Complete ammonia-oxidizing bacteria
COP21	21st Conference of the Parties
DCD	Dicyandiamide
DMPP	3,4-dimethylpyrazole phosphate
DMPSA	(3,4-dimethyl-1H-pyrazol-1-yl) succinic acid isomeric mixture
DNRA	Dissimilatory nitrate reduction to ammonia
DOC	Dissolved organic carbon
EF	N_2O emission factor
Eq.	Equation
EU	European Union
FAO	Food and Agriculture Organization
f_p	Fraction of N_2O and N_2 emitted from the soil NO_3^- pool undergoing denitrification
GC	Gas chromatograph
GHG	Greenhouse gas
GLM	Generalized linear models
GWP	Global warming potential
H_2O	Water
H_2SO_4	Sulfuric acid
HAO	Hydroxylamine oxidoreductase
HCl	Hydrochloric acid
I	Ion current
IMK-IFU	Institute of Meteorology and Climate Research Atmospheric Environmental Research
IPCC	Intergovernmental Panel on Climate Change
IRMS	Isotope Ratio Mass Spectrometer
KCl	Potassium chloride
KIT	Karlsruhe Institute of Technology
KNO_3	Potassium nitrate
LSD	Least significant difference
m/z	Mass-to-charge ratio

MgO	Magnesium oxide
N	Nitrogen
N_2	Dinitrogen
N_2O	Nitrous oxide
N_2O_D	Soil derived N_2O from nitrifier denitrification
N_2O_d	N_2O emissions derived from denitrification pathways
$N_2O_d/(N_2O_d + N_2)$	Denitrification product ratio
N_2O_N	Soil derived N_2O nitrification, abiotic N_2O production, and fungal denitrification
N_2O_n	N_2O emission derived from nitrification pathways
NH_2OH	Hydroxylamine
NH_3	Ammonia
NH_4^+	Ammonium
NI	Nitrification inhibitor
NO	Nitric oxide
NO_2^-	Nitrite
NO_3^-	Nitrate
N_r	Reactive nitrogen
ns	Statistically not significant
NUE	Nitrogen use efficiency
O_2	Oxygen
O_3	Ozone
P	*P* value
P1	Period 1
P2	Period 2
P3	Period 3
PVC	Polyvinyl chloride
S.E.	Standard error
SIAR	Sistema de Información Agroclimática para el Regadío
SIdI-UAM	Interdepartmental Investigation Service at Universidad Autónoma de Madrid
SOC	Soil organic carbon
UNFCCC	United Nations Framework Convention on Climate Change

VCl_3	Vanadium chloride
WFPS	Water-filled pore space
WMO	World Meteorological Organization
YSNE	Yield-scaled N_2O emissions

CHAPTER 1

INTRODUCTION

1.1. The effects of climate change in the Mediterranean area

Climate change is considered as one of the main environmental problems of the 21st century. Mediterranean-type ecosystems are characterized by their high interannual and seasonal variability precipitation, with long and intense dry periods occurring during the warm summer season, and with mild, wet winters. These regions are located between 30º and 45º latitude and are located in the Mediterranean Basin, California (USA), southwestern and southern Australia, central Chile and southern Africa. The Mediterranean Basin is the largest of these regions, covering 1.68 million km^2, which accounts for 60% of the total Mediterranean climate area (Figure 1.1) (Joffre and Rambal, 2001).

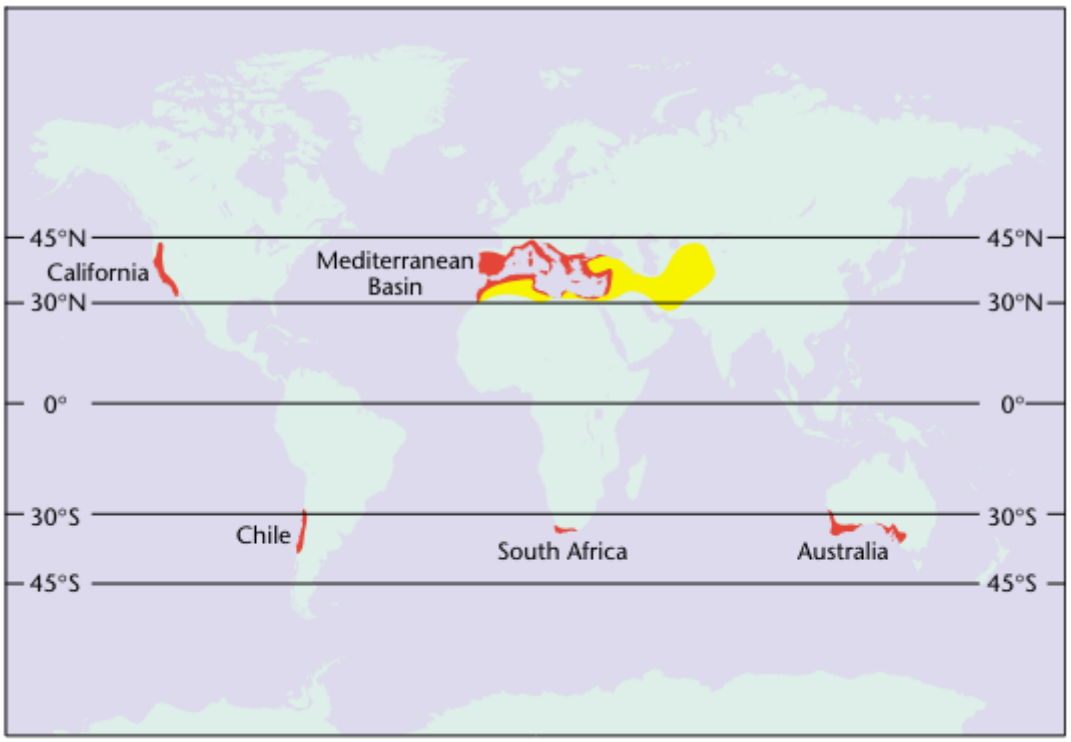

Figure 1.1. Map of the five regions with Mediterranean-type climate (red). The yellow area corresponds to the Mediterranean-steppe domain (mean annual rainfall between 100 and 400 mm) according to Le Houérou, 1997. Source: Joffre and Rambal (2001)

The specific climatic conditions of Mediterranean-type ecosystems make these regions to be considered as "hot-spots" in terms of climate change and climate variability (Giorgi, 2006). For instance, Mediterranean regions are expected to warm at a rate approximately 20% greater than

the global annual mean surface temperature. This warming will be especially pronounced during summer and in the continental areas north of the basin, where temperatures are projected to increase by around 50% more than the global average. In some localized areas, the temperature rise could even be double that of the global scale. Daytime temperatures are expected to rise more than nighttime temperatures, and summers are likely to experience greater increases compared to winters, resulting in an increase of amplitude of both daily and annual temperature ranges (Lionello and Scarascia, 2018). Furthermore, a global atmospheric temperature increase of 2 ºC will likely be accompanied by a 10-30% reduction in summer precipitation in the Mediterranean Basin (Cramer et al., 2018). The rising temperatures and declining precipitation due to ongoing climate change are expected to intensify water scarcity in this region, leading to longer, more intense, and more frequent droughts (García-Ruiz et al., 2011). Together with climate change, increasing water demand for irrigated agriculture −essential for stabilizing production and ensuring food security− is likely to further exacerbate water scarcity (Iglesias et al., 2012).

1.2. The use of N-based fertilizers in agriculture

As mentioned above, climate change is expected to negatively impact food production due to increasing water scarcity and rising temperatures. Agriculture, therefore, faces the urgent challenge of ensuring food security for a growing global population. Nitrogen (N) is, together with water, one of the most important limiting factors for crop productivity in terrestrial ecosystems (Quemada et al., 2020). Although N is the most abundant element on Earth's atmosphere, accounting for 78% of atmospheric composition as dinitrogen (N_2), most plants are unable to use this unreactive N_2. Only certain species, such as legumes, are capable of fixing atmospheric N_2. Plants need to incorporate N into their biomass as reactive N (Nr) compounds such as ammonia (NH_3), ammonium (NH_4^+), nitrate (NO_3^-), or nitrite (NO_2^-), and organic N

compounds which are naturally scarce in the natural environment. The scarcity of Nr was addressed with the development of the Haber-Bosch process, which enables the industrial synthesis of NH_3 from N_2 and hydrogen in a reduced energy cost process (Haber, 1920). This breakthrough allowed for the large-scale production of synthetic N-based fertilizers, which have played a crucial role in enhancing global agricultural productivity. Since the 1950s, the use of synthetic N fertilizers has increased dramatically, supporting a rapid expansion of the human population (Figure 1.2). It is estimated that synthetic N fertilizers have contributed to approximately 50% of global food production (Erisman et al., 2008). Increased fertilizer use has been driven by the demand for higher crop yields. Globally, the use of N fertilizers has increased a 41% between 1990 and 2019, according to the Intergovernmental Panel on Climate Change (IPCC, 2022). In the Mediterranean Basin, synthetic N fertilizer use has tripled between the 1960s and the first decade of the XXI century (Lassaletta et al., 2021).

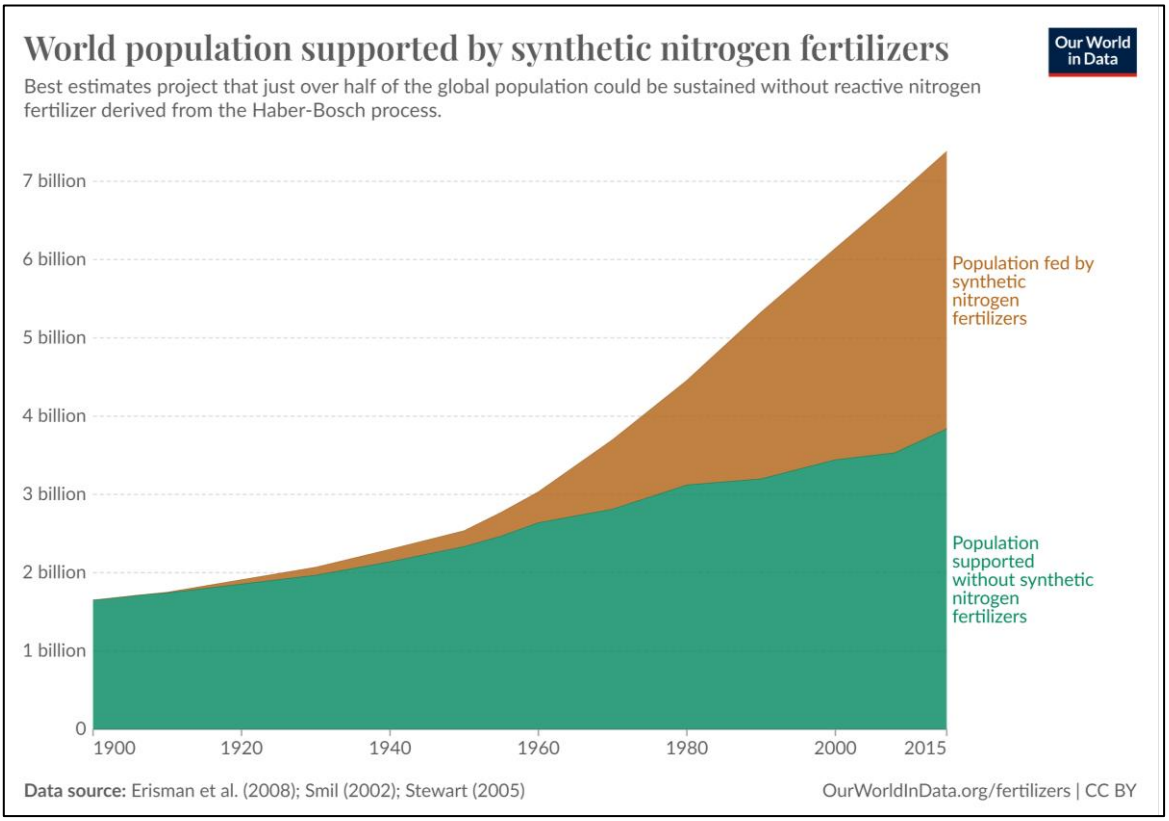

Figure 1.2. Word population supported by synthetic N fertilizers. Chart source: Ritchie (2017)

World population has increased from 6,108 million habitants in 2000 to over 7,800 million by 2020 (United Nations, 2022) and is expected to reach 9.7 billion by 2050. This increase will also affect the Mediterranean Basin, particularly in the coastal regions of eastern and southern Mediterranean countries. The use of N-based fertilizers, together with the implementation of irrigation, has significantly boosted crop yields without requiring the expanding of agricultural land. Thus, to ensure food security for the growing population, higher fertilizer inputs together with increased water demand are expected (Cramer et al., 2018). However, the excessive use of synthetic N-based fertilizers in agriculture has led to an imbalance in the N cycle since not all applied N is absorbed by crops. The N surplus in cropping systems –calculated as the difference between N inputs and outputs (i.e., the N exported by plants at harvest)– has negative effects on human health and environment. It contributes to water and air pollution, increases greenhouse gas (GHG) emissions to the atmosphere, and leads to biodiversity loss (Quemada et al., 2020). Currently, the average crop use efficiency of applied N in the Mediterranean region is estimated as less than 50% (Lassaletta et al., 2021), thus threatening agricultural, economic and environmental sustainability goals. Consequently, agriculture research has met the challenge of looking for ways to enhance crop yields optimizing the use of resources (e.g., fertilizers, soil quality, water, etc…) while minimizing negative environmental impacts. To select region-specific agricultural practices that enhance N utilization and mitigate its losses, it is crucial to understand and quantify the biochemical processes involved in the N cycle.

1.3. Nitrous oxide emissions from agriculture

Nitrous oxide (N_2O) is a major global concern due to its significant contributions to climate change and stratospheric ozone (O_3) depletion. Agriculture, responsible for 12% of global GHG emissions, is the largest anthropogenic source of N_2O, accounting for 66% of total

anthropogenic emissions (Figure 1.3) (IPCC, 2022). Within the agricultural sector, 28% of its GHG emissions are released as N_2O (Rosa and Gabrielli, 2023).

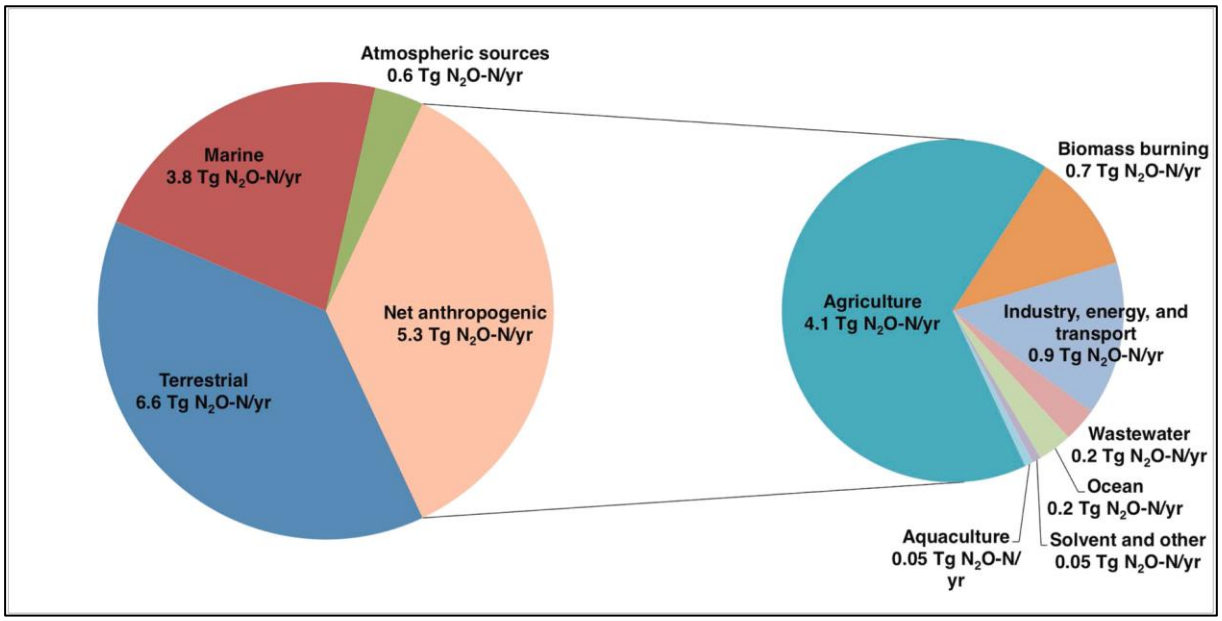

Figure 1.3. Natural and anthropogenic N_2O emissions in 2005. Source: Davidson and Kanter (2014)

The atmospheric concentration of N_2O has risen dramatically since the Industrial Revolution, increasing from 270 ppb to over 337 ppb by 2023 (Figure 1.4) (IPCC, 2021; WMO, 2024). This increase is primarily driven by agricultural activities, particularly the intensified use of N−based fertilizers and manure to maximize crop yields (Tian et al., 2020). Agricultural soils have been identified as the dominant source of these emissions, highlighting the critical role of agriculture in driving N_2O emissions.

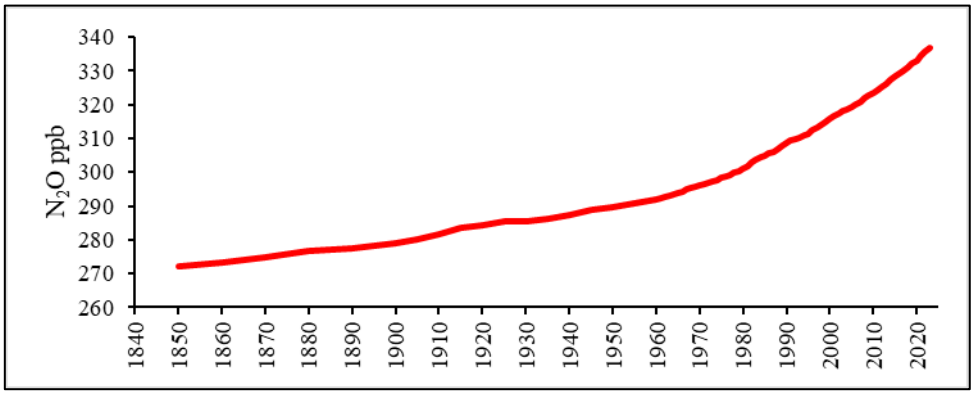

Figure 1.4. Evolution of N_2O atmospheric concentration from 1850 until 2019. Data obtained from the IPCC (2021) and the WMO (2024).

The atmospheric lifetime of N_2O is estimated at 116 ± 9 years, making it a long-lasting contributor to global warming (Prather et al., 2015). Moreover, its global warming potential (GWP) over a 100-year horizon is 273 times greater than that of carbon dioxide (CO_2) (IPCC, 2021). Beyond its impact as a potent GHG, N_2O is the most significant ozone-depleting substance currently emitted into the atmosphere (Foster et al., 2021; Ravishankara et al., 2009).

1.4. Nitrous oxide emission pathways

If N_2O emissions continue to rise at their current pace, achieving the goal of limiting global temperature increase to 1.5°C above pre-industrial levels within the framework of sustainable development, as outlined in the United Nations Framework Convention on Climate Change (UNFCCC) Paris Agreement adopted in 2015, will become unfeasible. Addressing the agricultural drivers of N_2O emissions and minimizing the negative impacts of N-based fertilizers, particularly through improved N management practices, is essential to effectively reducing N_2O emissions from agriculture and mitigating its environmental and climatic impacts (Christensen and Rousk, 2024). According to the European Environment Agency, agricultural GHG emissions in the European Union (EU) are projected to be 7% lower than 2005 levels by 2030, with the implementation of additional, currently planned measures. Thus, greater efforts must be made to reduce non-CO_2 emissions to achieve the targets set by the EU for 2030, which aim for a 55% reduction in net GHG emissions. Mitigating N_2O emissions will play a critical role in achieving these objectives.

In this sense, it is necessary to understand the biochemical processes involved in the N cycle that are responsible for N_2O production in soil. The production and consumption of N_2O in agricultural soils are primarily related to microbial processes, with nitrification and denitrification being the main microbial processes leading to N_2O production in soils (Butterbach-Bahl et al., 2013; Ussiri and Lal, 2013).

Nitrification is the oxidation of reduced forms of N (NH_3 or NH_4^+), ultimately to NO_3^- in the presence of oxygen (O_2) (Figure 1.5). The major sources of reduced forms of N are the mineralization of organic N compounds from manures or plant residues, and the application of NH_3-based fertilizers. It is an aerobic process that can occur by two pathways: autotrophic and heterotrophic nitrification (Butterbach-Bahl et al., 2013), with the latter being less studied and mainly occurring in soils that are typically too acid for autotrophic nitrification to take place (Martikainen, 2022). During autotrophic nitrification, the reduced forms of N are first oxidized to hydroxylamine (NH_2OH) through the action of the ammonia monooxygenase (AMO) enzyme. Further, NH_2OH is oxidized to NO_2^- via nitric oxide (NO) production (Caranto and Lancaster, 2017), being implied the hydroxylamine oxidoreductase (HAO) enzyme, and it is finally used by NO_2^- oxidizers to produce NO_3^- (Prosser et al., 2020), which can be lost from agroecosystems via leaching (Quemada et al., 2013; Wang and Li, 2019). Nitrous oxide can be released during nitrification due to the incomplete oxidation of the unstable NH_2OH and during the formation of NO_2^- (Figure 1.5). There are three groups of chemolithoautotrophic ammonia-oxidizers that contain the AMO enzyme: ammonia-oxidizing bacteria (AOB), ammonia-oxidizing archaea (AOA) and complete ammonia-oxidizing bacteria (comammox) (Beeckman et al., 2018). Nitrification is considered to be the preferential source of N_2O fluxes from well-aerated soils, such as those found in agricultural Mediterranean areas (Lassaletta et al., 2021; Montoya et al., 2022).

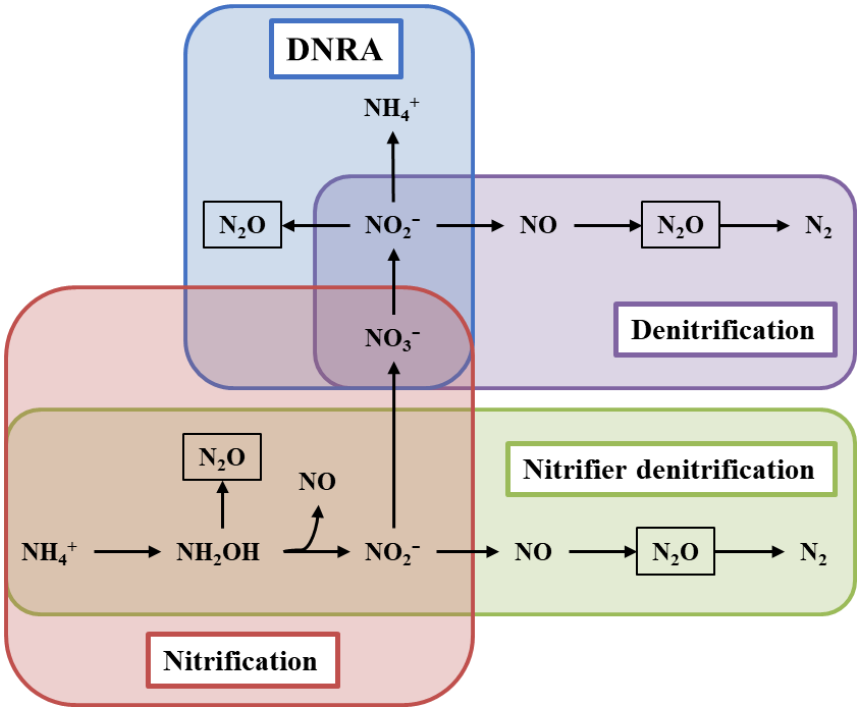

Figure 1.5. Soil processes showing the most relevant N substrate transformations for N_2O emissions. Own elaboration based on Barrat et al. (2021)

Denitrification is the microbial reduction of NO_3^- or NO_2^- to N oxides (NO and N_2O) and to the stable, unreactive N_2 (Figure 1.5). This process occurs predominantly under anaerobic conditions of limited O_2, when NO_3^- is available in soil (consequence of NH_4^+ nitrification or N fertilization with NO_3^-) and when high concentrations of easily available carbon (C) are present in the soil (Martens, 2005). Thus, a source of organic C is required for heterotrophic bacteria metabolism, with NO_3^- acting as the electron acceptor in environments with limited O_2. The final step of the denitrification pathway is the reduction of N_2O to N_2. The enzyme that catalyzes this reaction, the N_2O reductase (NosZ), is the only known enzyme capable of carrying out this reaction, making it the only known biological sink of N_2O. The NosZ has traditionally been attributed to bacteria and archaea (Hallin et al., 2018). Denitrification is considered as the major process of N loss in terrestrial ecosystems, with an average daily loss of 0.25 kg N ha^{-1} d^{-1}, being denitrification rate the highest in wetlands and the lowest in upland fields (Pan et al., 2022). Furthermore, it is considered as the major N_2O production process in agricultural soils with high organic matter content and elevated water-filled pore space (WFPS)

values (Butterbach-Bahl et al., 2013). In Mediterranean semiarid areas, climatic conditions do not always favor denitrifying activity. However, N_2O emissions associated with the increase of denitrifying activity can occur in soil micro-sites. Furthermore, this process has been reported in these areas because of soil rewetting after irrigation or intense summer precipitation events, which lead to increases in WFPS (Guardia et al., 2024a; Montoya et al., 2022).

Despite autotrophic nitrification and heterotrophic denitrification are the main processes leading to N_2O emissions from soil, accounting for approximately 70% of global N_2O emissions (Butterbach-Bahl et al., 2013), other microbial processes can also produce this Nr compound.

Nitrifier denitrification is carried out by AOB under anaerobic conditions when nitrification is incomplete. In this process, O_2 is substituted by NO_2^- as the terminal electron acceptor, which is then directly reduced to NO, followed by denitrification to N_2O and finally N_2 (Wrage et al., 2001) (Figure 1.5). Thus, in contrast to nitrification, this microbial process can occur in environments with low O_2 conditions (Zhu et al., 2013). When NO_2^- accumulates and moisture conditions or organic matter content are suboptimal for denitrification, nitrifier denitrification could be a significant contributor to N_2O emissions (Kool et al., 2011; Wrage-Mönnig et al., 2018). Together with nitrification, nitrifier-denitrification is a particularly relevant mechanism responsible for soil N_2O emissions in agricultural systems in Mediterranean climate areas, where soil moisture is favorable for both aerobic and anaerobic microsites (Butterbach-Bahl et al., 2013; Shaaban, 2024).

Coupled nitrification-denitrification occurs when the NO_3^- produced during nitrification is consumed by denitrifiers under conditions favorable for both microbial processes (Wrage et al., 2001). During this process, nitrification occurs in oxic conditions of the topsoil layer, while denitrification takes place in anoxic microsites.

There are other processes, such as **dissimilatory nitrate reduction to ammonia** (DNRA), **codenitrification,** and **chemodenitrification,** that can also result in N_2O emissions from soil. However, their contribution to N_2O emissions in semiarid Mediterranean areas is lower than that of the processes mentioned above. Dissimilatory nitrate reduction to ammonia occurs when NO_3^- is reduced to NO_2^-, and then further reduced to NH_4^+ (Figure 1.5). Although DNRA is considered of importance due to its capacity to increase N retention in soil, as NO_3^- is transformed into NH_4^+ (Pandey et al., 2020), N losses can occur during DNRA, as N_2O may be emitted as a byproduct (Rütting et al., 2011). Smith and Zimmerman (1981) concluded that the potential for significant DNRA exists in most soils, particularly in anaerobic microsites with anoxic conditions and when C is readily available. During chemodenitrification, NO_2^- released into the soil through both nitrification and denitrification can be chemically reduced to N_2O by soil organic matter or transition metals (Venterea, 2007; Wei et al., 2019). Codenitrification is a process that co-metabolizes organic N compounds to produce N_2O and/or N_2. However, it remains one of the least studied N loss pathways, and its contribution to agricultural N gas losses remains unclear (Spott et al., 2011).

These processes, in addition to being directly affected by the addition of external N sources, are also influenced by environmental conditions (e.g., climate, soil) and agricultural practices, which can have a significant effect on soil N_2O emissions (Cayuela et al., 2017; IPCC, 2022; Shaaban, 2024). Furthermore, agricultural soils play a significant role in CO_2 and methane (CH_4) emission, as discussed further in Section 1.8 of this thesis.

1.5. Use of conservation agriculture practices

Conservation agriculture is defined by the Food and Agriculture Organization (FAO) as an agroecosystem management system to ensure food security and improve profitability while preserving environmental resources. This approach can be considered as one of the main ways

to achieve agricultural sustainability by combining environmental protection with high crop productivity (Cárceles Rodríguez et al., 2022). Conservation agriculture practices include reduced tillage or no-till, retention of crop residues by either incorporating them into the soil or leaving them on the soil surface, and crop rotations including cover crops. These practices are considered to provide multiple ecosystem services, such as regulating wind and water erosion, climate regulation through enhanced C sequestration, and the provision and regulation of water and nutrients by increasing the soil organic matter content (Bohoussou et al., 2022; Cárceles Rodríguez et al., 2022; Palm et al., 2014). These practices align with the goals of various international initiatives, such as the Farm to Fork strategy proposed by the European Commission in 2020, which aims to transition to a sustainable food system, and the "4 per 1000" international initiative established at the 21st Conference of the Parties (COP21) of the UNFCCC (www.4p1000.org). This last initiative indicates that a yearly 4‰ increase of the soil organic C (SOC) stocks to a depth of 1 meter in managed agricultural lands, through the implementation of better management practices, could potentially reduce the CO_2 emissions while simultaneously enhancing the capability of agricultural systems to adapt to climate change and ensure food security (Minasny et al., 2017). Additionally, at the national level, frameworks such as the Royal Decree on Sustainable Nutrition of Agricultural Soils (RD 1051/2022) aim to regulate and promote practices that improve soil fertility and sustainability, further reinforcing the importance of conservation agriculture in achieving both environmental and policy-driven goals.

The challenge of conservation agriculture practices is to manage soils in a way that sequesters additional C from the atmosphere while sustaining high crop productivity (Shah and Wu, 2019). The positive effects of these practices on SOC have been extensively studied, and several reviews and meta-analyses have highlighted their benefits (Bai et al., 2019; Bohoussou et al., 2022; Cárceles Rodríguez et al., 2022; Palm et al., 2014). The agricultural practice of leaving

crop residues on the surface or incorporating them into the soil offers numerous benefits compared to their complete removal after harvesting, such as improving soil quality and reducing soil erosion (Blanco-Canqui and Lal, 2009; Malhi et al., 2006; Turmel et al., 2015). Crop residue retention has been proposed as a potential strategy for increasing SOC stocks in agricultural soils, with increases ranging from 2.7% to 18.2% when crop residues are incorporated into the soil, compared to their complete removal (Bolinder et al., 2020). Furthermore, a recent meta-analysis of P. Li et al. (2023) reported significant increments in N use efficiency (NUE) and yields, with average increases of 23% and 9%, respectively, associated with straw inputs. The integration of crop residues in the N cycle is also a key factor for the sustainability of agriculture in semiarid areas (Berhane et al., 2020).

The retention of crop residues can be carried out in different ways, such as incorporating them into the soil through conventional tillage or retaining them on the soil surface through no tillage. Lal (2003) indicated that soil C storage can be significantly increased with appropriate conservation tillage management. In fact, no tillage practices have been applied globally to maintain or increase SOC stocks and mitigate CO_2 emissions (Dimassi et al., 2014). Overall, the meta-analysis by Abdalla et al. (2016) showed that soil CO_2 emissions were 21% significantly higher in tilled soils compared to no tillage soils. This difference was even greater in soils with low SOC content, with a 27% increase in CO_2 emissions under tillage systems. However, the benefits of no tillage for CO_2 emission mitigation or the enhancement of SOC stocks strongly depend on factors such as the soil depth considered and the duration of no tillage implementation, among other environmental and management factors (Powlson et al., 2014).

Cover cropping has been shown to improve soil structure (Blanco-Canqui et al., 2011), enhance wildlife and soil microbial diversity (Muhammad et al., 2021), regulate weed and pathogen control, improve pollination, enhance soil fertility and hydrology, mitigate the influence of extreme meteorological events (Quintarelli et al., 2022; Van Eerd et al., 2023), reduce soil

erosion (Poeplau and Don, 2015), and prevent NO_3^- leaching (Quemada et al., 2013). Additionally, cover cropping has been proposed as a potential strategy to increase SOC stocks in agricultural soils, with an average increase of 7.3% compared to bare fallow (Joshi et al., 2023; Peng et al., 2023). Furthermore, Peng et al. (2023) found that increasing precipitation and using non-legume cover crops is likely to be more effective for improving SOC stocks, compared to legumes and mixtures. However, the effects of cover crops on cash crop yields have been more variable and controversial (Garba et al., 2022). These effects depend on factors such as the type of cash crop (e.g., maize, soybean or rice), the cover crop species (e.g., legume, non-legume or mixtures), soil properties, fertilizer management for the cash crop, and the duration of cover cropping (Van Eerd et al., 2023).

1.6. Effects of conservation agriculture practices on N_2O emissions

Nitrous oxide emissions, which have a significantly higher GWP than CO_2, may offset the climate change mitigation potential of SOC sequestration achieved through conservation agriculture practices (Guenet et al., 2021). The frequency and magnitude of N_2O emissions are linked to soil structure, which is determined by factors such as bulk density, soil C content, and aggregation, all of which are influenced by tillage practices, crop rotations and residue inputs. Therefore, despite the previously mentioned benefits of conservation agriculture practices, their impacts on N_2O emissions need to be carefully evaluated.

1.6.1. Retention of crop residues in soil

The management of crop residues lays a crucial role in influencing N_2O emissions (Huang et al., 2018). According to the meta-analysis by Abalos et al. (2022b), on average, the N supplied to soil microorganisms by crop residues when incorporated into the soil leads to a 40-50%

increase in N_2O emissions compared to when residues are removed. These findings align with those of De Notaris et al. (2022), who reported that residue removal could provide significant potential for N_2O mitigation. Abalos et al. (2013) observed that incorporating maize stover residues with a high (> 70) C:N ratio increased N_2O emissions by ca. 105% during the experimental period. This increase could be associated with enhanced denitrification due to the interaction between high-C crop residues with mineral N from dressing fertilization.

Abalos et al. (2022a) and Snyder et al. (2009) reported that several factors, including residue maturity, management practices, the timing of residue incorporation, and interactions with N fertilization, influence N_2O emissions from crop residues. For example, incorporating mature residues such as cereal straw, maize stover, or grain legume residues –typically characterized by a high C:N ratio (> 30)– promotes soil N immobilization, thereby reducing N_2O emissions compared to the incorporation of immature crop residues (Abalos et al., 2022b; Li et al., 2016). However, N immobilization from these residues generally occurs within the first few months after application, followed by net mineralization after this period (i.e., 4-6 months after their incorporation), and therefore releasing labile C and N for nitrifying and/or denitrifying microorganisms (Abalos et al., 2013). Additionally, mineral N inputs can alter the rate of microbial decomposition of SOM, and increases in SOC content have frequently been observed (Bolinder et al., 2020). This priming effect may also contribute to increase the N_2O emissions (Daly et al., 2024). Recent ^{15}N-tracing laboratory experiments have reported increases in N_2O fluxes of 19% (Roman-Perez and Hernandez-Ramirez, 2021) and 13-24% (Thilakarathna and Hernandez-Ramirez, 2021) following urea application.

1.6.2. Reduced tillage or no tillage

In non-tilled soils, SOC accumulates in the topsoil, increasing the availability of labile organic C for denitrifiers and mineral N for both nitrifiers and denitrifiers (Shakoor et al., 2021).

Denitrification may be enhanced due to the combination of greater soil moisture and higher available C from crop residues left on topsoil under conservation tillage (i.e., no tillage or minimum tillage). However, the effects of different tillage systems on N_2O emissions remain uncertain and depend primarily on the initial soil C content and on soil moisture conditions (Y. Li et al., 2023a; Shakoor et al., 2021). A recent meta-analysis by Y. Li et al. (2023a) reported that no tillage decreased N_2O emissions by 11% compared to conventional tillage. Similar results were obtained by Shakoor et al. (2024) with 14% to 21% reductions in China and the United States, respectively. However, reduced tillage may increase N_2O emissions by increasing soil organic matter content, which could provide additional energy for denitrifying organisms, and by reducing soil porosity, thereby favoring anaerobic conditions (Guenet et al., 2021). Meta-analyses by Mei et al. (2018) and Shakoor et al. (2021) reported average increases in N_2O emissions of 19.2% and 12%, respectively, under no tillage compared to conventional tillage. Field assays in Mediterranean agroecosystems have reported higher (Plaza-Bonilla et al., 2014) and lower (García-Marco et al., 2016) N_2O fluxes in no-tillage systems compared conventional tillage. However, studies by Guardia et al. (2016b) and Plaza-Bonilla et al. (2018) found a consistently neutral effect of tillage intensity on N_2O emissions. These variable effects are, in any case, quantitatively low compared to other components of the GWP balance, such as SOC stocks or emissions from field operations.

1.6.3. Cover crops and rotations

The implementation of diversified crop rotations has been shown to mitigate N_2O emissions while providing additional benefits such as reducing the GWP, increasing crop yields, and enhancing soil health (Xiaolin Yang et al., 2024). The meta-analysis by Y. Li et al. (2023a) found that cover crops increased, decreased, or had neutral effects on soil N_2O emissions. According to the meta-analysis by Muhammad et al. (2019), cover crops reduced N_2O

emissions compared to bare fallow. However, this effect was observed only for non-legume cover crops, probably due to their higher efficiency in increasing crop N uptake and thereby reducing the pool of residual soil NO_3^- content (Abdalla et al., 2019; Gabriel et al., 2012; Thapa et al., 2018). In contrast, legume cover crops, due to their ability to fix atmospheric N_2, can increase soil available N through rhizodeposition and plant decomposition, potentially leading to higher N_2O losses (Ussiri and Lal, 2013). The effects of cover crops on N_2O emissions strongly depend on cover crop species –and their associated functional traits– as well as on biochemical properties such as the C:N ratio (Fernandez Pulido et al., 2023; Muhammad et al., 2019). However, results vary depending on the cropping period under consideration, namely the cover cropping phase (with crucial influence of N uptake potential), the period following cover crop termination, or the early stages of cash crop development (when plant material decomposition plays a key role). Y. Li et al. (2023a) reported that N_2O emissions tended to increase during the active growth phase of cover crops, being explained by the C supply from rhizodeposition through actively growing root systems, which promotes denitrification. These results have also been reported in field studies under Mediterranean climate (Guardia et al., 2016a; Sanz-Cobena et al., 2014a). According to Basche et al. (2014), during the cover crop decomposition period most N_2O is emitted from cover cropping, and the easily decomposable C from the low C:N residues –especially from legume species– provides an energy source for denitrifying microorganisms (Li et al., 2016). Y. Li et al. (2023a) identified key soil properties influencing the effects of cover crops on N_2O emissions. Their findings suggest that neutral soil pH, soil total N concentrations of approximately 0.3%, and soil organic C concentrations of around 2% result in the lowest soil N_2O emissions associated with cover crops.

Cover crops are widely recommended for recycling residual N from the previous cash crop (which is often intensively fertilized), and for increasing total soil N (Bohoussou et al., 2022). However, the critical influence of the legacy effect of synthetic fertilizers and surplus N across

the different cover cropping stages remains largely unexplored, particularly in combination with the input of cash crop residues left on the soil surface. This topsoil layer plays a fundamental role for driving N_2O emissions (Butterbach-Bahl et al., 2013; Kuang et al., 2023). Additionally, the simultaneous N input from the mineralization of recalcitrant cash crop residues (typically maize) several months after its incorporation in autumn (Abalos et al., 2022b), the more labile cover crop residues incorporated in spring, and the readily available synthetic N applied to the subsequent cash crop typically in early summer (Guardia et al., 2016a) can dramatically boost N_2O emissions. Given these complex interactions, a robust assessment of N_2O fluxes with high temporal resolution, alongside crop yield measurements, is essential for identifying the best strategies for the sustainable management of cover crop-based rotations from both environmental and agronomic viewpoints.

1.7. Use of nitrification inhibitors

In recent decades, the use of nitrification inhibitors (NIs) has been proposed as a strategy to enhance NUE and mitigate N losses, thereby reducing the environmental risks associated with N fertilization (Abalos et al., 2014; Akiyama et al., 2010; Ming et al., 2024; Quemada et al., 2013; Tufail et al., 2022; Yin et al., 2023). These products are capable to chelate copper (Cu), a cofactor of the AMO enzyme, which catalyzes the first step of nitrification (Corrochano-Monsalve et al., 2021; Morales et al., 2015). By inhibiting the conversion of NH_4^+ to NH_2OH (Figure 1.5), NIs slow down the subsequent oxidation of NO_2^- to NO_3^-, effectively reducing NO_3^- availability and limiting N losses through leaching and gaseous emissions.

Several molecules have been identified with the capacity to inhibit nitrification, with commercialized dicyandiamide (DCD) and 3,4-dimethylpyrazole phosphate (DMPP) (Figure 1.6), a DMP-based NI, being the most widely used NIs. The adoption of DMPP has increased over DCD due to their comparable effectiveness in mitigating N_2O emissions (Yang et al.,

2016), its lower required application rate, and concerns regarding plant uptake of DCD (Macadam et al., 2003; Marsden et al., 2015). However, the high volatility of the pyrazole ring poses a disadvantage for pyrazole-based NIs. In this context, the NI (3,4-dimethyl-1H-pyrazol-1-yl) succinic acid isomeric mixture (DMPSA) (CA 2933591 A1 2015/06/18 Patent) (Figure 1.6) has been proposed as a more stable pyrazole-based NI. The non-polarity of DMPSA improves the availability of DMP in the soil and allows for a broader range of fertilizer formulations that it can be combined with (e.g., urea, calcium ammonium nitrate, diammonium phosphate) compared to DMPP (Pacholski et al., 2016).

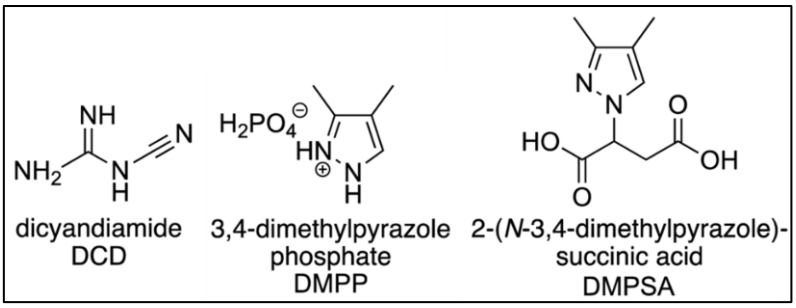

Figure 1.6. Chemical structure of the nitrification inhibitors DCD, DMPP and DMPSA.

When NIs are applied alongside NH_4^+-based fertilizers, the soil NH_4^+ concentration is expected to be kept for a longer period, favoring NH_4^+ adsorption to soil colloids and thus preventing NO_3^- losses via leaching or further denitrification. Quemada et al. (2013) indicated that NIs could decrease NO_3^- leaching in agricultural soils by 17%. Furthermore, one of the most effective strategies for mitigating N_2O emissions in fertilized crops is the use of NIs (Xia et al., 2017). The meta-analysis by Tufail et al. (2022) found that DMPP application resulted in a 39% reduction of N_2O emissions. Similarly, Ming et al (2024) reported a 63% decrease of GWP when using NIs in dryland ecosystems associated to a reduction of 58% and 9.8% in N_2O and CO_2 emissions, respectively. The effectiveness of NIs in reducing N_2O emissions has also been confirmed in Mediterranean agricultural systems, both in the meta-analysis by Cayuela et al. (2017) and in field experiments using DMPP (Abalos et al., 2017; Guardia et al., 2017b) and DMPSA (Corrochano-Monsalve et al., 2020; Guardia et al., 2018, 2017a; Recio et al., 2019).

However, the prolonged retention of NH_4^+ in the soil due to NI application has been associated with an increased risk of NH_3 volatilization (Castellano-Hinojosa et al., 2020; Pan et al., 2016; Qiao et al., 2015), particularly in alkaline soils (Cui et al., 2021).

It has been observed that the N_2O mitigation potential of DMPSA is enhanced by no tillage systems compared to conventional tillage under humid rainfed conditions (Corrochano-Monsalve et al., 2020). However, limited information is available regarding the interaction between tillage practices and NIs under semiarid (e.g., dry Mediterranean) conditions. The efficiency of these strategies may be compromised by the emission patterns in semiarid regions, especially during dry seasons, when rewetting events can significantly influence annual N_2O fluxes (Barrat et al., 2021; Guardia et al., 2024a).

1.8. CO_2 and CH_4 emissions from agriculture

In addition to N_2O, N fertilization also has relevant effects on the emission of other GHG, such as CH_4 and CO_2 (Sanz-Cobena et al., 2017). Since the Industrial Revolution, atmospheric CO_2 concentrations have increased from about 286 ppm to 410 ppm (Figure 1.7a), while CH_4 concentrations have risen from approximately 0.7 ppm to around 1.9 ppm (Figure 1.7b), according to the IPCC (2021) and the World Meteorological Organization (WMO) (WMO, 2024).

Soil represents the largest C pool in terrestrial ecosystems, with nearly 80% of its C stored within the top 1-meter layer. Despite being a huge C reservoir, soil respiration can contribute significantly to increasing atmospheric CO_2 concentrations. Carbon dioxide emissions from soil are associated with soil respiration, which includes soil microbial and root respiration. This process occurs when organic C compounds are completely oxidized into CO_2 and water (H_2O). The C stock within the top 30 cm of the soil contains twice the amount of C present in the atmosphere. In this context, increasing SOC sequestration through conservation agriculture

practices has been proposed as a strategy to reduce atmospheric CO_2 concentrations (Rumpel et al., 2020). On the other hand, a meta-analysis by Xiao et al. (2020) found an average 7% increase in soil CO_2 emissions in response to N addition, with a more pronounced increase (27%) in croplands. Soil rewetting episodes, consequence of intense rainfall events following long dry periods or due to irrigation, also have a significant impact on soil respiration, triggering CO_2 emission pulses (Liang et al., 2016; Sang et al., 2022). These effects have also been reported in Mediterranean cropping systems after the addition of N fertilizer and/or after rewetting events (Guardia et al., 2023). In general, the use of NIs in field experiments has led to a significant reduction (8%, on average) in CO_2 emissions (S. Li et al., 2023). However, studies by Guardia et al. (2021, 2017a) and Guardia et al. (2023) in Mediterranean cropping systems reported no significant effects from the use of DMPSA or DMPP, respectively.

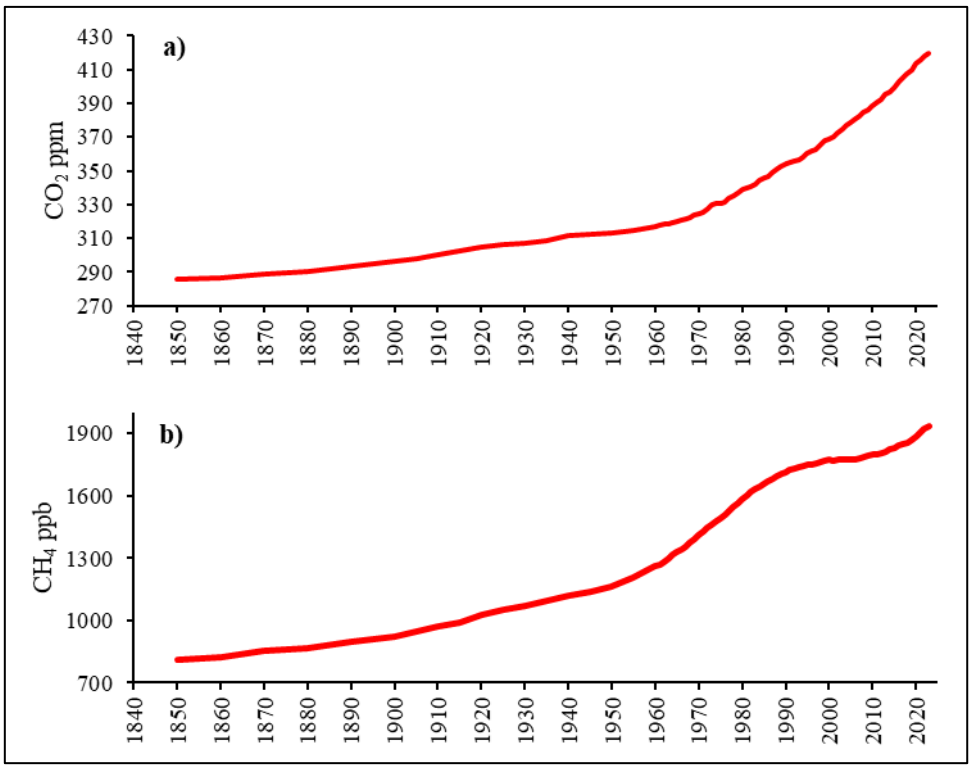

*Figure 1.7. Evolution of CO_2 **(a)** and CH_4 **(b)** atmospheric concentration from 1850 until 2019. Data obtained from the IPCC (2021) and WMO (2024).*

Between 2007 and 2016, agriculture was responsible for 39% of anthropogenic CH_4 emissions (IPCC, 2019a). Despite atmospheric concentration of CH_4 being much lower than that of CO_2 (Figure 1.7), CH_4 GWP is 25 times greater than that of CO_2 over a 100-year horizon, or 80 times greater in a 20-year horizon (IPCC, 2021). Due to its relatively short atmospheric lifetime (approximately 12 years), reducing CH_4 emissions could result in a rapid decrease of global temperatures, making it an important factor for short-term global warming mitigation (Wu et al., 2022).

Two microbiological processes are responsible for the production (methanogenesis) and consumption (methanotrophy) of CH_4 in the terrestrial and aquatic ecosystems. Methanogenesis is favored in anaerobic ecosystems, while methanotrophy is favored under aerobic conditions (Le Mer and Roger, 2001). The net flux of CH_4 to the atmosphere depends on the balance between these two processes. In agriculture, most CH_4 emissions are related to enteric fermentation and rice cultivation, while aerobic conditions in agricultural arable soils promote CH_4 oxidation, causing these soils to act as CH_4 sinks (Aronson et al., 2013). However, the meta-analysis by Aronson and Helliker (2010) indicated that agricultural soils, particularly those fertilized with N, exhibit significantly lower CH_4 oxidation rates compared to natural soils. Fertilizing with high N rates could compromise CH_4 consumption by soil microorganisms. Methanotrophs and ammonia oxidizers can switch substrates, thus NH_4^+ could compete with CH_4 and inhibit the CH_4 uptake by soil microorganisms when are exposed to high NH_4^+ concentrations (Wu et al., 2022). Several studies conducted in non-flooded Mediterranean agroecosystems have shown that soil acts as a net CH_4 sink, with no significant impact on CH_4 oxidation regardless N fertilization (Guardia et al., 2020; Montoya et al., 2021a, 2018). Agricultural practices such as tillage can also influence methanotrophic organisms. The recent review by Lim et al. (2024) and the meta-analyses by Maucieri et al. (2021) showed no apparent effects or even a reduction in CH_4 emissions when comparing no tillage and conventional tillage

in upland agricultural soils. According to the global meta-analysis by Qiao et al. (2015), and studies performed in semiarid Mediterranean (e.g., Guardia et al., 2023, 2021), the use of NIs had no effect on CH_4 soil fluxes.

The effect of residue input and temporal mineralization pattern is expected to influence both ecosystem respiration and CH_4 uptake in cover cropping systems, also depending on cover crop species and synthetic N application (Sanz-Cobena et al., 2014a; Wang et al., 2022). In this context, Ho et al. (2015) observed an enhancement in methanotrophic activity in soil after amendment with different biobased residues in an incubation experiment, probably due to increased nutrient availability in these soils. However, under field conditions, there is limited information about the effect of different crop residues on CH_4 oxidation capacity, particularly when both green manure and maize stover are co-applied.

1.9. Use of stable isotope ^{15}N tracing techniques in Mediterranean croplands and pre-alpine grasslands

The use of the stable isotope ^{15}N is one of the most powerful tools for studying N flows in agroecosystems (Scheer and Rütting, 2023) and is critical in the pursuit of sustainable agriculture. By using ^{15}N tracing techniques, it is possible to determine the sources of N_2O emissions (Guardia et al., 2016a; Ibraim et al., 2019), quantify the soil N transformation rates (Elrys et al., 2021; He et al., 2020), accurately calculate NUE in crops (Yan et al., 2020), asses soil N_2 losses (Friedl et al., 2023; Yankelzon et al., 2024), and ultimately to determine the fate of N applied via organic or synthetic fertilization (Ding et al., 2019; Guardia et al., 2018).

Tracing the fate of fertilizer-derived N in soil has gained increasing attention in recent years due to its direct implications for NUE and its environmental impact (Sha et al., 2020). Labeled ^{15}N tracing techniques have been widely used to monitor the fate of applied N across various

pools (i.e., crop biomass, soil, gaseous emissions and leachates), thereby allowing accurate quantification of fertilizer recovery in crops and other N reservoirs (Couto-Vázquez and González-Prieto, 2016; Guardia et al., 2018; Wang et al., 2016). The meta-analysis by Yan et al. (2020) indicated that, based on results from unfertilized plots used as control, approximately 55% of the N uptake in crops came from sources other than current-year fertilizer, while fertilizer N recovery increased to 61% in studies using ^{15}N-labeled methods. Field experiments conducted under Mediterranean conditions reported fertilizer N recovery rates of 33% in wheat (Ichir et al., 2003) and 68% in maize (Guardia et al., 2018) when synthetic fertilizers were applied. In grassland systems, cattle slurry application led to N recoveries ranging from 42% to 47.5% (Schreiber et al., 2023) and from 7% to 16% (Zistl-Schlingmann et al., 2020a). The effects of enhanced-efficiency fertilizers on N recovery have also been extensively studied. A meta-analysis of ^{15}N enrichment experimental data reported an average increase of 10.5% in crop fertilizer N recovery when NIs such as DCD or DMPP were applied (Sha et al., 2020). However, this study highlighted a knowledge gap regarding the effects of DMPSA application, particularly in rainfed semiarid cropping systems. In an irrigated Mediterranean maize field study, no significant differences in plant N recovery were reported when using DMPSA (Guardia et al., 2018).

The use of ^{15}N tracing techniques can also provide accurate insights into the contribution of N pools other than synthetic N fertilizers (e.g., soil endogenous mineral N, N mineralized from crop residues) to crop N uptake (Guardia et al., 2018; Taveira et al., 2020). Despite numerous studies addressing N recovery from fertilizer in crops (Gardner and Drinkwater, 2009; Yan et al., 2020), field data on N recovery from crop residues remain scarce. Taveira et al. (2020) reported residue-N recovery ranging from 10% to 30% depending on the type of crop residue and the subsequent cash crop. Similarly, Hu et al. (2015) reported an initial crop residue N recovery of 3.1% in the first year, with cumulative recovery up to 21% over four consecutive

cropping cycles. To our knowledge, no field studies have investigated crop residue N recovery under Mediterranean climate conditions.

Attributing N_2O emissions to the different processes responsible for its production is challenging, as these processes can occur simultaneously in different soil microsites (Butterbach-Bahl et al., 2013). The use of ^{15}N tracing techniques allows an accurate mechanistic understanding of N_2O production in soil and the contribution of the different N sources, both endogenous and exogenous (Guardia et al., 2018; Machado et al., 2021; X. Zhu et al., 2019). For instance, in an irrigated maize crop in central Spain, between 10% and 20% of N_2O emissions were derived from synthetic N fertilizer, with a higher contribution when barley was used as a cover crop compared to vetch (Guardia et al., 2016a). Under similar conditions, Guardia et al. (2018) reported that NH_4^+ from fertilizer was the major contributor to N_2O emissions during the days of highest emissions, with emissions significantly reduced when DMPSA was applied. Using a simulation model based on studies with ^{15}N–enriched wheat, barley and mustard crop residues, Delgado et al. (2010) found that crop residues contributed less to emissions than synthetic fertilizers. To date, no studies have investigated the contribution of crop residues to total N_2O emissions or fertilizer N recovery in cover crop-maize rotations in Mediterranean agricultural soils using ^{15}N-tracing techniques. In grassland soils, the contribution of sources other than fertilizer N to N_2O emissions has also been reported, with 60% of total cumulative N_2O emissions derived from the applied fertilizer (Dannenmann et al., 2024).

Another method that enables source partitioning of different N_2O emission processes is the measurement of N_2O isotopocules ($^{14}N^{14}N^{16}O$, $^{14}N^{15}N^{16}O$, $^{15}N^{14}N^{16}O$, and $^{14}N^{14}N^{18}O$) (Ibraim et al., 2020, 2019). The site-specific $^{15}N/^{14}N$ isotope-ratios at the central (alpha, α) and external (beta, β) positions of N_2O allow differentiation between soil-derived N_2O from nitrifier denitrification (referred to as N_2O_D) and N_2O produced via nitrification, abiotic pathways, and

fungal denitrification (referred to as N_2O_N). The intramolecular distribution of the ^{15}N into the α and β positions in N_2O, referred to as site preference, is lower for N_2O_D (-0.9 ± 4.1‰) compared to N_2O_N (32.8 ± 2.2‰) (Denk et al., 2017; Koba et al., 2009). Using isotopocule methods in grasslands, Bracken et al. (2021) reported a generally higher contribution of nitrification to N_2O emissions compared to denitrification, with an increased proportion of denitrification-derived N_2O at higher soil water contents. Furthermore, Buchen et al. (2018) suggested that nitrifier denitrification and/or denitrification coupled with nitrification are also relevant N_2O-producing processes in grassland soils.

In addition to N_2O, another potential N loss from agroecosystem is N_2 emissions from denitrification (Butterbach-Bahl et al., 2013). The commonly applied non-isotopic techniques allow for the quantitative analysis of NO and N_2O as intermediate products of denitrification, but do not measure the final product, N_2. Although N_2 emissions are environmentally benign, they result in economic losses and detrimental effects on crop productivity and NUE. Recently, Pan et al. (2022) reported a global mean denitrification emission factor ($N_2 + N_2O$) of 4.7% of applied fertilizer based on a global synthesis. However, due to limitations in the dataset used in the study, this emission factor may be underestimated. For instance, in a grassland experiment, N_2 losses represented 31-42% of the applied slurry-N (Zistl-Schlingmann et al., 2019). However, the N_2 losses were lower (7.5% of the applied N) when applying synthetic fertilizer in a wheat experiment (Yankelzon et al., 2024). Dinitrogen emissions remain a major uncertainty in ecosystem N balances, primarily due to the challenges of measuring soil N_2 emissions against the high atmospheric N_2 background (Friedl et al., 2020). The helium/oxygen (He/O_2) atmosphere method and the ^{15}N gas flux method (^{15}NGF method) enable the measurement of both N_2O and N_2 denitrification fluxes (Friedl et al., 2020). The former is an incubation system that replaces the soil atmosphere with He and is limited to laboratory experiments. In contrast, the ^{15}NGF method is suitable for field experiments, making it one of

the most effective techniques for in situ denitrification measurement (Micucci et al., 2023). The ^{15}NGF method employs a stable isotopic tracer ($^{15}NO_3^-$) with a high ^{15}N atom% enrichment to quantify denitrification by monitoring the ^{15}N signature of soil N_2 and N_2O emissions. Using the ^{15}NGF method, studies have demonstrated that N_2 losses are higher than N_2O emissions.

Another important application of N isotopes in agriculture is their use in calculating gross N transformation rates in soil through the ^{15}N pool dilution technique. The principle of this technique involves labeling a specific N pool with ^{15}N and subsequently monitoring its dilution due to the influx of naturally occurring N (Hart et al., 1994; Murphy et al., 2003). Gross N transformation rates provide a more accurate estimation compared to net N rates, which usually underestimate N dynamics in soil. The first calculations were developed by Kirkham and Bartholomew (1954), who derived equations for calculating gross mineralization and nitrification rates. Currently, numerical models have been developed to calculate gross N transformation rates using algorithms that consider the kinetics of individual N transformation processes (He et al., 2020; Müller et al., 2007, 2004a). However, there is a lack of ^{15}N−tracing field experiments investigating how different tillage systems (conventional tillage vs. tillage) in combination with N fertilizer application (with or without the NI DMPSA) could influence gross N transformation rates and fertilizer N recovery.

CHAPTER 2

OBJECTIVES

The mitigation of N_2O emissions from agricultural practices is a critical component in the fight against climate change. Reducing atmospheric N_2O concentrations is essential for limiting global temperature increases to 1.5°C above pre-industrial levels. Effective mitigation requires a comprehensive understanding of the biochemical processes driving N_2O production, which are primarily mediated by soil microbial activity. In this context, the research gaps that have been addressed in this thesis are related to: i) the effectiveness of DMPSA in reducing N_2O emissions under conservation tillage and in Mediterranean croplands, ii) the effect of the combination of conservation agricultural practices, such as cover crops and the input of crop residues, on GHGs emissions and crop yields, iii) the effect of crop residue C:N ratio and the different periods of the cover cropping cycle on GHGs emissions, iv) the effect of cover crops on N dynamics when applying maize crop residues and N synthetic fertilization, and v) the N transformation processes responsible of gaseous N losses in agricultural soils. Thus, implementing agricultural practices that reduce N_2O emissions without compromising crop yields is imperative. This not only involves adopting best management practices but also gaining a deeper understanding of the N cycle within agricultural ecosystems. One of the most valuable tools in this effort is the use of experimental ^{15}N tracing studies. These studies provide accurate insights into the fate of applied N, distinguishing between N used for plant growth and N lost through gaseous emissions, including N_2O. Furthermore, ^{15}N tracing enables the identification of specific pathways and environmental conditions that drive N_2O production, facilitating the development of targeted mitigation strategies. Consequently, these studies not only contribute to the understanding of N dynamics in agricultural soils but also support the design of more sustainable agricultural systems aligned with climate change mitigation and adaptation goals.

In this context, the main objective of this thesis is:

"To evaluate sustainable agricultural practices that combine crop residue management and N fertilization in rainfed and irrigated crops, with the aim of mitigating N_2O emissions without compromising crop yields, focusing on the mechanisms involved in N cycle transformations".

To achieve this, the research has been structured into three experiments conducted under Mediterranean climatic conditions, along with an additional experiment carried out in a pre-alpine grassland in southern Germany as part of a predoctoral stay. These experiments are presented in four distinct chapters, each with its own specific objective and related hypotheses. The hypotheses were formulated before the experiments were conducted, taking into account the available scientific literature.

Objective 1: *To evaluate the effect of the combination of different tillage management (conventional tillage, T, or no tillage, NT) with the application of N fertilizer enhanced with DMPSA as nitrification inhibitor or without DMPSA on the biochemical processes responsible for N_2O emissions and on the N fate in a rainfed barley crop under Mediterranean conditions using a ^{15}N-labeled fertilizer*.

Related hypotheses:

H1.1) DMPSA would mitigate N_2O emissions from nitrification of both exogenous and endogenous NH_4^+-N in T and, particularly, in NT.

H1.2) Nitrification would be the main process affecting N_2O emissions, as commonly observed in calcareous and low soil organic matter content soils.

Objective 2: *To assess the combined effect of residual N from the previous crop and the residues management (higher residue input when left on the surface, or reduced input after partial removal and deep incorporation) with the integration of different cover crop species (vetch as a legume and barley as a cereal) compared to bare fallow on GHG emissions and cash crop (maize) yield under Mediterranean conditions.*

Related hypotheses:

H 2.1) Greater inputs of maize residue (high C:N ratio) may reduce N_2O emissions before maize fertilization in a subsequent campaign, due to immobilization, while also increasing N_2O emissions after synthetic N application, due to the release of N and particularly labile C for denitrifiers.

H 2.2) The legume cover crop would increase N_2O emissions due to its reduced effectiveness in terms of offsetting residual N and due to the mineral N input increase from the decomposition of their N-rich residues, which would increase yield-scaled N_2O losses in comparison to the cereal cover crop and bare fallow.

H 2.3) The residual N from the previous cropping season would increase N_2O emissions and drive the performance of cover crops compared to bare fallow, especially during the cover cropping phase.

Objective 3: *To evaluate the combined effect of the incorporation of maize residues with two different cover crop species (barley and vetch) compared to bare fallow on the biochemical processes responsible for N_2O emissions and on the N fate of synthetic N applied in a maize crop under Mediterranean conditions using ^{15}N-labeled maize residues and a ^{15}N-labeled fertilizer.*

Related hypotheses:

H 3.1) The use of vetch as a legume cover crop and as green manure would increase N_2O emissions derived from both soil endogenous N and maize residues from the previous cropping system.

H 3.2) The incorporation of recalcitrant crop residues, such as those from maize stover, would be slowly mineralized, resulting in a limited contribution to N_2O emissions during the subsequent cropping year.

H 3.3) Despite irrigated conditions, nitrification would be a relevant process influencing N_2O emissions, particularly when no C-rich cover crop residues are applied.

Objective 4: *To quantify the fate of N (soil, plant and leaching) and the N_2O and N_2 emissions in a pre-alpine grassland soil, as well as the relative contribution of nitrification and denitrification processes to N gas fluxes, using a ^{15}N-labeled fertilizer*.

Related hypotheses:

H 4.1) Denitrification rather than nitrification would be the dominant process contributing to N_2O emissions under high WFPS values.

H 4.2) N_2 could be a major N loss pathway and predominantly explain the unrecovered N in the crop.

CHAPTER 3

MATERIALS AND METHODS

3.1. Site description

3.1.1. Experiments 1, 2 and 3

Three field experiments were conducted at the "Centro Nacional de Tecnología de Regadíos" (CENTER), located in San Fernando de Henares, Madrid, Spain (40° 25' 1.31'' N, 3° 29' 45.07'' W) (Figure 3.1).

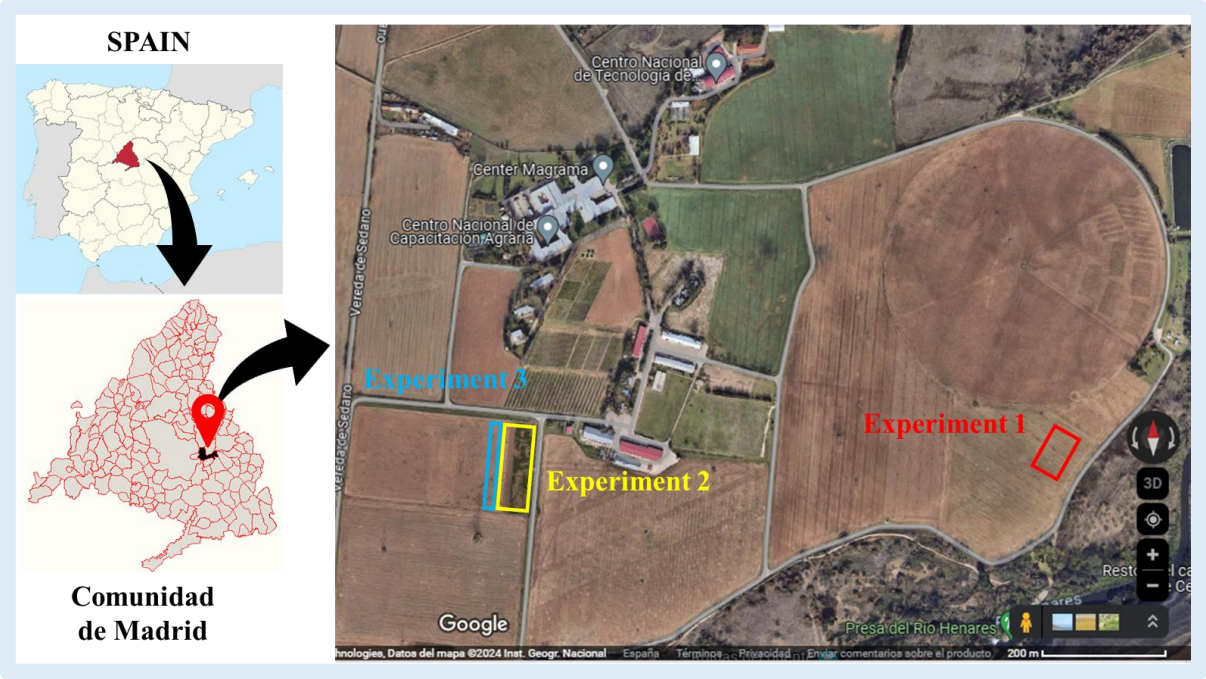

Figure 3.1. Location of Experiments 1 – 3 at the "CENTER" experimental field.

The area is characterized by a semiarid Mediterranean climate with high interannual variability. The mean air temperature and accumulated rainfall from 2006 to 2021 were 14.2°C and 401 mm, respectively. The climatological data (rainfall, air and soil temperature) were collected from the information of a meteorological station located at the CENTER and provided by the "Sistema de Información Agroclimática para el Regadío" (SIAR) webpage (https://eportal.mapa.gob.es/websiar/SeleccionParametrosMap.aspx?dst=1). The soil has been classified as a Typic Xerofluvent (Soil Survey Staff, 2014) which main physicochemical properties of the topsoil before the experimental studies are included in Table 3.1.

Table 3.1. Main physicochemical properties of the topsoil in Experiments 1 – 3.

Property	**Value**		**Method**
	Experiment 1 (0 – 10 cm)	Experiments 2 and 3 (0 – 10 cm)	
pH	8.16 ± 0.02	8.16 ± 0.02	H_2O (1:2.5)
Electric conductivity (mS cm^{-1})	0.49 ± 0.02	0.2	H_2O (1:5)
Texture	Silt loam	Silt loam	Bouyoucos
Clay (%)	9.2 ± 0.3	10.0	
Silt (%)	59.5 ± 1.0	59.5	
Sand (%)	31.3 ± 0.9	30.5	
$CaCO_3$ (%)	9.86 ± 0.92	8.16	Bernard calcimeter
N (%)	0.13 ± 0.00	0.16 ± 0.01	Kjeldhal
Organic matter (%)	1.44 ± 0.03	2.07	Walkey-Black
Bulk density (g cm^{-3})		1.20 ± 0.01	Core method
Non-tilled plots	1.19 ± 0.06		
Tilled plots	1.12 ± 0.05		

3.1.2. Experiment 4

The experiment was set up in the installations of the Institute of Meteorology and Climate Research Atmospheric Environmental Research (IMK-IFU) at the Karlsruhe Institute of Technology (KIT), located in Garmisch-Partenkirchen, southern Germany (Figure 3.2). The area is characterized by a humid continental climate, with an average annual temperature of 7.7 ºC and approximately 1,400 mm annual precipitation. To conduct the experiment, intact plant-soil mesocosms from the Graswang experimental site (DE-Gwg, 864 m a.s.l.) (Kiese et al., 2018) were translocated to a similar grassland site at Garmisch-Partenkirchen (Alpine Campus of KIT, IMK-IFU, 730 m a.s.l.) on 7 July 2023. The soil of the mesocosms is a C-rich (9% soil organic carbon in the topsoil) Haplic Cambisol, with 0.8% total N, silt loam texture (10% sand, 68% silt and 23% clay) and neutral pH due to carbonate content. More information about the main physicochemical characteristics of the soil are available in Schreiber et al. (2023). The vegetation is dominated by perennial herbs, including *Plantago lanceolata* L., *Trifolium repens*

L. and *Prunella vulgaris* L., as well as the perennial grass *Festuca rubra* L. (Zistl-Schlingmann et al., 2020b). During 2022-2023, the mesocosms were under extensive management, receiving two cattle manure fertilizer applications per year (40 kg N ha^{-1} each) and undergoing two harvests per year.

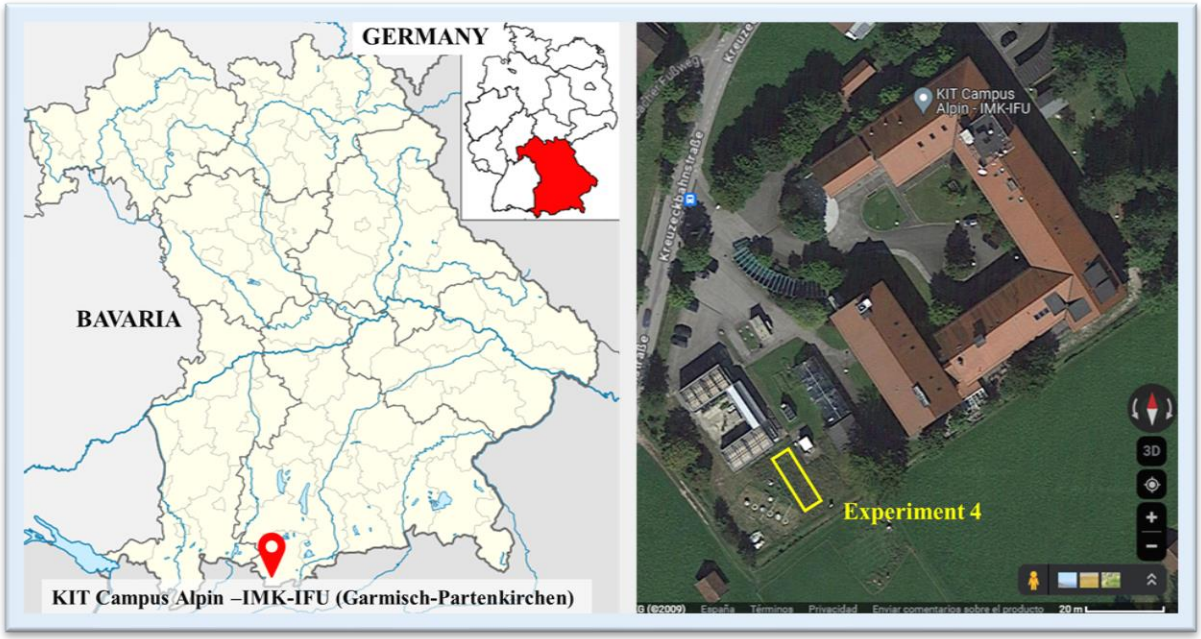

Figure 3.2. Location of Experiment 4 at the IMK-IFU.

3.2. Experimental design

3.2.1. Experiment 1

A field experiment using barley *(Hordeum vulgare* L. 'Esterel R1') was carried out at the "CENTER" experimental field (Figure 3.1). The barley crop was sown on 17 December 2018, at a seeding rate of 200 kg ha^{-1}. The experiment consisted of a three-replicate split-plot design with tillage as the main factor (no tillage, NT, and conventional tillage, T) arranged in a randomized block design. The second factor consisted of three fertilizer treatments applied at top-dressing: (1) calcium ammonium nitrate (CAN), (2) CAN with the nitrification inhibitor DMPSA (CAN+DMPSA), and (3) a control without N fertilization (N0). The distribution of subplots (8 m x 8 m) is shown in Figure 3.3. Fertilized subplots received 40 kg ha^{-1} of urea at

sowing (27 November 2018) and 80 kg N ha^{-1} of CAN at top dressing (14 March 2019). Rape residues (4492 kg ha^{-1}, with an average C:N ratio of 22.7) were incorporated with a disc harrow and cultivator in T plots or left on the soil surface in NT plots two months before barley sowing. In the NT plots, glyphosate 36% w/v was applied by spraying before barley seeding.

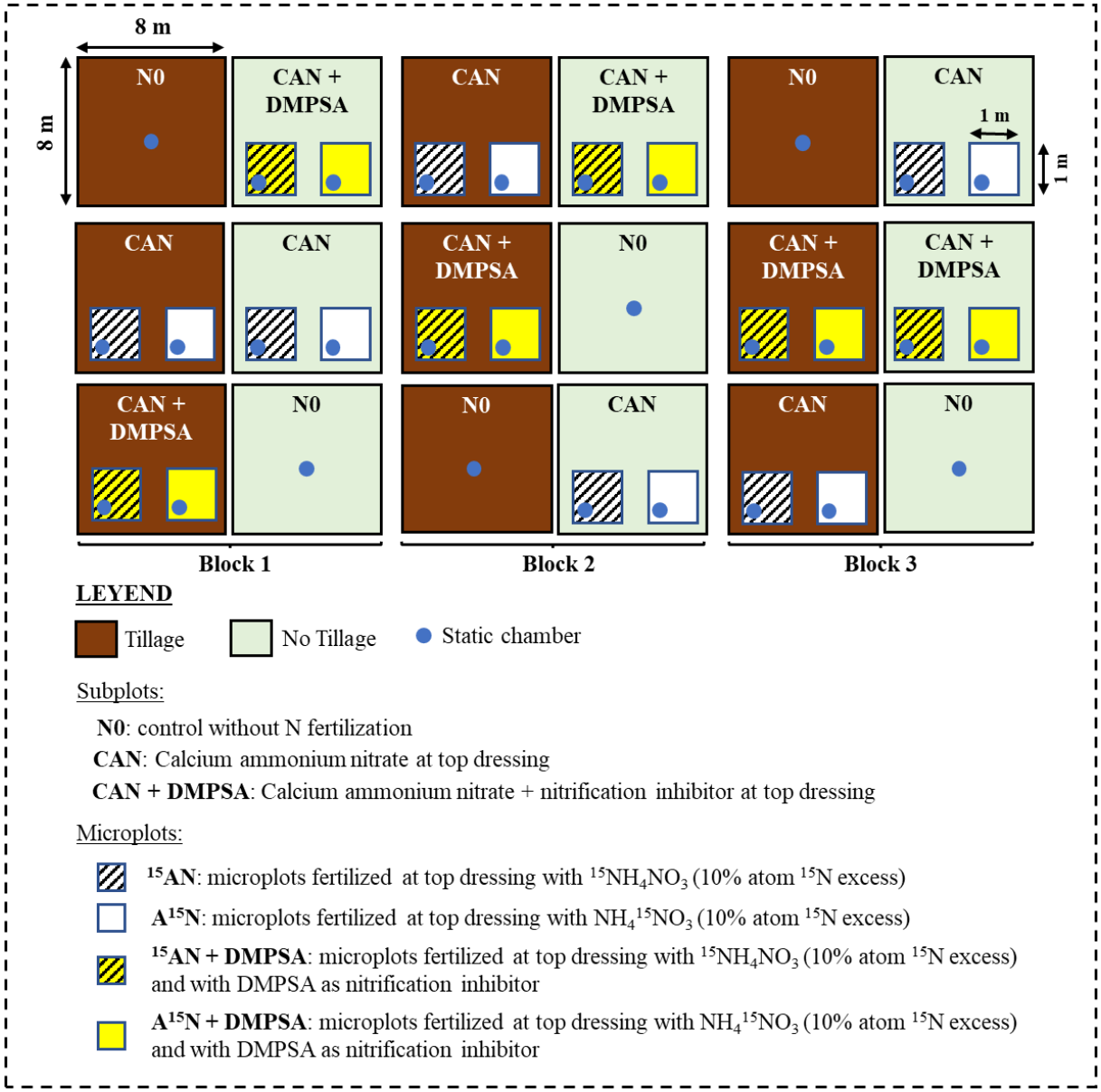

Figure 3.3. Experimental design at dressing fertilization of Experiment 1 at the "CENTER" field station.

Additionally, two microplots (1 m x 1 m) were established within every subplot before top dressing fertilization, except in the unfertilized plots (Figure 3.3). The microplots consisted of 0.3 m high galvanized sheet iron inserted into the soil to a depth of 0.2 m. Each microplot was

amended with 2 L of NH_4NO_3 (AN) solutions enriched with ^{15}N at a N rate of 80 kg N ha^{-1} on 14 March 2019. The solutions consisted of $^{15}NH_4{}^{14}NO_3$ (^{15}AN) or $^{14}NH_4{}^{15}NO_3$ (A^{15}N) (10 atom % ^{15}N, Campro Scientific) with or without DMPSA. To achieve a homogeneous distribution of ^{15}N–enriched products in the soil is crucial in isotopic tracing studies (Murphy et al., 2003). For this purpose, the microplots were divided into four quadrants (0.25 m^2 each) where 0.5 L of the fertilizer solution were homogeneously applied in the surface of each quadrant with a hand sprayer (Figure 3.4).

Figure 3.4. Application of the ^{15}N–enriched fertilizer solution in barley crop of Experiment 1.

The DMPSA inhibitor was provided by EuroChem Agro in a liquid solution and was applied at a rate of 0.8% of the NH_4^+-N content of the fertilizer. Pests were managed following local practices and irrigation was used on two occasions, on 26 March and 13 May 2019 (20 mm in each event), due to the severe drought conditions. The barley was harvested on 13 June 2019. The results presented in this thesis (Section 4.1 in Chapter 4) are based on the analyses performed in the ^{15}N fertilized microplots and on the N0 subplots after top-dressing N fertilization.

In Table 3.2 are summarized the principal agricultural management events and the sampling dates of **Experiment 1**.

Table 3.2. Principal agricultural management events and sampling dates of Experiment 1.

Agricultural management event	
Tillage (or no tillage)	Mid-October 2018
Basal fertilization	27 November 2018
Barley sowing	17 December 2018
Top-dressing fertilization: ^{15}N fertilizer application	14 March 2019
Emergency irrigation	26 March 2019 (12 DAF)*
Emergency irrigation	13 May 2019 (60 DAF)*
Barley harvest	13 June 2019 (91 DAF)*
Sampling dates	
Soil sampling at the end of experiment for ^{15}N recovery	7 November 2019 (238 DAF)*
Gas sampling for N_2O and $^{15}N_2O$ analyses (DAF)*	0, 1, 4, 6, 8, 13, 15, 19, 21, 26, 29, 34, 39, 42, 46, 50, 61, 63, 67, 68, 165, 166, 169, 182, 186, 193, 194, 237, 238
Soil sampling for mineral N analysis (DAF)*	0, 1, 4, 6, 13, 21, 39, 46, 67, 166, 238
Soil sampling for mineral ^{15}N analysis (DAF)*	0, 1, 4, 6, 13, 21

* DAF: days after top-dressing fertilization

3.2.2. Experiment 2

A field experiment was conducted from November 2020 to November 2021 at the "CENTER" field station (Figure 3.1). The experiment consisted of a three-replicated split-plot design with maize residue input as the main factor and cover cropping as the split factor. Within the main factor, two different types of plots were established: i) maize residue maintained and incorporated by a shallow disk harrow pass at 10-15 cm depth, thus leading to a higher input of residue in the topsoil (+R), and ii) removal of maize residue from the topsoil followed by deep incorporation of the remaining residue up to 40 cm depth, thus leading to a lower input of maize residue in the topsoil (−R) (Figure 3.5).

Figure 3.5. Different maize residue input in Experiment 2: lower input (-R) after partial removal of maize residue from the topsoil followed by deep incorporation of the remaining residue, and higher input (+R) with maize residues being incorporated in the topsoil by a shallow disk harrow pass.

In the previous cropping season (summer 2020), maize was fertilized with urea at a rate of 200 kg N ha^{-1}, obtaining 10,000 kg ha^{-1} grain yield (data obtained from personal communication with the field technicians). The different cover cropping treatments were bare fallow (F), a legume (L) cover crop (vetch, *Vicia sativa* L. var "Rada") and a cereal (C) cover crop (barley, *Hordeum vulgare* L. var "RGT PLANET"). Bare fallow was maintained with sporadic weeds and no labor or herbicides were applied. After cover crops termination, the bare fallow subplots were managed in a similar way to the cover crop subplots, applying the farming procedures described below prior to sowing the maize crop. The main factor was arranged in a completely randomized design, while the split factor was set out with a completely randomized set-up (Figure 3.6).

Control plots (which did not receive any synthetic N fertilization in either the 2020 maize cropping season or the 2021 cash crop maize phase) received the same maize residue input and cover cropping treatments. The experimental design of the control plots was similar to that of the fertilized plots (a split-plot design with residue input and cover cropping as the main and split factors, and with three replicates) (Figure 3.6). Control plots were located in the same

experimental area as the fertilized plots. The dimensions of all the subplots (both fertilized and unfertilized) were 5 m x 30 m.

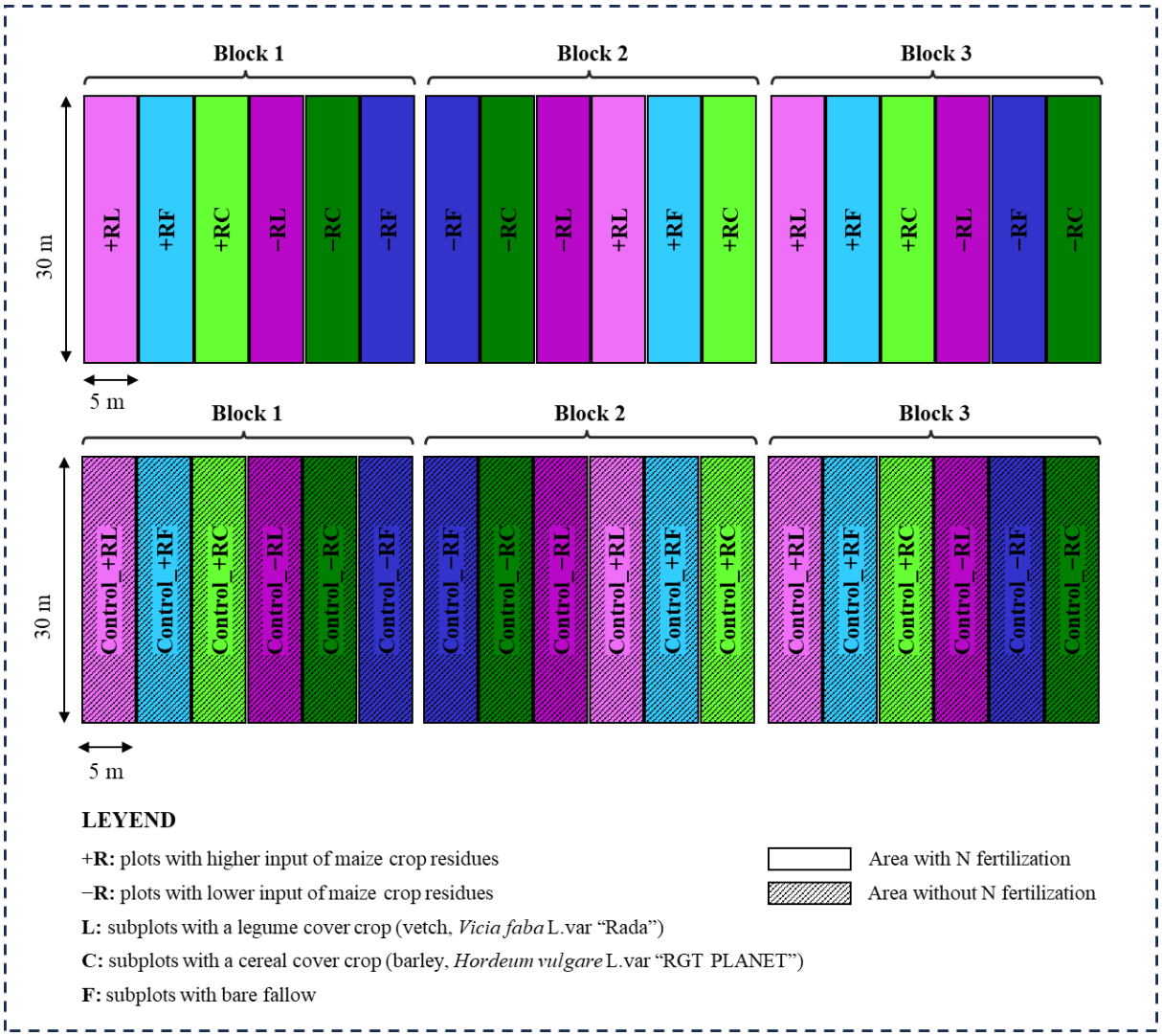

Figure 3.6. Experimental design of Experiment 2 at the "CENTER" field station.

The experiment started in mid-November with the management of maize straw from the previous cropping season. The average C:N of the maize residue was 89.5. Vetch and barley were sown at a rate of 200 kg ha^{-1} on November 17, chemically terminated on April 13 using herbicide (Roundup®, glyphosate 36%, 5 L ha^{-1}) and incorporated into the soil with a disc harrow pass at 10-15 cm depth on May 6. Maize (*Zea mays* L. var. "Pioneer 0725" FAO 500) was sown as the cash crop on June 10 at a rate of 9.5 plants m^{-2} and was irrigated by sprinkler using a ranger system during its cropping cycle accounting for a total of 700 mm water (ca. 50

mm per week split into two irrigation events per week). Maize was hand-fertilized on July 19 with CAN, which was homogeneously distributed over the soil surface of each plot. Moreover, the stainless steel rings −where the chambers for gas sampling were subsequently placed− were fertilized prior to the entire plot with the proportional share of the total N rate (Charteris et al., 2020). Maize was fertilized following integrated soil fertility management practices. Briefly, the gross N rate was calculated considering the expected yield and grain N extraction, while the net N rate was adjusted considering the soil mineral N concentration before dressing fertilization as well as the availability of N from the mineralization of cover crop residues. The N from cover crop residues available for maize was estimated by multiplying the total N content in cover crop dry biomass by the predicted % of plant available N at 10 weeks after cover crop residue application following the approach described in Sullivan et al. (2019). As a result, N fertilization rates of 170, 220 or 210 kg N ha^{-1} were applied in the L, C or F subplots, respectively. Maize was harvested at physiological maturity on November 19.

The experiment was split into three periods: 1) from mid-November 2020 to mid-April 2021, thus considering the development of cover crops until their termination during the intercrop period (P1); 2) from the end of P1 to maize dressing fertilization on 19 July 2021, thus considering the incorporation of cover crops and the beginning of the development of maize under irrigated conditions (P2); and 3) from maize fertilization to maize harvest on 11 November 2021 (P3).

The principal agricultural management events and the sampling dates of **Experiment 2** are shown in Table 3.3.

Table 3.3. Principal agricultural management events and sampling dates of Experiment 2.

Agricultural management event	
Maize residue incorporation	Mid-November 2020
Cover crops sowing	17 November 2020
Cover crops harvest	12 April 2021
Cover crops chemical termination	13 April 2021
Cover crops incorporation	6 May 2021
Maize cash crop sowing	10 June 2021
Start of maize irrigation	11 June 2021
Maize fertilization	19 July 2021
End of maize irrigation	End of September 2021
Maize harvest	19 November 2021
Sampling dates	
Gas sampling for GHG analysis in P1 (DACCS)*	7, 15, 31, 35, 43, 69, 71, 85, 90, 98, 106, 126, 137, 139, 146
Gas sampling for GHG analysis in P2 (DACCT)**	6, 10, 14, 24, 28, 50, 58, 60, 63, 66, 72, 78, 85, 92
Gas sampling for GHG analysis in P3 (DAF)***	2, 4, 7, 9, 11, 14, 16, 23, 28, 31, 37, 45, 52, 63, 79, 100, 109
Soil sampling for mineral N and DOC analyses in P1 (DACCS)*	7, 31, 69, 90, 137
Soil sampling for mineral N and DOC analyses in P2 (DACCT)**	10, 24, 50, 66, 85
Soil sampling for mineral N and DOC analyses in P3 (DAF)***	2, 9, 16, 23, 37, 63, 109

* DACCS: days after cover crops sowing
** DACCT: days after cover crops termination
*** DAF: days after maize top-dressing fertilization
P1: from cover crops sowing to cover crops chemical termination
P2: from cover crops chemical termination to maize fertilization
P3: from maize fertilization to maize harvest

3.2.3. Experiment 3

A ^{15}N tracing field experiment using microplots (1 m × 1 m) was conducted from November 2020 to November 2021 at the "CENTER" field station (Figure 3.1). This microplot experiment was carried out simultaneously in the N-fertilized area of **Experiment 2** (see Figure 3.6 in Section 3.2.2). The microplots established in this experiment consisted of 30 cm height stainless steel plates that were inserted into the soil to a depth of 10 cm. At mid-November 2020, nine initial microplots were established in the subplots of **Experiment 2** where maize residues from the previous cropping season were removed from the topsoil (−R, see Section 3.2.2 for detailed

information). Enriched ^{15}N maize residues, ^{15}RES (1.06% N, 42.6% C, 40.3 C:N ratio, 7.03% atom ^{15}N) obtained from a previous field experiment (Guardia et al., 2018) were incorporated into the topsoil of the nine initial microplots using a hoe at a rate of 950 g m^{-2}, thus applying a total N rate of 100 kg N ha^{-1} (Figure 3.7).

Figure 3.7. Incorporation of ^{15}N–enriched maize residues in Experiment 3.

After that, barley (*Hordeum vulgare* L. var "RGT PLANET") and vetch (*Vicia sativa* L. var "Rada") cover crops were manually sown in the microplots at the same rate as that on the subplots of **Experiment 2** (i.e., 20 g m^{-2}), and bare fallow was also implemented in similar microplots. Before maize (*Zea mays* L. var. "Pioneer 0725" FAO 500) fertilization, eighteen additional microplots were established in the subplots of **Experiment 2** where the maize residues from the previous cropping season were incorporated into the topsoil (i.e., non-enriched ^{15}N maize residues) (+R, see Section 3.2.2 for detailed information). Considering the grain yield of the previous cropping season (10,000 kg ha^{-1}), a 0.44% N content in maize stover (data from a two-year maize experiment under similar climatic and management conditions (Monistrol et al., 2024)), and a maize harvest index of 0.52 (Hütsch and Schubert, 2017), the total N rate applied in the non-enriched ^{15}N maize residue microplots was estimated to be 41 kg N ha^{-1}. The microplots were positioned so that six maize plants were inside each microplot. Fertilization of the twenty-seven microplots was performed by applying 2 L per microplot of fertilizer solution at a rate of 210 kg N ha^{-1} on 19 July 2021, following the same procedure as

that in **Experiment 1**. Briefly, the microplots were divided into four quadrants (0.25 m^2 each) with 0.5 L of fertilizer solution homogeneously applied to the surface of each quadrant using a hand sprayer (Figure 3.8). The fertilizer solution for the nine initial microplots (i.e., those receiving ^{15}N–enriched maize residues) consisted of AN at ^{15}N natural abundance. The eighteen microplots located in the subplots with non-enriched maize residues were fertilized with ^{15}N−enriched AN (20% ^{15}N atom), with nine of them receiving ^{15}AN and the other nine receiving $A^{15}N$.

Figure 3.8. Application of the ^{15}N-enriched fertilizer solution in Experiment 3

Three replicates per treatment were established in a completely randomized block design with cover crop as main factor (barley, B, vetch, V, and bare fallow, F). The experiment was split into two periods. The first period (P1) started in November 2020 with the incorporation of the ^{15}N–enriched maize residues into the soil and covered the development of the cover crops, their incorporation after being chemically terminated in mid-April, and ended before maize fertilization on 19 July 2021. The second period (P2) started with maize fertilization and finished with the maize harvest on 17 November 2021. An outline of the experimental design during P1 and P2 is shown in Figure 3.9a and Figure 3.9b, respectively.

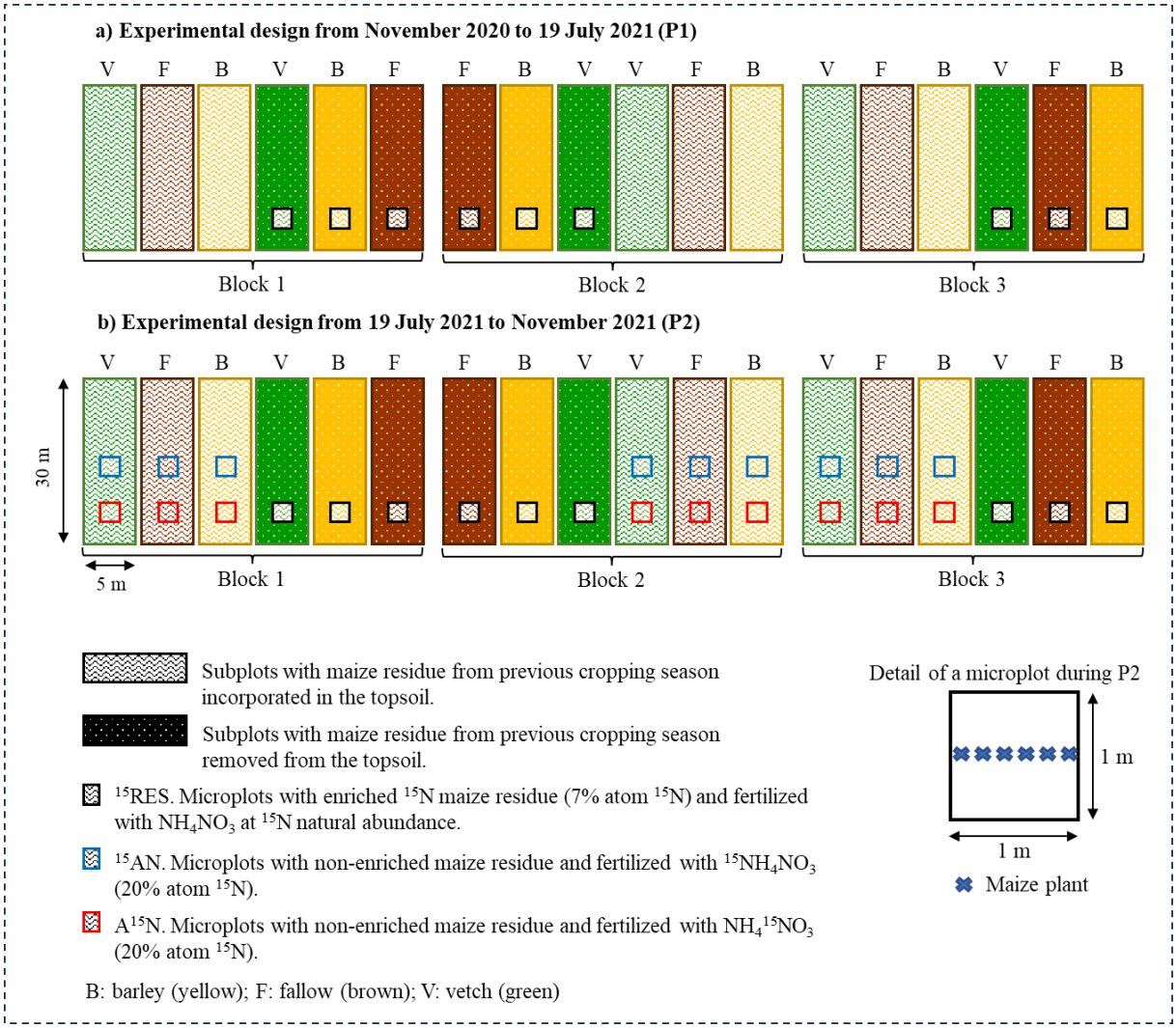

Figure 3.9. Experimental design of Experiment 3 at the "CENTER" field station.

The principal agricultural management events and the sampling dates of **Experiment 3** are shown in Table 3.4.

Table 3.4. Principal agricultural management events and sampling dates of Experiment 3.

Agricultural management event	
^{15}N-enriched maize residue incorporation	10 December 2020
Cover crops sowing	10 December 2020
Cover crops harvest	12 April 2021 (123 DARI*)
Cover crops chemical termination	13 April 2021 (124 DARI*)
Cover crops incorporation	7 May 2021 (148 DARI*)
Maize cash crop sowing	10 June 2021 (182 DARI*)
Start of maize irrigation	11 June 2021 (183 DARI*)
Maize fertilization with ^{15}AN, A^{15}N or AN	19 July 2021
End of maize irrigation	End of September 2021
Maize harvest	17 November 2021 (DAF**)
Sampling dates	
Gas sampling for GHG analysis in P1 (DARI)*	12, 20, 28, 43, 46, 62, 67, 83, 103, 116, 123, 130, 134, 138, 148, 152, 174, 182, 184, 187, 190, 196, 202, 209, 216
$^{15}N_2O$ analysis in P1 (DARI)*	46, 148, 184, 190, 216
Gas sampling for GHG analysis in P2 (DAF)**	0, 1, 2, 4, 7, 9, 11, 14, 16, 23, 28, 31, 37, 45, 52, 63, 79, 100, 109
$^{15}N_2O$ analysis in P2 (DAF)*	1, 2, 4, 7, 9, 11, 16, 23, 45
Soil sampling for mineral N and DOC analyses in P1 (DARI)*	12, 46, 67, 116, 148, 174, 190, 216
Soil sampling for mineral N analysis in P2 (DAF)**	0, 1, 2, 4, 7, 9, 11, 16, 23, 37, 52, 109
Soil sampling for DOC analysis in P2 (DAF)**	2, 9, 16, 23, 37, 52, 109
Soil sampling at the end of experiment for ^{15}N recovery	5 November 2021 (109 DAF**)

* DARI: days after maize residues incorporation

** DAF: days after maize top-dressing fertilization

P1: from maize residue incorporation to maize cash crop top-dressing fertilization

P2: from maize top-dressing fertilization to maize harvest

3.2.4. Experiment 4

A ^{15}N tracing field experiment using mesocosms was conducted from July to September 2023 at the IMK-IFU installations (Figure 3.2). The mesocosms consisted of 30 cm diameter x 40 cm height polyvinyl chloride (PVC) cylinders that were established in Graswang in August

2016 (Schreiber et al., 2023) and translocated to the IMK-IFU installations at Garmisch-Partenkirchen at the beginning of July 2023.

A total of fifteen mesocosms were used: six were used for calculating N_2O and N_2 losses by applying the ^{15}NGF method and for calculating N recovery in soil, plant, and the mineral N leaching (set M1); six mesocosms were used for destructive soil mineral N concentration and WFPS analyses (set M2); and three were used for soil moisture and temperature determination at 10 cm depth (set M3) (Figure 3.10).

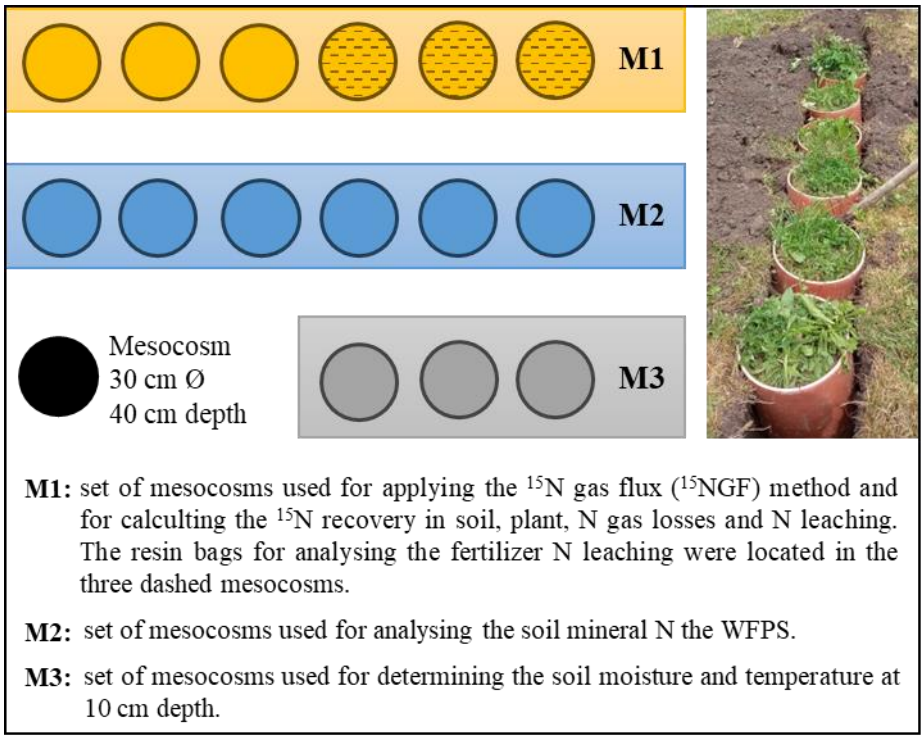

Figure 3.10. Experimental design of Experiment 4 at the IMK-IFU.

The mesocosms were fertilized with a N rate of 80 kg N ha^{-1} on 14 August and 29 August (i.e., a total N rate of 160 kg N ha^{-1}). To distribute the ^{15}N–enriched fertilizer with optimized homogeneity, a fertilizer solution was applied following the indications by Dannenmann et al. (2016) with some modifications. Briefly, during each fertilization event, the six mesocosms used for the ^{15}NGF method and ^{15}N recovery (set M1) were fertilized at a rate of 40 kg $N–NH_4^+$ ha^{-1} and 40 kg $N–NO_3^-$ ha^{-1} by applying 250 mL of fertilizer solution containing both

ammonium sulphate, $(NH_4)_2SO_4$, and potassium nitrate, KNO_3, (98% atom $^{15}N{-}NO_3^-$). A 10 mL syringe was used to homogenously distribute 25 injections of 10 mL of the fertilizer solution all over the mesocosms surface area (Figure 3.11). After that, 250 mL distilled water were applied twice over the mesocosms surface (30 and 60 min after fertilizer solution application). Therefore, a total volume of 750 mL (250 mL fertilizer solution + 500 mL water) was applied per mesocosm (i.e., 10 L ha^{-1}), promoting soil denitrifying conditions.

Figure 3.11. Application of the fertilizer solution in the mesocosms.

The fertilizer solution applied to the remaining nine mesocosms, used for soil mineral N concentration analyses (set M2) and for soil moisture and temperature determinations (set M3), consisted of $(NH_4)_2SO_4$ and KNO_3, both with ^{15}N at natural abundance, and was distributed over the mesocosms surface following the same procedure as for the mesocosms of set M1. To promote denitrifying conditions, one week after both fertilization events (i.e., on 21 August and on 4 September 2023), the mesocosms were irrigated to simulate a precipitation event of 30 mm by applying three doses of tap water within 1.5 hours. A summary of the principal management events and the sampling dates of **Experiment 4** are shown in Table 3.5.

Data of air temperature and pressure was obtained from a meteorological station located near the Alpine Campus of IMK-IFU (Kiese et al., 2018). Data of soil moisture and temperature was

obtained by inserting two sensors at 10 cm depth of each of the three mesocosms of set M3 (one for temperature and other for moisture) connected to a data logger.

Table 3.5. Principal agricultural management events and sampling dates of Experiment 4.

Agricultural management event	
Mesocosms translocation to IMK-IFU installations and installations of the moisture and temperature soil sensors	11-14 July 2023
Installation of the resin bags	10 August 2023
Fertilization	14 and 29 August 2023
Irrigation	22 August and 4 September 2023
Grass harvest	12 September 2023 (29 DAF*)
Sampling dates	
Gas sampling for GHG analyses	−25, −24 and −18 DAF* 0, 1, 2, 3, 4, 7, 8, 9, 10, 11, 14, 15, 16, 17, 18, 21, 22, 23 and 28 DAF*
Gas sampling for $^{15}N_2O$ and ^{15}N analyses	0, 1, 2, 3, 4, 7, 8, 9, 10, 11, 14, 15, 16, 17, 18, 21, 22, 23 and 28 DAF*
Soil sampling for mineral N analysis	−4, 2, 7, 10, 14, 17, 20 and 23 DAF*
Resin bags sampling for mineral ^{15}N leaching analysis	12 September 2023 (29 DAF*)
Soil sampling at the end of experiment for ^{15}N recovery	12 September 2023 (29 DAF*)

* DAF: days after 1st fertilizer application

3.3. Gas sampling, analysis and calculations

3.3.1. Greenhouse gases

The closed chamber system was used to measure the GHG (i.e., N_2O, CH_4 and CO_2) fluxes from the soil using manual static chambers. The chambers used were opaque and made of PVC.

3.3.1.1. Experiments 1, 2 and 3 at the CENTER experimental field

The chambers were placed over stainless steel rings that were inserted 4 cm into the soil surface to avoid the lateral diffusion of the gases. The rings were removed only during management events. Gas samples were taken at times t_0, t_{30} and t_{60} (60-min interval) from the headspaces of each chamber as described in Harvey et al. (2020) using 100 ml syringes that were inserted to 3-way stopcocks fitted to the chambers. Samples were transferred to 20 ml gas chromatography

vials sealed with a gas-tight butyl septum. Details of a manual chamber and the material used for gas sampling are shown in Figure 3.12.

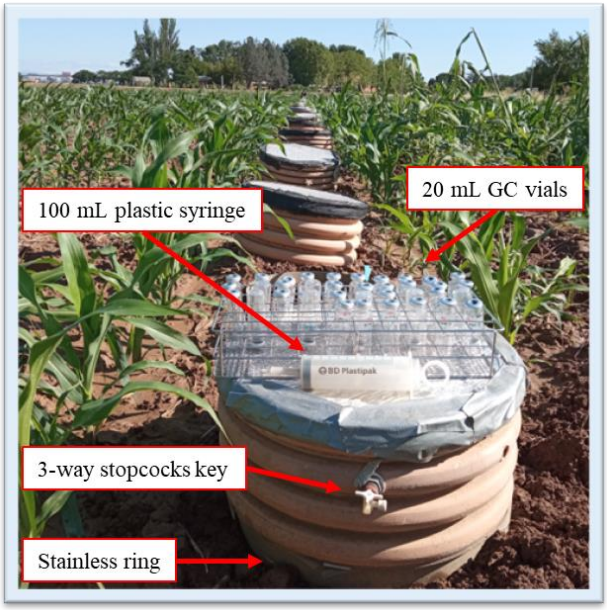

Figure 3.12. Detailed image of a closed manual chamber and the materials used for sampling greenhouse gases.

To minimize the effects of diurnal variation emissions, the samples were always taken at the same time of day (10-12 am). The GHG concentration in the samples was determined with an HP-6890 gas chromatograph (GC) equipped with an HTC-3 Headspace autosampler, both from Agilent Technologies (Barcelona, Spain). The samples were carried through HP Plot-Q capillary columns connected to a ^{63}Ni micro electro capture detector to analyze N_2O, and to a flame ionization detector to measure CH_4 and CO_2. Two gas standards with lower (500.0 ± 2.5 ppm CO_2, 2.00 ± 0.10 ppm CH_4 and 500 ± 15 ppb N_2O) and higher (1500.0 ± 7.5 ppm CO_2, 10.0 ± 0.1 ppm CH_4 and 2.0 ± 0.1 ppm N_2O) GHG concentrations were provided by Carburos Metálicos S.A. (Barcelona, Spain). The two standards were diluted with N_2 (1:1; v:v) to perform a calibration curve for the GHGs with four different concentrations: two original standards and two diluted standards. The response of GC was linear within the CO_2, CH_4 and N_2O concentrations of the standards (250 – 1500 ppm CO_2; 1 – 10 ppm CH_4 and 250 – 2000 ppb

N_2O). The increases in GHG concentrations within the chamber headspace were generally linear ($R^2 > 0.95$) during the chamber closure time (60 min).

Daily GHG fluxes (mg N_2O−N m^{-2} d^{-1}, mg CO_2−C m^{-2} d^{-1}, and mg CH_4−C m^{-2} d^{-1}) were estimated as the slope of the linear regression between concentration and time, and the ratio between chamber volume and soil surface area. Cumulative gas emissions of the different GHGs (mg N_2O−N m^{-2}; g CO_2−C m^{-2}, and mg CH_4−C m^{-2}) analyzed during the experimental period were estimated by multiplying the average flux of two successive determinations by the time interval between samplings, and then adding that amount to the previous cumulative total (Venterea et al., 2020).

In **Experiment 1,** one chamber (13 cm height × 35 cm dimeter, 12.5 L volume) was placed in every microplot, and the aboveground biomass of barley plants was placed inside the chamber's headspace during samplings (Figure 3.13). Cumulative N_2O emissions were calculated distinguishing the period before barley harvest and the postharvest period.

Figure 3.13. Location of the manual static chambers used for gas sampling in the barley crop of Experiment 1.

In **Experiment 2** one chamber (24 cm height × 35 cm diameter, 23.1 L volume) was placed in every subplot. During cover crop development the aboveground biomass of the plants were located inside the chambers during gas sampling. During the maize cropping phase, the chambers were located between two maize lines (Figure 3.14).

Figure 3.14. Location of the manual static chambers used for gas sampling in the barley cover crop (left) and in the maize cash crop (right) in Experiment 2.

Cumulative GHG emissions were calculated at the end of the three different periods of the experiment (see Section 3.2.2). Yield-scaled N_2O emissions (YSNE) expressed as g N_2O−N kg grain^{-1} were calculated as the ratio between the total cumulative N_2O−N emissions and maize grain yield. The N_2O emission factor (EF) was estimated as the ratio of total cumulative N_2O−N emissions, subtracting those of the corresponding control, to the synthetic 170, 220 or 210 kg N ha^{-1} applied in the legume, cereal or fallow plots, respectively.

In **Experiment 3**, soil-atmosphere exchange of N_2O and CO_2 was measured using similar static chambers than those used in **Experiment 1**. The aboveground biomass of the cover crops was placed inside the chamber's headspace during samplings (Figure 3.15). The chambers were placed next to the maize rows during maize growing phase (Figure 3.16). Cumulative GHG

emissions were calculated at the end of the two different periods of the experiment and considering the whole experimental period (see Section 3.2.3).

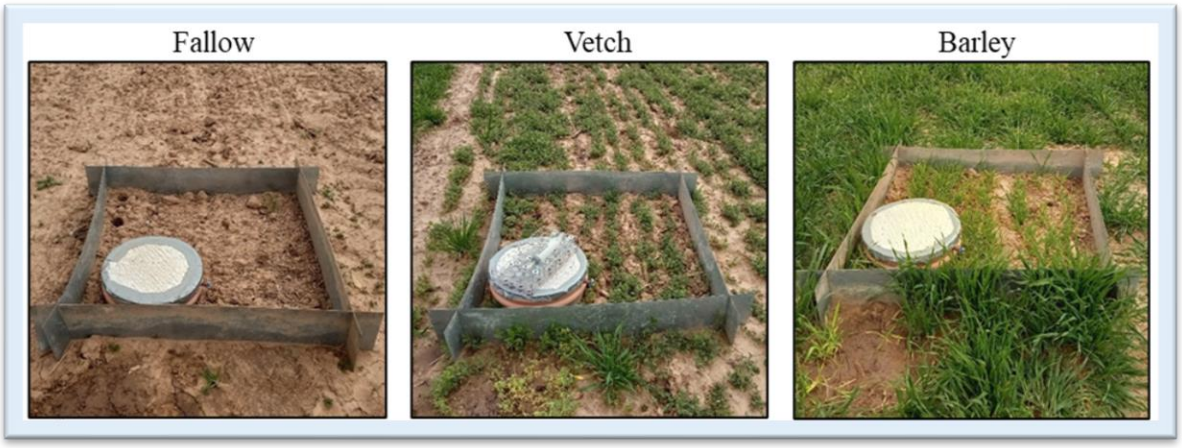

Figure 3.15. Location of the manual static chambers used for gas sampling during cover crop development and until maize fertilization (P1) of Experiment 3.

Figure 3.16. Location of the manual static chambers used for gas sampling after maize fertilization and until maize harvest (P2) of Experiment 3.

3.3.1.2. Experiment 4 at the IMK-IFU

Greenhouse gases from the soil mesocosms of set M1 (Figure 3.10 in Section 3.2.4) were sampled using 13 cm height × 30 cm diameter PVC chambers. During sampling, the chambers were fitted to the top of the PVC cylinder of the mesocosms (Figure 3.17). Greenhouse gas samples from the chamber headspace were taken using a 30 mL syringe fitted to a three-way stopcock connected to the chambers, and the gas sample was overpressure flushed into 10 mL

GC vials. The concentrations of GHGs (N_2O, CH_4 and N_2O) were analyzed using a GC analyzer connected to an autosampler (SRI 8610C, SRI Instruments, Torrance, USA), following the method described by Rehschuh et al. (2019). Fluxes of GHGs were calculated from the slope of the linear increase or decrease in the four concentrations measured during the closure time (t = 0, 15, 45 and 180 min). Gases flux rates (µg N_2O-N m^{-2} h^{-1}, mg CO_2-C m^{-2} h^{-1} and µg CH_4-C m^{-2} h^{-1}) were calculated according to the equations described by Scheer et al. (2014), and corrected for air temperature, atmospheric pressure, and the ratio of chamber volume to surface area.

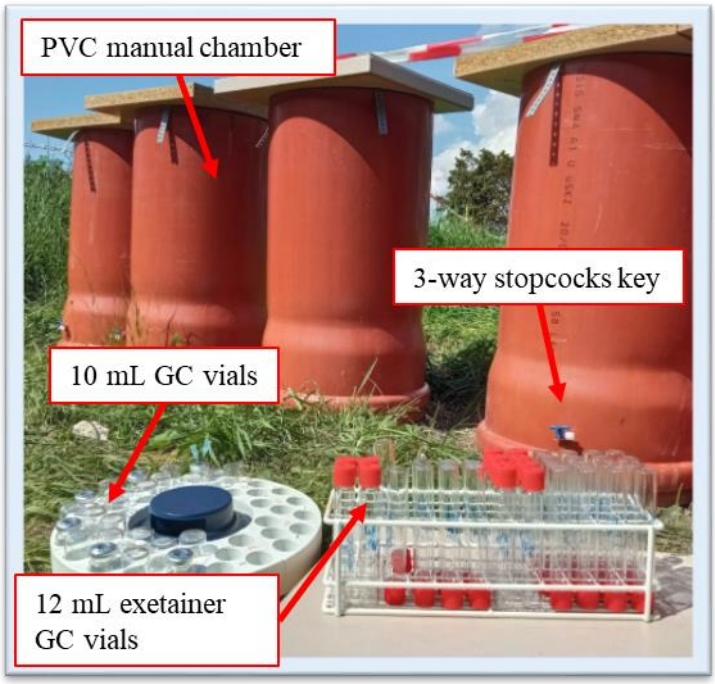

Figure 3.17. Manual static chambers used for greenhouse gas sampling at the IMK-IFU

3.3.2. $^{15}N_2O$ analysis in Experiments 1 and 3

In the microplots amended with a ^{15}N source ($^{15}NH_4NO_3$, ^{15}AN; $NH_4{}^{15}NO_3$, $A^{15}N$ or ^{15}N−enriched maize residues, ^{15}RES) in **Experiments 1** and **3**, on the same dates when GHGs were sampled, pre-evacuated 12 ml exetainer GC vials (Labco Limited, Lampeter, UK) were filled with gas samples from the headspace of the chambers at t = 0 min for one replicate of each treatment, and at t = 60 min closure time for every chamber.

The gas samples of **Experiment 1** were sent to Rothamsted Research (North Wyke, UK) to measure the ^{15}N enrichment of N_2O using a TG2 trace gas analyzer interfaced to a 20-22 isotope ratio mass spectrometer (IRMS) (both from SerCon Ltd., Crewe, UK).

The gas samples of the **Experiment 3** were sent to the stable isotope facility at the University of California (Davis, California, USA) to analyze the ^{15}N enrichment of N_2O using a Thermo Scientific GasBench + PreCon trace gas concentration system interfaced to a Thermo Scientific Delta V Plus IRMS (Bremen, Germany). Of all the gas samples taken during the experiment, only those that were considered most useful for understanding the dynamics of N_2O emissions were sent for ^{15}N analysis. For this purpose, the N_2O concentrations previously measured in the laboratory with the GC, as well as relevant agronomic events (e.g., the incorporation of cover crops, the start of maize irrigation, or the period after maize fertilization) were considered.

The equations used for calculating the different parameters related to $^{15}N_2O$ analysis are shown in Table 3.6. The N_2O in the headspace of the chamber was a mix of atmospheric N_2O at the time of chamber closure and the N_2O emitted from the soil. Equations 1 and 2 were used for calculating the ^{15}N abundance of emitted N_2O ($atom\ \%\ ^{15}N\text{–}N_2O_{em}$) considering the ^{15}N abundance of the headspace sample ($atom\ \%\ ^{15}N\text{–}N_2O_{mix}$) and the ambient air ($atom\ \%\ ^{15}N\text{–}N_2O_{air}$), and the N_2O concentrations of headspace samples (C_{mix}), the ambient air (C_{air}) and the emitted N_2O (C_{em}).

The atom % excess (*ape*) of the emitted N_2O ($ape\ ^{15}N_2O_{em}$), as well as that of the ^{15}AN ($ape\ ^{15}AN$) and $A^{15}N$ fertilizers ($ape\ A^{15}N$), and of the maize residue ($ape\ ^{15}RES$), were calculated according to Equations 3 and 4, by subtracting the 20 atom % or 10 atom % in the ^{15}AN and $A^{15}N$ fertilizers used in **Experiment 3** and **Experiment 1**, respectively (Campro Scientific), or to the 7.03 atom % in the maize residues used in **Experiment 3**.

The proportion of N_2O emitted derived from the ^{15}AN ($\%N_2O{-}N_{15AN}$) or A^{15}N fertilizers ($\%N_2O{-}N_{A15N}$), or from the ^{15}RES ($\%N_2O{-}N_{15RES}$) was calculated following Equation 5. The proportion of N_2O emitted derived from the fertilizer ($\%N_2O\text{-}N_{fert}$) was calculated by adding the $\%N_2O{-}N_{15AN}$ to the $\%N_2O{-}N_{A15N}$ (Eq. 6). Equations 7, 8 and 9 were used to calculate the proportion of N_2O emitted from soil endogenous N ($\%N_2O{-}N_{soil}$). Equation 7 was used in **Experiment 1**, while Equations 8 and 9 were used during P1 and P2 of **Experiment 3**, respectively. Note that soil endogenous N refers to all the N in the soil except for that derived from the applied ^{15}N–enriched sources (i.e., from the ^{15}N−labeled fertilizers in **Experiment 1**, and from the ^{15}N−labeled fertilizers together with the N from the ^{15}N−enriched maize residues in **Experiment 3**). Therefore, soil endogenous N includes the available mineral N at the beginning of the experiment from previous cropping season, N from the mineralization of SOM, and, in the case of **Experiment 3**, also N from cover crops residues mineralization and from biological N fixation.

The daily fluxes of $N_2O{-}N$ derived from the ^{15}AN fertilizer, from the A^{15}N fertilizer or from the ^{15}RES ($N_2O{-}N_{15AN}$, $N_2O{-}N_{A15N}$ or $N_2O{-}N_{15RES}$) were calculated according to Equation 10. The daily fluxes of $N_2O{-}N$ derived from the fertilizer ($N_2O\text{-}N_{fert}$) were calculated according to Equation 11. The daily fluxes of $N_2O{-}N$ derived from the endogenous soil N ($N_2O{-}N_{soil}$) during P1 and during P2 were calculated according to Equations 12, 13 and 14. Equation 15 explains the calculations of the N_2O EF following maize fertilization using the ^{15}N tracing technique.

Table 3.6. Equations for calculating parameters related to $^{15}N_2O$ analysis.

Parameter	Units	Equation	Eq. number	References
C_{em}	µL N_2O L^{-1}	$C_{em} = C_{mix} - C_{air}$	Eq. 1	Li et al. (2016) Xu et al. (2019)
$atom\ \%\ ^{15}N{-}N_2O_{em}$	%	$atom\ \%\ ^{15}N{-}N_2O_{em} = (atom\ \%\ ^{15}N{-}N_2O_{mix} \times C_{mix} - atom\ \%\ ^{15}N{-}N_2O_{air} \times C_{air})/C_{em}$	Eq. 2	
$ape\ ^{15}N_2O_{em}$	%	$ape^{15}N_2O_{em} = atom\ \%^{15}N{-}N_2O_{em} - atom\ \%^{15}N{-}N_2O_{air}$	Eq. 3	
$ape\ ^{15}AN$ $ape\ A^{15}N$ $ape\ ^{15}RES$	%	$ape^{15}AN$ (or $ape\ A^{15}N$ or $ape^{15}RES$) $= atom\ \%^{15}AN$ (or $atom\ \%\ A^{15}N$ or $atom\ \%^{15}RES$) $- atom\ \%^{15}N_{background}$	Eq. 4	
$\%N_2O{-}N_{15AN}$ $\%N_2O{-}N_{A15N}$ $\%N_2O{-}N_{15RES}$	%	$\%N_2O\text{-}N_{15AN}$ ($or\ \%N_2O\text{-}N_{A15N}\ or\ \%N_2O\text{-}N_{15RES}$) $= \left(\frac{ape\ ^{15}N_2O_{em}}{ape\ ^{15}AN\ (\text{or}\ ape\ A^{15}N\ \text{or}\ ape\ ^{15}RES)}\right) \times 100$	Eq. 5	
$\%N_2O{-}N_{fert}$	%	$\%N_2O\text{-}N_{fert} = \%N_2O\text{-}N_{15AN} + \%N_2O\text{-}N_{A15N}$	Eq. 6	
$\%N_2O{-}N_{soil}$	%	$\%N_2O\text{-}N_{soil} = 100 - \%N_2O\text{-}N_{fert}$ or $\%N_2O\text{-}N_{soil} = 100 - \%N_2O\text{-}N_{15RES}$ or $\%N_2O\text{-}N_{soil} = 100 - (\%N_2O\text{-}N_{fert} + \%N_2O\text{-}N_{15RES})$	Eq. 7 Eq. 8 Eq. 9	
$N_2O{-}N_{15AN}$ $N_2O{-}N_{A15N}$ $N_2O{-}N_{15RES}$	mg N m^{-2} d^{-1}	$N_2O\text{-}N_{15AN}$ (or $N_2O\text{-}N_{A15N}$ or $N_2O\text{-}N_{15RES}$) $= \frac{\%N_2O\text{-}N_{15AN}\ (\text{or}\ \%N_2O\text{-}N_{A15N}\ \text{or}\ \%N_2O\text{-}N_{15RES})}{100} \times N_2O\text{-}N_{total}$	Eq. 10	
$N_2O{-}N_{fert}$	mg N m^{-2} d^{-1}	$N_2O\text{-}N_{fert} = N_2O\text{-}N_{15AN} + N_2O\text{-}N_{A15N}$	Eq. 11	
$N_2O{-}N_{soil}$	mg N m^{-2} d^{-1}	$N_2O\text{-}N_{soil} = N_2O\text{-}N_{total} - N_2O\text{-}N_{fert}$ or $N_2O\text{-}N_{soil} = N_2O\text{-}N_{total} - N_2O\text{-}N_{15RES}$ or $N_2O\text{-}N_{soil} = N_2O\text{-}N_{total} - (N_2O\text{-}N_{fert} + N_2O\text{-}N_{15RES})$	Eq. 12 Eq. 13 Eq. 14	
EF	%	$EF = (\frac{total\ N_2O{-}N_{fert}}{total\ N_{fert}}) \times 100$	Eq. 15	

'C_{mix}' is the concentration of the total N_2O (µL N_2O L^{-1}) in the chamber headspace at t = 60 min at each sampling date.

'C_{em}' is the concentration of the emitted N_2O (µL N_2O L^{-1}) in the chamber headspace at t = 60 min at each sampling date.

'C_{air}' is the concentration of the atmospheric air N_2O (µL N_2O L^{-1}) in the chamber headspace at t = 0 min at each sampling date.

*'**atom % ^{15}N-N_2O_{em}**'* is the ^{15}N abundance of the emitted N_2O after 60 min chamber closure at each sampling date.

'atom % ^{15}N-N_2O_{mix}' is the ^{15}N abundance of the N_2O in the chamber headspace at t = 60 min at each sampling date.

'atom % ^{15}N-N_2O_{air}' is the average ^{15}N abundance of N_2O in the chamber headspace at t = 0 min at each sampling date.

'ape $^{15}N_2O_{em}$' is the atom % ^{15}N excess of the emitted N_2O after 60 min chamber closure at each sampling date.

'ape ^{15}AN'*, *'ape $A^{15}N$' and ***'ape ^{15}RES'*** are the atom % ^{15}N excess of the $^{15}NH_4NO_3$ (^{15}AN), $NH_4{}^{15}NO_3$ ($A^{15}N$) and ^{15}N-enriched maize residues (^{15}RES), respectively.

'%N_2O-N_{15AN}', '%N_2O-N_{A15N}' and ***'%N_2O-N_{15RES}'*** are the proportion of N_2O derived from the ^{15}AN fertilizer, from the $A^{15}N$ fertilizer and from the ^{15}RES, respectively.

'N_2O-N_{15AN}', 'N_2O-N_{A15N}' and *'**N_2O-N_{15RES}'*** are the daily fluxes of N_2O derived from the ^{15}AN fertilizer, from the $A^{15}N$ fertilizer and from the ^{15}RES measured in the chamber headspace at each sampling date, respectively.

'N_2O-N_{total}' is the daily flux of the total N_2O measured in the chamber headspace at each sampling date.

'EF' is the fertilizer N_2O emission factor.

'Total N_2O-N_{fert}' is the cumulative N_2O emissions derived from the applied fertilizer (kg N ha^{-1}).

'Total N_{fert}' is the fertilizer N rate (kg N ha^{-1}). The N fertilization rate was 80 kg N ha^{-1} and 210 kg N ha^{-1} in **Experiment 1** and **3**, respectively.

The atom % of the ^{15}AN and $A^{15}N$ fertilizers used in **Experiment 1** and **Experiment 3** were 10% and 20%, respectively.

The atom % of the ^{15}RES used in **Experiment 3** was 7.03%.

The atom % of the air background used for calculating the *ape ^{15}AN*, *ape $A^{15}N$* and *ape ^{15}RES* was 0.3667%.

3.3.3. ^{15}N gas flux method in Experiment 4

The ^{15}NGF method was used to quantify N_2 losses from the fertilizer as described in detail by Dannenmann et al. (2024) and Yankelzon et al. (2024). Pre-evacuated 12 mL Labco exetainer GC vials were filled with gas samples taken from the chamber headspace of mesocosms of set M1 (Figure 3.10) at the same closure times as for GHGs measurement (i.e., 0, 15, 45 and 180 min after chamber close) using 20 mL syringes. These vials were analyzed for N_2 and N_2O isotopologues ($^{15}N^{14}N$, $^{15}N^{15}N$; [$^{14}N^{15}N^{16}O$ + $^{15}N^{14}N^{16}O$] and $^{15}N^{15}N^{16}O$) using an Isoprime PrecisION IRMS (Elementar UK Ltd. Stockport, UK), coupled to an iso FLOW GasBench (Elementar UK Ltd. Stockport, UK).

Emissions of N_2 were calculated using the ^{15}NGF method (Friedl et al., 2020). Briefly, measurements of the ion currents (I) via IRMS at the mass-to-charge ratios (m/z) 44, 45, and 46 enabled the molecular ratios ^{45}R ($^{45}I/^{44}I$) and ^{46}R ($^{46}I/^{44}I$) to be calculated for N_2O. The I at m/z 28, 29, and 30 allowed the molecular ratios ^{29}R ($^{28}I/^{29}I$) and ^{30}R ($^{28}I/^{30}I$) to be calculated for N_2. Assuming that all N_2 and N_2O produced by denitrification originate from the same pool of NO_3^-, the ^{15}N enrichment of the soil NO_3^- pool undergoing denitrification (a_p N_2 and a_p N_2O) and the fraction of N_2O and N_2 emitted from this pool (f_p) were calculated according to Friedl et al. (2023) and Spott et al. (2006). Furthermore, a_p N_2O was used to calculate N_2 fluxes (Stevens and Laughlin, 2001).

The headspace concentrations of N_2O and N_2 were multiplied by the respective f_p values giving N_2O and N_2 produced via denitrification (referred to as N_2 and N_2O_d), with their respective fluxes expressed in g N_2 or N_2O_d–N emitted g^{-1} soil day^{-1}. Emissions of N_2O derived from nitrification mediated pathways (N_2O_n) were calculated as the difference between daily N_2O emissions and N_2O_d.

The precision of the IRMS for N_2 based on the standard deviation of atmospheric air samples (n = 18) at 95% confidence interval (Friedl et al., 2020) was 1.2×10^{-6} and 2.4×10^{-7} for ^{29}R and ^{30}R, respectively. The corresponding method detection limit ranged from 14 g N_2–N ha^{-1} day^{-1} with a_p assumed at 60 atom % to 24 g N_2–N ha^{-1} day^{-1} with a_p assumed at 35 atom %. The product ratio of denitrification ($N_2O_d/(N_2O_d + N_2)$) was used to calculate N_2 fluxes, if both ^{29}R and ^{30}R were below the respective precision of the IRMS. Calculated $N_2O_d/(N_2O_d + N_2)$ ratios were gap filled using linear interpolation between calculated ratios for the respective chambers, and if that was not possible, by using the average across calculated ratios for the respective day. Product ratios were then used to calculate N_2 fluxes using the corresponding N_2O_d fluxes.

The percentage of fertilizer losses via N_2 emissions was calculated as the ratio of ^{15}N atom excess % of N_2 emitted and the ^{15}N atom excess % of the N fertilizer applied and multiplying it per 100.

3.4. Soil sampling, analysis and calculations

In **Experiments 1 – 3**, samples of the topsoil (0-10 cm depth) were taken using stainless steel cores (4.5 cm diameter, 10 cm length) to analyze soil mineral N, dissolved organic C (DOC) and for calculating the WFPS throughout the experiments. Samples were taken at least once a month, with the sampling frequency being increased up to 2-3 times per week after fertilizer application, irrigation, or agricultural management events such as cover crops incorporation (see the sampling frequency for **Experiment 1**, **Experiment 2**, and **Experiment 3** in Table 3.2, Table 3.3, and Table 3.4, respectively). Soil samples were stored at -20 ºC when the mineral N and/or DOC extractions were not performed immediately after soil was brought to the laboratory.

In **Experiment 4**, the topsoil (0 – 15 cm) of the mesocosms of set M2 (Figure 3.10 in Section 3.2.4) was sampled using a stainless core (3 cm diameter × 15 cm length) the day before first fertilization to calculate the background mineral N content, and the day before and two days after every fertilization and irrigation event (Table 3.5). Soil samples were brought to the laboratory and extracted for mineral N analysis and WFPS determination immediately after sampling.

3.4.1. Mineral N

In **Experiments 1 – 3**, mineral N (NH_4^+-N and NO_3^--N) was extracted from fresh homogenized soil samples using 1 M potassium chloride, KCl, (1:6.25, w:v) for 1 h at 180 rpm, centrifuged for 10 min at 4000 rpm, and then filtered using 0.45 µm cellulose syringe filters (Agilent). After that, soil extracts were frozen at −20ºC until being analyzed. The mineral N concentration in soil extracts was determined using a flow injection analyzer provided with a UV–vis spectrophotometer detector (FIAS 400, Perkin Elmer and SFA FUTURA, AMS Alliance for NH_4^+ and NO_3^- analyses, respectively). Ammonium determination in the soil extracts was performed by gaseous diffusion of NH_4^+ previously transformed into NH_3(g) in an alkaline medium. The NH_3(g) was defunded through a permeable membrane and reacted with an acid–base indicator, being detected by the spectrophotometer at λ = 590 nm (PerkinElmer, 2001). The NO_3^- in soil extracts was previously reduced to NO_2^- with vanadium chloride (VCl_3), then reacted with sulphanilamide and an aromatic amine and was transformed into a chromophore aromatic species that is detected at λ = 540 nm (Miranda et al., 2001).

In **Experiment 4**, fresh soil samples were homogenized removing the roots and extracted with 1 M KCl solution in a 1:2 soil:extractant ratio. Following extraction, the samples were filtered using a vacuum pump and porcelain funnels with Whatman GF/A filters with a second filtration step to 0.45 µm using syringe filters and were stored at -20 °C until further analyses.

Concentrations of NH_4^+ and NO_3^- in the extracts were determined using colorimetric methods and measuring the absorbance of the samples using a microplate UV-vis spectrometer analyzer (Epoch, BioTek Inc., USA). The reactions with the Griess reagent were used to analyze the NO_3^--N concentration (Patton and Kryskalla, 2011) and the indophenol method was used to analyze the NH_4^+-N concentration (Bolleter et al., 1961) in the extracts.

3.4.2. $^{15}NH_4^+$ and $^{15}NO_3^-$

The microdiffusion technique described by Hart and Stark (1994) was carried out with some modifications to analyze the ^{15}N enrichment in soil mineral N of **Experiment 1**. The microdiffusion technique consists of the sequential diffusion of NH_3 coming from both NH_4^+ and NO_3^-. Soil samples taken at field were immediately extracted at the laboratory for mineral N as described in Section 3.4.1. Soil extracts were filtered using Filter-Lab 1250 cellulose filters previously washed with 1 M KCl. Stainless steel wire pieces (60 mm length) covered with plastic were placed on 100 ml specimen cup lids. Pieces of Whatman no. 3 cellulose filters (0.6 cm^2) were attached to the wire. Filter pieces were humidified with 20 µl 1.5 M sulfuric acid (H_2SO_4). To separately liberate the NH_4^+–N and the NO_2^-+NO_3^-–N in the form of NH_3, two sequential diffusion were carried out. 40 mL aliquots of KCl soil extracts were placed in 100 ml plastic containers. Then, two glass beads (4 mm in diameter) previously acid-washed with 0.5–1.0 M hydrochloric acid (HCl) and gently rinsed with deionized water, were incorporated into the specimen cups to promote further swirling process. For carrying out the first diffusion, 0.2 g magnesium oxide (MgO) was added, and the specimen cups were immediately closed. MgO makes the solution basic causing NH_3 vapor to be released and subsequently captured on the acidified filter piece. After 7 days of incubation at room temperature (under 25ºC to avoid water condensing on the cup taps) (Bremner, 1965) and gently swirling the solution two or three times a day, the filter papers and the wires were removed and replaced with new ones. For

carrying out the second diffusion, 0.4 g Devarda's alloy and 0.2 g MgO were added to the soil extracts and the containers were immediately closed. The extracts were incubated for 7 days under the same conditions described above. The filter pieces from both diffusion steps were dried overnight after every incubation by placing the taps with the wires and the filter pieces in a desiccator over concentrated H_2SO_4. Dried filter papers were stored in 1.5 mL Eppendorf tubes and sent to the Interdepartmental Investigation Service at Universidad Autónoma of Madrid (SIdI-UAM) for total N and ^{15}N analysis through combustion of samples using an elemental analyzer Thermo 1112 Flash HT hyphenated to an IRMS Thermo Delta V Advantage.

To determine how much NH_4^+–N or NO_3^-–N in the soil came from the fertilizer or from the soil, the following equations (Eq. 16 and Eq. 17) were used:

$$NH_4^+\text{-}N_{15AN}\ (or\ NH_4^+\text{-}N_{A15N}) = Total\ NH_4^+\text{-}N \times \left(\frac{ape\ ^{15}N_{filter}}{ape\ ^{15}N_{fert}}\right) \quad \text{Eq. 16}$$

$$NH_4^+\text{-}N_{soil} = Total\ NH_4^+\text{-}N - \left(NH_4^+\text{-}N_{15AN}\right) - \left(NH_4^+\text{-}N_{A15N}\right) \quad \text{Eq. 17}$$

where 'NH_4^+-N_{15AN}' (or NH_4^+-N_{A15N}) is the NH_4^+-N in the soil that was derived from ^{15}AN or A^{15}N fertilizer (kg N ha^{-1}), respectively. The '*Total* NH_4^+-*N*' is the concentration of NH_4^+-N total in soil obtained from the results of the first microdiffusion. The '*ape* $^{15}N_{filter}$' was obtained by subtracting the background atom % ^{15}N (0.3663 atom % ^{15}N) from the atom % ^{15}N in the filters of the first microdiffusion. Similar calculations were carried out to obtain 'NO_3^--N_{15AN}', 'NO_3^--N_{A15N}', and 'NO_3^--N_{soil}' using the results obtained in the second microdiffusion. For these calculations, '*Total* NO_3^--*N*' is the concentration of NO_3^--N in soil obtained by the results from the second microdiffusion.

3.4.3. Dissolved organic C

The DOC was extracted from fresh homogenized topsoil samples (8 g soil: 50 mL Milli-Q water) for 1 hour at 180 rpm and then centrifuged for 10 min at 4000 rpm and filtered (Filterlab

1300/800). After that, 40 mL of soil extracts were frozen at −20ºC until being analyzed. Quantification of DOC was performed by a total organic carbon analyzer (Analytik Jena multi N/C 3100) equipped with an infrared detector.

3.4.4. Water-filled pore space

The WFPS in soil samples was calculated according to Equation 18:

$$WFPS\ (\%) = \frac{H\ \times\ Db}{1 - \frac{Db}{Dp}} \times\ 100 \qquad \text{Eq. 18}$$

where '*H*' is the gravimetric water content in dry basis, '*Db*' is the soil bulk density, and '*Dp*' is the soil particle density, assumed to be 2.65 g cm^{-3}. The gravimetric water content was determined by oven-drying 5 g fresh soil samples for 24h at 105ºC. The bulk density was determined by taking soil samples at different depths using 100 cm^3 stainless steel cores and oven-drying the samples for 24h at 105ºC.

3.4.5. Total N and ^{15}N

At the end of **Experiments 1** and **3**, soil was sampled at three depths using a stainless-steel auger: 0−10, 10−20, and 20−40 cm in **Experiment 1,** and 0−20, 20−40, and 40−60 cm in **Experiment 3**. At the laboratory, fresh soil samples were homogenized and then separated into two subsamples. One subsample was stored at −20 °C for mineral N analysis according to the protocol described in Section 3.4.1. The other subsample was air-dried, ground using a ball mill (Retsch MM 400, Retsch GmbH, Haan, Germany), and the total N and ^{15}N contents were analyzed by IRMS at SIdI-UAM.

At the end of **Experiment 4**, the mesocosms from set M1 (Figure 3.10) were dug, and the soil columns were pulled out the PVC cylinders, separated into three layers using a saw (depths 0−5 cm, 5−15 cm, and 15−40 cm), and weighted to determine the bulk density of each layer. After

taking representative samples of the belowground biomass (see Section 3.5.4), the soil from each layer was homogenized by hand in a bucket for at least 10 minutes. After that, two representative soil samples from each mesocosms layer were taken. One sample was oven-dried at 105 °C for 24 h to determine the gravimetric soil water content needed to calculate the bulk density. The other sample was oven-dried at 60 °C to constant weight to determine the total soil N and the total soil ^{15}N enrichment. Dry soil samples were homogenized, and representative subsamples were ground to a fine powder using a ball mill (Retsch Schwingmühle MM2, Haan, Germany) and stored in a desiccator over silica gel until total N and ^{15}N contents were analyzed by elemental analysis (Flash EA, Thermo Scientific, Waltham, MA, USA) coupled to IRMS (Delta PlusXP, Thermo Scientific, Waltham, MA, USA) at the IMK-IFU stable isotopes laboratory (Yankelzon et al., 2024).

3.5. Plant sampling, analysis and calculations

3.5.1. Experiment 1

Barley plants (shoot and root systems) were sampled using a 0.25 m^2 frame, which was placed in the middle of each microplot. The shoot system was cut by sickle at the soil level and was separated into spikes (that were threshed out to obtain the grain) and stems (aboveground biomass). Roots were cleaned with a brush, rinsed thoroughly with tap water (5 min) to separate soil from roots, and washed in an ultrasound-assisted bath for 15 min with tap water followed by 5 min with deionized water (García-Gómez et al., 2015). The aboveground biomass (straw and grain) and roots were oven-dried to a constant weight at 75 °C, ground using a ball mill (Retsch MM 400, Retsch GmbH, Haan, Germany), and stored at room temperature until total N and ^{15}N content were analyzed by IRMS at the SIdI-UAM.

3.5.2. Experiment 2

Before barley and vetch cover crops were chemically terminated, the aboveground biomass was sampled and fresh-weighed in the field. The samples taken from each subplot consisted of a representative mixture of three subsamples, collected using a 0.25 m^2 frame. In the laboratory, dry biomass production was determined by oven-drying the samples at 70 °C until constant weight. The dry samples were then ground (IKA® MF 10 Basic Microfine Grinder Drive) to analyze the N and C contents, using an elemental analyzer (TruMac CN Leco®) and applying the Dumas method (AOAC, 2005).

At physiological maturity, aboveground maize biomass was harvested by collecting fifteen maize plants randomly in every subplot. The aboveground biomass was weighed at harvest. To determine dry matter grain and stover (aboveground biomass without grain) yields, the stover and grain moisture were determined after over-drying plant samples at 70 °C. Maize grain and stover were ground (IKA® M 20 universal mill and IKA® MF 10 Basic Microfine Grinder Drive, respectively), and the total N concentration was analyzed by Kjeldahl digestion. The NUE was calculated as the apparent recovery efficiency of applied N, using the following equation (Eq. 19) by Congreves et al. (2021):

$$NUE = \frac{(U_N - U_0)}{F_N} \qquad \text{Eq. 19}$$

where 'U_N' represents the total N uptake in the aboveground biomass at maturity with applications of N fertilizer; 'U_0' is the total N uptake in the aboveground biomass at maturity without applications of N fertilizer; and 'F_N' is the amount of N fertilizer applied (170, 220, and 210 kg N ha^{-1}, for legume, cereal, and bare fallow plots, respectively).

3.5.3. Experiment 3

Aboveground biomass samples of barley and vetch cover crops grown in the initial microplots with ^{15}N–enriched maize residues (^{15}RES) were harvested using a 0.096 m^2 frame, leaving the remaining biomass in the microplots for their chemical termination. Furthermore, representative roots samples from the cover crops in the ^{15}RES microplots were collected. At the laboratory, the rhizosphere soil was separated from the roots. The roots were then rinsed with tap water for 5 min and washed in an ultrasound-assisted bath for 10 min using deionized water (García-Gómez et al., 2015). All plant material was oven-dried at 70 ºC for 48 h and ground using a ball mill (Retsch MM 400, Retsch GmbH, Haan, Germany). The aboveground biomass yield was calculated based on the 0.096 m^2 frame area used for harvesting, while the root biomass yield was estimated according to Hu et al. (2018). The total C content in the aboveground biomass of the cover crops was determined by the Dumas method using an elemental analyzer (TruMac CN Leco®, USA).

Maize was harvested at physiological maturity. The aboveground biomass of the six plants in every microplots was fresh weighted in the field. To estimate the crop yield on a dry basis, the stover and grain moisture content was determined by oven-drying subsamples at 70 ºC until constant weight. The aboveground biomass (stover and grain) of the four central plants and the root and rhizosphere soil of one of the central plants of every microplot were used for analyzing the total N and ^{15}N content. After separating the rhizosphere soil from the roots, the roots were cleaned following the same procedure described above for the cover crop roots and then were oven-dried at 70 ºC for 48 h.

The total N and ^{15}N content in the cover crops (aboveground and belowground biomass) and in maize (roots, grain and stover) samples were analyzed by IRMS at the SIdI-UAM.

3.5.4. Experiment 4

One month after the first fertilization, both aboveground and belowground biomass (AGB and BGB, respectively) of the six mesocosms receiving ^{15}N fertilizer (set M1) were sampled. The AGB was harvested by cutting the grass directly above the soil with scissors. After digging out the mesocosms, representative BGB samples from the first two layers were taken using 95 cm^3 stainless steel soil sampling cores. The roots in these cores were separated from the soil by rinsing the samples with tap water using a 0.5 mm mesh sieve. The ABG and BGB were oven-dried at 60 °C to constant weight immediately after sample preparation and weighted for determining the biomass yield. Plant samples were homogenized, and representative subsamples were ground into a fine powder using a ball mill (Retsch Schwingmühle MM2, Haan, Germany), then stored in a desiccator over silica gel until total N and ^{15}N contents were analyzed by elemental analysis coupled to IRMS at the IMK-IFU stable isotopes laboratory (Yankelzon et al., 2024).

3.6. Mineral N leaching

In **Experiment 4**, mineral N (NH_4^+ + NO_3^-) leaching was determined from accumulation of NH_4^+ and NO_3^- on resin bags (Dannenmann et al., 2018). For this purpose, 30 cm diameter polyester bags containing 300 g anion exchange resin (AmberChrom™ 1X8 50-100 Mesh [Cl^--ion exchanger resin], Sigma Aldrich) and 300 g cation exchange resin (Amberlite™ IRC120 [Na^+-ion exchanger resin], Thermo Scientific Chemicals) were placed at the bottom of three mesocosms of set M1 (Figure 3.10 in Section 3.2.4) before applying the ^{15}N–enriched fertilizer solution. These bags were harvested at the end of the experiment to analyze the N leaching from the ^{15}N–enriched fertilizer. The resin bags were rinsed in the laboratory with distilled water to remove the soil particles adsorbed to the fabric bags and then the resin beads were extracted with 500 mL 1M NaCl by shaking for 30 min at 160 rpm. The resin extracts were filtered and

analyzed for mineral N in following the same steps described in Section 3.4.1 of this chapter. The NH_4^+ and NO_3^- of the resin extracts were sequentially trapped on acidified filter papers following the diffusion technique used in **Experiment 1** (Section 3.4.2) with the specifications described by Dannenmann et al. (2016) and Schreiber et al. (2023). Briefly, the resin extracts were placed in 250 mL Duran glass bottles. In each step of the diffusion, two pieces of pin-holed Whatman ash less paper filter were acidified with 10 µL of 1 M oxalic acid each (instead of 1.5 M H_2SO_4) and placed on a hook of a custom-made cap. In each step of the diffusion, the samples were shaken on a rotary shaker for 24 h at 30 ºC. For increasing the pH of the solution, N-free NaOH pellets were used instead of MgO. After harvesting the filters, they were placed into micro titer plates and dried by storing the plates in desiccators over silica gel. After drying, the filters were transferred into tin capsules. Total N and total ^{15}N in the filters were analyzed via elemental analysis (Flash EA, Thermo Scientific, Waltham, MA, USA) coupled to IRMS (Delta PlusXP, Thermo Scientific, Waltham, MA, USA) in the stable isotopes laboratory at the IMK-IFU to calculate the mineral N leaching from the fertilizer.

3.7. N recovery

3.7.1. Experiments 1 and 3

The equations used for calculating the N recovery in the soil at the end of **Experiment 1** and **Experiment 3** are shown in Table 3.8.

The recovery of N from the fertilizer in soil at the end of the experiment ($soil\_NR_{fert}$) was calculated according to Equation 25. For that, the soil N concentration derived from both the ^{15}AN fertilizer ($soil\_N_{15AN}$) and the $A^{15}N$ fertilizer ($soil\_N_{A15N}$) in the different soil layers, as well as the total soil N concentration derived from the fertilizer NH_4NO_3 ($soil\_N_{fert}$), were calculated according to Equations 20 – 24. Furthermore, the soil N recovery from the ^{15}AN

fertilizer (*soil_NR$_{15AN}$*) and from the A^{15}N fertilizer (*soil_NR$_{A15N}$*) were calculated using Equations 26 and 27, respectively. The amount of N in the different soil layers *(soil_TN*, kg N ha^{-1}) was calculated by multiplying the N content (%) of each soil layer by its bulk density measured at the end of the experiments (Table 3.7) and by the soil thickness of each layer.

Table 3.7. Bulk density of soil samples at different depths at the end of Experiment 1 and Experiment 3.

Experiment 1		**Experiment 3**	
Soil layer (cm)	Bulk density (g cm^{-3})	Soil layer (cm)	Bulk density (g cm^{-3})
0-10	1.15 ± 0.02	0-20	1.46 ± 0.07
10-20	1.30 ± 0.09	20-40	1.52 ± 0.03
20-40	1.43 ± 0.01	40-60	1.55 ± 0.01

Data are expressed as the mean (n = 3) ± S.E.

Table 3.8. Equations for calculating parameters related to ^{15}N analysis in soil

Parameter	Units	Equation	Equation number	References
Soil_TN$_{15AN}$	kg N ha^{-1}	$soil\_TN_{15AN} = soil(1st\ layer)\_TN_{15AN} + soil(2nd\ layer)\_TN_{15AN} + soil(3rd\ layer)\_TN_{15AN}$	Eq. 20	Taveira et al. (2020)
Soil (1st layer)_TN$_{15AN}$ *Soil (2nd layer)_TN$_{15AN}$* *Soil (3rd layer)_TN$_{15AN}$*	kg N ha^{-1}	$soil\ layer\_TN_{15AN} = \frac{soil\ layer\_ape^{15}N_{15AN}}{ape^{15}AN} \times soil\ layer\_N\ amount$	Eq. 21	
Soil_TN$_{A15N}$	kg N ha^{-1}	$soil\_TN_{A15N} = soil(1st\ layer)\_TN_{A15N} + soil(2nd\ layer)\_TN_{A15N} + soil(3rd\ layer)\_TN_{A15N}$	Eq. 22	
Soil (1st layer)_TN$_{A15N}$ *Soil (2nd layer)_TN$_{A15N}$* *Soil (3rd layer)_TN$_{A15N}$*	kg N ha^{-1}	$soil\ layer\_TN_{A15N} = \frac{soil\ layer\_ape^{15}N_{A15N}}{ape\ A^{15}N} \times soil\ layer\_N\ amount$	Eq. 23	
Soil_TN$_{fert}$	kg N ha^{-1}	$soil\_TN_{fert} = soil\_TN_{15AN} + soil\_TN_{A15N}$	Eq. 24	
Soil_NR$_{fert}$	%	$soil\_NR_{fert} = \frac{soil\_TN_{fert}}{total\ N_{fert}} \times 100$	Eq. 25	
Soil_NR$_{15AN}$	%	$soil\_NR_{15AN} = \frac{soil\_TN_{15AN}}{NH_4^+ - N_{fert}} \times 100$	Eq. 26	
Soil_NR$_{A15N}$	%	$soil\_NR_{A15N} = \frac{soil\_TN_{A15N}}{NO_3^- - N_{fert}} \times 100$	Eq. 27	

'Soil_N_{15AN}' and ***'Soil_N_{A15N}'*** are the N content (kg N ha^{-1}) in soil derived from the $^{15}NH_4NO_3$ (^{15}AN) fertilizer and from the $NH_4{}^{15}NO_3$ ($A^{15}N$) fertilizer.

'Soil_N_{fert}' is the total N content (kg N ha^{-1}) in soil derived from the fertilizer.

'Soil *(1st layer)_N_{15AN}*', 'Soil *(2nd layer)_N_{15AN}*' and **'Soil *(3rd layer)_N_{15AN}*'** are the N contents (kg N ha^{-1}) in the different soil layers derived from the ^{15}AN fertilizer.

'Soil *(1st layer) N_{A15N}*', 'Soil *(2nd layer)_N_{A15N}*' and **'Soil *(3rd layer)_N_{A15N}*'** are the N contents (kg N ha^{-1}) in the different soil layers derived from the $A^{15}N$ fertilizer.

'Soil layer_TN amount' is the total N amount (kg N ha^{-1}) in the different soil layers.

'*Soil_NR_{fert}*', '*Soil_NR_{15AN}*' and **'*Soil_NR_{A15N}*'** are the recoveries of N (%) derived from the NH_4NO_3 fertilizer, from the NH_4^+−N in the fertilizer, and from the NO_3^-−N in the fertilizer.

'Total N_{fert}' is the fertilizer N rate (kg N ha^{-1}). The N rate was 80 kg N ha^{-1} and 210 kg N ha^{-1} in **Experiments 1 and 3**, respectively.

'*NH_4^+−N_{fert}*' and **'*NO_3^-−N_{fert}*'** are the kg N ha^{-1} applied as NH_4^+ and NO_3^- (40 kg N ha^{-1} and 105 kg N ha^{-1} in **Experiment 1** and **Experiment 3**, respectively).

Depth of the different soil layers in **Experiment 1**: 1st layer, 0 – 10 cm; 2nd layer, 10 – 20 cm; 3rd layer, 20 – 40 cm.

Depth of the different soil layers in **Experiment 3**: 1st layer, 0 – 20 cm; 2nd layer, 20 – 40 cm; 3rd layer, 40 – 60 cm.

The atom % of the ^{15}AN and $A^{15}N$ fertilizers used in **Experiment 1** and **Experiment 3** were 10% and 20%, respectively.

The atom % of the air background used for calculating the *ape ^{15}AN* and *ape $A^{15}N$* was 0.3667%.

The equations used for calculating the N recovery in the plants in **Experiment 1** and **Experiment 3** are shown in Table 3.9.

The recovery of N from the fertilizer (*plant_NR$_{fert}$*) was calculated according to Equation 35. For that, the N uptake derived from both the ^{15}AN fertilizer (*plant_N$_{15AN}$*) and the A^{15}N fertilizer (*plant_N$_{A15N}$*) in the different plant tissues, and the total N uptake derived from the fertilizer NH_4NO_3 (*plant_N$_{fert}$*), were calculated (Eq. 30 – Eq. 34). Furthermore, the plant N recovery from the ^{15}AN fertilizer (*plant_NR$_{15AN}$*) and from the A^{15}N fertilizer (*plant_NR$_{A15N}$*) were calculated using Equations 36 – 37.

The recovery of N from the ^{15}N–enriched maize residue (*plant_NR$_{15RES}$*) was calculated according to Equation 40. For that, the N uptake derived from the ^{15}RES (*plant_N$_{15RES}$*) (Eq. 38) was calculated considering the N uptake derived from the ^{15}RES in the different plant tissues (*plant tissue_N$_{15RES}$*) (Eq. 39)

The total N uptake in the different plant tissues (*TN uptake*, kg N ha^{-1}) was calculated as shown in Equation 28:

$$TN\ uptake = (N\ content\ \times Yield)/100 \qquad \text{Eq. 28}$$

Where '*N content*' is the percentage of N in each plant tissue and '*Yield*' is expressed as kg plant tissue ha^{-1} in dry weight.

The total N recovery from the fertilizer (*total_NR$_{fert}$*) was calculated according to Equation 29:

$$total\_NR_{fert} = plant\_NR_{fert}\ + soil\_NR_{fert} \qquad \text{Eq. 29}$$

Table 3.9. Equations for calculating parameters related to ^{15}N analysis in plant.

Parameter	Units	Equation	Equation number	References
Plant_N_{15AN}	kg N ha^{-1}	$plant\_N_{15AN} = \sum plant\ tissues\_N_{15AN}$	Eq. 30	Taveira et al. (2020)
Plant tissue_N_{15AN}	kg N ha^{-1}	$plant\ tissue\_N_{15AN} = \frac{plant\ tissue\_ape^{15}N_{15AN}}{ape^{15}AN} \times plant\ tissue\_TN\ uptake$	Eq. 31	
Plant_N_{A15N}	kg N ha^{-1}	$plant\_N_{A15N} = \sum plant\ tissues\_N_{A15N}$	Eq. 32	
Plant tissue_N_{A15N}	kg N ha^{-1}	$plant\ tissue\_N_{A15N} = \frac{plant\ tissue\_ape^{15}N_{A15N}}{ape\ A^{15}N} \times plant\ tissue\_TN\ uptake$	Eq. 33	
Plant_N_{fert}	kg N ha^{-1}	$plant\_N_{fert} = plant\_N_{15AN} + plant\_N_{A15N}$	Eq. 34	
Plant_NR_{fert}	%	$plant\_NR_{fert} = \frac{plant\_N_{fert}}{total\ N_{fert}} \times 100$	Eq. 35	
Plant_NR_{15AN}	%	$plant\_NR_{15AN} = \frac{plant\_N_{15AN}}{NH_4^+ - N_{fert}} \times 100$	Eq. 36	
Plant_NR_{A15N}	%	$plant\_NR_{A15N} = \frac{plant\_N_{A15N}}{NO_3^- - N_{fert}} \times 100$	Eq. 37	
Plant_N_{15RES}	kg N ha^{-1}	$plant\_N_{15RES} = \sum plant\ tissues\_N_{15RES}$	Eq. 38	
Plant tissue_N_{15RES}	kg N ha^{-1}	$plant\ tissue\_N_{15RES} = \frac{plant\ tissue\_ape^{15}N_{15RES}}{ape^{15}RES} \times plant\ tissue\_TN\ uptake$	Eq. 39	
Plant_NR_{RES}	%	$plant\_NR_{RES} = \frac{plant\_N_{15RES}}{total\ N_{RES}} \times 100$	Eq. 40	

*Plant tissues in **Experiment 1**: barley straw, grain and roots.*

*Plant tissues in **Experiment 3**: maize stover, grain and roots.*

'Plant_N_{15AN}', 'Plant_N_{A15N}' and ***'Plant_N_{15RES}'*** are the N uptake (kg N ha^{-1}) in plant derived from the $^{15}NH_4NO_3$ (^{15}AN) fertilizer, from the $NH_4{}^{15}NO_3$ ($A^{15}N$) fertilizer and from the ^{15}N−enriched maize residue (^{15}RES).

'Plant_N_{fert}' is the total N uptake (kg N ha^{-1}) in plants derived from the fertilizer.

'*Plant tissue_N_{15AN}*' is the N uptake (kg N ha^{-1}) in the different plant tissues (i.e., barley straw, grain and root in **Experiment 1** and maize stover, grain and root in **Experiment 3**) derived from the ^{15}AN fertilizer.

'*Plant tissue_N_{A15N}*' is the N uptake (kg N ha^{-1}) in the different plant tissues (i.e., barley straw, grain and root in **Experiment 1** and maize stover, grain and root in **Experiment 3**) derived from the $A^{15}N$ fertilizer.

'*Plant tissue_N_{15RES}*' is the N uptake (kg N ha^{-1}) in maize stover, grain and root derived from the ^{15}RES in **Experiment 3**.

'*Plant tissue_TN uptake*' is the total N uptake (kg N ha^{-1}) in the different plant tissues (i.e., barley straw, grain and root in **Experiment 1** and maize stover, grain and root in **Experiment 3**).

'*Plant_NR_{fert}*', '*Plant_NR_{15AN}*', '*Plant_NR_{A15N}*' and **'*Plant_NR_{15RES}*'** are the recoveries of N (%) derived from the NH_4NO_3 fertilizer, from the $NH_4{}^+$−N in the fertilizer, from the $NO_3{}^-$−N in the fertilizer and from the N in the ^{15}N−enriched maize residue.

'Total N_{fert}' is the fertilizer N rate (kg N ha^{-1}). The N fertilization rate was 80 kg N ha^{-1} and 210 kg N ha^{-1} in **Experiment 1** and **Experiment 3**, respectively.

'Total N_{RES}' is the N rate applied via maize residue incorporation in **Experiment 3** (100 kg N ha^{-1}).

'*$NH_4{}^+$−N_{fert}*' and **'*$NO_3{}^-$−N_{fert}*'** are the kg N ha^{-1} applied as $NH_4{}^+$ and $NO_3{}^-$ (40 kg N ha^{-1} and 105 kg N ha^{-1} in **Experiment 1** and **Experiment 3**, respectively).

The atom % of the ^{15}AN and $A^{15}N$ fertilizers used in **Experiment 1** and **Experiment 3** were 10% and 20%, respectively.

The atom % of the ^{15}RES used in **Experiment 3** was 7.03%.

The atom % of the air background used for calculating the *ape ^{15}AN*, *ape $A^{15}N$* and *ape ^{15}RES* was 0.3667%.

3.7.2. Experiment 4

The total N recovery from the fertilizer was calculated by adding the N recovery from all the investigated pools (N_2 emissions, NR_{N2}; N_2O emissions, NR_{N2O}; AGB, NR_{AGB}; BGB, NR_{BGB}; soil, NR_{soil}; and NH_4^+ and NO_3^- leaching, NR_{NH4+} and NR_{NO3-}, respectively). The N recovery in the different pools (NR_{pool}) was calculated according to Taveira et al. (2020) (Eq. 41 – 43).

$$NR_{pool}(\%) = \frac{TN_{dff}\,in\ the\ pool}{N_{fert}} \times 100 \qquad \text{Eq. 41}$$

$$TN_{dff}\,in\ the\ pool\ = N_{dff}\,in\ the\ pool\,\frac{N_{dff}\,in\ the\ pool}{100} \times TN\ in\ the\ pool \qquad \text{Eq. 42}$$

$$N_{dff}\,in\ the\ pool = \frac{^{15}\,Natom\%\ excess\ in\ the\ pool}{^{15}\,N\ atom\%\ excess\ in\ the\ fertilizer} \qquad \text{Eq. 43}$$

Where "N_{fert}" is the total N-NO_3^- rate (80 kg N ha^{-1}) applied in the two fertilizer applications; the "*TN in the pool*" and 'TN_{dff} *in the pool*' are the total N content and the total N content derived from the fertilizer, respectively, in the different pools (total soil N, TN_{soil}; total N uptake by AGB, TN_{AGB}; total N uptake by BGB, TN_{BGB}; total N leached, TN_{leach}; and cumulative N_2O and N_2 emissions) at the end of the experiment expressed as kg N ha^{-1}; and the '^{15}N *atom% excess*' is calculated by subtracting the ^{15}N atom 0.3667% background to the ^{15}N atom% analyzed in the different pools. The amount of N in the different soil layers was calculated by multiplying the N content (%) of each soil layer by its bulk density (Table 3.10) and by the soil thickness of each layer.

Table 3.10. Bulk density of soil samples at different depths at the end of Experiment 4.

Soil layer (cm)	**Bulk density (g cm^{-3})**
0-5	0.43 ± 0.03
5-15	0.73 ± 0.02
15-40	1.31 ± 0.03

Data are expressed as the mean (n = 6) ± S.E.

3.8. Gross N transformation rates

The gross N mineralization rate (i.e., an indicator of the amount of organic-N that is mineralized to NH_4^+ by ammonifiers) in **Experiment 1** was estimated from the rate of dilution of ^{15}N enrichment in the NH_4^+ pool and from the change in the total NH_4^+ pool size, following the equations of Kirkham and Bartholomew (1954). Calculation of the gross N mineralization rate is shown in Equation 44.

$$m = \frac{M_0 - M}{t} \times \frac{\log(\frac{H_0 \times M}{H \times M_0})}{\log(\frac{M_0}{M})} \quad \text{Eq. 44}$$

where 'm' is the mineralization rate (mg N kg^{-1} d^{-1}); 'H_0' is the $^{15}NH_4^+$ concentration in soil at t = 0; 'M_0' is the total NH_4^+ concentration in soil at time t = 0; 'H' is the $^{15}NH_4^+$ concentration in soil at time $t = t$; 'M' is the total NH_4^+ concentration in soil at time $t = t$; and 't' is the time between measurements for H_0, M_0 and H, M.

The gross N nitrification rate was calculated from the equations of Ruppel et al. (2006) and is shown in the Equation 45.

$$n = \frac{a'NO3_t - a'NO3_0}{\Delta t} \times \frac{NO3_0}{a'NH4_0 - a'NO3_t} \quad \text{Eq. 45}$$

where 'n' is the gross N nitrification rate (mg N kg^{-1} d^{-1}); '$NO3_0$' is the total NO_3^- concentration in soil at time t = 0 (mg N kg^{-1}); '$a'NO3_t$' and '$a'NO3_0$' are the atom % ^{15}N excess in the NO_3^- pool at time $t = t$ and time $t = 0$, respectively; and '$a'NH4_0$' is the atom % ^{15}N excess in the NH_4^+ pool at time t = 0.

3.9. Statistical analysis

Data analysis of the experiments was performed using Statgraphics® Centurion 19 and R Studio 4.3.2 software.

In **Experiments 1 – 3**, data distribution normality and variance uniformity were verified in the studied variables by the Shapiro–Wilk test and Levene's test, respectively. Inverse or log transformations were applied when necessary before analysis. Analyses of variance (two-way ANOVAs) were conducted using generalized linear models (GLM) to assess significant differences in the studied variables, except for the meteorological ones (Table 3.11). The analyses were done as follows: i) for tillage and fertilization factors (and their interaction) in **Experiment 1**, ii) for crop residue management and cover crop factors (and their interaction) in **Experiment 2,** and iii) for cover crop factors in **Experiment 3**. The least significant difference (LSD) test at $P < 0.05$ was used for multiple comparisons between means.

In **Experiment 1**, to analyze the differences between N derived from ^{15}AN and N derived from A^{15}N, an additional factor (^{15}N labelling: ^{15}AN or A^{15}N) was included in the GLM for the ANOVA, in addition to tillage and fertilization factors (i.e., split-split-plot).

In **Experiment 2**, the Pearson's correlation was used to study the relationship between i) daily GHG fluxes and soil properties (NH_4^+, NO_3^-, DOC concentrations, WFPS and temperature), ii) cumulative GHG emissions, average NH_4^+, NO_3^-, and DOC concentrations during the three experimental periods, and iii) total cumulative GHG emissions, YSNE, maize N content, NUE, and N_2O EF.

In **Experiment 3**, the Pearson's correlation test was performed to study the relationship between daily N_2O, $^{15}N_2O$, and CO_2 emissions, soil mineral N and DOC concentrations, WFPS, and soil and air temperature in the two different periods of the experiment and also considering the whole experimental period.

In **Experiment 4**, the Pearson's correlation test was performed to study the relationship between daily N_2O, N_2, N_2O-N_{fert}, N_2-N_{fert}, N_2O_d, N_2O_n, CO_2, and CH_4 emissions, $N_2O_d/(N_2O_d+N_2)$, soil mineral N, WFPS, and soil and air temperature.

Table 3.11. Variables studied in the different experiments.

Experiment 1	N_2O and $^{15}N_2O$ emissions
	Soil NH_4^+, NO_3^-, $^{15}NH_4^+$, $^{15}NO_3^-$ concentrations and WFPS
	Gross mineralization and nitrification rates
	Total N and ^{15}N contents and N recovery in barley and soil
	Soil and air temperatures
Experiment 2	N_2O, CH_4 and CO_2 emissions, yield-scaled N_2O emissions and N_2O emission factor
	Soil NH_4^+, NO_3^-, DOC concentrations and WFPS
	Total C and N in cover crop aboveground biomass
	Total N content, N uptake and maize yield in maize grain and stover
	Nitrogen use efficiency
	Soil and air temperatures
Experiment 3	N_2O, $^{15}N_2O$ and CO_2 emissions
	Soil NH_4^+, NO_3^-, DOC concentrations and WFPS
	Total C, N and ^{15}N content and N uptake in cover crops biomass
	Total N and ^{15}N contents, N uptake and yield in maize stover, grain and root
	Total N and ^{15}N contents in soil
	N recovery in maize and soil
	Soil and air temperatures
Experiment 4	N_2O, CH_4 and CO_2 emissions
	Soil NH_4^+ and NO_3^- concentrations and WFPS
	N_2O emissions derived from nitrification and from denitrification
	N_2 emissions
	Total N and ^{15}N contents in aboveground and belowground grass biomass and in soil
	N recovery in plant, soil, leaching and gases
	Soil and air temperatures

CHAPTER 4

RESULTS AND DISCUSSION

4.1. Experiment 1 – Combined effect of different tillage systems and the use of DMPSA on N fate and N_2O emissions: a ^{15}N tracing study with barley under rainfed conditions

This section reports the results of this experiment, previously published in the journal *Geoderma* (ISSN 0016-7061; JIF (2023) = 5.3). DOI: 10.1016/j.geoderma.2023.116424

4.1.1. Environmental conditions

From top-dressing fertilization (14 March) to harvest (13 June), the accumulated rainfall was 96 mm (136 mm including irrigation events). This accumulated rainfall was lower than the 15-year average in the area (118 mm). A remarkable rainfall event (35.6 mm) took place during the postharvest period (26 August) after several weeks of drought and high air and soil temperatures (Figure 4.1a). Throughout the experimental period (from March to November), the minimum and maximum soil temperatures (10 cm depth) were 10.9 ºC and 25.8 ºC, respectively, with a mean temperature of 19.3 ºC (Figure 4.1a).

The WFPS (Figure 4.1b) ranged from 10.2% to 62.6% during the preharvest period, with values below 30% in the upper soil layer most of this time. It was only above 45% at the end of April and in mid-May as a consequence of rainfall or irrigation events. During summer, the soil remained dry (WFPS < 20%); however, after the rainfall event on 26 August, the WFPS increased from 10.2% to 44.7%. No significant differences in WFPS were found between the tillage systems.

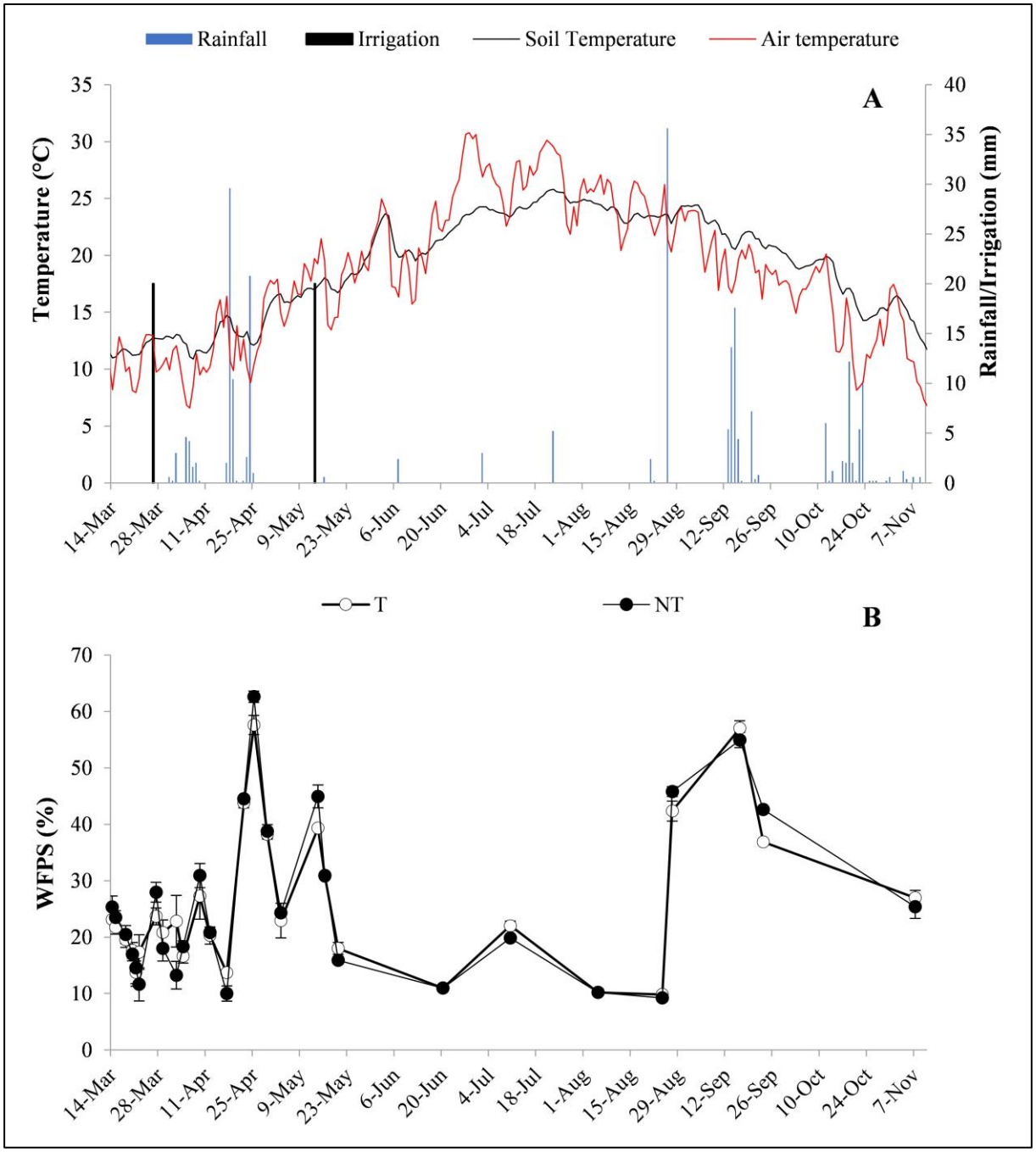

Figure 4.1. ***A)*** *Daily mean air and soil (10 cm depth) temperature and daily rainfall during the experimental period (14 March to 9 November 2019). Two irrigation events (black bars, 20 mm each) were performed on 26 March and 13 May.* ***B)*** *Evolution of soil WFPS (0-10 cm) in the different tillage (conventional tillage, T, no tillage, NT) plots. The black arrows denote irrigation events (26 March and 13 May). Vertical bars indicate standard errors of the means.*

4.1.2. Mineral N, $^{15}N\text{-}NH_4^+$ and $^{15}N\text{-}NO_3^-$ in soil

The soil NH_4^+ concentration was < 10 mg NH_4^+-N kg^{-1} the day before top-dressing fertilizer application (13 March) in all plots, without significant differences between tillage management or fertilization treatments (Figure 4.2a). Until harvest, the mean NH_4^+ concentrations in the soil were in the following order: AN+DMPSA > AN > N0, with no effect of tillage (Table 4.1).

The results of NH_4^+-N obtained from the microdiffusions in soil extracts from 14 March to 4 April are included in Figure 4.3, showing that 75.4% (on average) of NH_4^+-N was derived from top-dressing N fertilization (Table 4.2). Significant differences in fertilization treatments were observed only for NH_4^+-N_{15AN}, which was higher in AN+DMPSA (by 75.1% on average) with respect to AN.

Table 4.1. Mean soil mineral N (NH_4^+-N and NO_3^--N) concentrations in the preharvest period.

	NH_4^+ (mg N kg $soil^{-1}$)	**NO_3^- (mg N kg $soil^{-1}$)**
Tillage		
T	8.16	48.9 b
NT	5.90	24.4 a
S.E.	0.76	2.2
***P* value**	**0.171**	**0.016**
Fertilizer		
N0	2.73 a	19.8 a
AN	7.71 b	41.8 b
AN+DMPSA	10.65 c	48.4 b
S.E.	0.95	2.4
***P* value**	**0.000**	**0.000**
Tillage × Fertilizer		
***P* value**	**0.711**	**0.179**

Different letters within columns indicate significant differences within each effect according to the LSD test at $P < 0.05$. S.E.: Standard error of the mean.

The soil NO_3^- concentration ranged from 10.3 ± 3.9 to 52.3 ± 5.8 mg NO_3^--N kg^{-1} the day before top-dressing fertilizer application (13 March), with a significantly higher concentration in the T plots than in the NT plots (Figure 4.2b). The mean NO_3^- concentration in the T plots was

double that of the NT plots in the preharvest period (Table 4.1). However, DMPSA did not affect the NO_3^- concentration with respect to AN-only, and both fertilized treatments led to higher values compared with N0. At the end of the experiment, the NO_3^- concentration increased with depth, and the highest values were reported in the T_AN treatment (Table 4.3).

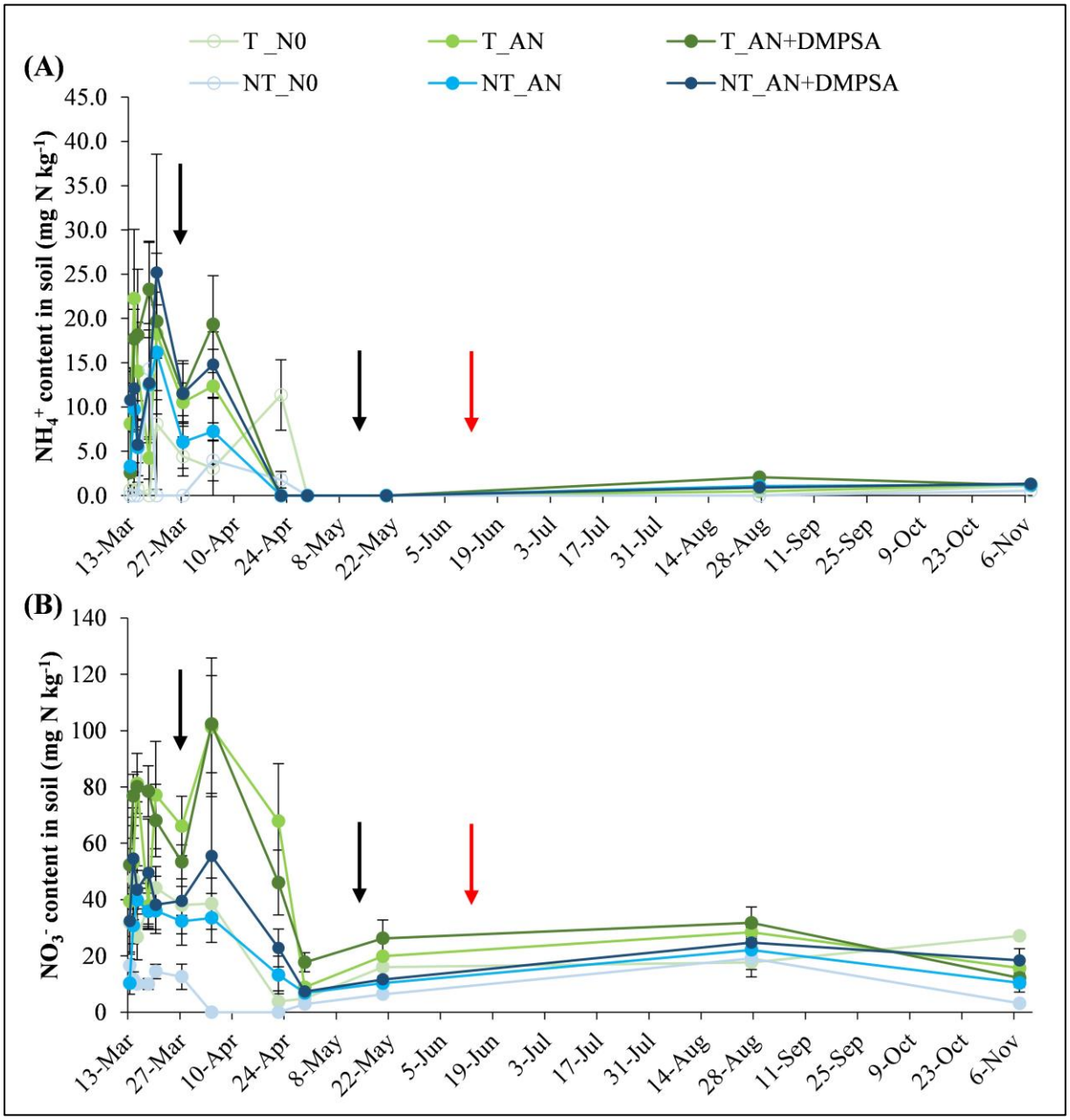

*Figure 4.2. Evolution of NH_4^+-N **(A)** and NO_3^--N **(B)** topsoil (0-10 cm) concentrations for the different soil tillage (conventional tillage, T, no tillage, NT) and fertilizer (unfertilized N control, N0, NH_4NO_3, AN, NH_4NO_3 with DMPSA, AN+DMPSA) treatments over the whole experimental period: from 13 March (i.e., one day before top dressing fertilization) until 9 November 2019. The black arrows denote irrigation events. The red arrow denotes the day of harvest. Vertical lines indicate standard errors of the means (n = 3).*

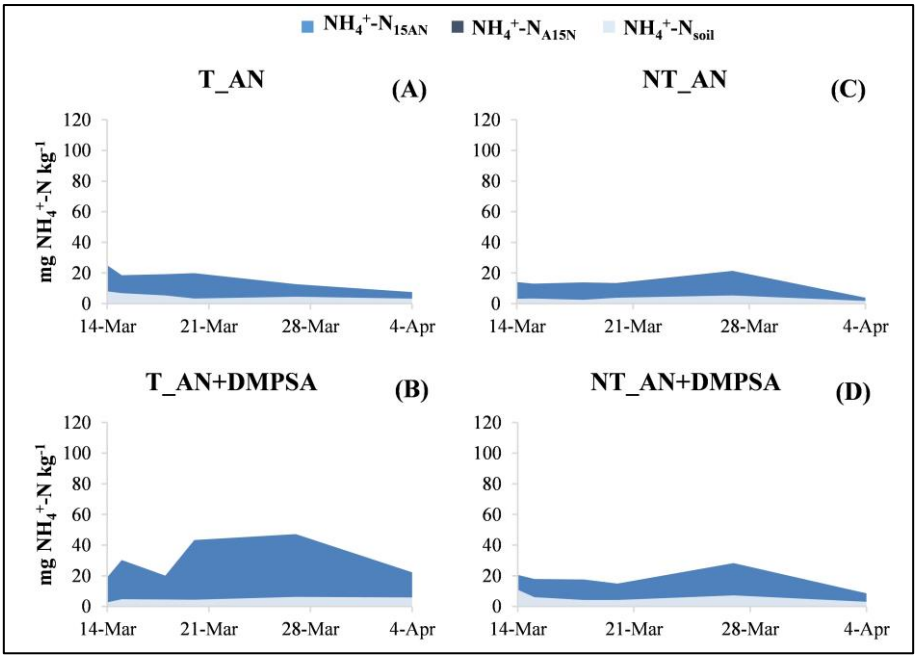

*Figure 4.3. Evolution of NH_4^+-N concentration derived from soil ($NH_4^+-N_{soil}$), from $^{15}NH_4NO_3$ ($NH_4^+-N_{15AN}$) and from $NH_4{}^{15}NO_3$ ($NH_4^+-N_{A15N}$) during 21 days following top dressing fertilization (14 March) in the different soil tillage (conventional tillage, T, no tillage, NT) and fertilizer (NH_4NO_3, AN, NH_4NO_3 with DMPSA, AN+DMPSA) treatments. T_AN **(A)**, T_AN+DMPSA **(B)**, NT_AN **(C)** and NT_AN+DMPSA **(D)**.*

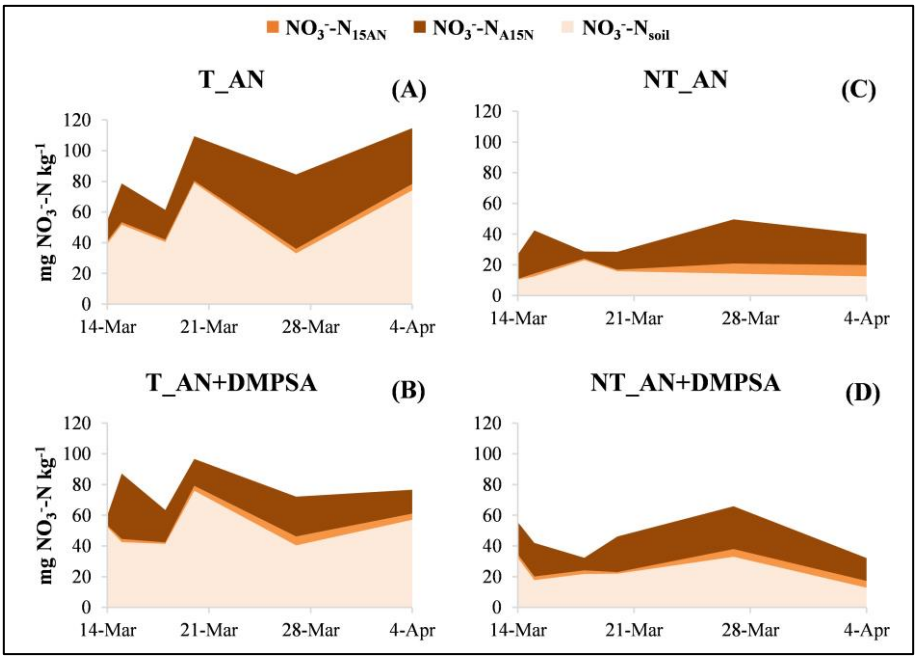

*Figure 4.4. Evolution of NO_3^--N concentration derived from soil ($NO_3^--N_{soil}$), from $^{15}NH_4NO_3$ ($NO_3^--N_{15AN}$) and from $NH_4{}^{15}NO_3$ ($NO_3^--N_{A15N}$) during 21 days following top dressing fertilization (14 March) in the different soil tillage (conventional tillage, T, no tillage, NT) and fertilizer (NH_4NO_3, AN, NH_4NO_3 with DMPSA, AN+DMPSA) treatments. T_AN **(A)**, T_AN+DMPSA **(B)**, NT_AN **(C)** and NT_AN+DMPSA **(D)**.*

During the period from 14 March to 4 April, significant differences in soil management were observed for NO_3^--N_{soil} (Figure 4.4), which was on average 2.5 times higher in T than in NT (Table 4.2). This was not observed for NO_3^--N_{fert} (neither for ^{15}AN nor for A^{15}N). On average, N fertilization (^{15}AN + A^{15}N) contributed to 35.5% and 52.9% of the NO_3^- concentrations in the soil in T and NT, respectively. The NO_3^--N_{15AN} concentrations were lower than those of NO_3^--N_{A15N} (Figure 4.4, Table 4.2).

The mean gross mineralization rate during the sampling period was 1.6 mg N kg^{-1} d^{-1} and no differences between treatments were observed (Table 4.4). In general, the largest values of gross mineralization rates were obtained during the first 24 hours, ranging from 1.1 mg N kg^{-1} d^{-1} (T_AN+DMPSA) to 5.2 mg N kg^{-1} d^{-1} (NT_AN+DMPSA) (data not shown). The mean gross nitrification rate was 0.7 mg N kg^{-1} d^{-1}, and values were numerically higher in NT and in AN than in T and AN+DMPSA, respectively (Table 4.4).

Table 4.2. Mean values obtained from microdiffusions (from 14 March to 4 April) of mineral N derived from $^{15}NH_4NO_3$ ($NH_4^+-N_{15AN}$ and $NO_3^--N_{15AN}$), derived from $NH_4{}^{15}NO_3$ ($NH_4^+-NA15N$ and $NO_3^--N_{A15N}$), and from the soil ($NH_4^+-N_{soil}$ and $NO_3^--N_{soil}$) (mg N kg^{-1}) in the different soil tillage (conventional tillage, T, no tillage, NT) and fertilizer (NH_4NO_3, AN, NH_4NO_3 with DMPSA, AN+DMPSA) treatments. Data in parentheses indicate the % with respect to total NH_4^+-N or NO_3^--N.

	NH_4^+-N_{15AN}	NH_4^+-N_{A15N}	NH_4^+-N_{soil}	NO_3^--N_{15AN}	NO_3^--N_{A15N}	NO_3^--N_{soil}
Tillage						
T	18.8 (79.1)	0.002 (0.0)	4.97 (20.9)	2.52 (3.3)	24.7 (32.2)	49.6 (64.5) b
NT	11.3 (69.9)	0.013 (0.1)	4.85 (30.1)	2.99 (7.2)	19.0 (45.7)	19.6 (47.1) a
S.E.	2.2	0.003	0.11	0.09	1.8	3.9
***P* value**	0.227	0.118	0.549	0.062	0.157	0.032
Fertilizer						
AN	10.9 (71.9) a	0.003 (0.0)	4.28 (28.1)	2.64 (4.6)	23.1 (40.6)	31.1 (54.8)
AN+DMPSA	19.1 (77.5) b	0.012 (0.0)	5.54 (22.5)	2.86 (4.7)	20.6 (33.6)	38.0 (61.8)
S.E.	1.2	0.003	0.81	0.27	3.3	3.3
***P* value**	0.033	0.089	0.332	0.597	0.627	0.238
Tillage x Fertilizer						
***P* value**	0.212	0.251	0.200	0.349	0.433	0.479

Different letters within columns indicate significant differences within each effect according to the LSD test at $P < 0.05$. S.E.: Standard error of the mean.

Table 4.3. Soil mineral N concentration at the end of the experiment (11 November 2019) in the different soil tillage (conventional tillage, T, no tillage, NT) and fertilizer (NH_4NO_3, AN, NH_4NO_3 with DMPSA, AN+DMPSA) treatments at three sampling depths (0–10 cm, 10–20 cm, 20–40 cm).

Treatment	NH_4^+ (mg N kg^{-1})				NO_3^- (mg N kg^{-1})			
	0 – 10 cm	10 – 20 cm	20 – 40 cm	S.E. Depth	0 – 10 cm	10 – 20 cm	20 – 40 cm	S.E. Depth
T_AN	1.26 AB ab	1.09 A	1.66 B	0.16	15.7 A	38.2 B b	41.6 B	4.0
T_AN+DMPSA	1.17 A a	0.97 A	1.77 B	0.12	12.2 A	29.9 B ab	38.0 B	5.4
NT_AN	1.22 A ab	1.10 A	1.65 B	0.13	10.4 A	14.5 A a	32.8 B	3.2
NT_AN+DMPSA	1.34 AB b	0.95 A	1.73 B	0.14	18.4 A	21.9 A ab	37.5 B	4.2
S.E. Treatment	0.05	0.23	0.12		3.6	5.4	3.3	

Different capital letters denote differences ($P < 0.05$) between soil depths within each treatment. Different lowercase letters denote differences ($P < 0.05$) between treatments at the same soil depth. S.E.: Standard error of the mean.

Table 4.4. Gross mineralization and nitrification rates (mean from 14 March to 4 April) in the different soil tillage (conventional tillage, T, no tillage, NT) and fertilizer (NH_4NO_3, AN, NH_4NO_3 with DMPSA, AN+DMPSA) treatments.

	Gross mineralization rate (mg N kg^{-1} d^{-1})	Gross nitrification rate (mg N kg^{-1} d^{-1})
Tillage		
T	1.56	0.62
NT	1.64	0.87
S.E.	0.18	0.21
***P* value**	**0.792**	**0.701**
Fertilizer		
AN	1.67	0.89
AN+DMPSA	1.53	0.60
S.E.	0.41	0.23
***P* value**	**0.825**	**0.767**
Tillage x Fertilizer		
***P* value**	**0.116**	**0.316**

S.E: Standard error of the mean.

4.1.3. N_2O and $^{15}N_2O$ emissions

4.1.3.1. Emissions after top dressing fertilization (preharvest period)

The main N_2O emission peaks occurred immediately after the second irrigation event (i.e., 61 days after N application), reaching 0.49 mg N m^{-2} d^{-1} in NT_AN (Figure 4.5a). Cumulative N_2O fluxes before harvest were in the following order: AN > AN+DMPSA > N0 (Figure 4.6), with the emissions from AN+DMPSA being 60% lower than those from AN. Most of the N_2O emitted (85%, on average) during this period was derived from the endogenous N of the soil (Figure 4.7), regardless of tillage or fertilizer treatments (Table 4.5). The use of DMPSA abated N_2O-N_{15AN} (by 74%), N_2O-N_{A15N} (by 46%) and N_2O-N_{soil} (by 60%) emissions compared with AN, regardless of tillage management ($P < 0.05$). The relative contribution of exogenous NO_3^- was lower than that of exogenous NH_4^+ or endogenous N, ranging from 4% in T_AN to 9% in NT_AN+DMPSA (Table 4.5).

4.1.3.2. Emissions during the postharvest period

Nitrous oxide emissions were negligible when daily effective rainfall was below 5 mm. However, after the rainfall event at the end of August (Figure 4.1a), N_2O fluxes peaked (Figure 4.5b).

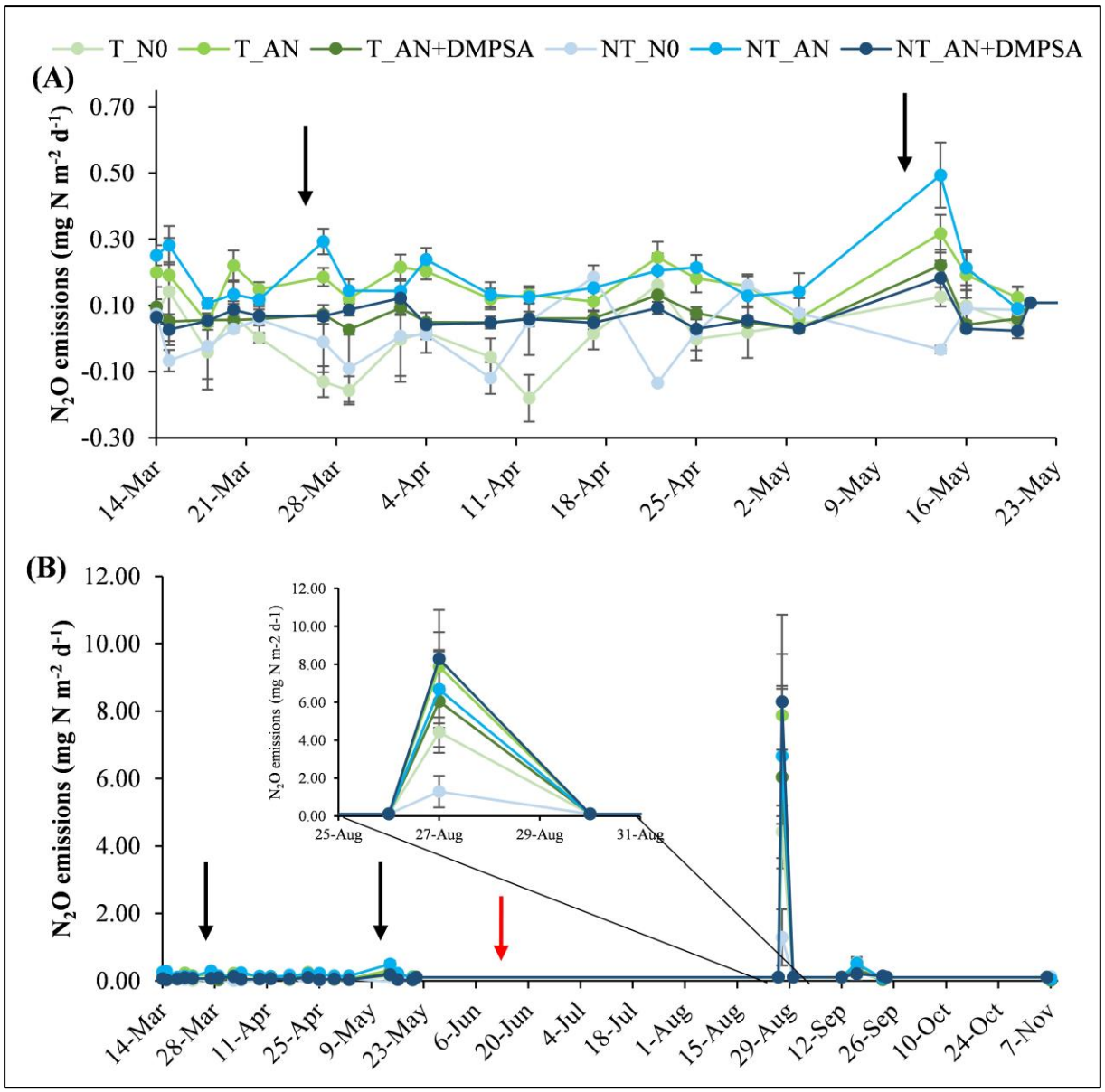

*Figure 4.5. Daily N_2O emissions in the preharvest period **(A)** and during the whole experimental period **(B)** for the different soil tillage (conventional tillage, T, no tillage, NT) and fertilizer (unfertilized N control, N0, NH_4NO_3, AN, NH_4NO_3 with DMPSA, AN+DMPSA) treatments. The black arrows denote irrigation events. The red arrow denotes the day of barley harvest. Vertical lines indicate standard errors of the means.*

The N_2O emissions during this summer peak were similar for all the tillage × fertilizer combinations except for the NT_N0 treatment, which had the lowest value ($P < 0.05$). The N_2O emitted during that pulse had a pivotal influence on total cumulative fluxes, leading to total emissions from AN to be numerically, but not statistically, higher than those from AN+DMPSA (Figure 4.6). In contrast to the preharvest period, N_2O-N_{15AN} emissions after harvest and until the end of the experiment were significantly lower than those derived from $A^{15}N$ (Table 4.5). Same as during the crop period, most N_2O emissions were derived from the soil (i.e., 95%, on average).

Table 4.5. Preharvest and postharvest cumulative N_2O-N emissions derived from $^{15}NH_4NO_3$ (N_2O-N_{15AN}), $NH_4{}^{15}NO_3$ (N_2O-N_{A15N}) and from the soil (N_2O-N_{soil}) in the different soil tillage (conventional tillage, T, no tillage, NT) and fertilizer (NH_4NO_3, AN, NH_4NO_3 with DMPSA, AN+DMPSA) treatments.

	N_2O (mg N m^{-2})					
	Preharvest			Postharvest		
	N_2O-N_{15AN}	N_2O-N_{A15N}	N_2O-N_{soil}	N_2O-N_{15AN}	N_2O-N_{A15N}	N_2O-N_{soil}
Tillage						
T	0.70	0.37	7.13	0.30 a	1.23	31.4
NT	1.08	0.49	7.55	0.74 b	0.91	32.7
S.E.	0.22	0.09	0.41	0.07	0.39	2.2
***P* value**	0.342	0.448	0.539	0.046	0.622	0.653
Fertilizer						
AN	1.41 b	0.56 b	10.5 b	0.52	1.10	32.3
AN+DMPSA	0.37 a	0.30 a	4.22 a	0.53	1.03	31.8
S.E.	0.26	0.05	0.41	0.12	0.25	2.1
***P* value**	0.018	0.016	0.000	0.974	0.841	0.640
Tillage x Fertilizer						
T_AN	0.87	0.57	9.84	0.32	1.31	32.8
T_AN+DMPSA	0.53	0.18	4.42	0.29	1.14	29.9
NT_AN	1.95	0.55	11.1	0.72	0.89	31.9
NT_AN+DMPSA	0.21	0.43	4.02	0.77	0.92	33.6
S.E.	0.37	0.06	0.58	0.17	0.35	3.0
***P* value**	0.071	0.110	0.231	0.842	0.783	0.526

Different letters within columns indicate significant differences within each effect according to the LSD test at $P < 0.05$. S.E.: Standard error of the mean.

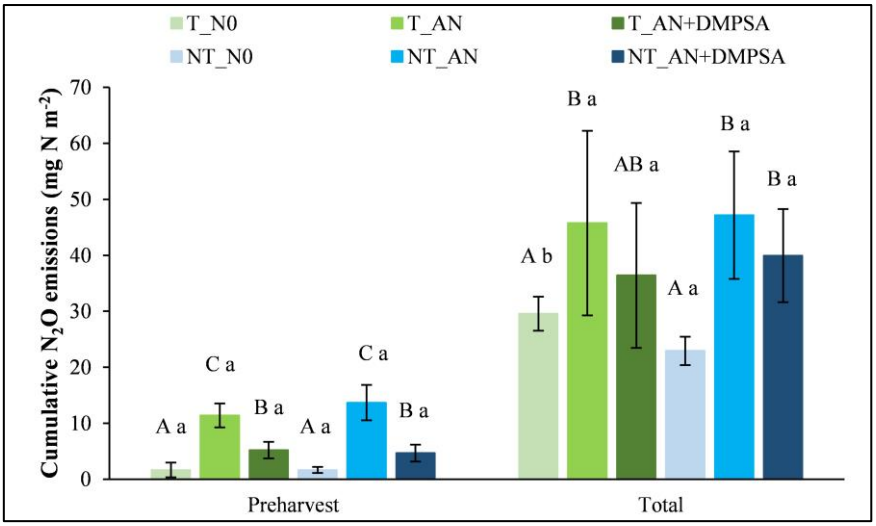

Figure 4.6. Cumulative N_2O emissions at preharvest and total N_2O emissions at the end of the experiment (i.e., preharvest + postharvest) in the different soil tillage (conventional tillage, T, no tillage, NT) and fertilizer (unfertilized N control, N0, NH_4NO_3, AN, NH_4NO_3 with DMPSA, AN+DMPSA) treatments. Vertical lines indicate standard errors of the means. Different capital letters indicate differences ($P < 0.05$) between fertilizer treatments within each tillage treatment. Different lowercase letters indicate significant differences ($P < 0.05$) between tillage treatments within each fertilizer treatment.

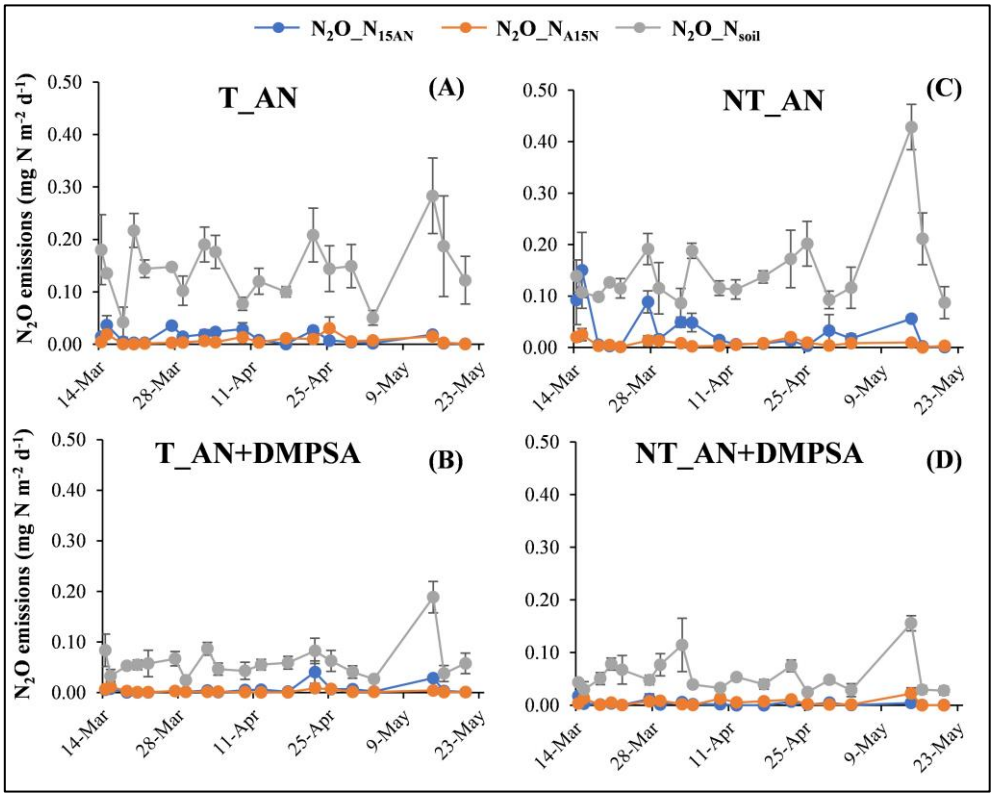

*Figure 4.7. Daily $N_2O{-}N$ emissions derived from soil ($N_2O{-}N_{soil}$), from $^{15}NH_4NO_3$ ($N_2O{-}N_{15AN}$) and from $NH_4{}^{15}NO_3$ ($N_2O{-}N_{A15N}$) after top dressing fertilization (14 March) in the different soil tillage (conventional tillage, T, no tillage, NT) and fertilizer (NH_4NO_3, AN, NH_4NO_3 with DMPSA, AN+DMPSA) treatments. T_AN **(A)**, T_AN+DMPSA **(B)**, NT_AN **(C)** and NT_AN+DMPSA **(D)**. Vertical lines indicate standard errors of the means.*

4.1.4. Total N and ^{15}N in barley plants

The mean total N in grain, aboveground biomass and root biomass of barley plants was 2.3%, 1.1% and 1.4%, respectively, with no significant differences between any of the tillage-fertilizer combinations (Table 4.6). Plant N uptake was increased in AN+DMPSA, with respect to AN, in grain (by 9% on average), biomass (by 24% on average) and roots (by 11% on average), although these increases were only significant for NT plots (Table 4.6).

Table 4.6. Total N uptake (kg N ha^{-1}) and total N (%) in grain, aboveground biomass and root biomass in barley plants in the different soil tillage (conventional tillage, T, no tillage, NT) and fertilizer (NH_4NO_3, AN, NH_4NO_3 with DMPSA, AN+DMPSA) treatments.

	Total N uptake (kg N ha^{-1})			% N		
	Grain	Biomass	Root	Grain	Biomass	Root
Tillage						
T	42.2	27.9 a	2.00	2.34	1.13	1.45
NT	61.0	36.6 b	2.67	2.32	1.07	1.32
S.E.	6.2	0.8	0.21	0.03	0.05	0.05
***P* value**	0.164	0.020	0.155	0.627	0.464	0.202
Fertilizer						
AN	49.3 a	28.8 a	2.22 a	2.35	1.06	1.38
AN+DMPSA	53.9 b	35.8 b	2.45 b	2.30	1.15	1.40
S.E.	1.4	1.4	0.06	0.03	0.05	0.03
***P* value**	0.041	0.007	0.015	0.338	0.211	0.606
Tillage × Fertilizer						
T_AN	43.1 Aa	27.3 Aa	2.03 Aa	2.37	1.10	1.46
T_AN+DMPSA	41.3 Aa	28.5 Aa	1.97 Aa	2.31	1.17	1.45
NT_AN	55.6 Ab	30.2 Aa	2.41 Aa	2.33	1.01	1.29
NT_AN+DMPSA	66.4 Bb	43.0 Bb	2.93 Bb	2.30	1.12	1.35
S.E.	2.0	2.0	0.09	0.05	0.07	0.04
***P* value**	0.007	0.038	0.004	0.801	0.808	0.393

Different letters within columns indicate significant differences within each effect according to the LSD test at $P < 0.05$. Different capital letters in the "Tillage × Fertilizer" interaction indicate significant differences between fertilizers within each tillage system, while different lowercase letters indicate significant differences between tillage systems within each fertilization treatment. S.E.: Standard error of the mean.

Table 4.7. Plant ^{15}N percentage (% ^{15}N), plant N derived from fertilizer (Plant_N_{fert}), plant N derived from soil (Plant_N_{soil}) and plant N recovery in the different soil tillage (conventional tillage, T, no tillage, NT) and fertilizer (NH_4NO_3, AN, NH_4NO_3 with DMPSA, AN+DMPSA) treatments and in the different ^{15}N labelling treatments ($^{15}NH_4NO_3$, ^{15}AN, $NH_4{}^{15}NO_3$, $A^{15}N$).

	% ^{15}N			Plant_N_{fert} (kg N ha^{-1})			Plant_N_{soil} (kg N ha^{-1})			N recovery (%)
	Grain	Biomass	Root	Grain	Biomass	Root	Grain	Biomass	Root	Plant
Tillage										
T	1.49 b	1.39	1.10	9.74	5.95 a	0.31	32.5	22.0	1.69	20.0
NT	1.36 a	1.32	1.11	12.3	7.53 b	0.40	48.7	30.8	2.27	25.3
S.E.	0.02	0.05	0.03	1.34	0.08	0.03	4.9	1.8	0.18	1.7
***P* value**	0.046	0.393	0.9499	0.309	0.005	0.182	0.144	0.068	0.158	0.161
Fertilizer										
AN	1.50	1.42	1.16	11.5	6.68	0.36	37.8 a	23.8	1.86	23.2
AN+DMPSA	1.34	1.29	1.05	10.5	6.80	0.35	43.4 b	29.0	2.11	22.1
S.E.	0.13	0.12	0.08	0.62	0.34	0.02	1.3	1.9	0.08	1.2
***P* value**	0.391	0.414	0.326	0.306	0.819	0.576	0.008	0.056	0.097	0.533
Tillage x Fertilizer										
T_AN	1.53	1.42	1.14	10.4	6.06	0.33	32.6 Aa	21.3	1.70	21.0
T_AN+DMPSA	1.45	1.36	1.07	9.05	5.84	0.29	32.3 Aa	22.7	1.69	19.0
NT_AN	1.75	1.42	1.18	12.6	7.30	0.40	43.0 Ab	26.3	2.01	25.4
NT_AN+DMPSA	1.24	1.21	1.03	12.0	7.76	0.40	54.4 Bb	35.2	2.52	25.2
S.E.	0.18	0.17	0.11	0.85	0.48	0.03	1.8	2.7	0.12	1.6
***P* value**	0.668	0.631	0.715	0.689	0.519	0.472	0.005	0.197	0.084	0.597
Label										
^{15}AN	1.09 a	1.04 a	0.90 a	3.89 a	2.10 a	0.12 a				
$A^{15}N$	1.76 b	1.67 b	1.31 b	7.13 b	4.64 b	0.23 b				
S.E.	0.05	0.04	0.03	0.23	0.16	0.01				
***P* value**	0.000	0.000	0.000	0.000	0.000	0.000				

Different letters within columns indicate significant differences within each effect according to the LSD test at $P < 0.05$. Different capital letters in the "Tillage x Fertilizer" interaction indicate significant differences between fertilizers within each tillage system, while different lowercase letters indicate significant differences between tillage systems within each fertilization treatment. S.E.: Standard error of the mean.

Regarding ^{15}N analyses, differences were observed in the % ^{15}N in grain, with higher values obtained in barley plants grown in T compared with those from NT plots and in plants fertilized with A^{15}N versus ^{15}AN (Table 4.4). The use of DMPSA affected plant_N_{soil}, which was higher in AN+DMPSA than in AN in grain (by 14.8%, $P < 0.05$) and by 21.1% and 13.5% in biomass and roots, respectively ($0.05 < P < 0.10$). Generally, no differences in the plant_N_{fert} were observed between tillage or fertilization treatments, except for the higher values in NT than in T for biomass (21% increment, $P < 0.05$) (Table 4.7). Accordingly, NT plots had higher N recovery in aboveground biomass (Table 4.8) and tended to have larger total recovery in plants with respect to T. On average, 22% of the N applied at top dressing fertilization was recovered in barley plants, with no significant effect of tillage or DMPSA addition. Values corresponding to plant_N_{A15N} were statistically higher than those from plant_N_{15AN} for all components of barley yield (Table 4.7).

Table 4.8. Plant N recovery in the different soil tillage (conventional tillage, T, no tillage, NT) and fertilizer (NH_4NO_3, AN, NH_4NO_3 with DMPSA, AN+DMPSA) treatments.

		Plant N recovery (%)		
		Grain	Biomass	Root
Tillage				
	T	12.2	7.44 a	0.38
	NT	15.4	9.00 b	0.50
	S.E.	1.7	0.24	0.04
	***P* value**	0.313	0.043	0.181
Fertilizer				
	AN	14.4	7.94	0.45
	AN+DMPSA	13.2	8.50	0.43
	S.E.	0.7	0.51	0.02
	***P* value**	0.299	0.487	0.169
Tillage x Fertilizer				
	***P* value**	0.648	0.316	0.470

Different letters within columns indicate significant differences within each effect according to the LSD test at $P < 0.05$. S.E.: Standard error of the mean.

4.1.5. Retention of ^{15}N in soil

At the end of the experiment, soil_N_{15AN} was mainly retained in the upper soil layer, showing higher values with the use of DMPSA (9.7 kg N ha^{-1}) compared with AN (4.9 kg N ha^{-1}, Figure 4.8). Tillage management did not affect soil_N_{15AN} or soil_N_{A15N} in the upper layer. However, soil_N_{A15N} at deeper soil layers (10–20 cm and 20–40 cm) was higher in the T plots than in the NT plots, while no differences were observed between fertilization treatments (Figure 4.8). Total soil N retention ranged from 28.6% (in NT_AN) to 49.5% of synthetic N applied (in T_AN+DMPSA) without significant differences between treatments (Table 4.9). On average, the non-accounted N reached 41%.

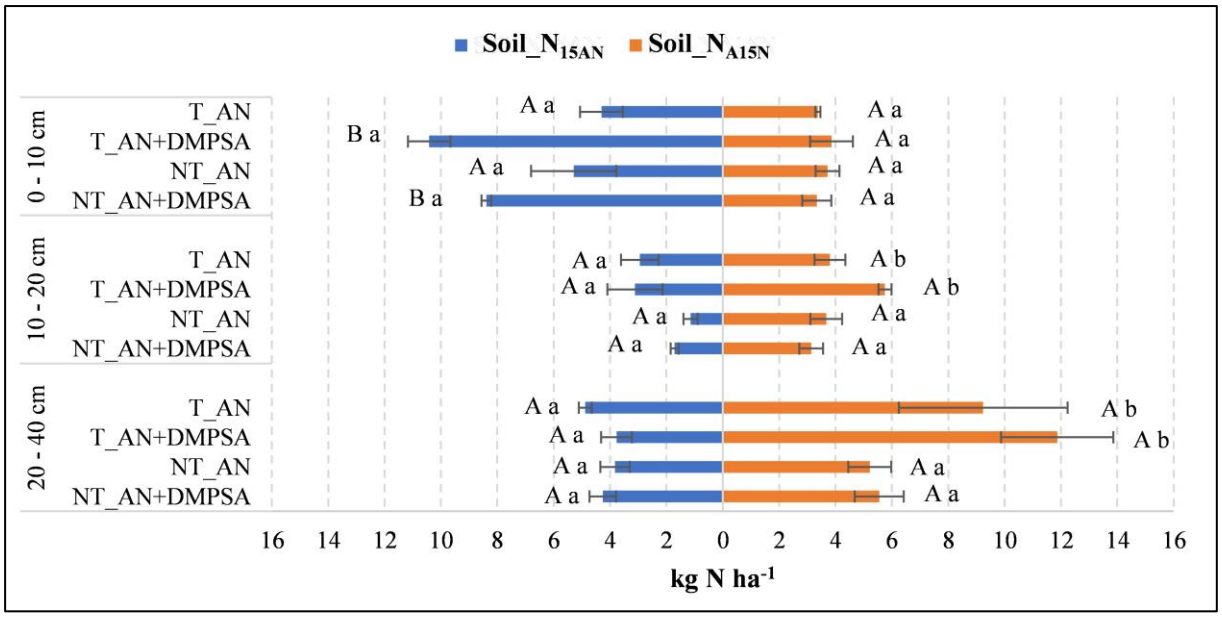

Figure 4.8. Average soil N derived from ^{15}AN (Soil_N_{15AN}) and derived from $A^{15}N$ (Soil_N_{A15N}) at 0–10 cm, 10–20 cm and 20–40 cm depths at the end of the experiment (7 November) in the different soil tillage (conventional tillage, T, no tillage, NT) and fertilizer (NH_4NO_3, AN, NH4NO3 with DMPSA, AN+DMPSA) treatments. Horizontal lines indicate standard errors. Different capital letters indicate differences (P < 0.05) between fertilizers within each soil management system, while different lowercase letters indicate significant differences (P < 0.05) between soil management within each fertilization treatment.

Table 4.9. Soil N derived from fertilizer (Soil_N_{fert}) and soil N retention at the end of the experiment in the different soil tillage (conventional tillage, T, no tillage, NT) and fertilizer (NH_4NO_3, AN, NH_4NO_3 with DMPSA, AN+DMPSA) treatments and in the different ^{15}N labelling ($^{15}NH_4NO_3$, ^{15}AN, $NH_4{}^{15}NO_3$, $A^{15}N$).

	Soil_N_{fert} (kg N ha^{-1})			**Soil N Retention (%)**			
Effect	0 – 10 cm	10 – 20 cm	20 – 40 cm	0 – 10 cm	10 – 20 cm	20 – 40 cm	Total
Tillage							
T	11.6	7.81	14.9 b	14.5	9.76	18.6 b	42.9
NT	10.4	4.83	9.42 a	13.0	6.04	11.8 a	30.8
S.E.	1.2	0.66	0.76	1.6	0.82	0.9	3.3
***P* value**	0.545	0.085	0.037	0.545	0.085	0.037	0.120
Fertilizer							
AN	8.57 a	5.78	11.6	10.7 a	7.23	14.5	32.4
AN+DMPSA	13.4 b	6.86	12.7	16.8 b	8.57	15.9	41.3
S.E.	0.88	0.47	2.0	1.9	0.58	2.5	3.9
***P* value**	0.018	0.178	0.708	0.018	0.179	0.708	0.184
Tillage x Fertilizer							
***P* value**	0.161	0.189	0.902	0.162	0.189	0.902	0.466
Label							
^{15}AN	7.32 b	2.23 a	4.18 a				
$A^{15}N$	3.68 a	4.09 b	7.97 b				
***P* value**	0.001	0.001	0.001				

Different letters within columns indicate significant differences within each effect according to the LSD test at $P < 0.05$. S.E.: Standard error of the mean

4.1.6. Discussion

There is a remarkable inter-annual meteorological variability in semiarid Mediterranean croplands. However, the frequency of cropping campaigns with low cumulative precipitation is increasing in these areas (Paniagua et al., 2019). The results of our study were obtained in a dry cropping period (see Section 3.1). However, half of the campaigns during the last 15-years reported even lower cumulative rainfall in the March-July period than in our experiment (considering the irrigation events) (Table 4.10).

Table 4.10. Cumulative rainfall (mm) during the typical barley cropping period (November-July) and the typical post-dressing fertilization period (March-July) during the last 15 years. Data highlighted in yellow and red denote the values lower than the cumulative rainfall in the experimental campaign (2018/2019), with and without considering the irrigation events, respectively.

November – July	**Rainfall (mm)**	**March – July**	**Rainfall (mm)**
2004/2005	97	2005	31
2005/2006	295	2006	124
2006/2007	412	2007	220
2007/2008	301	2008	208
2008/2009	219	2009	85
2009/2010	487	2010	195
2010/2011	388	2011	220
2011/2012	188	2012	96
2012/2013	311	2013	190
2013/2014	278	2014	103
2014/2015	276	2015	120
2015/2016	310	2016	217
2016/2017	280	2017	113
2017/2018	428	2018	294
2018/2019	**195**	**2019**	**104**
2018/2019 + 40 mm irrigation	**235**	**2019 + 40 mm irrigation**	**144**
Average	298	Average	155

These meteorological conditions affect the environmental impacts of N fertilization and N dynamics that should be explored mechanistically. Field experiments shed light on N fate, N cycling and the potential benefits of recommended agricultural practices. Under the conditions of our study, we can conclude that i) dry seasons could decrease N_2O losses after fertilization

but lead to critical peaks after rewetting, thus limiting the effectiveness of mitigation strategies; ii) NIs modulate the nitrification process from both fertilizer-N and endogenous-N (which is the main contributor to plant uptake), affecting soil residual N at the end of the cropping period; and iii) the effect of no tillage on N_2O fluxes and soil and plant recovery could be mainly related to plant N acquisition.

4.1.6.1. Soil mineral N during the preharvest period

Crop residue management practices affected NO_3^--N concentrations in the soil (0–10 cm depth), with higher values for the tilled plots than in the non-tilled plots (Table 4.1). Similar results were reported previously under rainfed Mediterranean conditions (Corrochano-Monsalve et al., 2020; Plaza-Bonilla et al., 2014). This could be related to the higher crop density and early crop development observed in the non-tilled plots that could have enhanced crop N acquisition, thus reducing the soil N pool. Improved crop development using conservation tillage management under Mediterranean conditions has been previously reported by Morell et al. (2011b).

The effectiveness of DMPSA in inhibiting NH_4^+ oxidation has been previously reported in several studies under similar climatic conditions (Guardia et al., 2021; Volpi et al., 2017). Our results confirm this with an increase of 39% in the average soil NH_4^+-N in AN+DMPSA compared with AN during the preharvest period (Table 4.1). These results are in agreement with the well-known effect of NIs at a global scale (Qiao et al., 2015) and are related to the increase in the amount of NH_4^+-N derived from the fertilizer (Table 4.2). The reduced effect of DMPSA on non-tilled plots (in comparison with conventional tillage) could be associated with the potentially higher NH_4^+ uptake in NT plots (see Section 4.1.4) or with the generally higher N losses through volatilization in non-tilled than in tilled soils (Pinheiro et al., 2018).

The decrease in NH_4^+-N_{15AN} in fertilized plots coinciding with an increase in the NO_3^--N_{15AN} concentrations during the 3 following weeks after N fertilization (Figure 4.3 and Figure 4.4,

respectively) could have been the result of nitrification (He et al., 2020; G. Zhu et al., 2019), considering the low WFPS values (Pilegaard, 2013). The gross nitrification rates reported in the present study (0.7 mg N kg^{-1} d^{-1} on average, Table 4.4) are of the same order of magnitude as those obtained previously under field conditions, e.g., 0.3 mg N kg^{-1} d^{-1} in a neutral pH soil in England (Geens et al., 1991) and 0.8 mg N kg^{-1} d^{-1} in a calcareous soil in England (Unkovich et al., 1998). As mentioned above, DMPSA effectively inhibited NH_4^+ oxidation. Thus, higher gross nitrification rates in AN compared with AN+DMPSA would be expected. We observed high variability in the gross nitrification rates (0.89 ± 0.33 and 0.60 ± 0.10 mg N kg^{-1} d^{-1} in AN and AN+DMPSA respectively, Table 4.4), thus masking the effect of DMPSA at a statistical level. However, despite this variability, we observed a decrease of 32% in the AN+DMPSA treatment with respect AN. These results highlight the challenges when developing ^{15}N tracing studies under field conditions, such as ensuring the uniform distribution of the applied ^{15}N-label throughout the soil (Murphy et al., 2003), the presence of plants that are known to influence gross N transformation rates (He et al., 2020; Inselsbacher et al., 2013) or adverse meteorological conditions or unaccounted for N losses via NH_3 volatilization (Pan et al., 2016), which should be taken into account in future studies to better understand the N dynamics in agricultural fields.

Our values of gross mineralization (1.6 mg N kg^{-1} d^{-1} on average, Table 4.4) were lower than those reported by Geens et al. (1991) (2.4 kg N ha^{-1} d^{-1}), Unkovich et al. (1998) (3.6 mg N kg^{-1} d^{-1}), Ruppel at al. (2006) (3.7 mg N kg^{-1} d^{-1}) and Harty et al. (2017) (5.2 mg N kg^{-1} d^{-1}). Our lower values could be explained by the low organic matter content of this soil (< 2%) and the dry conditions during the two weeks following fertilization (Figure 4.1a, b).

4.1.6.2. N_2O emissions

4.1.6.2.1 Emissions after top dressing fertilization (preharvest period)

The scarce precipitation during the experiment (Figure 4.1a) was likely a key driver of the low N_2O emissions after N top dressing fertilization (Figure 4.5a, Table 4.5), with lower values than those reported in other studies in rainfed crops under semiarid Mediterranean conditions, e.g., 9 – 80 mg N m^{-2} in Guardia et al. (2021) or 20 – 124 mg N m^{-2} in Montoya et al. (2021b), the latter including the postharvest period. Dry conditions, low soil moisture and organic C content, and calcareous soils are all factors that are expected to lead to low N_2O fluxes (Aguilera et al., 2013b; Cayuela et al., 2017). Moreover, dry conditions are expected to favor conservation over conventional tillage with regards to crop development and plant recovery (Morell et al., 2011b), thus changing soil N availability and N_2O emission dynamics (Huang et al., 2018) and, therefore, modifying the relevance of the post-harvest N_2O emission peaks after rewetting (Barrat et al., 2021).

The low WFPS in the upper soil layer reported after top dressing fertilization (Figure 4.1b) could have favored top-dressing fertilizer retention in this layer. Most N_2O emissions were derived from endogenous soil N (Table 4.5, Figure 4.7), which could be related to the previously reported priming effect that occurs after synthetic N addition (Schleusner et al., 2018; Thilakarathna and Hernandez-Ramirez, 2021). These endogenous N_2O emissions could also be derived from the N remaining from the fertilizer application at sowing. When focusing on N_2O emissions derived from dressing N fertilization, the N_2O coming from NH_4^+ was higher than that from NO_3^- (Table 4.5), suggesting that nitrification (*per se* or coupled with denitrification) was a relevant process for N_2O emissions during this period, as usually observed in Mediterranean cropping systems (Aguilera et al., 2013b) and in agreement with our second hypothesis.

The effectiveness of DMPSA in reducing N_2O emissions until harvest was demonstrated with the 61% lower cumulative fluxes reported in the microplots that received DMPSA (Table 4.5). In addition to the well-known effect of DMPSA inhibiting nitrification from fertilizer NH_4^+-N (Guzman-Bustamante et al., 2022; Huérfano et al., 2016; Montoya et al., 2021b; Torralbo et al., 2017), we observed that DMPSA also mitigated the N_2O emissions derived from the endogenous N in both tillage systems, thus supporting our first hypothesis. Our results suggest that DMPSA can move within the soil profile, as seen for DMPP (another DMP-based NI) from another study (Marsden et al., 2016), and inhibit the oxidation of the remaining NH_4^+ from basal fertilization and SOM mineralization, which had rates that were higher than those of nitrification. Besides the understandable effect of DMPSA on the N_2O coming from endogenous or exogenous NH_4^+, a significant effect of the inhibitor was also observed in N_2O derived from fertilizer NO_3^--N (Table 4.5), as reported by Guardia et al. (2018), who also used single-labeled ammonium nitrate (i.e., ^{15}AN and A^{15}N) but in a maize crop. It has been demonstrated that soils with rapid nitrification rates (e.g., calcareous or alkaline) promote O_2 depletion and NO_2^- accumulation, thus stimulating denitrification and increasing the N_2O:N_2 ratio (Y. Li et al., 2023b; Petersen et al., 1996). Therefore, the inhibiting effect of DMPSA is also expected to detrimentally affect denitrification rates and the amount of N_2O derived from A^{15}N. A clear effect of NIs such as DMPP or DMPSA on denitrifying microorganisms has also been observed by e.g., Torralbo et al. (2017) or Barrena et al. (2017), decreasing the abundance of genes involved in the stepwise reduction of NO_3^- to NO_2^- and NO, and/or increasing those involved in the reduction of N_2O to N_2. These changes in microbial populations could be due to the direct effect of NIs on denitrifying microorganisms or due to the indirect effect of reducing the availability of NO_3^-. Therefore, the addition of DMPSA could be effective when conditions are favorable for high N_2O losses, e.g., significant SOM mineralization rates stimulated from the addition of N fertilizers (Thilakarathna and Hernandez-Ramirez, 2021) and

even when a NO_3^--N-based synthetic fertilizer is applied. With regards to the effect of tillage, non-tilled microplots tended to reduce N_2O losses from ^{15}AN (compared with conventional tillage) but only when DMPSA was applied (Table 3, $P < 0.10$). Therefore, our findings were consistent with those of Corrochano-Monsalve et al. (2020) under a humid Mediterranean climate, suggesting that the combination of both strategies could be a good option for mitigating N_2O emissions.

4.1.6.2.2 Emissions after harvest

Under our climate and soil conditions, the highest N_2O flux regardless of fertilization or soil management was observed two months after harvest (Figure 4.5b), after an intense rainfall event that was preceded by several weeks of drought and elevated temperatures (Figure 4.1a). This pulse effect has been reported in several field studies under similar climatic conditions (Montoya et al., 2022, 2021b). The intensity of N_2O peaks after rewetting is greater when the soil remains close to the permanent wilting point during several weeks both with (Bergstermann et al., 2011) and without fertilizer application (Barrat et al., 2021), as was the case in our experiment.

The accumulated N_2O emissions derived from that pulse effect represented 71.5% of the total N_2O emissions, on average, thus highlighting the importance of measuring N_2O fluxes during the postharvest period in semiarid regions. Neither the fertilizer source (except the low peak in NT−N0) nor the tillage management affected the magnitude of the rewetting peak. Moreover, most of the N_2O released after harvest came from endogenous N rather than from the applied fertilizer (Table 4.5). This result could suggest that i) the opportunities for abating these rewetting peaks through fertilization or tillage management could be limited; ii) this type of peak could be mostly explained by the reactivation of microorganisms after rewetting (Barrat et al., 2021; Montoya et al., 2022; Priemé and Christensen, 2001) rather than by the

accumulation of residual or surplus N. However, we speculate that denitrifying microorganisms could have played a significant role in the evolution of this peak because i) N_2O emissions derived from the NO_3^-−N applied at top-dressing fertilization were higher than those derived from NH_4^+−N (in contrast with the trend observed before harvest) and ii) the mean NH_4^+ concentration at the rewetting event (0.8 mg N kg^{-1}) was much lower than that of NO_3^- (24.0 mg N kg^{-1}). The recent study of Montoya et al. (2022) also reported an increase in the abundance of nitrifying archaea and denitrifying populations (but not of nitrifying bacteria) during a postharvest rewetting peak.

4.1.6.3. Plant N recovery

Most N uptake of barley plants was obtained from soil/endogenous N instead of the N applied through top-dressing fertilization (Table 4.7). This result is in accordance with the review of Gardner and Drinkwater (2009). It is important to highlight that ^{15}N application was performed at top-dressing, but the crop also received a basal fertilization of 40 kg N ha^{-1} at seeding. This fact could partially explain our lower values compared with the 42% of plant N recovery and the 37% of N uptake derived from fertilizer reported for small grain crops by Yan et al. (2020). In addition, the fertilizer N losses that were not accounted for, e.g., NH_3 volatilization, N leaching, denitrification, could have also contributed to explaining the low N recoveries in barley (Harmsen, 2003). Both the % ^{15}N and the N derived from fertilizer in the crop (Table 4.7) revealed that barley plants preferably took up N from NO_3^- fertilization rather than from NH_4^+. These results are in accordance with those from Inselsbacher et al. (2013) in a barley crop and with those from Liu et al. (2019) in wheat cultivated in an alkaline soil.

Our results were also in accordance with most studies reviewed by Smith and Chalk (2020), in which tillage management did not affect fertilizer N recovery by crops, and with the meta-analysis of Gardner and Drinkwater (2009), which concluded that the use of NIs had no

significant impact on crop N recovery. The meta-analysis by Sha et al. (2020) suggested that the use of NIs can enhance the crop recovery of N from fertilizer, particularly when applied with organic fertilizers or urea in soils with medium SOM contents and neutral pH, rather than in soils with low organic matter content and calcareous soils, as in our experiment. Moreover, this meta-analysis reported that DMPP did not have a significant effect on fertilizer-N recovery.

The use of DMPSA combined with no tillage enhanced the plant uptake of endogenous N, particularly in the grain (Table 4.7). This increase was attributable to the improvement of plant development and yields, rather than an effect on plant N concentrations. The results of the study by Montoya et al. (2022) under similar experimental conditions than those of the present experiment reported an increase of ca. 60% in barley biomass and grain yields in NT compared with T plots regardless of the application of NIs in the fertilized treatments. The increase in N uptake and crop yield in non-tilled compared with tilled plots was also reported in the review of Shakoor et al. (2021) or by e.g., Soon and Arshad (2005) or Pittelkow et al. (2015a) during dry years (as in our study) and/or in rainfed crops. This has also been observed under Mediterranean conditions (Morell et al., 2011b; Plaza-Bonilla et al., 2014), being attributed to the improvement of chemical fertility and water retention capacity (Abdalla et al., 2016). The meta-analysis by Li et al. (2018) suggest that the enhancement in crop yield and/or NUE when applying NIs tend to diminish with high soil pH (>8) such as that of our study, and also that NIs are apparently more effective in enhancing NUE in irrigated cropping systems compared with rainfed ones. Recent studies using DMPSA did not find effects on crop yield in neither irrigated (Allende-Montalbán et al., 2022) nor rainfed (Guardia et al., 2020) cropping systems under Mediterranean climatic conditions.

4.1.6.4. Soil N at the end of the experimental period

Soil N that was derived from ^{15}AN fertilization was preferably retained in the topsoil (0–10 cm) (Figure 4.8), which could be related to the adsorption capacity of NH_4^+ to the soil colloid, thus partially preventing its lixiviation to deeper layers. The concentration of soil N derived from fertilizer NH_4^+-N was higher than that derived from NO_3^--N fertilization in the first 10 cm, but the opposite trend was observed at 10–40 cm, thus indicating the higher leaching potential and mobility of synthetic NO_3^--N-based fertilizers (Figure 4.8). This higher concentration of residual N derived from fertilizer NH_4^+-N fertilization in the top layer could also be related to the abovementioned barley preference of NO_3^- uptake by roots. It should be highlighted that under the conditions of the study, a significant amount of residual mineral N was present at the end of the experiment (Table 4.3).

The use of DMPSA significantly increased the topsoil retention of N-derived NH_4^+-N fertilization (Figure 4.8), thus enhancing the potential biological uptake and adsorption by the soil matrix (Sha et al., 2020). Regarding tillage management, the higher residual N contents in the deepest layer in tilled plots could be related to the lower N uptake in comparison with no tillage and the vertical movement of this non-absorbed N. These results support the recommendation of combining no tillage and NIs such as DMPSA to reduce the environmental impacts during current and subsequent cropping campaigns.

Rainfed Mediterranean croplands are characterized by high inter-annual variability in the amount and distribution of precipitation. The present study took place during a dry campaign. However, different dynamics could be expected in humid campaigns. For instance, rainy seasons may stimulate aboveground and belowground biomass production, thus increasing plant N recovery. On the other hand, leaching losses are expected to increase under high-rainfall

conditions, thus possibly decreasing both soil and plant recovery in coarse well-drained soils (Quemada et al., 2013). Moreover, the input of endogenous N from the mineralization of organic matter and crop residues is evidently driven by soil water availability (Quemada and Gabriel, 2016). To explore and disentangle these dynamics, further research is required under contrasting meteorological and soil (i.e., texture, pH) conditions.

4.2. Experiment 2 - Maize residue input rather than cover cropping influenced N_2O emissions and soil–crop N dynamics during the intercrop and cash crop periods

This section reports the results of this experiment, previously published in the journal *Agriculture Ecosystems & Environment* (ISSN 0167-8809; JIF (2023) = 6.0).

DOI: 10.1016/j.agee.2023.108873

4.2.1. Environmental conditions

The mean air and soil (10 cm) temperatures during the whole experimental period were 14.3 °C and 16.1 °C (Figure 4.9a), with minimum air temperature in mid-January (-16.3 °C, Table 4.11) and maximum air temperature reached during the summer season in P3. The cumulated precipitation during P1 and P2 (156 and 74 mm, respectively) was 12% and 30% lower than that of the 15-year average in the area (Table 4.11).

Table 4.11. Climatological data (accumulated rainfall and air temperature) and WFPS in the three periods (P1, P2 and P3) of the experiment. The WFPS mean values (n = 15, n = 14 and n = 17 in P1, P2 and P3, respectively) are expressed as the average during each period ± standard error of the mean. Average accumulated rainfall and air temperature during the 15 years before the experiment.

			Air Temperature (ºC)			**WFPS (%)**		
		Accumulated rainfall (mm)	**Mean**	**Min.**	**Max.**	**Mean**	**Min.**	**Max.**
Experimental year (2020-2021)	P1	156	7.52	-16.3	23.8	39.8 ± 2.4	13.2	52.7
	P2	74	19.1	-0.0	39.8	34.7 ± 2.9	15.1	49.4
	P3	188	18.8	-1.3	41.6	35.6 ± 3.3	13.5	64.4
15-years average (2006-2020)	P1	177	7.13					
	P2	105	19.4					
	P3	104	19.1					

The WFPS values ranged from 13.2% to 64.4% during the whole experiment (Table 4.11), with 72% reported values ranging between 30% and 50% (Figure 4.9b). The average WFPS during the whole experiment was 36.7%, with no difference between the three experimental periods (Table 4.11).

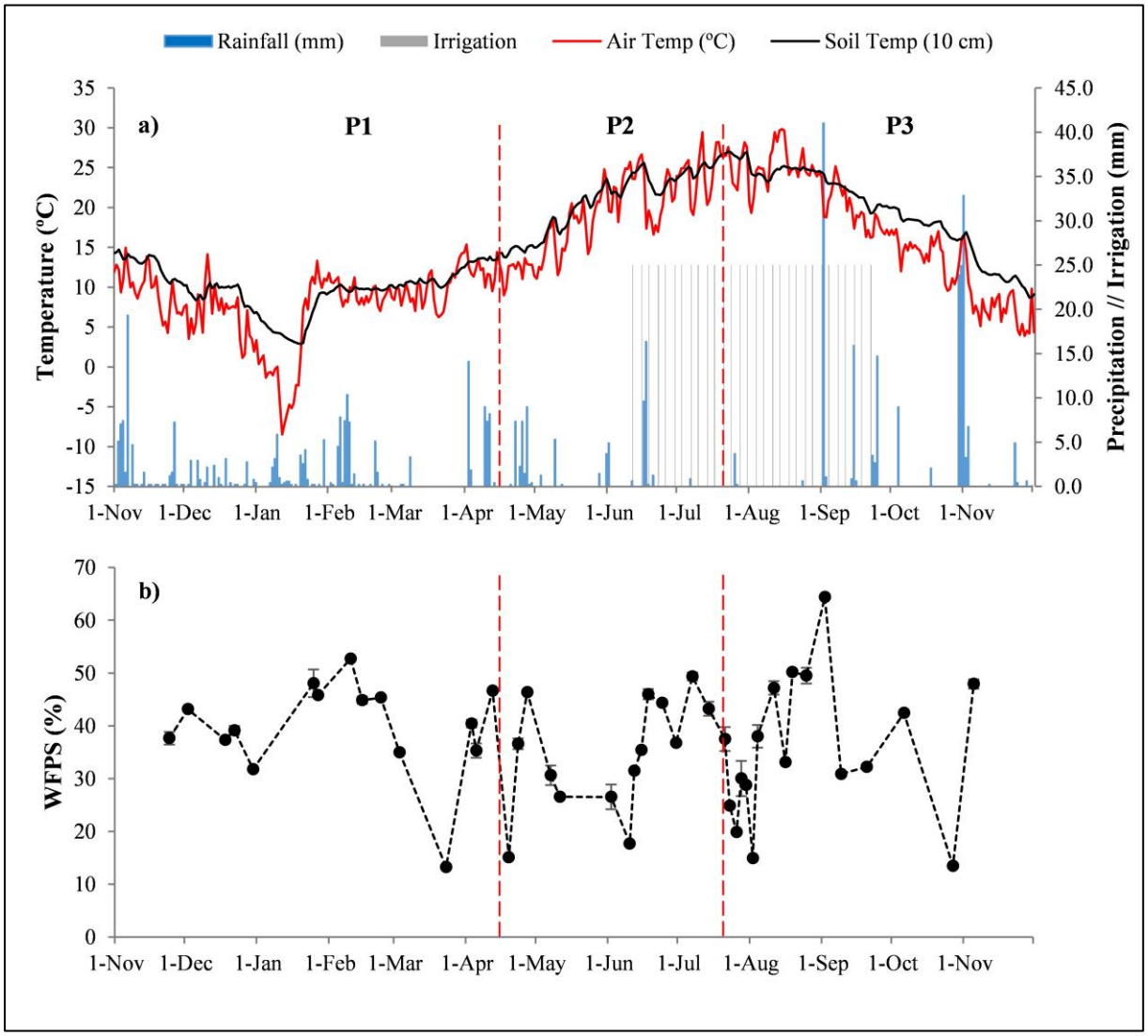

Figure 4.9. Mean air and soil temperature (°C), rainfall and irrigation (mm) ***(a)*** *and mean WFPS (%) in the upper soil layer (10 cm)* ***(b)*** *during the three experimental periods (P1, P2 and P3).*

4.2.2. N_2O emissions

The N_2O emissions were lower in the control area than in the N-fertilized area even before maize N fertilization (Figure 4.10a). In the N-fertilized area, the mean N_2O cumulative emissions during P1 and P2 (25.7 ± 2.9 and 47.2 ± 6.1 mg N m^{-2}, respectively) were lower than those reported in P3 (107.4 ± 23.8 mg N m^{-2}) (Figure 4.11a-c). The highest N_2O emission peak during P1 (Figure 4.12a) was reported after a freeze–thaw period at the end of January (Figure 4.9a). Another emission peak was reported in both areas after the beginning of maize irrigation and after several days of rainfall during P2, with values up to 8.82 mg N m^{-2} d^{-1} in −RC (Figure 4.12a) and 1.33 mg N m^{-2} d^{-1} in control_−RF (Figure 4.13a). The highest correlation reported during P1 was between N_2O emissions and soil NO_3^- concentration (r = 0.708), but this was not statistically significant (Figure 4.14a). A positive correlation was reported between N_2O emissions and WFPS values during P2 ($P < 0.05$; r = 0.558, Figure 4.14b). The cover crops only affected the N_2O emissions after their incorporation during P2, being 92.4% higher in C than in F (Figure 4.11b). The higher input of maize residues in +R significantly mitigated N_2O emissions during P1 and P2, being 39.2% and 46.8% lower in +R than in −R, respectively (Figure 4.11a,b). Furthermore, N_2O emissions were mitigated in control_+R compared to control_−R during P1 by 37.6% (Table 4.12). However, the opposite occurred after N fertilization in maize, with cumulative N_2O emissions 2.7 times higher in the +R plots than in the −R plots during P3 (Figure 4.11c). Three emissions peaks were reported during the first month after fertilization coinciding with samplings made the day after irrigation events, with the highest values reported in the +RL and +RC treatments, reaching up to 20.2 and 29.7 mg N m^{-2} d^{-1}, respectively (Figure 4.12a). These values decreased three or four days after irrigation events. The average EF and YSNE were 0.63% and 0.11 g N_2O-N kg^{-1} grain without differences reported between maize residue incorporation or cover cropping treatments (Figure 4.11e,f).

When considering the whole experimental trial, daily N_2O emissions were strongly correlated ($P < 0.05$) positively with soil NO_3^- (r = 0.601) and negatively with DOC concentration (r = -0.535) (Figure 4.14d), although the relationships were significant only for the L and +R treatments (data not shown). Furthermore, a moderate correlation was reported with CO_2 emissions ($P < 0.01$; r = 0.359) and with air and soil temperature at 10 cm depth ($P < 0.01$; r = 0.471 and r = 0.403) (Figure 4.14d).

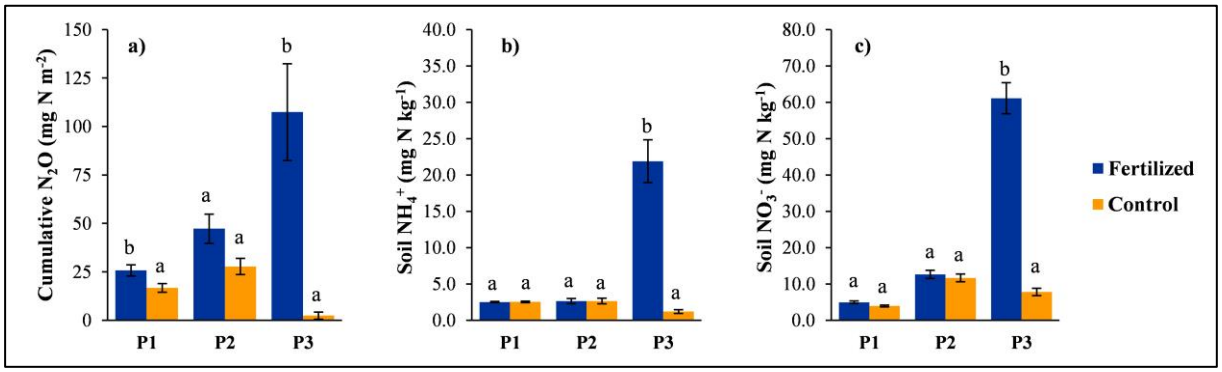

*Figure 4.10. Average **(a)** cumulative N_2O emissions, **(b)** soil NH_4^+-N concentration and **(c)** soil NO_3^-–N concentration for the three experimental periods (P1, P2 and P3) in the N-fertilized (blue bars) and unfertilized control areas (orange bars). Different letters in each period denote significant differences ($P < 0.05$) between areas according to the LSD test*

.

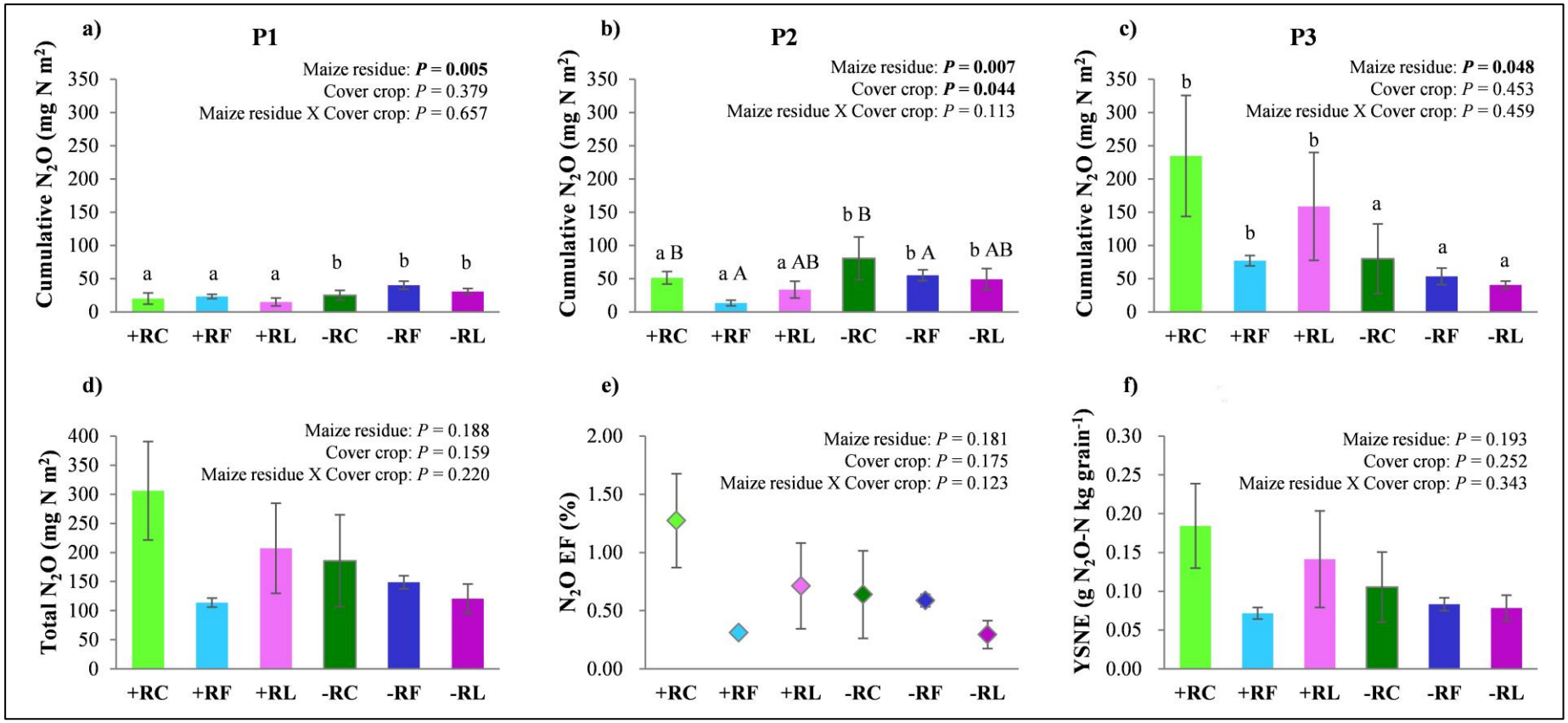

Figure 4.11. ***(a, b, c)*** *Cumulative N_2O-N emissions over the three experimental periods: P1, P2 and P3, respectively;* ***(d)*** *Total cumulative N_2O-N emissions at the end of the experiment;* ***(e)*** *the N_2O emission factor (EF) and* ***(f)*** *yield-scaled N_2O emissions (YSNE) in the different maize residue (higher input, +R, and lower input, –R) and cover crop (cereal, C; legume, L; and bare fallow, F) treatments in the N−fertilized area. Different lowercase letters denote significant differences in maize residue management for the same cover crop, while different uppercase letters denote significant differences between cover crops for the same maize residue management scheme, at the 95% confidence level and having applied the LSD test. Vertical lines represent the standard error of the mean (n = 3).*

Table 4.12. Cumulative N_2O-N and CO_2-C emissions over the three experimental periods (P1, P2 and P3), total cumulative N_2O-N, CO_2-C and CH_4-C emissions for the different maize residue (higher input, +R, and lower input, –R) and cover crop (cereal, C; legume, L; and fallow, F) treatments in the unfertilized control area.

	N_2O cumulative emissions (mg N m^{-2})			**Total N_2O (mg N m^{-2})**	**CO_2 cumulative emissions (g C m^{-2})**			**Total CO_2 (g C m^{-2})**	**CH_4 cumulative emissions (mg C m^{-2})**			**Total CH_4 (mg C m^{-2})**
	P1	**P2**	**P3**		**P1**	**P2**	**P3**		**P1**	**P2**	**P3**	
Maize residue	***P* = 0.024**	*P* = 0.292	*P* = 0.846	*P* = 0.707	***P* = 0.001**	*P* = 0.576	*P* = 0.802	***P* = 0.015**	*P* = 0.832	*P* = 0.314	*P* = 0.879	*P* = 0.623
Control_+R	12.8 a	32.2	3.26	48.3	87.8 a	85.2	87.6	261 a	8.55	-17.5	-26.7	-35.6
Control_–R	20.6 b	23.3	1.51	45.4	149.7 b	80.6	85.3	316 b	6.41	-9.06	-24.5	-27.1
S.E.	1.8	5.4	2.55	5.3	9.3	5.5	6.2	14	6.81	5.44	9.6	11.6
Cover crop	*P* = 0.650	*P* = 0.197	*P* = 0.513	*P* = 0.143	***P* = 0.000**	***P* = 0.000**	***P* = 0.008**	***P* = 0.000**	*P* = 0.600	*P* = 0.586	*P* = 0.666	*P* = 0.790
Control_C	18.4	21.4	5.31	45.1	132.2 b	102.7 b	81.8 a	317 b	12.6	-16.8	-29.2	-33.4
Control_F	15.6	22.8	-1.22	37.2	61.2 a	41.7 a	68.5 a	171 a	9.35	-15.7	-30.9	-37.2
Control_L	16.1	39.0	3.06	58.2	162.8 b	104.3 b	109.1 b	376 c	0.51	-7.44	-16.6	-23.6
S.E.	5.0	10.6	41.1	6.4	19.0	19.7	20.0	39	8.34	6.67	11.8	11.98
Maize residue × Cover crop	***P* = 0.016**	*P* = 0.552	*P* = 0.345	*P* = 0.210	***P* = 0.001**	***P* = 0.014**	***P* = 0.021**	*P* = 0.298	*P* = 0.324	*P* = 0.252	*P* = 0.696	*P* = 0.253
Control_+RC	14.0 ab	21.1	3.56	38.6	89.9 ab	93.4 b	86.9 b	270	22.8	-28.1	-24.7	-30.1
Control_+RF	18.6 bc	26.1	3.99	48.7	77.5 ab	36.2 a	50.3 a	164	11.6	-10.1	-29.2	-27.7
Control_+RL	6.0 a	49.4	2.21	57.6	96.1 b	126.0 c	125.6 c	348	-8.73	-14.4	-26.0	-49.2
Control_–RC	22.9 bc	21.7	7.06	51.6	174.6 c	112.1 bc	76.7 ab	363	2.40	-5.40	-33.7	-36.7
Control_–RF	12.6 ab	19.5	-6.44	25.6	44.9 a	47.3 a	86.7 b	179	7.10	-21.3	-32.6	-46.8
Control_–RL	26.3 c	28.7	3.92	58.9	229.6 d	82.6 b	92.6 bc	405	9.74	-0.47	-7.25	2.0
S.E.	3.1	9.4	4.4	9.1	16.1	9.6	10.8	24	11.8	9.43	16.7	20.1

Different letters within columns denote significant differences ($P < 0.05$) between maize residue management or between cover crops by applying the LSD test. S.E.: standard error.

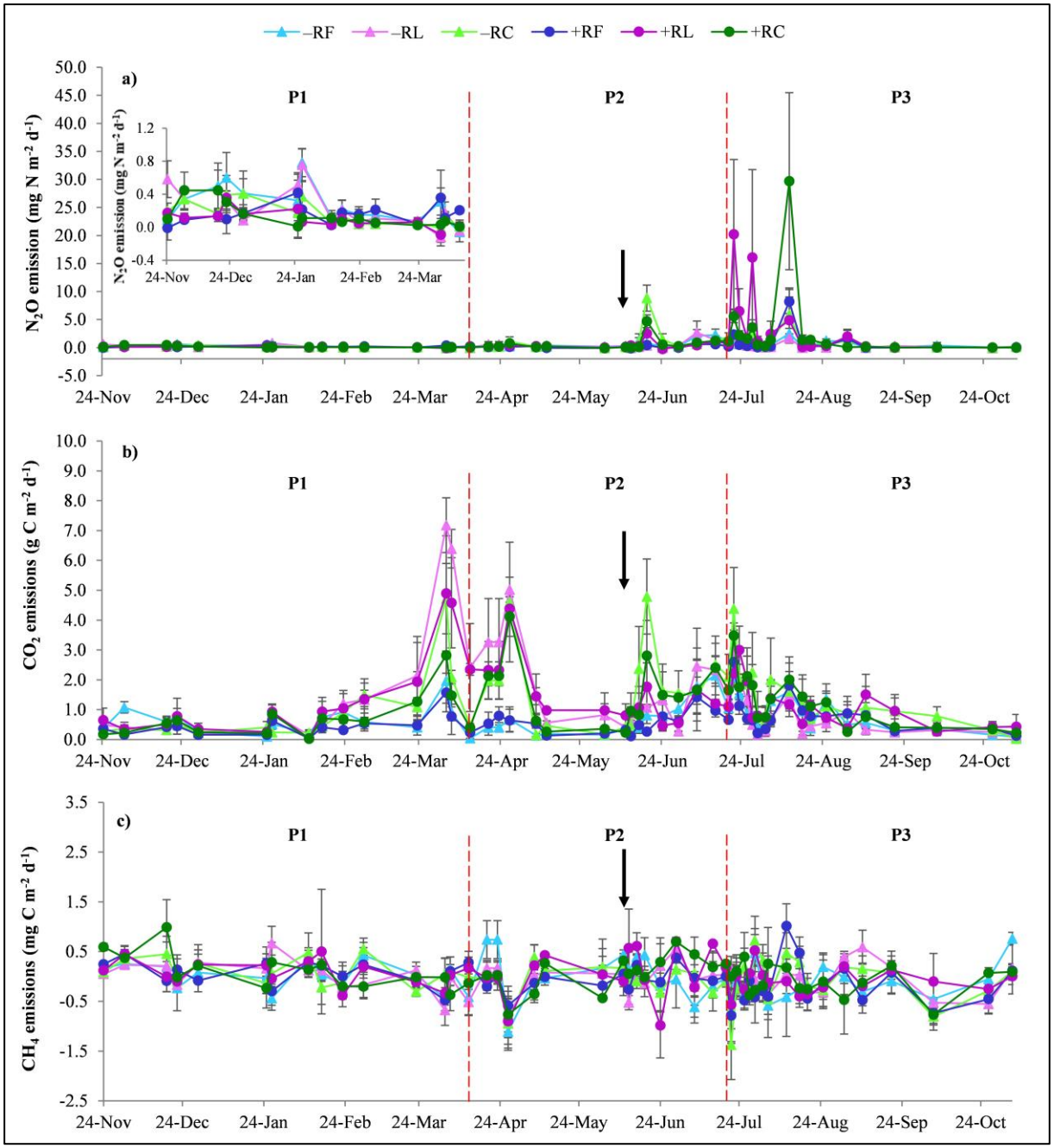

Figure 4.12. Daily fluxes of ***(a)*** *N_2O-N,* ***(b)*** *CO_2-C and* ***(c)*** *CH_4-C for the different maize residue (higher input, +R, and lower input, –R) and cover crop (cereal, C; legume, L; and bare fallow, F) treatments during the three experimental periods (P1, P2 and P3) in the N-fertilized area. Vertical lines denote standard errors of the means. The black arrow denotes maize sowing and the beginning of the irrigation.*

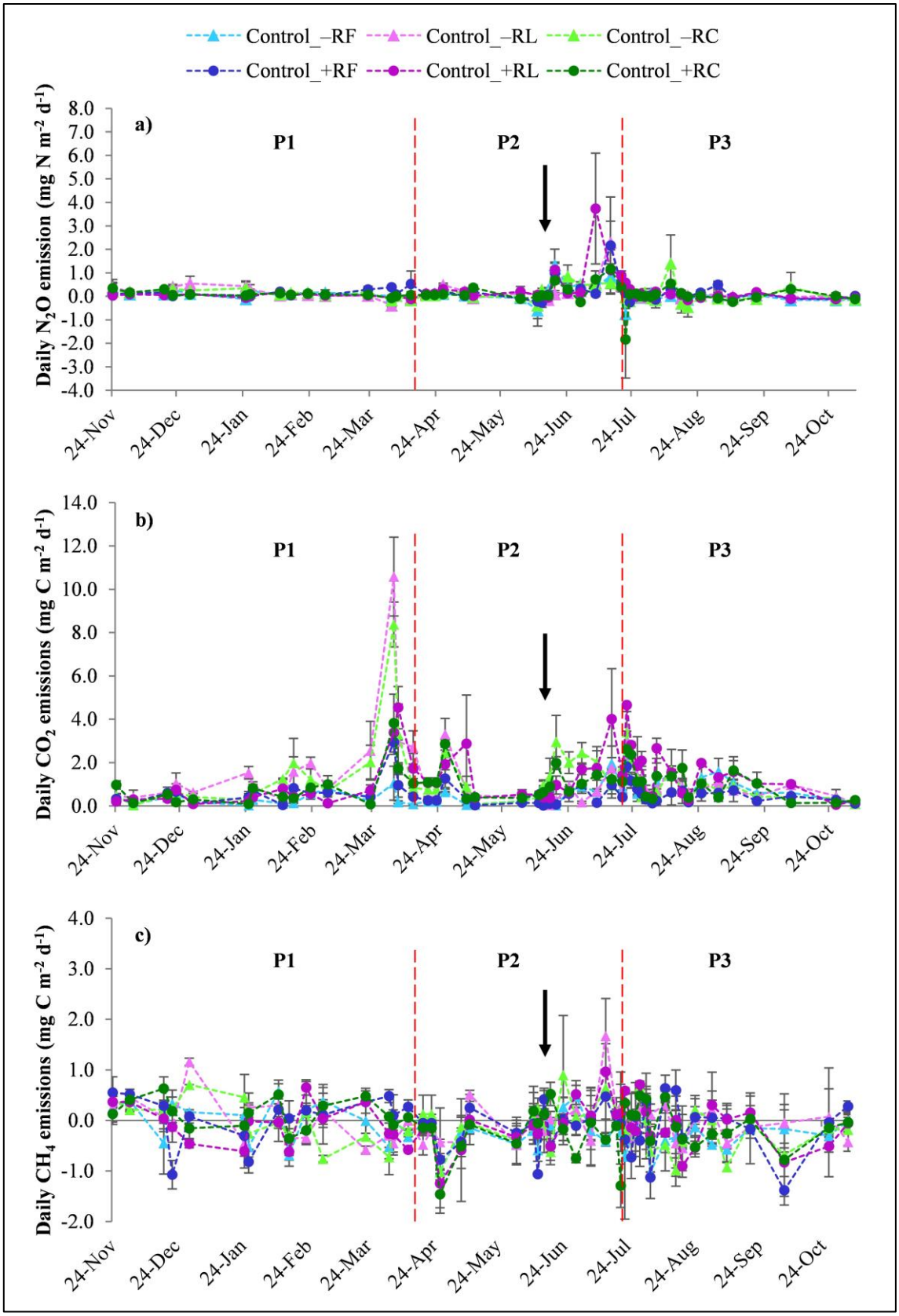

Figure 4.13. Daily fluxes of ***(a)*** *N_2O,* ***(b)*** *CO_2 and* ***(c)*** *CH_4 in the unfertilized control plots for the different maize residue (higher input, +R, and lower input, –R) and cover crop (cereal, C; legume, L; and fallow, F) treatments during the three experimental periods (P1, P2 and P3). Vertical lines denote standard errors of the mean. The black arrow denotes maize sowing and the beginning of irrigation.*

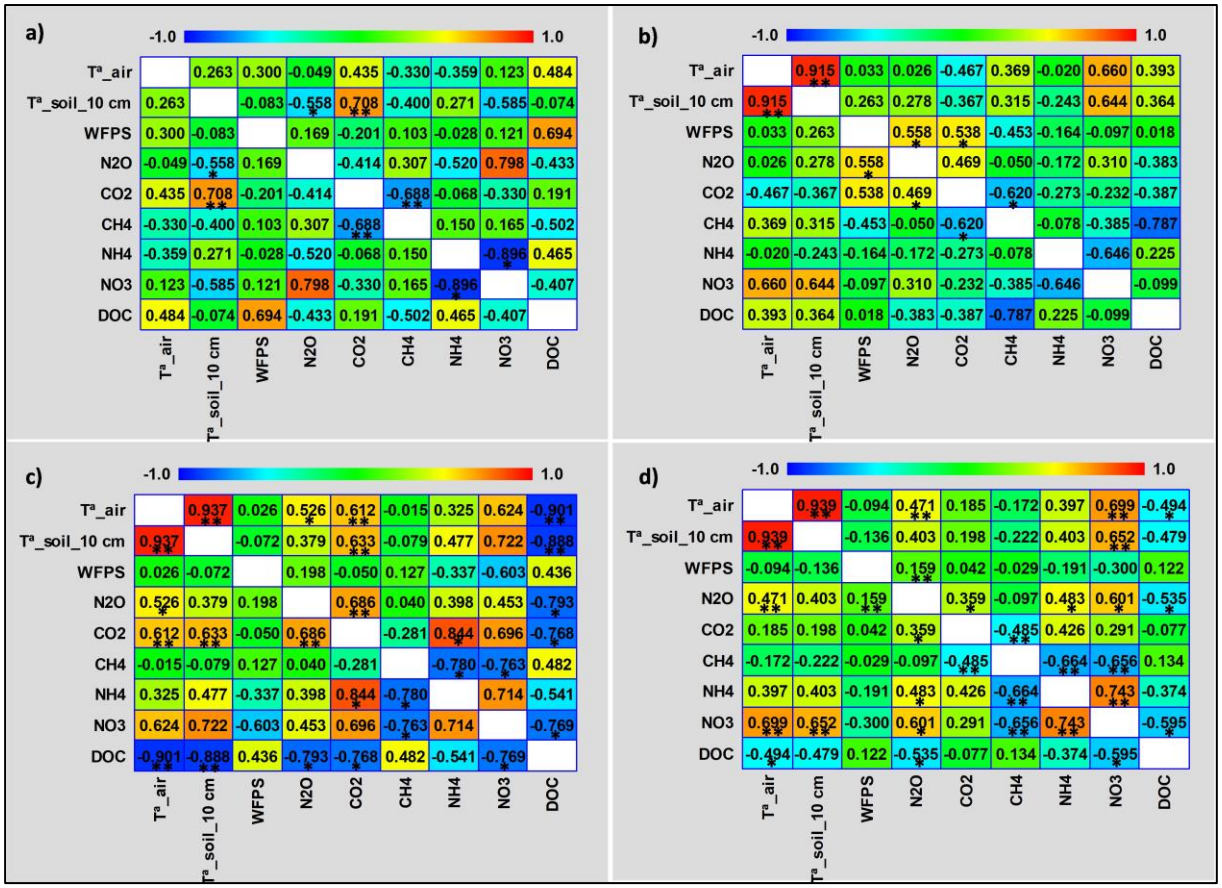

*Figure 4.14. Pearson correlation coefficients for the daily air and soil (at 10 cm depth) temperature, the daily N_2O, CO_2 and CH_4 fluxes, and daily soil properties (WFPS, NH_4^+, NO_3^- and DOC) analyzed over three experimental periods (**(a)** P1, **(b)** P2 and **(c)** P3, respectively) and over the whole experimental trial **(d)** in the N-fertilized area. The asterisks indicate the level of significance level (* P < 0.05, ** P < 0.01).*

4.2.3. CO_2 and CH_4 fluxes

Cumulative CO_2 emissions were only affected by cover crops before maize fertilization in the N-fertilized area (Table 4.13). At the end of the experiment, the total CO_2 emissions were respectively 77% and 105% higher for the cereal and legume cover crops than for bare fallow (Table 4.13). The cover crops influenced CO_2 emissions throughout the experiment in the unfertilized control area (Table 4.12). In the unfertilized area, the highest total cumulative CO_2 emissions were reported in control_L (119% higher than in control_F), followed by control_C (85% higher than in control_F) (Table 4.12). The highest input of maize residues only reduced CO_2 emissions during P1 in the control area (Table 4.12). The highest CO_2 fluxes were observed

in early spring, when they reached 7.2 g C m^{-2} d^{-1} in –RL (Figure 4.12b) and 10.6 g C m^{-2} d^{-1} in control_–RL (Figure 4.13b). Furthermore, CO_2 fluxes were increased after cover crop chemical termination and incorporation at the end of April and after intense rainfall and the beginning of irrigation in mid-June in both N-fertilized and control areas (Figure 4.12b and Figure 4.13b, respectively). In the N-fertilized area, the application of synthetic fertilizer also led to a CO_2 emissions peak. Cumulative CO_2 emissions at the end of the experiment were similar in the N-fertilized and control areas (average 301 ± 21 g C m^{-2}).

Daily CH_4 fluxes ranged from -1.46 to 1.67 mg C m^{-2} d^{-1} (Figure 4.12c), with no differences between maize residue management or cover cropping systems in the N-fertilized and control areas (Table 4.13 and Table 4.12, respectively). During P1, net cumulative CH_4 emissions were reported in both areas, while during P2 and P3, the soil acted as a CH_4 sink, with higher CH_4 consumption in the control area during P2 compared to the N-fertilized area. Considering the whole experimental period, the cumulative CH_4 oxidation rates in the control area were 7.5 times higher ($P < 0.05$) than those reported in the N-fertilized area (-31 mg C m^{-2} and -3.7 mg C m^{-1}, respectively).

Table 4.13. Cumulative CO_2-C and CH_4-C emissions over the three experimental periods (P1, P2 and P3) and total cumulative emissions at the end of the experiment for the different maize residue (higher input, +R, and lower input, –R) and cover crop (cereal, C; legume, L; and bare fallow, F) treatments in the N-fertilized area.

	CO_2 cumulative emissions (g C m^{-2})			**Total CO_2 (g C m^{-2})**	**CH_4 cumulative emission (mg C m^{-2})**			**Total CH_4 (mg C m^{-2})**
	P1	**P2**	**P3**		**P1**	**P2**	**P3**	
Maize residue	*P* = 0.239	*P* = 0.499	*P* = 0.703	*P* = 0.635	*P* = 0.905	*P* = 0.720	*P* = 0.979	*P* = 0.855
+R	102	108	84.5	295	14.0	0.30	-16.3	-1.98
–R	125	122	79.6	327	11.7	-1.39	-15.8	-5.48
S.E.	20	10	20.8	40	12.0	2.90	11.6	12.0
Cover crop	***P* = 0.005**	***P* = 0.003**	*P* = 0.570	***P* = 0.016**	*P* = 0.672	*P* = 0.746	*P* = 0.142	*P* = 0.480
C	103 a	138 b	101	342 b	16.8	-0.10	-16.1	0.59
F	68.3 a	56.0 a	69.3	194 a	9.3	-4.45	-20.8	-16.0
L	168 b	153 b	75.6	397 b	12.5	2.92	-11.2	4.20
S.E.	19.0	19.7	20.0	39	5.8	6.72	3.0	12.0
Maize residue × Cover crop	*P* = 0.962	*P* = 0.939	*P* = 0.869	*P* = 0.895	*P* = 0.912	*P* = 0.837	*P* = 0.648	*P* = 0.858

Different letters within columns denote significant differences ($P < 0.05$) between maize residue management or between cover crops by applying the LSD test. S.E.: standard error.

4.2.4. Mineral N and DOC

Maize stover management affected the NH_4^+ concentration during P1 in both the fertilized and control areas, with an average increase of 16.3% in +R compared to −R (Table 4.14and Table 4.15). The NH_4^+ concentration during P2 was significantly greater in L than in F and C in both areas (Table 4.14 and Table 4.15), with the highest values being reported 50 days after cover crop incorporation (12.6 ± 10.9 mg N kg^{-1} in −RL) (Figure 4.15a). Before maize N fertilization (P1 and P2), no differences were observed between the N-fertilized and control areas in terms of soil NH_4^+ (average 2.52 and 2.64 mg N kg^{-1}, respectively) and NO_3^- (average 4.55 and 12.2 mg N kg^{-1}, respectively) concentrations (Figure 4.10b,c). In the N-fertilized area, the average NO_3^- soil concentration during P2 was 44.5% lower in C compared to F and 52.7% lower in C than in L (Table 4.14).

Immediately after maize fertilization (P3), the mineral N concentration increased to 221 mg NH_4^+-N kg^{-1} in −RL and 212 NO_3^--N kg^{-1} in −RC and fell to levels similar to those reported before fertilization two weeks and two months after N fertilization for NH_4^+ and NO_3^-, respectively (Figure 4.15a and b, respectively). During P3, the F plots reported the lowest NH_4^+ concentrations (52% and 37% lower than L and C, respectively), and NO_3^- was 22.6% higher in −R than in +R in the N-fertilized area (Table 4.14). The mineral N content in the control area during P3 was similar to that registered in previous periods, without any significant differences between treatments (Table 4.15).

In the case of DOC concentrations, no significant differences were reported between the N-fertilized and control areas throughout the experimental year. In the fertilized area (Figure 4.15c), significant differences were only observed during P2, due to the interaction of the two factors (maize residue input and cover cropping), with lower DOC concentrations being registered on plots receiving lower inputs of maize residue (except for −RL) (Table 4.14). In

the control area, higher values were reported for the +R control plots than for the –R control plots during P1 and P3 (Table 4.15). In addition, the development of cover crops during P1 reduced the DOC values in control_C and control_L compared to control_F (by 34.5% and 20.8%, respectively), with the opposite happening during P2 (47.7% increase in control_L compared to control_F). The average DOC concentrations registered during P3 (16.6 and 16.3 mg C kg^{-1} in the fertilized and control areas, respectively) were both lower than those reported before maize fertilization (Table 4.14 and Table 4.15).

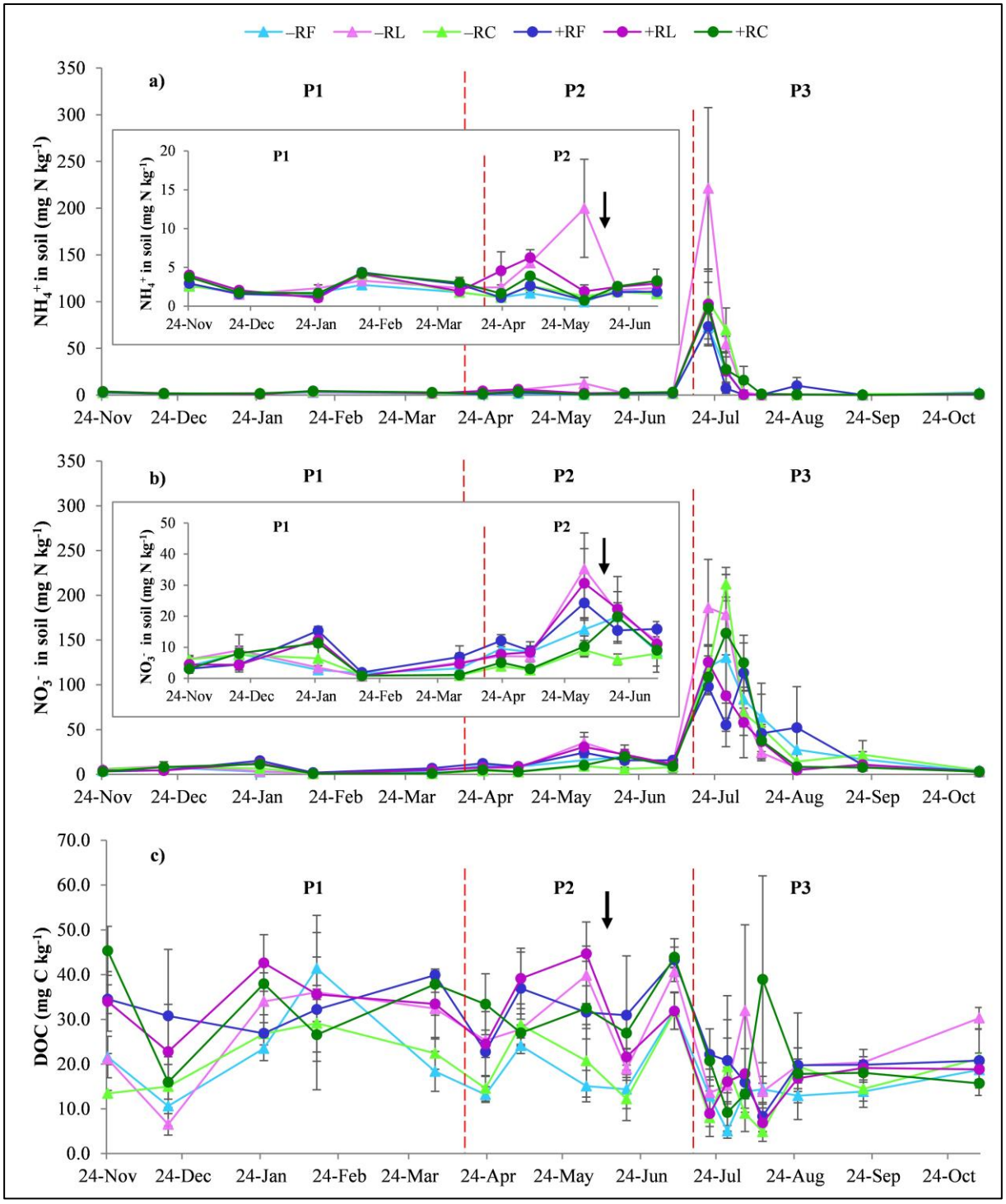

Figure 4.15. ***(a)*** *Soil NH_4^+-N,* ***(b)*** *soil NO_3^--N and* ***(c)*** *soil DOC concentrations for the different maize residue (higher input, +R, and lower input, –R) and cover crop (cereal, C; legume, L; and bare fallow, F) treatments during the three experimental periods (P1, P2 and P3) in the N-fertilized area. Vertical lines denote standard errors of the means. The black arrow denotes maize sowing and the beginning of irrigation.*

Table 4.14. Soil NH_4^+, NO_3^- and DOC concentrations over the three experimental periods (P1, P2 and P3) for the different maize residue (higher input, +R, and lower input, –R) and cover crop (cereal, C; legume, L; and fallow, F) treatments in the N-fertilized area.

	NH_4^+ concentration (mg N kg^{-1} soil)			**NO_3^- concentration (mg kg^{-1} soil)**			**DOC concentration (mg C kg^{-1} soil)**		
	Period 1	**Period 2**	**Period 3**	**Period 1**	**Period 2**	**Period 3**	**Period 1**	**Period 2**	**Period 3**
Maize residue	***P* = 0.023**	*P* = 0.074	*P* = 0.283	*P* = 0.069	*P* = 0.380	***P* = 0.015**	*P* = 0.140	*P* = 0.198	*P* = 0.444
+R	2.71 b	2.56	17.0	5.53	13.6	54.9 a	32.0	34.2	17.4
–R	2.33 a	2.33	26.7	4.39	11.6	67.3 b	22.5	25.5	15.8
S.E.	0.07	0.16	4.7	0.22	1.2	1.07	2.8	3.2	1.9
Cover crop	*P* = 0.184	***P* = 0.002**	***P* = 0.038**	*P* = 0.782	***P* = 0.006**	*P* = 0.606	*P* = 0.418	*P* = 0.056	*P* = 0.687
C	2.64	2.06 b	22.5 b	4.66	7.71 a	67.0	26.5	27.9	16.4
F	2.36	1.53 a	14.1 a	5.11	13.9 b	58.8	26.3	28.5	15.6
L	2.56	3.74 c	29.1 b	5.11	16.3 b	57.5	29.0	33.0	17.8
S.E.	0.12	0.35	3.9	0.52	1.37	7.0	1.5	1.4	1.8
Maize residue × Cover crop	*P* = 0.401	*P* = 0.441	*P* = 0.214	*P* = 0.344	*P* = 0.562	*P* = 0.711	*P* = 0.383	***P* = 0.044**	*P* = 0.107
+RC	2.89	2.42	20.1	4.89	9.5	64.0	32.8	32.5 b	19.1
+RF	2.59	1.63	13.1	6.34	15.3	54.1	31.2	35.6 b	18.2
+RL	2.64	3.62	17.9	5.36	16.0	46.6	32.1	34.3 b	14.9
–RC	2.38	1.70	24.9	4.43	5.9	70.0	20.2	23.3 a	13.8
–RF	2.12	1.44	15.0	3.88	12.5	63.5	21.4	21.4 a	13.1
–RL	2.47	3.86	40.3	4.87	16.6	68.5	25.9	31.8 b	20.7
S.E.	0.17	0.50	5.5	0.73	1.9	9.9	2.2	1.9	2.6

Different letters within columns denote significant differences ($P < 0.05$) between maize residue management or between cover crops by applying the LSD test. S.E.: standard error.

Table 4.15. Soil NH_4^+, NO_3^- and DOC concentrations over the three experimental periods (P1, P2 and P3) for the different maize residue (higher input, +R, and lower input, –R) and cover crop (cereal, C; legume, L; and fallow, F) treatments in the unfertilized control area.

	NH_4^+ concentration (mg N kg^{-1} soil)			**NO_3^- concentration (mg kg^{-1} soil)**			**DOC concentration (mg C kg^{-1} soil)**		
	P1	**P2**	**P3**	**P1**	**P2**	**P3**	**P1**	**P2**	**P3**
Maize residue	***P* = 0.022**	*P* = 0.210	*P* = 0.505	*P* = 0.840	*P* = 0.381	*P* = 0.081	***P* = 0.000**	*P* = 0.104	***P* = 0.003**
Control_+R	2.71 b	2.98	1.25	3.90	12.2	9.16	33.6 b	34.4	20.0 b
Control_–R	2.34 a	2.32	1.79	3.95	11.2	6.43	21.2 a	28.8	12.6 a
S.E.	0.08	0.33	0.54	0.19	0.7	0.92	0.8	2.1	1.1
Cover crop	*P* = 0.973	***P* = 0.021**	*P* = 0.417	***P* = 0.020**	***P* = 0.003**	*P* = 0.125	***P* = 0.001**	***P* = 0.041**	*P* = 0.117
Control_C	2.52	2.14 a	2.18	4.59 b	7.8 a	6.09	22.0 a	31.7 ab	15.4
Control_F	2.52	1.86 a	1.54	3.95 ab	12.1 b	7.38	33.6 c	25.4 a	14.7
Control_L	2.54	3.96 b	0.84	3.23 a	15.1 b	9.92	26.6 b	37.5 b	18.9
S.E.	0.10	0.41	0.66	0.24	0.9	1.13	1.1	2.5	1.3
Maize residue × Cover crop	***P* = 0.029**	*P* = 0.732	*P* = 0.608	*P* = 0.053	*P* = 0.443	*P* = 0.129	*P* = 0.434	*P* = 0.369	*P* = 0.294
Control_+RC	2.97 c	2.57	2.23	4.89	9.5	64.0	32.8	32.6	19.1
Control_+RF	2.73 bc	2.36	0.71	6.34	15.3	54.1	31.2	35.6	18.2
Control_+RL	2.44 ab	4.02	0.81	5.36	16.0	46.6	32.1	34.3	14.9
Control_–RC	2.08 a	1.70	2.13	4.43	5.9	70.0	20.2	23.3	13.8
Control_–RF	2.30 ab	1.37	2.37	3.88	12.5	63.5	21.4	21.4	13.1
Control_–RL	2.64 bc	3.90	0.88	4.87	16.6	68.5	25.9	31.8	20.7
S.E.	0.14	0.58	0.94	0.73	1.9	9.9	2.2	1.9	2.6

Different letters within columns denote significant differences ($P < 0.05$) between maize residue management or between cover crops by applying the LSD test. S.E.: standard error.

4.2.5. N uptake and yields in cover crops and maize

The average aboveground N uptake of cover crops was 53% higher (P = 0.071) in the legume than in the cereal cover crop, regardless of residue management (Table 4.16). The C:N ratio in the cereal cover crop was twice that in the legume cover crop, and the total aboveground biomass in barley was also higher than that in vetch ($0.1 < P < 0.05$). The differences between cover crop species in N content and in C:N ratio were intensified in the −R treatment (Table 4.16).

Table 4.16. Percentage of C and N, C:N ratio, aboveground N uptake (kg N ha^{-1}) and dry aboveground biomass (Mg ha^{-1}) of cover crops (cereal, C and legume, L) for the different maize residue management (higher input, +R, and lower input, –R) treatments in the N-fertilized area.

	C content (%)	**N content (%)**	**C:N ratio**	**Aboveground N uptake (kg N ha^{-1})**	**Total aboveground biomass (Mg D.M. ha^{-1})**
Maize residue	P = 0.191	P = 0.846	P = 0.078	P = 0.724	P = 0.729
+R	40.3	2.53	16.8	112	4.45
–R	40.8	2.44	21.1	105	4.63
S.E.	0.2	0.04	0.9	13	0.33
Cover crop	***P* = 0.048**	***P* = 0.000**	***P* = 0.000**	P = 0.071	P = 0.072
C	40.2 a	1.70 a	25.3 b	85.5	5.08
L	40.9 b	3.27 b	12.6 a	131.1	3.99
S.E.	0.2	0.08	1.5	13.2	0.32
Maize residue × Cover crop	P = 0.084	***P* = 0.001**	***P* = 0.018**	P = 0.618	P = 0.201
+RC	40.2	2.01 b	20.3 b	94.1	4.65
+RL	40.4	3.06 c	13.2 a	129.6	4.24
–RC	40.2	1.53 a	30.3 c	76.9	5.51
–RL	41.5	3.48 c	12.0 a	132.6	3.75
S.E.	0.3	0.06	1.33	18.7	0.45

Different letters within columns denote significant differences (P < 0.05) between maize residue management or between cover crops by applying the LSD test. D.M.: dry matter. S.E.: standard error.

The average maize grain yield in the N-fertilized area was 16.6 Mg ha^{-1} (Table 4.17). Legumes significantly reduced the grain yield by 7.9% and 9.5% compared to F and C, respectively. The

stover yield and the stover N content tended to be lower ($P < 0.1$) in the L-plots compared to C and F. The N yield in maize stover was also 16.3% and 19.3% lower in L compared to C and F, and the NUE was 149% and 151% higher in C and F compared to L, respectively. The grain N content and grain N uptake were strongly and negatively correlated with cumulative N_2O emissions after maize fertilization (r = -0.651, $P < 0.01$ and r = -0.485, $P < 0.05$, respectively) (Figure 4.16).

All the abovementioned parameters (yield, % N and N uptake) were higher when maize was grown in the N-fertilized area compared to the control area ($P < 0.01$). In contrast to the fertilized area, grain yield and N uptake in control_L were 28% and 40% higher than those in control_C and 30% and 46% higher than those in control_F, respectively. Furthermore, in unfertilized plots, both grain yield and grain N uptake were 17% and 22% higher in +R than in –R, respectively (Table 4.18).

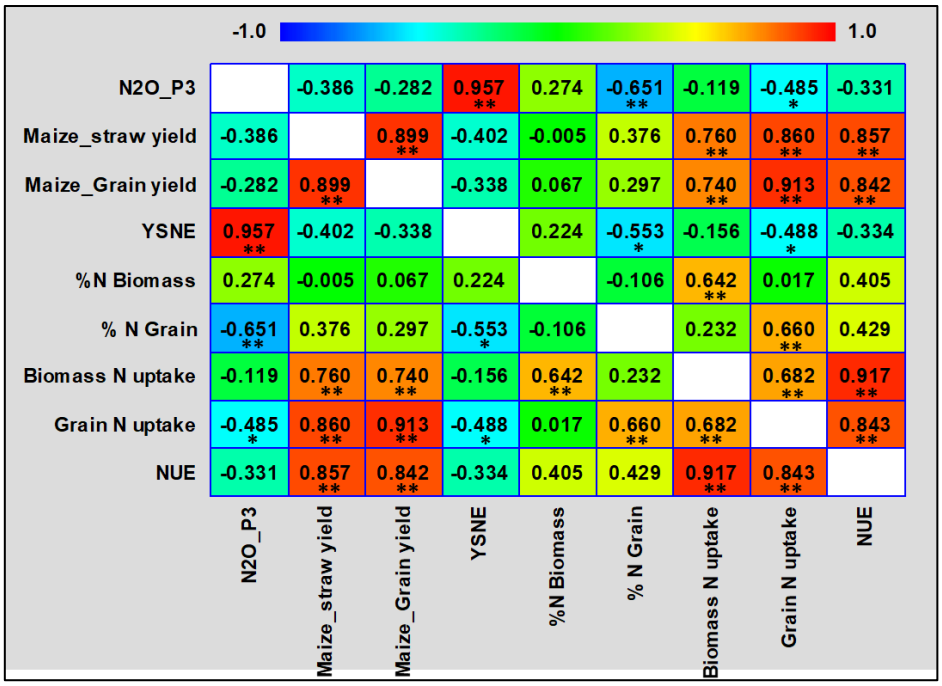

Figure 4.16. Pearson correlation coefficients for cumulative N_2O emissions after maize fertilization (N_2O_P3), and the yield maize parameters for the N-fertilized area. The asterisks indicate the levels of significance ($P < 0.05$, ** $P < 0.01$).*

Table 4.17. Maize yield, N content and N uptake in maize stover (aboveground biomass without grain) and maize grain, weight of 100 maize grains and NUE for the different maize residue (higher input, +R, and lower input, –R) and cover crop (cereal, C; legume, L; and bare fallow, F) treatments in the N-fertilized area.

	Stover yield (Mg ha^{-1})	**Grain yield (Mg ha^{-1})**	**100 grain weight (g)**	**N stover (%)**	**N Grain (%)**	**Stover N uptake (kg N ha^{-1})**	**Grain N uptake (kg N ha^{-1})**	**NUE (%)**
Maize residue	*P* = 0.334	*P* = 0.426	*P* = 0.965	*P* = 0.927	*P* = 0.012	*P* = 0.246	*P* = 0.197	*P* = 0.107
+R	16.2	16.2	37.8	0.54	0.99 a	86.0	160	37.9
–R	17.7	17.0	37.9	0.54	1.03 b	95.8	176	57.3
S.E.	0.9	0.6	0.9	0.02	0.00	4.2	6	4.9
Cover crop	***P* = 0.066**	***P* = 0.046**	*P* = 0.449	*P* = 0.079	*P* = 0.835	***P* = 0.011**	*P* = 0.340	***P* = 0.000**
C	17.7 b	17.3 b	38.5	0.56 ab	1.00	98.4 b	173	63.2 b
F	16.7 ab	17.0 b	37.3	0.57 b	1.01	94.9 b	172	54.1 b
L	16.1 a	15.6 a	37.9	0.50 a	1.02	79.4 a	160	25.4 a
S.E.	0.4	0.4	0.6	0.02	0.02	3.5	7	3.7
Maize residue × Cover crop	*P* = 0.172	*P* = 0.221	*P* = 0.259	*P* = 0.401	*P* = 0.696	*P* = 0.112	*P* = 0.407	*P* = 0.271

Different letters within columns denote significant differences ($P < 0.05$) between maize residue management or between cover crops by applying the LSD test. S.E.: standard error.

Table 4.18. Maize stover (aboveground biomass without grains) and grain yield, weight of 100 maize grains, N content and N uptake in maize stover and maize grain and yield scaled N_2O emissions (YSNE) in the different maize residue (higher input, +R, and lower input, –R) and cover crop (cereal, C; legume, L; and bare fallow, F) treatments in the unfertilized control area.

	Stover yield (Mg ha^{-1})	**Grain yield (Mg ha^{-1})**	**100 grain weight (g)**	**N stover (%)**	**N Grain (%)**	**Stover N uptake (kg N ha^{-1})**	**Grain N uptake (kg N ha^{-1})**	**YSNE (g N kg grain^{-1})**
Maize residue	*P* = 0.895	***P* = 0.008**	*P* = 0.171	*P* = 0.185	*P* = 0.368	*P* = 0.225	***P* = 0.019**	*P* = 0.481
Control_+R	11.4	11.8 b	35.1	0.50	0.93	56.4	110 b	0.04
Control_–R	11.4	10.1 a	32.5	0.41	0.89	47.4	91 a	0.04
S.E.	0.4	0.3	1.2	0.04	0.03	4.7	4	0.00
Cover crop	***P* = 0.047**	***P* = 0.002**	*P* = 0.176	*P* = 0.815	*P* = 0.212	*P* = 0.272	***P* = 0.004**	*P* = 0.365
Control_C	11.0 a	10.1 a	32.6	0.45	0.89	49.2	90 a	0.04
Control_F	10.6 ab	9.9 a	32.5	0.44	0.87	46.3	86 a	0.04
Control_L	12.6 b	12.9 b	36.4	0.48	0.97	60.2	125 b	0.05
S.E.	0.80.5	0.4	1.4	0.05	0.04	5.7	5	0.00
Maize residue × Cover crop	*P* = 0.848	*P* = 0.465	*P* = 0.856	*P* = 0.525	*P* = 0.458	*P* = 0.568	*P* = 0.337	*P* = 0.100

Different letters within columns denote significant differences ($P < 0.05$) between residue management or between cover crops by applying the LSD test. S.E.: standard error.

4.2.6. Discussion

4.2.6.1. Maize residue input as a key driver of N_2O fluxes

In line with the first hypothesis, during P1 and P2, the higher inputs of maize residue (+R) resulted in a significant reduction in soil N_2O emissions compared to the plots from which residues were removed (−R). This was consistent with the negative relationship that is frequently found between the return of crop residues with high C:N ratios, such as maize residues, and N_2O emissions (Abalos et al., 2022b; Chen et al., 2013; Hu et al., 2019). The abatement of N_2O emissions when high C:N ratio residues (> 30) are incorporated has been associated with a decrease in soil mineral N levels as a result of their immobilization during residue degradation (Chen et al., 2013). This immobilization has a detrimental effect on the nitrification and denitrification processes, which are the main processes controlling soil N_2O production (Ussiri and Lal, 2013).

In contrast to the results obtained before fertilization, the cumulative N_2O emissions during P3 were 170% higher on the +R than on the −R plots (Figure 4.11a-c). This was probably because coupled nitrification-denitrification was favored when it was combined with: i) the incorporation of large amounts of C:N crop residue from maize (Sarkodie-Addo et al., 2003); ii) the addition of easily available NH_4^+-N and NO_3^--N via synthetic fertilization; iii) the irrigation of the cash crop, with the consequent increase in soil moisture, which favors mineralization (Elrys et al., 2021) and other biochemical processes involved in the release of N_2O (Butterbach-Bahl et al., 2013) (Figure 4.9b); and iv) the warm soil and air temperatures registered in the summer season during the cash crop phase (Figure 4.9a), which are positively related to microbial activity and N_2O emissions (Ussiri and Lal, 2013). This increase in microbial activity during the summer season was supported by the correlations reported in P3 between CO_2 and air and soil temperature ($P < 0.01$; r = 0 .612 and r = 0.633, respectively) and

between N_2O emissions and air temperature ($P < 0.05$; r = 0.526) (Figure 4.14c). Purportedly greater microbial activity on the plots with the highest residue inputs was supported by lower soil mineral N concentrations (in comparison with those with low topsoil residue inputs) (Table 4.14) during P3.

The results obtained indicate that any potential benefits relating to N_2O mitigation deriving from the topsoil retaining residues during the intercrop period (P1 and P2) (Figure 4.11a,b) were no doubt offset by increased N_2O emissions during the cash crop phase (Figure 4.11c). Thus, the N_2O emissions after cash crop fertilization had an important influence on total N_2O losses (i.e., cumulative emissions after fertilization represented up to 75% and 38% of total N_2O emissions in +R and –R, respectively).

4.2.6.2. Influence of cover cropping on N_2O fluxes

Contrary to the initial hypothesis, using different cover cropping systems during the growing period had no effect on N_2O emissions (P1, Figure 4.11a). Greater fluxes would, however, have been expected from plots with legume cover crops, as reported by Sanz-Cobena et al. (2014a), as a consequence of the capacity of legumes to fix atmospheric N_2 and thus influence the balance between soil N uptake and release. The meta-analysis by Basche et al. (2014) also revealed that using legume species as cover crops had a positive relationship with N_2O emissions when no additional N was applied. However, no significant differences in soil mineral N values were observed between the cover crops during their growing phase (P1, Table 4.14). This could explain similar results for N_2O emissions during this same period. In line with the results found in this study, Basche et al. (2014) suggested that the growth periods of cover crops were responsible for reduced effects in terms of N_2O emissions compared to those following their incorporation and decomposition, or the cash crop phase. This could be related

to the limiting low temperatures usually reported during the winter season, which coincide with cover crop growth (Ussiri and Lal, 2013).

Although it is frequently observed that the incorporation of legume cover crop residue increases N_2O emissions compared to that from nonlegume species (Muhammad et al., 2019), the opposite was observed in the present study during P2. During that period, the cereal cover crop produced higher cumulative emissions than the legume after their incorporation (Figure 4.11b); this contradicted the second hypothesis. The highest N_2O fluxes observed during this period occurred in mid-June (Figure 4.12a), immediately after soil rewetting. They were a consequence of several days of rainfall and of the beginning of cash crop irrigation resulting in a significant increase in WFPS, which coincided with warmer soil and air temperatures (Figure 4.9). In fact, WFPS was the only variable that significantly correlated with N_2O emissions during this period ($r = 0.558$, Figure 4.14b). Furthermore, the average WFPS values during P2 were 8 % and 7% significantly higher in barley compared to the fallow and vetch subplots respectively (data not shown). This increase in WFPS, together with the greater amount of aboveground biomass and higher C:N ratio in barley crop compared to that of vetch (Table 4.16), could have stimulated N_2O production after rewetting (Barrat et al., 2021). Previous findings have reported higher N_2O emissions associated with less recalcitrant and lower C:N residues (Abalos et al., 2022a) due to the higher N availability from their mineralization. Indeed, during this decomposition period after cover crop termination, the rapid mineralization of the low C:N ratio vetch biomass (< 25) provided N in excess of the microbial N demand (Shan and Yan, 2013). This resulted in higher soil mineral N levels in the legume than in the nonlegume cover crop, in both the N-fertilized and control areas (Table 4.14and Table 4.15, respectively). These results suggest that this known and widely accepted pattern could be different in semiarid areas in which rewetting episodes are key drivers of annual N_2O emissions. These N_2O hot moments after rewetting could mainly be driven by denitrification (Butterbach-Bahl et al.,

2013; Montoya et al., 2022). As a result, under the conditions of the present study, the greater aboveground biomass, C:N ratio and easily available C in the cereal residue along with the higher WFPS values, may have promoted levels of anaerobicity and denitrification during rewetting events (Zhijie Li et al., 2021). These conditions may have exceeded the effects of the greater N release from the decomposition of the legume residue.

As previously reported by Guardia et al. (2016a), no significant differences between cover cropping systems regarding N_2O emissions were observed after integrated N fertilization. However, the higher C:N ratio for the aboveground barley biomass compared to that of vetch (Table 4.16) and the presence of readily decomposable carbon substrate for heterotrophic denitrifiers in immature residues (such as those from cover crops) could explain the numerically higher N_2O emissions from the barley plots than from the vetch and fallow plots (Abalos et al., 2022b; Butterbach-Bahl et al., 2013). It is important to highlight that incorporating vetch is a good strategy for mitigating the carbon footprint because it reduces the need for synthetic N fertilization and therefore upstream emissions associated with the industrial production of fertilizers (Guardia et al., 2019).

4.2.6.3. Legacy effect of synthetic N on N_2O emissions

In the present cover cropping field experiment, fertilized and unfertilized cash crop areas were established together with residue input and cover crop factors. This made it possible to shed light on the relevant residual N carry-over effect associated with intensively managed cash crops and the role of catch crops in surplus N recycling. The differences in cumulative N_2O emissions observed between the two areas during P2 were not as notable as those during P1 ($P < 0.05$ and $P < 0.1$ in P1 and P2, respectively) (Figure 4.10a). Thus, although there was no significant difference between the two areas in terms of soil mineral N (Figure 4.10b, c), the legacy effect of the N applied in the previous cropping season would have influenced the N_2O

emissions, especially at the beginning of the experiment, which is in line with the initial hypothesis.

On average, 59% of the total cumulative N_2O emissions were produced during P3 (i.e., after maize N fertilization) in the N-fertilized area (Figure 4.11c,d), while only 5% were emitted during P3 in the control area (Table 4.12). These results support those of Ferrari Machado et al. (2021), who identified N from fertilization as the dominant source of N_2O in studies involving crop residues.

Overall, no significant differences in N_2O EFs were reported in relation to maize residue management or cover cropping, despite barley cover crops and the incorporation of maize stover tending to increase them (Figure 4.11f). The average EF (0.64 ± 0.11%) observed in the present study was below the 0.91% average N_2O EF associated with cropping systems subjected to sprinkler irrigation under Mediterranean conditions (Cayuela et al., 2017), and was similar to the IPCC default value of 0.5% for dry climates (IPCC, 2019b).

4.2.6.4. Effects on soil respiration and CH_4 fluxes

CO_2 emissions are highly dependent on soil microbial activity, which tends to increase with moderate soil temperature and is negatively affected by low water content (Nilahyane et al., 2020). The present study revealed an interannual variation in CO_2 fluxes (Figure 4.12b and Figure 4.13b). Furthermore, and as predicted by Barnard et al. (2020), a peak in CO_2 emissions was observed in both the N-fertilized and control areas for the cover crop plots (vetch and barley) in mid-June. This was a consequence of the soil rewetting after the first intense spring rainfall, the onset of irrigation preceded by mild temperatures registered in the spring season (Figure 4.9**a**), and the incorporation of the cover crop in the topsoil. However, soil respiration decreased from mid-summer (at the beginning of P3), when the soil temperature increased (>25°C), thus limiting soil microbial activity. Opposite to the results reported by Wang et al.

(2019), no differences between the control and the N-fertilized area were reported for any of the three periods relating to average cumulative CO_2 fluxes. This suggests that respiration was not affected by N addition, which is contrary to what has been previously reported (Wang et al., 2019). This may indicate that root biomass and respiration were similar in fertilized and non-fertilized plots, and that soil moisture and soil temperature were the key drivers of ecosystem respiration fluxes.

Net methanogenic activity was reported in both areas during P1 (Table 4.12 and Table 4.13), when the lowest soil and air temperatures were registered. These results were in line with the review by Shukla et al. (2013), who observed that CH_4 oxidation was reduced when soil temperatures in many temperate areas fell below 5°C, with this being a result of reduced gas diffusion and physiological stress. The total cumulative CH_4 fluxes at the end of the experiment were negative in both the N-fertilized (Table 4.13) and control (Table 4.12) areas. This suggests that there was an overall sink effect for CH_4, regardless of the maize residue management or cover cropping system. Similar results have been reported by Guardia et al. (2016a) and Sanz-Cobena et al. (2014a) in field experiments conducted under similar climatic conditions. In accordance with the meta-analysis carried out by Wu et al. (2022) and with field studies involving irrigated maize (Huérfano et al., 2015), an 88% decrease in soil CH_4 consumption was observed in the N-fertilized area compared to the control area. This would suggest that the addition of N significantly reduced the rate of CH_4 uptake by the soil. The recent meta-analysis by P. Li et al. (2023) reported a significant decrease in cumulative CH_4 emissions associated with higher rates of straw input. However, similar to Wegner et al. (2018) in a corn–soybean rotation, no significant effect was reported for CH_4 fluxes between maize residue management systems or cover crops.

4.2.6.5. Maize yield, YSNE and NUE

As expected, the objective of enhancing maize yield when applying N via synthetic fertilization was evidently achieved (Table 4.17 and Table 4.18). However, the higher cumulative N_2O emissions in the N-fertilized area (Figure 4.10a) drove the YSNE, resulting in them being significantly higher in fertilized plots (average 0.11 g N kg grain^{-1}, Figure 4.11f) compared to those in the control area (average 0.04 g N kg grain^{-1}, Table 4.18). Maize stover management did not affect the maize yield parameters in the fertilized area (Table 4.17). However, on the unfertilized plots, there was a 17% increase in grain yield and a 22% increase in grain N uptake on the +R compared to the −R plots (Table 4.18). This supports the findings of the global meta-analysis carried out by P. Li et al. (2023), who reported overall increases in both crop yield and NUE, by 9% and 23%, respectively. It also suggests that the incorporation of maize stover successfully provided mineral N to the subsequent crop, although its effects were masked when N was applied via fertilization. Long-term experiments have also reported increases in maize yields after several years of stover incorporation (Urra et al., 2018).

The maize grown on vetch plots received the lowest mineral N via integrated soil fertility management (i.e., 170 kg N ha^{-1}) but produced the lowest grain ($P < 0.05$) and stover ($P < 0.10$) yields, as well as the lowest NUE values (Table 4.17). These differences were not related to grain weight but to the total number of grains on each cob (Table 4.17). These results were in line with those reported by Abdalla et al. (2019), who found that cover crops (both legumes and nonlegumes) reduced cash crop yields by around 4%, while the combination of legume and nonlegume cover crops increased cash crop yields by about 13%. The meta-analysis by Tonitto et al. (2006) also found that replacing fallow with a legume cover crop resulted in negative yield or had no effect on production. These yield penalties on vetch plots highlight the challenge inherent when trying to optimize integrated N management and to accurately predict the supply

of N from the decomposition of legume residues. The incorporation of low C:N residues from cover crops, and particularly legume cover crops, can produce a very rapid release of mineral N when cash crop N uptake is still low (Drinkwater et al., 2000). The amount of plant available N obtained from cover crops would then not be efficiently taken up and maize yields could be reduced in comparison with treatments involving greater N inputs via N fertilization at top-dressing coinciding with the highest crop demand and N acquisition potential. However, in the unfertilized control area, the maize grown after the legume cover crop produced the highest yields and N uptake rates (Table 4.18). These results confirmed the potential benefits of including legumes in rotations (Gou et al., 2023) and the need to appropriately integrate the N supplied by synthetic fertilization and legume residues in order to reduce the C footprint of croplands and avoid yield penalties.

4.2.6.6. Uncertainties and future research

For the first time, this one-year study sheds light on the interaction between cover cropping and the amount of cash crop residue in the N legacy. However, N_2O fluxes are often strongly driven by environmental conditions and this is the case with many rainfed Mediterranean croplands, which may exhibit large degrees of year-on-year variability (Lassaletta et al., 2021), as occurred at the experimental site highlighted in this study (Table 4.19). Under the conditions of this experiment, small influence of this variability could have been expected during the maize cropping phase (P3), since the meteorological and management conditions produced optimum conditions for the microbial communities commonly involved in nitrification, denitrification and mineralization (Zhaolei Li et al., 2021; Ussiri and Lal, 2013). This occurred and was the result of warm temperatures in summer and the presence of sufficient soil moisture due to water being supplied through irrigation. During the cover cropping phase (P1), meteorological conditions are often more unpredictable, but high N_2O emissions are usually prevented by low soil temperatures (Aguilera et al., 2013b). Relating to this point, a random-meta-forest analysis

conducted by Y. Li et al. (2023a) revealed that emissions from cover cropping systems were mainly driven by soil pH, N and SOC contents rather than by other variables, such as climate. However, after cover crop termination, temperature and soil moisture would seem to be the key drivers responsible for N release from labile residues, which is something that tends to occur to a significant degree in the first months after termination (Nyabami et al., 2023). They also influence the magnitude of N_2O peaks after rewetting, with these being intensified by intense periods of drought (Barrat et al., 2021). Even though the temperatures and amount of rainfall before the maize crop was sown were close to 15-year average values (Table 4.19), we hypothesize that extremely low and high quantities of rainfall during P2 could have resulted in lower than normal N_2O losses, respectively due to the reduced mineralization of crop residues and to the lower intensity of rewetting events. However, this will need to be confirmed in future multi-year field studies. Furthermore, it will be necessary to quantify the specific contributions made by nitrification, bacterial/fungal denitrification (which is relevant during N_2O rewetting pulses) and nitrifier denitrification through, e.g., site preference, is still needed (Wei et al., 2023; Wrage-Mönnig et al., 2018). It would also be relevant to study the dynamics of C and N mineralization (through ^{13}C and ^{15}N-labeled residues) in order to find ways of overcoming the limitations of integrated soil fertility management. It is therefore recommended to include the soil mineral N concentrations after cover cropping in calculations of N emission rates resulting from integrated fertilization. This is also strongly recommended in order to avoid potential yield penalties of the type reported in this study (Table 4.17).

Table 4.19. Cumulative rainfall, mean air temperature, average minimum and maximum temperature, absolute minimum and maximum temperature and evapotranspiration during every month corresponding to the cover crop phase of the experiment (November to June) and during the whole cover crop phase in the experimental year (2020/2021) and during the fifteen years before the experiment (2006-2020). Data in brackets indicate the minimum and maximum values of each parameter

		November	**December**	**January**	**February**	**March**	**April**	**May**	**June**	**Cover crop phase**
Cumulative Rainfall (mm)	2020/2021	59	21	32	47	4	69	12	33	277
	2006-2020	48 (8 - 128)	33 (4 - 128)	31 (7 - 71)	33 (1 - 102)	41 (4 - 137)	51 (10 - 137)	51 (10 - 89)	25 (2 - 57)	303
Mean T^a (˚C)	2020/2021	9.7	6.7	2.3	9.2	9.7	12.1	17.2	21.9	11.1
	2006-2020	8.8 (6.2 - 11.2)	5.3 (3.7 - 7.7)	5.0 (3.6 - 7.7)	6.5 (4.1 - 8.8)	9.6 (8.2 - 10.7)	12.8 (11.1 - 15.2)	16.9 (13.6 - 18.8)	21.8 (19.8 - 24.8)	10.9
Average Min. T^a (˚C)	2020/2021	4.9	1.9	-2.8	4.2	2.2	6.3	8.8	13.9	4.9
	2006-2020	3.4 (-1.5 - 7.3)	0.2 (-2.1 - 3.7)	0.0 (-3.8 - 3.4)	0.6 (-4.0 - 3.6)	2.9 (0.9 - 4.5)	6.1 (3.7 - 7.8)	9.2 (6.2 - 10.8)	13.2 (11.5 - 15.8)	4.4
Average Max. T^a (˚C)	2020/2021	15.8	11	8.1	15	17	18.3	24.8	29.4	17.4
	2006-2020	15.2 (13.0 - 18.1)	11.7 (10.0 - 14.8)	11.0 (8.5 - 12.8)	13.0 (10.4 - 16.3)	16.4 (12.9 - 19.2)	19.5 (16.7 - 23.0)	24.2 (20.5 - 26.9)	29.5 (27.1 - 32.8)	17.6
Absolute Min. T^a (˚C)	2020/2021	-1.8	-5	-16.3	0.6	-3.6	0	3.9	10	-1.5
	2006-2020	-3.7 (-9.7 - 1.5)	-6.3 (-10.9 - -2.4)	-6.4 (-11.9 - -2.3)	-4.8 (-9.6 - -2.0)	-2.9 (-4.7 - 0.0)	0.1 (-2.5 - 5.4)	2.9 (-0.3 - 6.2)	7.2 (4.7 - 9.9)	-1.7
Absolute Max. T^a (˚C)	2020/2021	21.5	16.6	18.8	19.5	23.8	23.7	32.5	35	23.9
	2006-2020	21.6 (18.6 - 24.4)	16.8 (15.3 - 18.8)	16.7 (14.0 - 19.6)	19.3 (15.5 - 22.4)	23.5 (16.5 - 26.9)	26.4 (22.5 - 28.9)	31.7 (26.4 - 35.1)	36.7 (33.7 - 40.3)	24.1
ET^o (mm)	2020/2021	28	29	23	40	81	83	147	169	75
	2006-2020	36 (28 - 49)	25 (19 - 30)	31 (26 - 35)	46 (40 - 62)	81 (61 - 99)	105 (84 - 129)	147 (113 - 174)	176 (152 - 196)	81

4.3. Experiment 3 – Contribution to N_2O emissions and N fate of crop residues and fertilizer N in a cover crop-maize rotation. A ^{15}N–tracing study

4.3.1. Meteorological conditions, soil mineral N and DOC

The cumulative rainfall during the experiment (from mid-November 2020 to mid-November 2021) was 417 mm, with a cumulative rainfall of 230 mm and 187 mm during P1 and during P2, respectively. The average temperature during the experimental year was 14.3 ºC, with minimum and maximum air temperatures of −16.3 °C and 41.6 °C, respectively, reported in mid-January and mid-August (Figure 4.17a). The average WFPS ranged from 13% to 52% before maize irrigation (i.e., during the cover cropping period), and from 15% to 64% during the maize irrigation period (Figure 4.17b).

The average soil NH_4^+ concentrations increased after maize fertilization, rising from 4 mg N kg^{-1} to 67 mg N kg^{-1}, and then decreased to baseline levels three weeks after fertilization (Figure 4.17c). Cover crops did not influence soil NH_4^+ concentrations throughout the whole experimental period (Figure 4.18a). Soil NO_3^- concentrations also increased after maize fertilization, reaching 122, 146 and 110 mg N kg^{-1} in F, V and B treatments, respectively, 4 to 9 days after fertilization. The soil NO_3^- concentration remained above 40 mg N kg^{-1} for 3 weeks in all cover cropping treatments, decreasing to baseline levels five weeks after maize fertilization in all treatments (Figure 4.17d). Before maize fertilization, the barley microplots reported the lowest soil NO_3^- concentration (average 7.2 mg N kg^{-1}) (Figure 4.18b). The average soil NO_3^- concentration in V during P2 (82.0 mg N kg^{-1}) was 36% and 33% higher compared to F and B, respectively ($P < 0.05$). No significant differences were observed in soil DOC between treatments (Figure 4.18c).

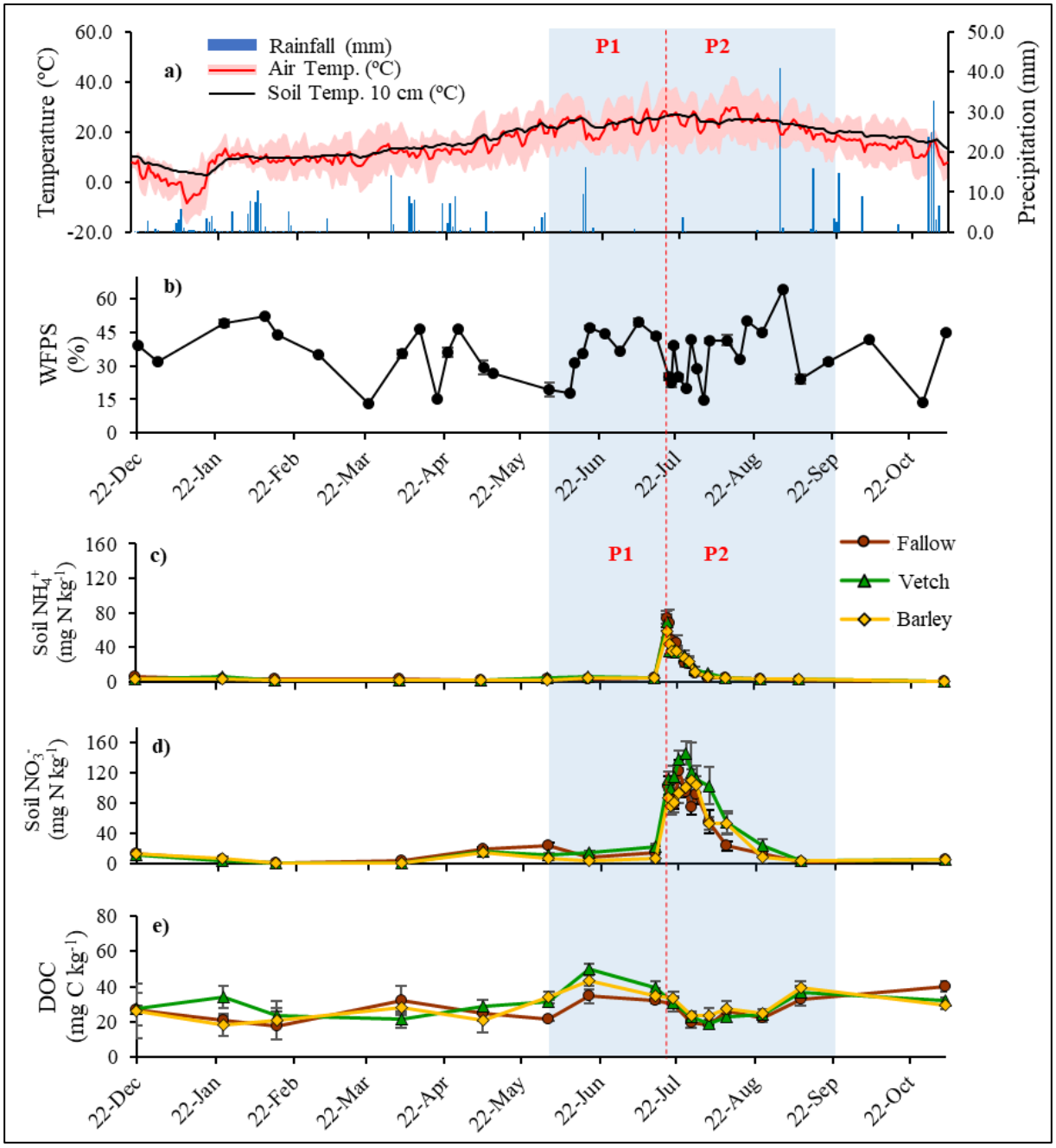

*Figure 4.17. Daily meteorological parameters (precipitation, average air temperature and average soil temperature at 10 cm depth). The reddish area corresponds to the daily thermal amplitude **(a)**; topsoil (10 cm depth) water-filled pore space (WFPS) **(b)**; daily soil NH_4^+, NO_3^- and DOC concentrations (**c**, **d** and **e**, respectively) before (P1) and after maize fertilization (P2) in the different cover crop treatments (bare fallow, F, vetch, V, and barley, B). Vertical bars denote the standard error of the mean (n = 3 in P1, n = 9 in P2). The dotted red line indicates the maize top-dressing fertilization date (19 July 2021) corresponding to the transition from P1 to P2. The blue shadow area corresponds with the maize irrigation period.*

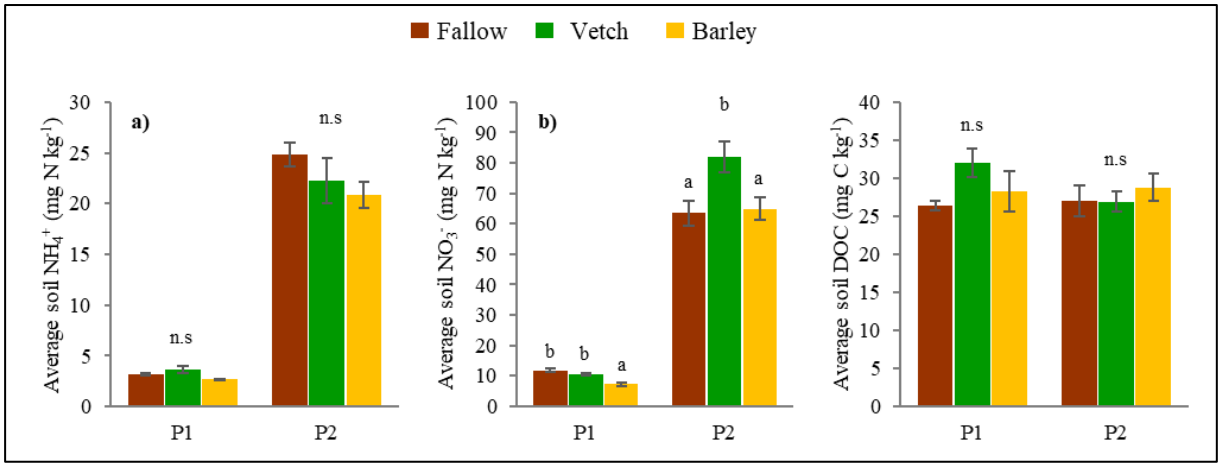

Figure 4.18. Average soil NH_4^+ ***(a)****, NO_3^-* ***(b)*** *and DOC* ***(c)*** *concentrations in the different cover crop treatments (bare fallow, vetch, and barley) before (P1) and after maize fertilization (P2). The vertical lines denote the standard error of the mean (n = 3 in P1, n = 9 in P2). Different letters within each period denote statistical differences (P < 0.05) between cover crop treatments in each period by applying the LSD test. n.s.: no significant difference.*

4.3.2. N_2O and CO_2 emissions

Before maize fertilization, most daily N_2O fluxes were below 0.5 mg N m^{-2} d^{-1} (Figure 4.19a). During P1, the average accumulated N_2O emission was 57.9 mg N m^{-2}, with no statistical differences between cover cropping treatments (Figure 4.19c). During this period, daily N_2O emissions were positively correlated with WFPS (r = 0.53; $P < 0.01$), CO_2 emissions (r = 0.53; $P < 0.05$), and soil NH_4^+ (r = 0.77; $P < 0.05$) (Figure 4.20a).

The highest N_2O emission flux during Period 2 (9.6 mg N m^{-2} d^{-1}) was reported one week after maize fertilization (Figure 4.19a). Four weeks after fertilization, emissions dropped below 0.5 mg N m^{-2} d^{-1}, with a short-term increase at the beginning of September, immediately following a 41 mm rainfall event (Figure 4.17a). The average accumulated N_2O emission flux during P2 was 98.0 mg N m^{-2}, with no significant differences between cover cropping treatments (Figure 4.19c). During both P1 and P2, vetch was the cover cropping treatment with the highest numerical accumulated N_2O emissions, being statistically significant ($P < 0.05$) when considering the total emissions at the end of the experiment (i.e., 47% increment in V compared with B, Figure 4.19c).

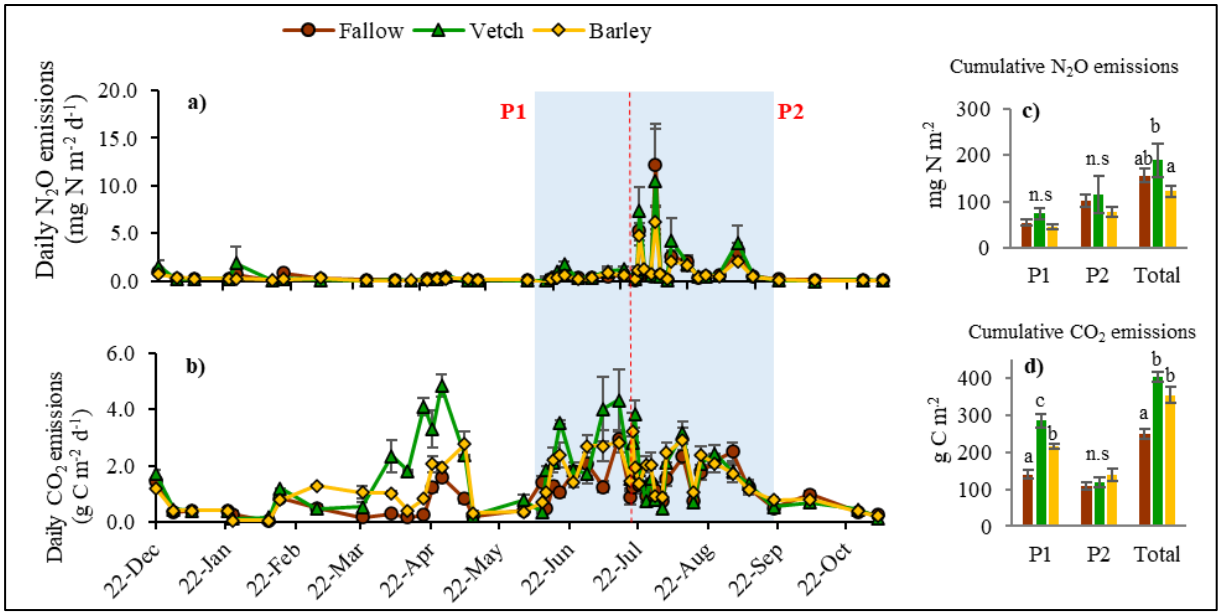

Figure 4.19. Daily N_2O ***(a)*** *and CO_2* ***(b)*** *emissions before (P1) and after maize fertilization (P2) in the different cover crop treatments (bare fallow, vetch and barley). The dotted red line indicates the maize top-dressing fertilization date (19 July 2021) corresponding with the transition from P1 to P2. The blue shadow area corresponds with the maize irrigation period. Cumulative N_2O* ***(c)*** *and CO_2* ***(d)*** *emissions during P1 and P2 and total cumulative emissions at the end of the experiment. Different letters within each period denote statistical differences ($P < 0.05$) between cover crop treatments in each period by applying the LSD test. n.s.: no significant difference. Vertical bars denote the standard error of the mean (n = 3 in P1, n = 9 in P2).*

During P2, daily N_2O emissions were strongly and positively correlated with both air and soil temperature, as well as CO_2 emissions (r = 0.66, $P < 0.01$; r = 0.66, $P < 0.01$ and r = 0.80, $P < 0.001$, respectively) (Figure 4.20b). These correlations were also significant considering the entire experimental period, with additional correlations ($P < 0.05$) found between N_2O emissions and soil WFPS and NH_4^+ (r = 0.31 and r = 0.48, respectively) (Figure 4.20c).

During P1, cumulative CO_2 emissions were 104% and 33% higher in V compared to F and B, respectively (Figure 4.19d). During this period, soil respiration fluxes increased in mid-April, after the termination of cover crops, and also in mid-June, coinciding with the onset of the maize irrigation period (Figure 4.19b).

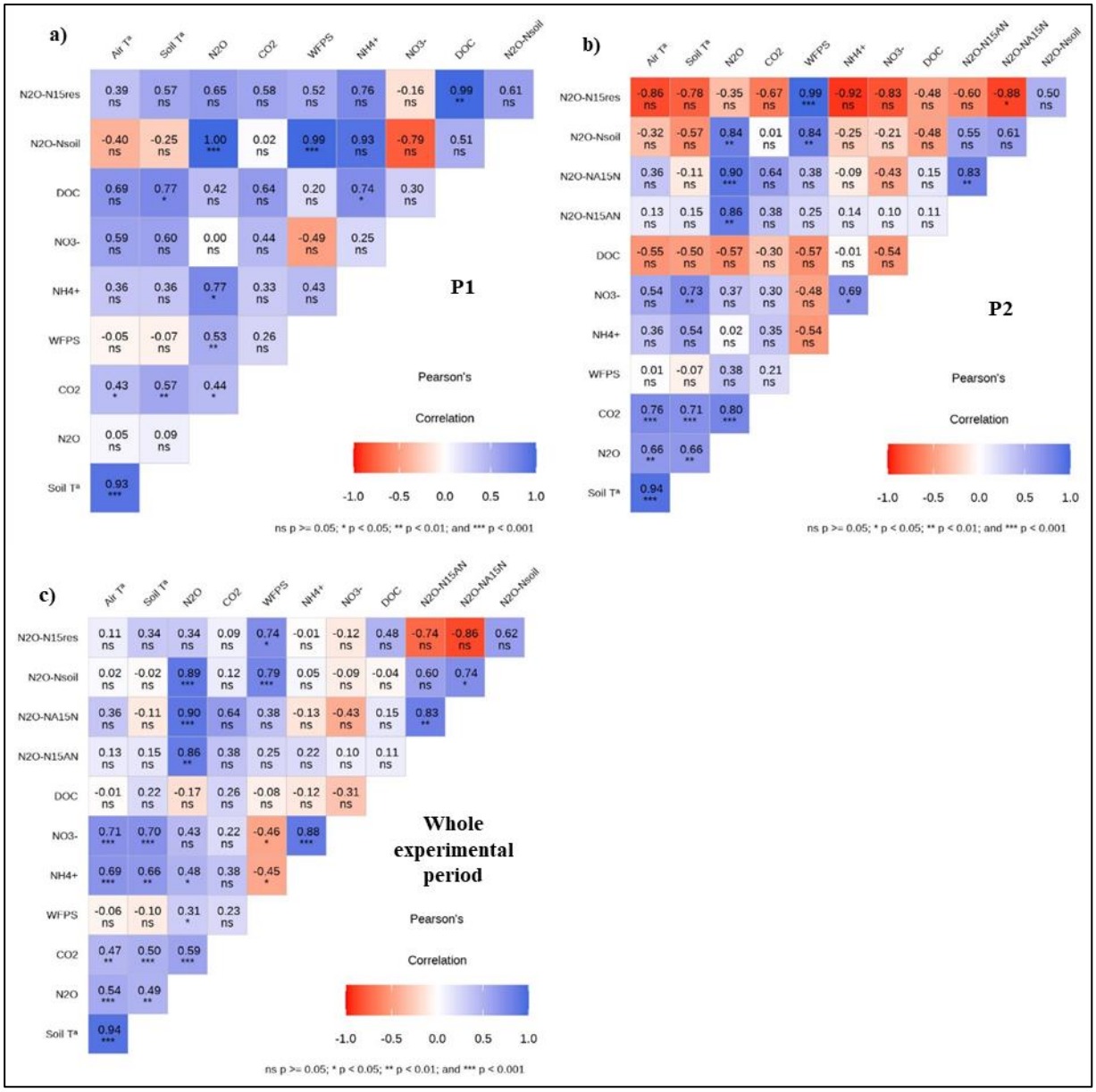

*Figure 4.20. Pearson correlation coefficients for the daily air and soil (at 10 cm depth) temperature, the daily N_2O and CO_2 fluxes, daily soil properties (WFPS, NH_4^+, NO_3^- and DOC) and daily N_2O emissions derived from $^{15}N-$enriched maize residues (N_2O-N_{15RES}), derived from $^{15}NH_4NO_3$ fertilizer (N_2O-N_{15AN}), derived from $NH_4{}^{15}NO_3$ fertilizer (N_2O-N_{A15N}) and derived from soil endogenous N (N_2O-N_{soil}) analyzed before maize fertilization (P1) **(a)**, after maize fertilization (P2) **(b)** and over the whole experimental trial **(c)**.*

During P2, no differences in cumulative CO_2 emissions were observed between cover crops. Considering the entire experimental period, cumulative CO_2 emissions were lower in F (249g C m^{-2}) compared to V and B (404 g C m^{-2} and 355 g C m^{-2}, respectively) ($P < 0.05$, Figure 4.19d). Similar to daily N_2O fluxes, air and soil temperatures were positively correlated with

daily CO_2 emissions throughout the whole experiment (Figure 4.20c), particularly during P2 (r = 0.72, $P < 0.001$ and r = 0.71, $P < 0.001$, respectively) (Figure 4.20b).

4.3.3. $^{15}N_2O$ emissions

Before maize fertilization (P1), the contribution of maize residues on N_2O emissions increased from 2% of daily N_2O fluxes at the beginning of the experiment to 7% after the start of maize on 11 June 2021 (Figure 4.21). During this period, contrary to our first hypothesis, the cover cropping treatments did not have a significant effect on emission from ^{15}N–enriched maize residues ($N_2O{-}N_{15RES}$) or from soil endogenous N ($N_2O{-}N_{soil}$) (Table 4.20). Nitrous oxide emissions derived from soil were strongly and positively correlated with WFPS (r = 0.99, $P < 0.001$), and $N_2O{-}N_{15RES}$ emissions were correlated with DOC (r = 0.99, $P < 0.01$) during P1 (Figure 4.20a).

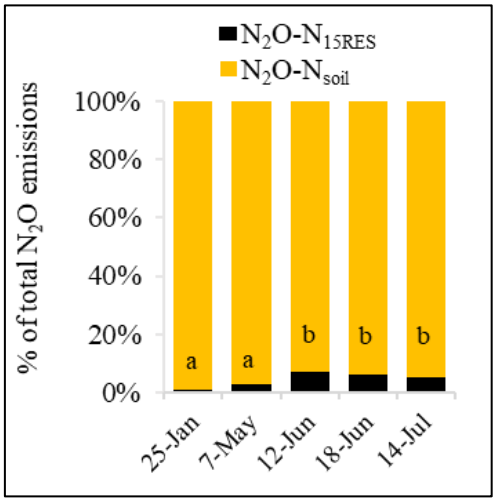

Figure 4.21. Proportion of N_2O emissions derived from ^{15}N–enriched maize residues ($N_2O{-}N_{15RES}$) and derived from soil endogenous N ($N_2O{-}N_{soil}$) at different simple dates during P1 (between ^{15}N–enriched maize residues incorporation on mid-November 2020 and maize cash crop fertilization on 19 July 2021). Different letters denote significant difference between sampling dates in $N_2O{-}N_{15RES}$ by applying the LSD test at 95% confidence level.

Table 4.20. Daily N_2O emissions (mg N m^{-2} d^{-1}) derived from ^{15}N–enriched maize residues (N_2O-N_{15RES}) and derived from soil N (N_2O-N_{soil}) during P1 (from maize residue incorporation on 17 November 2020 and until maize fertilization on 19 July 2021) in the different cover crop treatments (bare fallow, F, vetch, V and barley, B).

		N_2O-N_{15RES}	**N_2O-N_{soil}**
25-Jan	F	0.01 ± 0.01	0.70 ± 0.64
	V	0.02 ± 0.01	1.85 ± 1.71
	B	0.00 ± 0.00	0.24 ± 0.15
	P value	0.235	0.262
7-May	F	0.00 ± 0.00	0.07 ± 0.03 b
	V	0.00 ± 0.00	0.01 ± 0.00 a
	B	0.01 ± 0.00	0.21 ± 0.08 b
	P value	0.060	0.011
12-Jun	F	0.01 ± 0.00	0.15 ± 0.03
	V	0.03 ± 0.02	0.35 ± 0.17
	B	0.02 ± 0.02	0.22 ± 0.19
	P value	0.443	0.692
18-Jun	F	0.04 ± 0.01	0.61 ± 0.32
	V	0.10 ± 0.02	1.63 ± 0.24
	B	0.04 ± 0.01	0.61 ± 0.13
	P value	0.120	0.106
14-Jul	F	0.04 ± 0.02	0.61 ± 0.16
	V	0.05 ± 0.02	1.14 ± 0.24
	B	0.03 ± 0.01	0.51 ± 0.11
	P value	0.713	0.174

Values are expressed as the mean ± standard error. Different letters within columns denote significant differences ($P < 0.05$) between cover crop treatments for the different sources of N_2O emissions at the different sampling dates by applying the LSD test.
Data of ^{15}N-N_2O emissions were only obtained on selected days during the experiment. Data of daily N_2O emissions during the whole experiment are available in Figure 4.19a.

After fertilization (P2), the N_2O emissions derived from the different sources (i.e., maize residues, fertilizer, and soil N) were not affected by the incorporation of the different cover crops (Table 4.21), contrary to our initial hypothesis. The $^{15}N_2O$ analyses also showed that the contribution of ^{15}AN and A^{15}N fertilizers accounted for 42% to 61% and for 9% to 18% of daily N_2O emissions, respectively, during the first two weeks after fertilization. At the highest emission peak (July 28), fertilizer and soil contributed on average by 71% and 27% to N_2O emissions, respectively. Regarding maize residues, N_2O-N_{15RES} increased from 1% to 3% of total N_2O emissions at 16 days after fertilization (Figure 4.22). The contribution of endogenous

soil N to N_2O emissions during the first two weeks after fertilization was, on average, 36% of daily N_2O emissions, peaking on September 2 (i.e., 45 days after fertilization). The average N_2O EFs from NH_4NO_3 fertilizer and maize residues were 0.3% and 0.06%, respectively.

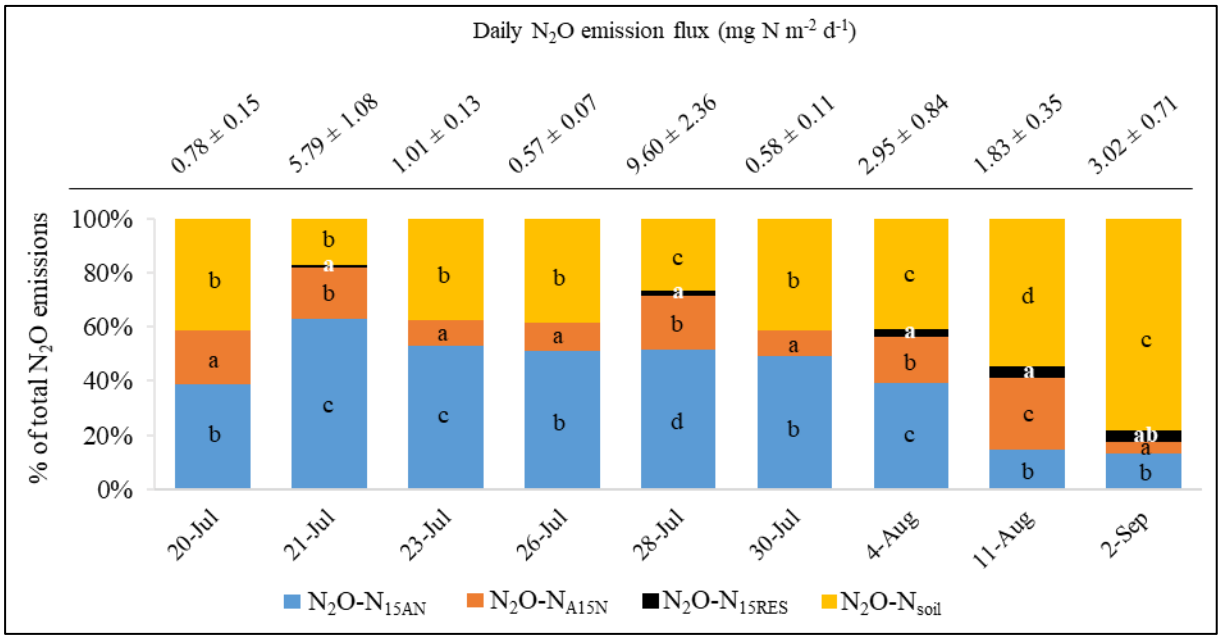

Figure 4.22. Proportion of daily N_2O emissions derived from $^{15}NH_4NO_3$ fertilizer ($N_2O{-}N_{15AN}$), from $NH_4{}^{15}NO_3$ fertilizer ($N_2O{-}N_{A15N}$), from ^{15}N–enriched maize residues ($N_2O{-}N_{15RES}$) and derived from soil endogenous N ($N_2O{-}N_{soil}$) during P2 (i.e., after maize fertilization on 19 July 2021). Different letters denote significant difference between N_2O sources in the different sampling dates by applying the LSD test at 95% confidence level (n = 9). Data above bars indicate the average daily N_2O emission flux in each sampling date (n = 9).

Table 4.21. Daily N_2O emissions (mg N m^{-2} d^{-1}) after maize fertilization (Period 2 of the experiment) derived from ^{15}N–enriched maize residues (N_2O-N_{15RES}), derived from $^{15}NH_4NO_3$ fertilizer (N_2O-N_{15AN}), from $NH_4{}^{15}NO_3$ fertilizer (N_2O-N_{A15N}) and derived from soil N (N_2O-N_{soil}) in the different cover crop treatments (bare fallow, F, vetch, V and barley, B).

		N_2O-N_{15RES}	N_2O-N_{15AN}	N_2O-N_{A15N}	N_2O-N_{soil}
20-Jul	F		0.24 ± 0.07	0.05 ± 0.02	0.15 ± 0.08
	V		0.26 ± 0.10	0.10 ± 0.03	0.45 ± 0.09
	B		0.40 ± 0.16	0.31 ± 0.24	0.37 ± 0.16
	P value		0.182	0.291	0.284
21-Jul	F	0.06 ± 0.02	3.23 ± 1.23	1.15 ± 0.39	0.88 ± 0.31
	V	0.05 ± 0.01	4.87 ± 1.61	1.44 ± 0.58	1.00 ± 0.46
	B	0.04 ± 0.02	2.82 ± 0.88	0.72 ± 0.26	1.12 ± 0.42
	P value	0.482	0.059	0.109	0.912
23-Jul	F		0.35 ± 0.14	0.05 ± 0.01	0.20 ± 0.02
	V		0.67 ± 0.14	0.13 ± 0.04	0.42 ± 0.16
	B		0.58 ± 0.03	0.10 ± 0.01	0.50 ± 0.11
	P value		0.287	0.178	0.185
26-Jul	F		0.23 ± 0.07	0.03 ± 0.01 a	0.16 ± 0.03
	V		0.28 ± 0.10	0.07 ± 0.00 b	0.22 ± 0.10
	B		0.37 ± 0.04	0.08 ± 0.02 b	0.28 ± 0.03
	P value		0.123	0.037	0.423
28-Jul	F	0.24 ± 0.04	6.16 ± 2.76	1.84 ± 0.50	3.92 ± 0.83
	V	0.18 ± 0.08	5.40 ± 3.10	2.55 ± 2.08	2.34 ± 1.09
	B	0.15 ± 0.02	3.37 ± 0.44	1.21 ± 0.30	1.46 ± 0.20
	P value	0.482	0.724	0.852	0.129
30-Jul	F		0.24 ± 0.11	0.05 ± 0.01	0.29 ± 0.20
	V		0.24 ± 0.13	0.06 ± 0.04	0.18 ± 0.05
	B		0.39 ± 0.08	0.05 ± 0.01	0.25 ± 0.09
	P value		0.629	0.788	0.769
4-Aug	F	0.09 ± 0.03	1.25 ± 0.14	0.26 ± 0.09	0.99 ± 0.66
	V	0.09 ± 0.03	1.43 ± 0.84	1.00 ± 0.75	1.68 ± 0.83
	B	0.05 ± 0.02	0.81 ± 0.33	0.25 ± 0.11	0.97 ± 0.32
	P value	0.155	0.553	0.497	0.409
11-Aug	F	0.11 ± 0.04	0.22 ± 0.06	0.61 ± 0.05	1.02 ± 0.27
	V	0.07 ± 0.03	0.25 ± 0.03	0.59 ± 0.31	0.91 ± 0.49
	B	0.06 ± 0.02	0.31 ± 0.04	0.25 ± 0.06	1.06 ± 0.31
	P value	0.298	0.344	0.132	0.909
2-Sep	F	0.17 ± 0.06	0.39 ± 0.31	0.16 ± 0.16	2.30 ± 0.78
	V	0.18 ± 0.09	0.50 ± 0.44	0.18 ± 0.16	3.13 ± 1.77
	B	0.06 ± 0.00	0.29 ± 0.08	0.02 ± 0.01	1.66 ± 0.41
	P value	0.274	0.784	0.737	0.739

Values are expressed as the mean ± standard error. Different letters within columns denote significant differences ($P < 0.05$) between cover crop treatments for the different sources of N_2O emissions at the different sampling dates by applying the LSD test.
Data of ^{15}N-N_2O emissions were only obtained on selected days during the experiment. Data of daily N_2O emissions during the whole experiment are available in Figure 4.19a.

4.3.4. Nitrogen recovery in plant (cover crop and maize cash crop)

4.3.4.1. Nitrogen recovery in cover crops

No differences were reported regarding aboveground cover crop biomass yield (average 3.11 Mg dry weight ha^{-1}) and C content (average 40.7%) between V and B (Table 4.22). The percentage of N and the total plant N in the aboveground biomass of cover crops were 2.4 and 2.1 times higher in V compared with B ($P < 0.05$), and 3.2 and 3.1 times higher in the belowground biomass. No differences were reported in the N uptake from ^{15}RES despite the ^{15}N enrichment being higher in B compared to V ($P < 0.05$, Table 4.22).

4.3.4.2. Nitrogen recovery in maize

The average maize N uptake at harvest was 76, 153, and 16 kg N ha^{-1} in stover, grain, and root, respectively, with no significant differences between cover crop treatments, as also found for yield and plant N concentrations (Table 4.23). The average ^{15}N content in all maize tissues in the ^{15}RES treatment was lower than in those receiving ^{15}N–enriched fertilizer, being higher in A^{15}N compared to ^{15}AN (i.e., by 69%, 68%, and 61% higher in stover, grain, and root, respectively) (Table 4.24). A 7.7% N recovery was obtained from the ^{15}N-maize residues in the subsequent maize crop, without significant differences between cover crop treatments (Figure 4.23).

Table 4.22. Aboveground and belowground cover crop production (Mg DW ha^{-1}), C and N content (%), total N (kg N ha^{-1}), atom ^{15}N % and N derived from the ^{15}N–enriched maize residue (N_{15RES}) and from endogenous soil N (N_{soil}) (kg N ha^{-1}) in the vetch and barley cover crops.

Aboveground biomass

Cover crop	Production (Mg DW ha^{-1})	N content (%)	Total N (kg N ha^{-1})	^{15}N (%)	N_{15RES} (kg N ha^{-1})	N_{soil} (kg N ha^{-1})	C content (%)
Vetch	2.9 ± 0.4	3.69 ± 0.04 b	106 ± 14	0.42 ± 0.01 a	0.79 ± 0.04	105 ± 14	41.3 ± 0.5
Barley	3.4 ± 0.6	1.52 ± 0.05 a	51 ± 7	0.49 ± 0.02 b	0.89 ± 0.11	50 ± 7	41.1 ± 0.3
P value	0.530	0.001	0.083	0.045	0.393	0.082	0.460

Belowground biomass

Cover crop	Production (Mg DW ha-1)	N content (%)	Total N (kg N ha^{-1})	^{15}N (%)	N_{15RES} (kg N ha^{-1})	N_{soil} (kg N ha^{-1})
Vetch	1.1 ± 0.0	2.03 ± 0.03 b	21.4 ± 0.3 b	0.44 ± 0.00 a	0.25 ± 0.01	21.1 ± 0.3 b
Barley	1.1 ± 0.0	0.64 ± 0.06 a	6.8 ± 0.7 a	0.65 ± 0.03 b	0.28 ± 0.02	6.5 ± 0.3 a
P value	[1]	0.002	0.001	0.024	0.430	0.001

Values are expressed as the mean ± standard error (n = 3). Different letters denote significant differences between cover crops by applying the LSD test at a 95% confidence level.

[1] The belowground biomass production was obtained from the study by Hu et al. (2018).

Table 4.23. Maize yield (Mg ha^{-1}), N content (%) and N uptake (kg N ha^{-1}) in the different plant tissues (stover, grain and root) in the different cover crop treatments (bare fallow, F, Vetch, V and barley, B).

	Maize yield (Mg ha^{-1})			**Maize N content (%)**			**Maize N uptake (kg N ha^{-1})**		
Cover crop treatment	Stover	Grain	Root	Stover	Grain	Root	Stover	Grain	Root
F	10.1 ± 0.3	10.5 ± 0.3	1.96 ± 0.05	0.72 ± 0.02	1.41 ± 0.02	0.75 ± 0.03	72.9 ± 3.1	147 ± 3	14.7 ± 0.6
V	10.0 ± 0.5	10.3 ± 0.6	1.93 ± 0.06	0.71 ± 0.04	1.42 ± 0.02	0.78 ± 0.03	71.5 ± 5.9	145 ± 3	15.0 ± 2.0
B	11.7 ± 0.9	11.5 ± 1.6	2.22 ± 0.16	0.70 ± 0.02	1.43 ± 0.02	0.81 ± 0.03	83.4 ± 6.8	165 ± 10	17.9 ± 1.4
P value	0.361	0.248	0.922	0.807	0.742	0.146	0.425	0.202	0.100

Values are expressed as the mean ± standard error (n = 9). Different letters denote significant differences between treatments by applying the LSD test at a 95% confidence level

Table 4.24. Maize ^{15}N content (%) in the different plant tissues (stover, grain and roots) in the different cover crop treatments (bare fallow, F, vetch, V and barley, B), in the different ^{15}N fertilizer treatments (^{15}N−enriched maize residues, ^{15}RES, $^{15}NH_4NO_3$ fertilizer, ^{15}AN and $NH_4{}^{15}NO_3$ fertilizer, $A^{15}N$) and in the different combination of the cover crops and fertilizer treatments.

	Maize ^{15}N content (atom % ^{15}N)		
Cover crop treatment	Stover	Grain	Root
F	1.83 ± 0.36	1.99 ± 0.42	2.16 ± 0.42
V	2.02 ± 0.43	2.25 ± 0.50	2.22 ± 0.46
B	2.42 ± 0.52	2.53 ± 0.54	2.78 ± 0.60
P value	0.100	0.423	0.796
^{15}N fertilizer treatment	Stover	Grain	Root
^{15}RES	0.57 ± 0.01 a	0.55 ± 0.01 a	0.66 ± 0.02 a
^{15}AN	2.12 ± 0.12 b	2.32 ± 0.13 b	2.50 ± 0.17 b
A^{15}N	3.58 ± 0.16 c	3.89 ± 0.15 c	4.01 ± 0.20 c
P value	0.000	0.000	0.000
CC×^{15}N	Stover	Grain	Root
F×^{15}RES	0.57 ± 0.01 a	0.56 ± 0.02 a	0.67 ± 0.02 a
F×^{15}AN	1.86 ± 0.02 b	2.00 ± 0.01 b	2.34 ± 0.05 b
F×A^{15}N	3.07 ± 0.01 d	3.40 ± 0.01 d	3.48 ± 0.03 cd
V×^{15}RES	0.57 ± 0.05 a	0.58 ± 0.08 a	0.71 ± 0.26 a
V×^{15}AN	1.90 ± 0.04 b	2.16 ± 0.06 b	2.07 ± 0.10 b
V×A^{15}N	3.55 ± 0.14 e	4.02 ± 0.07 e	3.88 ± 0.15 de
B×^{15}RES	0.57 ± 0.08 a	0.52 ± 0.24 a	0.59 ± 0.26 a
B×^{15}AN	2.56 ± 0.06 c	2.79 ± 0.14 c	3.08 ± 0.10 c
B×A^{15}N	4.13 ± 0.16 f	4.25 ± 0.06 e	4.67 ± 0.18 e
P value	0.003	0.003	0.015

Values are expressed as the mean ± standard error (n = 9 for the different cover crop and ^{15}N fertilizer treatment; n = 3 for the different CC×^{15}N combination). Different letters denote significant differences between treatments by applying the LSD test at a 95% confidence level.

The average N uptake from fertilizer (plant_N_{fert}) at maize harvest was 19.3, 43.1, and 4.7 kg N ha^{-1} in stover, grain, and root, respectively (Table 4.25). The plant N uptake derived from the A^{15}N fertilizer (46.4 kg N ha^{-1}) was 2.3 times higher than that derived from the ^{15}AN fertilizer (average 20.6 kg N ha^{-1}) (Table 4.25). Barley cover crops increased the plant_N_{15AN} in grain (by 39% and 33% compared to F and V, respectively, $P < 0.05$) and in root (by 31% and 55% compared to F and V, respectively, $0.05 < P < 0.10$). Furthermore, B significantly increased the stover_N_{A15N} and the root_N_{A15N} compared to F (by 94% and 76%, respectively) and V (by

70% and 34%, respectively) (Table 4.25). Consequently, the percentage of plant N recovery from the fertilizer was higher in B (42%) than in F (26%), with V showing intermediate results (30%) (Figure 4.24).

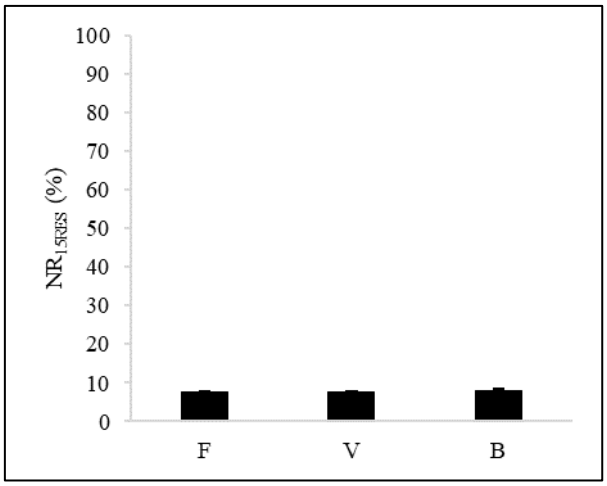

Figure 4.23. Nitrogen recovery in maize plants at harvest from the ^{15}N–enriched maize residues (Plant_NR_{15RES}) in the different cover crop treatments (bare fallow, F, vetch, V, and barley, B). No significant differences between treatments were obtained when applying the LSD test at 95% confidence level. Vertical bars denote the standard error of the mean (n=3).

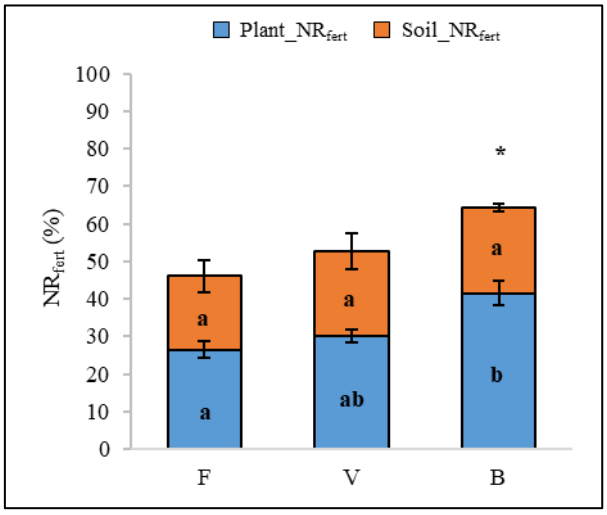

Figure 4.24. Nitrogen recovery from the NH_4NO_3 fertilizer in maize plants at harvest (Plant_NR_{fert}, %) and in soil at the end of the experiment (Soil_NR_{fert}, %) in the different cover crop treatments (bare fallow, F, vetch, V, and barley, B). Different lowercase letters denote significant differences between cover crop treatments in plant or soil NR_{fert}. (*) Denotes significant differences in the N recovery between plant (Plant_NR_{fert}) and soil (Soil_NR_{fert}) in each cover crop treatment (F, V or B). Statistical differences were obtained applying the LSD test at 95% confidence level. Vertical bars denote the standard error of the mean (n = 9).

Table 4.25. Nitrogen derived from ^{15}N–enriched maize residues (N_{15RES}), derived from $^{15}NH_4NO_3$ fertilizer (N_{15AN}), derived from $NH_4{}^{15}NO_3$ fertilizer (N_{A15N}) and derived from endogenous soil N (N_{soil}) in the different maize tissues (stover, grain and root) and in total maize plant in the different cover crop treatments (bare fallow, vetch, and barley). Data are expressed in kg N ha^{-1}.

	Cover crop treatment			
Stover	Fallow	Vetch	Barley	
N_{15RES}	2.55 ± 0.12 A	2.13 ± 0.08 A	2.91 ± 0.32 A	0.157
N_{15AN}	4.85 ± 0.01 B	5.75 ± 1.50 B	6.04 ± 0.59 B	0.725
N_{A15N}	10.1 ± 1.5 C a	11.6 ± 1.1 C a	19.6 ± 1.7 C b	0.022
N_{soil}	55.4 ± 1.6 D	52.1 ± 3.6 D	54.9 ± 4.5 D	0.826
	0.000	0.000	0.000	*P* value
Grain	Fallow	Vetch	Barley	
N_{15RES}	4.40 ± 0.21 A	4.73 ± 0.21 A	4.35 ± 0.03 A	0.202
N_{15AN}	11.8 ± 0.2 B a	12.3 ± 1.2 B a	16.4 ± 1.2 B b	0.014
N_{A15N}	23.5 ± 3.1 C	28.1 ± 0.9 C	37.2 ± 3.6 C	0.104
N_{soil}	108 ± 3 D	100 ± 2 D	107 ± 6 D	0.423
	0.000	0.000	0.000	*P* value
Root	Fallow	Vetch	Barley	
N_{15RES}	0.65 ± 0.01 A	0.69 ± 0.09 A	0.71 ± 0.18 A	0.909
N_{15AN}	1.50 ± 0.03 B ab	1.27 ± 0.18 B a	1.97 ± 0.11 B b	0.066
N_{A15N}	2.29 ± 0.21 C a	3.02 ± 0.52 C a	4.03 ± 0.25 C b	0.015
N_{soil}	10.3 ± 0.7 D	10.1 ± 1.3 D	11.2 ± 1.6 D	0.474
	0.000	0.000	0.000	*P* value
Plant	Fallow	Vetch	Barley	
N_{15RES}	7.59 ± 0.32 A	7.55 ± 0.36 A	7.96 ± 0.48 A	0.782
N_{15AN}	18.1 ± 0.2 B	19.3 ± 2.3 B	24.4 ± 1.7 B	0.105
N_{A15N}	35.9 ± 4.8 C a	42.7 ± 2.1 C ab	60.8 ± 5.1 C b	0.054
N_{soil}	173 ± 4 D	162 ± 7 D	173 ± 8 D	0.561
	0.000	0.000	0.000	*P* value

Values are expressed as the mean ± standard error (n = 3). Different capital letters denote significant differences between N sources and different lowercase letters denote significant differences between cover crop treatments by applying the LSD test at 95% confidence level.

4.3.5. Nitrogen recovery in soil

There were no differences between the soil N derived from ^{15}AN (average 20.5 kg N ha^{-1}) and from $A^{15}N$ fertilizer (average 25.5 kg N ha^{-1}) (Table 4.26). Considering the whole 0-60 cm depth, B significantly increased soil_N_{15AN} compared to V (by 84%) and F (by 123%).

However, there were no differences between treatments in the sum of both soil_N_{15AN} and soil_N_{A15N} (i.e., N_{fert}) (Table 4.26), with an average soil N recovery of 22% (Figure 4.24). Barley was the only treatment that resulted in significant differences between plant_NR_{fert} (42%) and soil_NR_{fert} (23%).

Table 4.26. Soil N derived from $^{15}NH_4NO_3$ fertilizer (soil_N_{15AN}) and from $NH_4{}^{15}NO_3$ fertilizer (soil_N_{A15N}) at the three different soil sampling depths (0 – 20 cm, 20 – 40 cm and 40 – 60 cm), considering the whole soil sampling depth (0 – 60 cm) and total soil N derived from the fertilizer (soil_N_{fert}) in the 0 – 60 cm depth in the different cover crop treatments (bare fallow, F, vetch, V and barley, B).

	0 – 20 cm		**20 – 40 cm**		**40 – 60 cm**		**Total (0 – 60 cm)**		
Cover crop treatment	Soil_N_{15AN} (kg N ha^{-1})	Soil_N_{A15N}	Soil_N_{15AN} (kg N ha^{-1})	Soil_N_{A15N}	Soil_N_{15AN} (kg N ha^{-1})	Soil_N_{A15N}	Soil_N_{15AN} (kg N ha^{-1})	Soil_N_{A15N}	N_{fert}
F	4.20 ± 0.74	6.19 ± 0.74	4.71 ± 2.21	11.8 ± 6.7	4.94 ± 2.68 ab	9.52 ± 3.65	13.8 ± 4.5 a	27.5 ± 10.2	41.3 ± 8.9
V	10.5 ± 3.9	5.50 ± 1.92	3.45 ± 0.88	9.70 ± 3.66	2.71 ± 0.63 a	15.3 ± 6.0	16.7 ± 5.3 a	30.5 ± 10.1	47.2 ± 10.2
B	9.63 ± 2.59	6.04 ± 0.72	10.3 ± 3.3	4.29 ± 1.62	10.9 ± 3.1 b	6.83 ± 0.23	30.8 ± 3.7 b	17.2 ± 1.4	48.0 ± 2.3
P value	0.287	0.878	0.068	0.621	0.045	0.501	0.009	0.752	0.842

Values are expressed as the mean ± standard error (n = 3). Different letters denote significant differences between cover crop treatments by applying the LSD test at 95% confidence level.

4.3.6. Discussion

4.3.6.1. Effects of cover crops on N_2O and CO_2 emissions

When total cumulative emissions are considered, vetch cover crop resulted in higher N_2O emissions compared to barley (Figure 4.19c). These results are opposite to those reported in the meta-analysis by Basche et al. (2014). During P1 (i.e., during their growing phase and after their incorporation into the soil before maize cash crop fertilization), the decomposition of N−rich vetch residues may have increased the soil organic N input, together with the NH_4^+ concentration, thus favoring nitrification processes responsible for N_2O emissions. This is supported by the positive correlation between daily NH_4^+ and N_2O emissions during this period (Figure 4.20a), as well as considering the whole experimental period (Figure 4.20c), and by the higher soil NO_3^- concentration in V compared to F and B after maize fertilization (Figure 4.18b). However, during P1, no significant differences in N_2O emissions were observed between bare fallow, barley, and vetch as cover crops. Studies conducted under similar climatic conditions have reported comparable results (Guardia et al., 2016a). Even though non-legume cover crops exhibit enhanced soil residual N-acquisition capacity compared to N-fixing legumes (Fernandez Pulido et al., 2023), our results align with the recent meta-analysis by Y. Li et al. (2023a), which supports that legume species can self-regulate in terms of N input via N_2 fixation and also develop active soil N uptake (De Notaris et al., 2021). Furthermore, Y. Li et al. (2023a) reported that N_2O emissions could be increased during the cover crop growing phase due to denitrification being promoted by the increased C supply from rhizodeposition. The balance between these two contrasting effects of cover crop roots on N_2O emissions (i.e., a direct mitigating effect by reducing the reactive N pool in the soil, and an indirect emission-increasing effect by raising soil DOC concentrations) could explain the variable and usually non-significant effects found during the cover crop growing period (Guardia et al., 2016a; Sanz-

Cobena et al., 2014a). Moreover, the incorporation of cereal cover crop residues with higher C:N ratios could increase N_2O emissions when rewetting events and N addition create favorable conditions for denitrification, as previously reported in **Experiment 2** of this thesis (see Section 4.2) and by Abalos et al. (2022a).

In accordance with the meta-analysis by Muhammad et al (2019), CO_2 emissions increased in the presence of cover crops when considering the whole experiment (Figure 4.19d). However, the differences in CO_2 emissions were observed only before maize fertilization, including the cover crops development and their incorporation into the soil. During this period, the vetch cover crop increased CO_2 emissions compared to the barley cover crop, with bare fallow reporting the lowest CO_2 emissions fluxes (Figure 4.19d). The increased CO_2 emissions observed with cover crops compared to bare fallow were likely due to enhanced C inputs into the soil, which increased the availability of C substrates and stimulated microbial activity. Furthermore, other studies have also reported higher CO_2 emissions in legume compared to non-legume cover crops (Chirinda et al., 2010; Sanz-Cobena et al., 2014a), what could be related to an increase in soil microbial community abundance and rhizosphere respiration (Muhammad et al., 2021).

4.3.6.2. Sources of N_2O emissions and N_2O EF

The chemical characteristics of recalcitrant crop residues such as high C:N ratios and high cellulose, hemicellulose, and lignin fractions (Abalos et al., 2022b), are related to their slow biodegradability rates (Jensen et al., 2005; Lashermes et al., 2022). Therefore, it would be expected that maize residues, which have these characteristics, would have a low contribution to N_2O emissions (Abalos et al., 2022b). This was confirmed by the 95% average N_2O emissions derived from endogenous soil N during the cover cropping period, supporting the second hypothesis of this study. The contribution of maize stover to N_2O during P1 increased

from 2% to 7% after maize irrigation (Figure 4.21), indicating increased mineralization rates of the maize stover under higher soil moisture conditions, as supported by the positive correlations between N_2O fluxes with DOC and WFPS. Furthermore, the low but continuously increasing contribution of ^{15}RES to N_2O emissions was observed after maize fertilization (Figure 4.22), with higher $N_2O{-}N_{15RES}$ daily fluxes during P2 compared to P1 (Table 4.21 and Table 4.20, respectively). Ferrari Machado et al. (2021) also reported a low contribution of crop residues (ranging from 0.3% to 1.3%) to total N_2O emissions in a 4-year crop rotation.

Our results align with those previously reported in **Experiment 1** of this thesis (see Section 4.1) and by Guardia et al. (2018), where NH_4^+ was identified as the main source of N_2O emissions in ^{15}N tracing experiments when fertilizing with NH_4NO_3 in Mediterranean agricultural soils. This supports the third hypothesis of this study, suggesting that $NH_4^+{-}N$ oxidation-based processes (nitrification, nitrifier-denitrification, or nitrification coupled with denitrification) could be relevant pathways leading to N_2O emissions. The WFPS values during this period were ca. 40%, thus being favorable the N_2O emissions associated to nitrification processes (Pilegaard, 2013). Three weeks after fertilization, WFPS values followed a similar trend (as irrigation was maintained for two months), but N_2O fluxes sharply declined, likely due to the limited availability of soil mineral N (Figure 4.17c,d), and consequently, the reduced substrates for N transformations that lead to N_2O emissions (García-Marco et al., 2014). Our findings are also in accordance with the recent global meta-analysis by Han et al. (2024), which reported higher N_2O emissions derived from nitrification than from denitrification in cropland experiments using ^{15}N-labeled fertilizers.

In addition to the fertilizer, the contribution of soil endogenous N (including N mineralized from cover crop residues) to N_2O emissions, as a consequence of the priming effect following synthetic N addition, should not be underestimated. In the present study, even immediately after

N fertilizer application, endogenous soil N accounted for ca. 40% of N_2O emissions (Figure 4.22). The application of organic amendments, such as cover crop residues, can alter the magnitude and direction of N_2O priming by introducing labile C sources for denitrifiers, increasing the availability of mineral N substrates, modifying microbial communities (Arcand and Congreves, 2020; Daly et al., 2024), and increasing soil moisture (Roman-Perez and Hernandez-Ramirez, 2021). Other studies that applied ^{15}N-labeled fertilizers in calcareous soils under Mediterranean climates, e.g., Guardia et al. (2018) in irrigated maize, or the results of **Experiment 1** in this thesis in rainfed barley (see Section 4.1) have also reported a significant contribution of soil endogenous N to N_2O emissions.

The N_2O EF from synthetic fertilizer under the experimental conditions of the present ^{15}N-tracing experiment (average 0.3%) was lower than the 0.5% default value for synthetic N inputs in dry climates (IPCC, 2019b) and the average 0.6% EF for irrigated Mediterranean crops (Cayuela et al., 2017). This experiment was conducted with maize as the cash crop under sparkling irrigation. If other agricultural practices (such as drip irrigation instead of sprinkler, the use of NIs, or ISFM) were implemented together with cover cropping, it would be possible to further reduce N_2O EFs in irrigated Mediterranean croplands (Aguilera et al., 2013b; Cayuela et al., 2017). Regarding maize residues, the average 0.06% N_2O EF was also lower than the 0.5% EF default value (IPCC, 2019b), but closer to the values reported for maize residues by Machado et al. (2021) and Ferrari Machado et al. (2021) (0.011 – 0.017% and 0.003 – 0.016%, respectively), for oilseed rape residues by Kesenheimer et al. (2019) (0.03 – 0.06%), and for cowpea residues by Gomes et al. (2019) (0.013 – 0.015%). Therefore, N_2O emissions could be notably overestimated if the 0.5% EF default value is applied, rather than considering the specific biochemical properties of the residues (i.e., C:N ratio, easily degradable fractions) which are in turn related to their maturity and potential for effective mineralization (Abalos et al., 2022b).

4.3.6.3. N recovery from maize residues and from fertilizer

The slow degradation and mineralization of recalcitrant maize residues resulted in most of the N that was incorporated in the cover crop biomass was derived from sources other than maize residues, such as endogenous soil N or biological N fixation (Table 4.22). Despite the total N in vetch biomass was higher than in barley, the ^{15}N content derived from ^{15}N–enriched maize residues was higher in the non-legume cover crop compared to the legume. This may be due to the biological N fixation capacity of legumes, which decreases their potential for soil N uptake (De Notaris et al., 2020). Opposite to legume, non-legume cover crops need to acquire soil N during their development, what can be beneficial for reducing the risk of N losses via leaching (Thapa et al., 2018). The results of the present experiment support this dynamic. First, soil NO_3^- concentrations during P1 in the barley microplots were lower compared to those in fallow or vetch (Figure 4.18b), confirming the higher soil N acquisition potential of non-legume cover crops compared to legumes. Furthermore, the proportion of N derived from ^{15}N–enriched maize residues was 2.3 times higher in B compared to V (Table 4.22). By implementing cover crop mixtures, it is possible to balance the benefits of the biological N fixation by legumes and N transfer to non-legumes, while enhancing soil N uptake from cereal cover crops through improved root traits (Rodriguez et al., 2020).

In the present experiment, the different cover cropping treatments (fallow, vetch, and barley) had no significant effect on N recovery in maize plants from the preceding maize residues. To date, no data are available regarding the effect of cover cropping on N recovery from mature crop residues in the subsequent cash crops. The average 7.7% plant_NR_{15RES} is within the range reported by other studies. Mubarak et al. (2003) observed a 9% N recovery in groundnut, followed by a 2% N recovery in maize after maize residue recycling. Similarly, Ding et al. (2019) reported a 9.2% N recovery from maize residues in wheat in a pot experiment, while

Taveira et al. (2020) reported a N recovery from aboveground and belowground biomass corn residue-N by 9.7% − 13.5% in soybean seed, highlighting the higher contribution of belowground biomass crop residues to N recovery in subsequent crops. In the present study, N recovery from maize residues was calculated considering only the aboveground crop residues. Thus, a higher N recovery would be expected if the belowground biomass was considered (Farzadfar and Congreves, 2022). Moreover, the relatively low N recovery from recalcitrant maize residues can be attributed to the greater availability of alternative N sources, such as synthetic fertilizer applied to maize and N from less mature cover crop residues. When cover crops are incorporated into the soil as green manure, they are more easily decomposed and mineralized by soil microorganisms, providing readily available nitrogen for the following cash crop (Liang et al., 2022).

The average 33 ± 3% plant N recovery from synthetic fertilizer reported in this experiment (Figure 4.24) was higher than the 17% reported by Taveira et al. (2020) and the 21% reported by Mubarak et al. (2003) in maize plants. Before maize fertilization, soil NO_3^- concentrations were lower in microplots where barley was grown (Figure 4.17d and Figure 4.18b). This was likely due to the higher N uptake by barley during its development, as well as the immobilization of mineral N promoted following the incorporation of the high C:N ratio barley residues (Chen et al., 2014; McSwiney et al., 2010). The limited availability of soil NO_3^- in the early development stages of maize grown after the barley cover crop caused an enhanced response of maize crop when synthetic fertilizer is applied, resulting in higher plant N recovery with barley cover crop compared to bare fallow (Figure 4.24). Additionally, the immobilization of soil mineral N by the barley cover crop could have temporarily reduced NO_3^- leaching after maize fertilization, thus resulting in enhanced NO_3^- uptake form the fertilizer (Meng et al., 2021). Contrary to these results, Gabriel and Quemada (2011) reported no differences in N recovery in maize regardless cover cropping treatment.

The average 22% soil N recovery from the fertilizer (Figure 4.24) was consistent with the values reported by Taveira et al. (2020) with maize at a 0–45 cm soil depth (17% - 29%). However, these recoveries were lower than those observed in rainfed crops, such as the 29% - 50% N recovery in barley reported in **Experiment 1** of this thesis (see Section 4.1) or the 29% in wheat reported by H. Li et al. (2023). This discrepancy could be attributed to the lower N leaching losses typically observed in rainfed systems compared to irrigated cropping systems. The soil N content derived from the ^{15}AN fertilizer (but not A^{15}N) was higher in B compared to F and V (Table 4.26). This could be related to an increase of NH_4^+ adsorption into soil colloids, which may have been further enhanced by the incorporation of high C:N ratio barley residues. Moreover, as discussed earlier, maize exhibits a preference for NO_3^- over NH_4^+, which could explain the observed differences in soil N retention across cover crop treatments.

Considering the fertilizer N recovery in both plant and in soil (average 55%) and the 0.3% of fertilizer N lost via N_2O emissions, approximately 45% of the applied N at fertilization remained unaccounted for. In addition to the loss of N oxides with low quantitative impact (Liu et al., 2017), the primary 'holes in the pipe' under the conditions of this study likely include NH_3 volatilization, NO_3^- leaching, and N_2 emissions via denitrification (Sutton et al., 2013; Ussiri and Lal, 2013). Globally, N_2 losses account for an average 5% of N applied but exhibit substantial variability (Pan et al., 2022). For instance, Guardia et al. (2018) reported significant N_2 emissions in irrigated maize (9.6 to 11.7 kg N ha^{-1} within 13 days after fertilization), despite the higher contribution of NH_4^+ oxidation processes leading to N_2O emissions compared to denitrification. The review by Pan et al. (2016) indicated that, on average, 13% of synthetic fertilizer N is lost through NH_3 volatilization in Europe, with residue retention increasing this lost by 25.5% (when N is applied as urea). Although urea and manure applications are the primary sources of NH_3 volatilization (Sanz-Cobena et al., 2014a), substantial NH_3 losses from NH_4NO_3 can also occur in calcareous soils, such as those in the present study −particularly

when fertilizers are not immediately incorporated by irrigation– (Recio et al., 2018). Additionally, NO_3^- leaching represents a potentially major N loss pathway, particularly under humid conditions or in semiarid agroecosystems where irrigation and fertilizer applications are not precisely aligned with crop demand (Quemada et al., 2013). The use of cover crops is an effective strategy to mitigate these losses during the postharvest period (Gabriel et al., 2013; Thapa et al., 2018). Our results evidence the critical need to identify site-specific N loss pathways, thereby optimizing fertilizer efficiency to minimize N surpluses and associated environmental risks (Galloway et al., 2003; Lassaletta et al., 2014).

4.4. Experiment 4 – Fate of mineral N fertilizer and processes involved in N_2O emissions in a pre-alpine grassland

4.4.1. Environmental conditions

The average air temperature during the experimental period was 18.8 ºC, with an average daily amplitude of 14.4 ºC. The lowest average air and soil temperatures (10.9 ºC and 16.5 ºC, respectively) and the highest soil volumetric water content (42.3 %) were reported after a period of intense rainfall, which coincided with the second fertilizer application (Figure 4.25). Total cumulative precipitation was 147 mm (227 mm considering the irrigation events) and was concentrated mainly in the second week of the experiment, reaching a daily precipitation of 50 mm on 28 August (i.e., 14 days after 1st fertilizer application) (Figure 4.25).

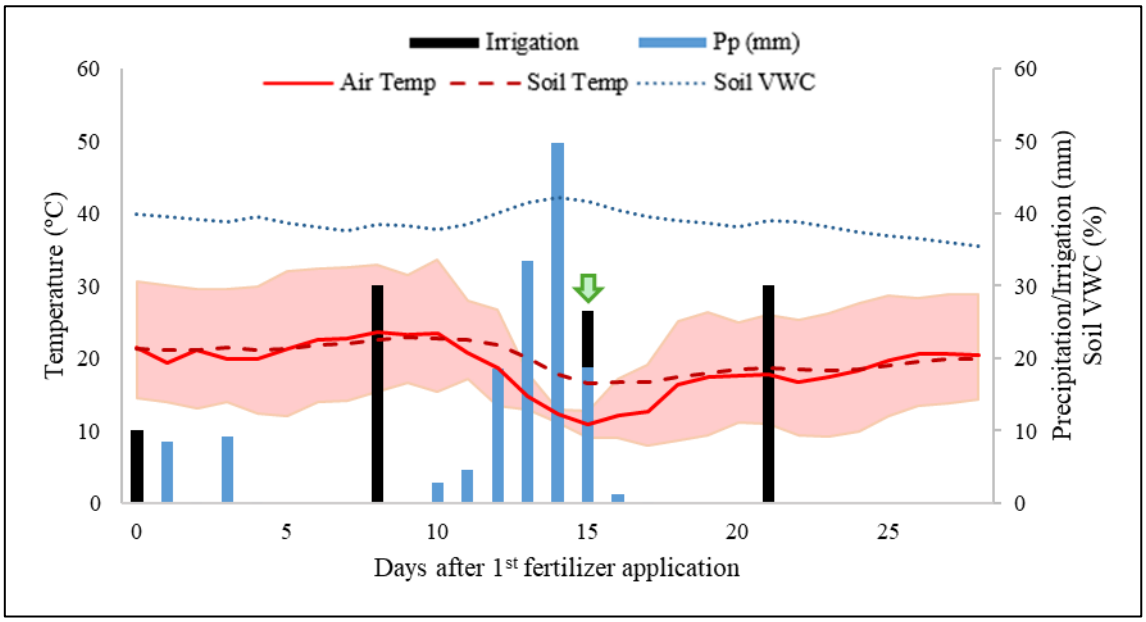

Figure 4.25. Daily precipitation (Pp), irrigation, average air temperature, average soil temperature at 10 cm depth and average soil volumetric water content (VWC). The reddish area corresponds to the daily air thermal amplitude. The green arrow denotes the date of the second fertilizer application (29 August 2023).

4.4.2. Soil mineral N and WFPS

The WFPS ranged from 64% to 80% throughout the experimental period (Figure 4.26), with the highest value reported the day before the second fertilizer application, following several days of intense precipitation (Figure 4.25). Baseline soil NH_4^+ and NO_3^- concentrations were 2.8 mg N kg^{-1} and 7.9 mg N kg^{-1}, respectively. Soil NO_3^- concentrations increased to 47.1 mg N kg^{-1} and 61.0 mg N kg^{-1} (44.5 and 57.6 kg N ha^{-1}) two days after the first and second fertilizer applications, respectively. However, soil NH_4^+ concentrations remained stable (< 7.8 mg N kg^{-1} or 7.4 kg N ha^{-1}) throughout the experimental period (Figure 4.26) despite the addition of 40 kg N–NH_4^+ ha^{-1} in both fertilization events.

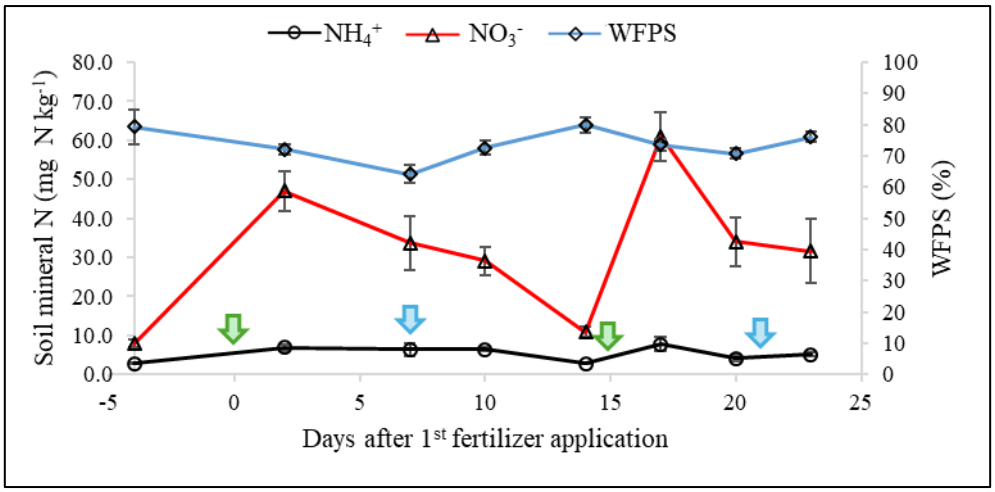

Figure 4.26. Daily soil NH_4^+ and NO_3^- concentrations and WFPS. The green arrows denote the two fertilization events (14 and 29 August 2023). The blue arrows denote the two irrigation events (22 August and 4 September 2023). Vertical lines correspond with the standard error of the mean (n = 6).

4.4.3. CO_2 and CH_4 fluxes

The average daily CO_2 emission flux (29.7 kg C ha^{-1} d^{-1}, Figure 4.27a) was in the order of the background fluxes (38 kg C ha^{-1} d^{-1}). The lowest CO_2 fluxes were reported in the middle of the experiment, coinciding with a decrease in temperature (Figure 4.25). In fact, daily CO_2 fluxes were strongly correlated with both air temperature (P < 0.001; r = 0.70) and soil temperature (P < 0.05; r = 0.66) (Figure 4.33). Daily CH_4 fluxes ranged from −0.98 to −5.31 g C ha^{-1} d^{-1}

(Figure 4.27b), remaining similar to background fluxes (−3.99 g C ha^{-1} d^{-1}). Daily CH_4 fluxes were negatively correlated with air temperature ($P < 0.05$; r = −0.53) and positively correlated with soil VWC ($P < 0.01$; r = 0.62) (Figure 4.33). At the end of the experiment, cumulative CO_2 and CH_4 fluxes were 862 ± 22 kg C ha^{-1} and −87.2 ± 9.0 g C ha^{-1}, respectively.

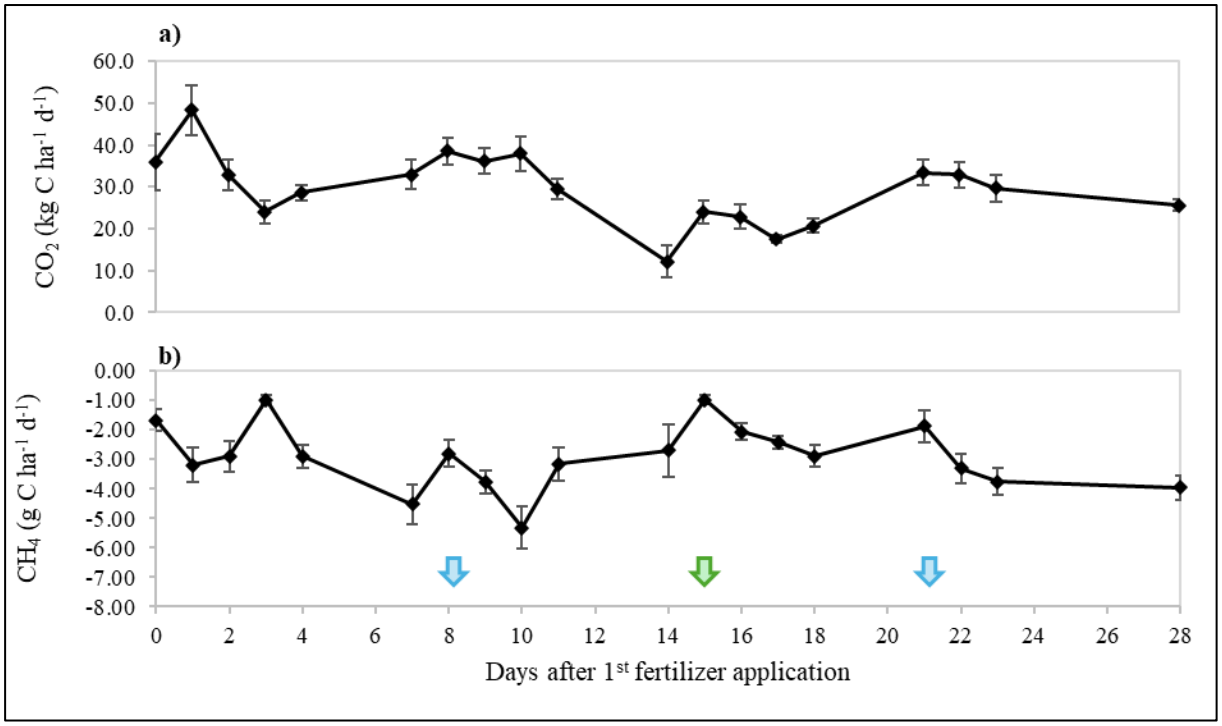

Figure 4.27. Daily CO_2 (a) and CH_4 (b) emission fluxes. The green arrow denotes the date of the second fertilizer application (29 August 2023). The blue arrows denote the two irrigation events (22 August and 4 September 2023). Vertical lines correspond with the standard error of the mean (n = 6).

4.4.4. N_2O and N_2 emissions

The basal N_2O flux measured during the three weeks preceding the first fertilizer application was 1.52 g N ha^{-1} d^{-1} (data not shown). The highest N_2O emission fluxes were reported immediately after the first fertilizer application (175 g N ha^{-1} d^{-1}) and the day following the second fertilization (25.7 g N ha^{-1} d^{-1}) (Figure 4.28). Between fertilization events, N_2O fluxes remained below 20 g N ha^{-1} d^{-1}. On average, daily N_2O emissions derived from the KNO_3 fertilizer (N_2O-N_{fert}) accounted for 17.2 % of total N_2O emissions (Figure 4.28), contributing to 27.5% of cumulative N_2O emissions over the experimental period (Table 4.27).

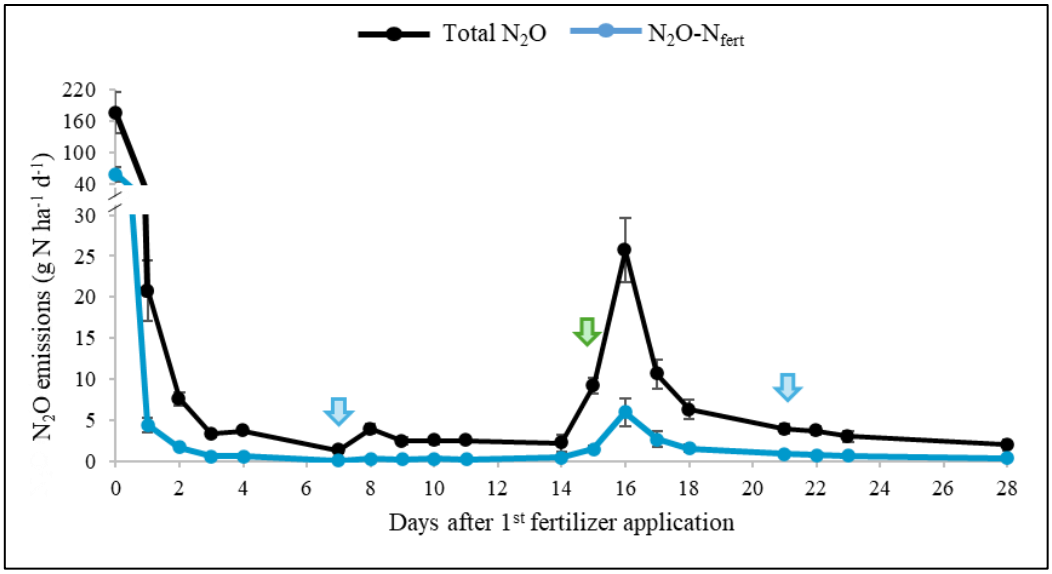

Figure 4.28. Daily total N_2O emission fluxes (Total N_2O) and daily N_2O emission fluxes derived from the KNO_3 fertilizer ($N_2O{-}N_{fert}$). The green arrow denotes the date of the second fertilizer application (29 August 2023). The blue arrows denote the two irrigation events (22 August and 4 September 2023). Vertical lines correspond with the standard error of the mean (n = 6).

Nitrification was the major contributor to N_2O emissions on most days (Figure 4.29). However, the days with the highest N_2O emission fluxes –specifically, the day of the first fertilization and the day following the second fertilization– N_2O_d exceeded N_2O_n (Figure 4.29). Consequently, by the end of the experiment, denitrification accounted for 62% of the total cumulative N_2O emissions (Table 4.27).

Table 4.27. Total N fertilization rate via KNO_3 (98% atom ^{15}N). Cumulative total N_2O emissions and N_2O emissions derived from the fertilizer ($N_2O{-}N_{fert}$), derived from denitrification (N_2O_d) and derived from nitrification (N2On). Cumulative total N_2 emissions and N_2 emissions derived from the fertilizer ($N_2{-}N_{fert}$). Denitrification ratios ($N_2O/(N_2O_d+N_2)$ and $N_2O_d/(N_2O_d+N_2)$).

Total KNO_3 fertilizer addition (kg N ha^{-1})	**80**
Total N_2O (g N ha^{-1})	320 ± 49
$N_2O{-}N_{fert}$ (g N ha^{-1})	87.9 ± 16.7
N_2O_d (g N ha^{-1})	198 ± 39
N_2O_n (g N ha^{-1})	122 ± 12
Total N_2 (kg N ha^{-1})	2.15 ± 0.67
$N_2{-}N_{fert}$ (kg N ha^{-1})	1.15 ± 0.33
$N_2O/(N_2O+N_2)$ (%)	16 ± 3
$N_2O_d/(N_2O_d+N_2)$ (%)	10 ± 1

Data are expressed as the mean (n = 6) ± standard error

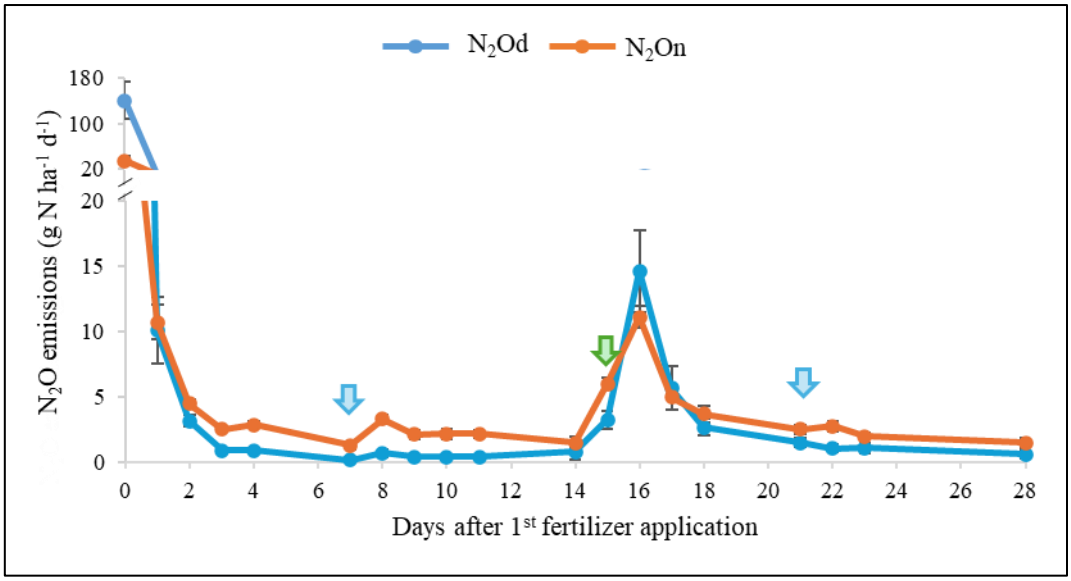

Figure 4.29. Daily N_2O emission fluxes derived from denitrification and nitrification processes (N_2O_d and N_2O_n, respectively). The green arrow denotes the second fertilizer application event (29 August 2023). The blue arrows denote the two irrigation events (22 August and 4 September 2023). Vertical lines correspond with the standard error of the mean (n = 6).

The N_2O emissions (including total N_2O, N_2O from $K^{15}NO_3$ fertilizer, N_2O_d, and N_2O_n) were positively corelated with soil NO_3^- concentration, with correlations coefficients ranging from 0.84 to 0.87 ($P < 0.05$) (Figure 4.33).

Regarding N_2 emissions, the highest fluxes were reported coinciding with both fertilizer applications (168 g N ha^{-1} d^{-1} and 137 g N ha^{-1} d^{-1} after the first and second fertilization, respectively) and with the second irrigation event (455 g N ha^{-1} d^{-1}) as shown in Figure 4.30. On average, 55% of the daily N_2 emissions were derived from the $K^{15}NO_3$ fertilizer (Figure 4.30). Thus, at the end of the experiment, N_2 emissions from the fertilizer accounted for 53% of total N_2 emissions (Table 4.27). Cumulative N_2 emissions derived from the fertilizer were 13 times higher than N_2O emissions from fertilizer (Table 4.27).

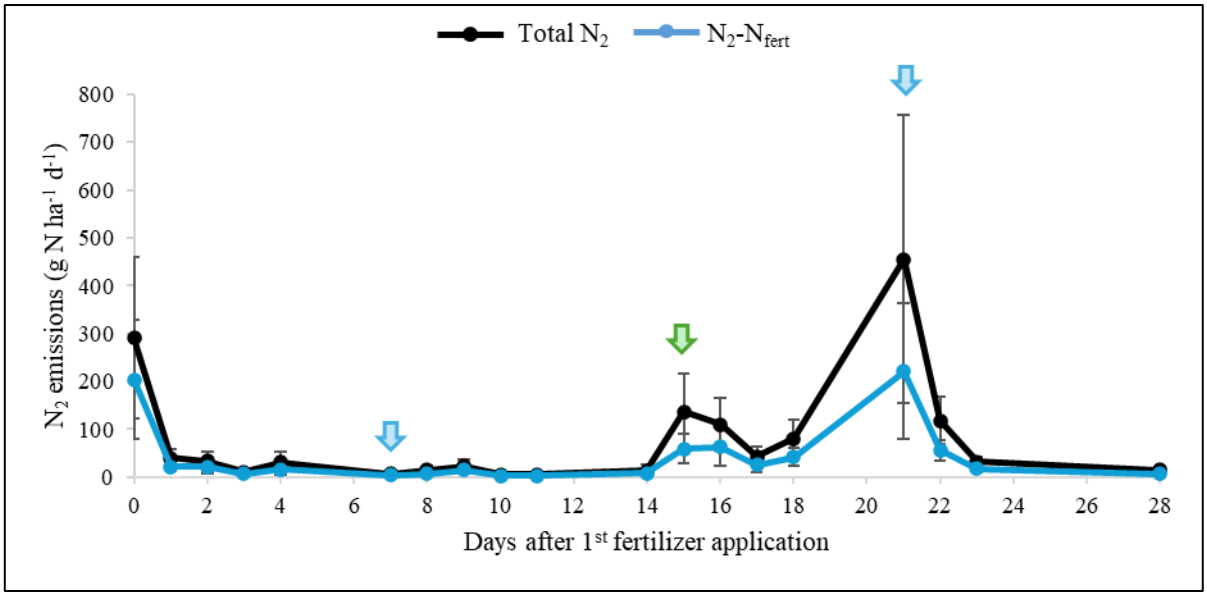

Figure 4.30. Daily total N_2 emission fluxes (Total N_2) and daily N_2 emission fluxes derived from the KNO_3 fertilizer (N_2-N_{fert}). The green arrow denotes the date of the second fertilizer application (29 August 2023). The blue arrows denote the two irrigation events (22 August and 4 September 2023). Vertical lines correspond with the standard error of the mean (n = 6).

The average ($N_2O_d/(N_2O_d+N_2)$) ratio was 0.10 (Table 4.27), reaching values of 0.45 and 0.20 after the first and second fertilization events, respectively (Figure 4.31).

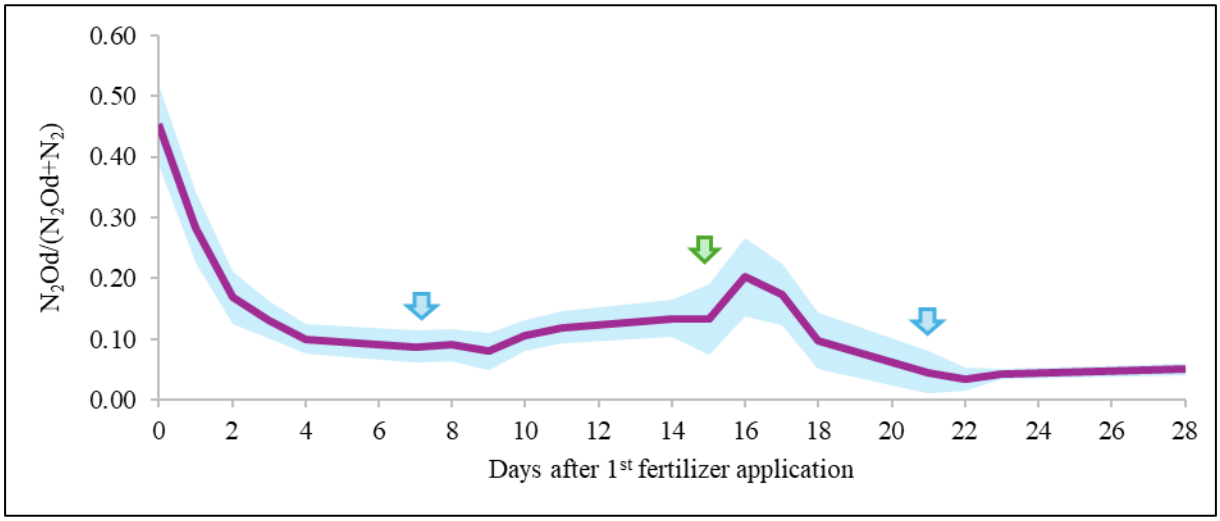

Figure 4.31. Daily $N_2O_d/(N_2O_d+N_2)$ ratio. The green arrow denotes the date of the second fertilizer application (29 August 2023). The blue arrows denote the two irrigation events (22 August and 4 September 2023). The blueish area corresponds with the standard error of the mean (n = 6).

4.4.5. Fertilizer N recovery

At the end of the experiment, 28.5 ± 1.1% of the N in AGB was derived from the $K^{15}NO_3$ fertilizer (Table 4.28). Although BGB yield was more than twice that of AGB, and that total N uptake was similar in both parts of the plants, fertilizer-derived N accounted for only 9.0 ± 1.1% of the N in BGB. This was because of the lower N and ^{15}N concentrations in BGB compared to AGB (Table 4.28). Given the low contribution of fertilizer-derived N to total plant N, total N recovery in plant was 37.2 ± 3.6%, while more than 50% of the fertilizer N was recovered in the soil (Figure 4.32), primarily within the top 15 cm layer. The measured N losses (N_2O, N_2, and mineral N leaching) represented less than 2% of the total N applied, with N_2 being the dominant loss pathway. Thus, 7.4 ± 1.6% of the N applied via ^{15}N-labeled fertilizer remained unaccounted for.

Table 4.28. Yield, total N uptake, N uptake derived from the $K^{15}NO_3$ fertilizer (plant_Nfert), N content and ^{15}N enrichment in aboveground biomass (AGB) and belowground biomass (BGB).

		Yield (D.W.) (t ha^{-1})	Total N uptake (kg N ha^{-1})	Plant_N_{fert} (kg N ha^{-1})	N content (%)	^{15}N (atom % excess)
AGB		1.8 ± 0.1	80.7 ± 4.0	23.0 ± 1.4	4.7 ± 0.1	28.2 ± 1.1
BGB	(0-5cm)	2.9 ± 0.3	46.9 ± 7.6	4.0 ± 1.4	1.6 ± 0.2	7.7 ± 1.3
	(5-15 cm)	2.0 ± 0.9	22.5 ± 7.3	2.8 ± 1.0	1.4 ± 0.2	11.9 ± 1.2
	(0-15 cm)	4.9 ± 1.0	69.4 ± 10.0	6.8 ± 1.7		

Data are expressed as the mean (n = 6) ± S.E.

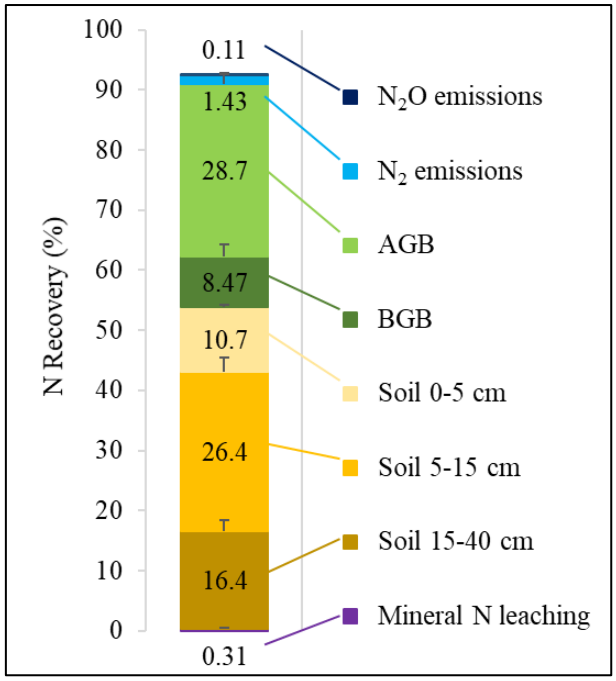

Figure 4.32. N recovery (%) from the KNO_3 fertilizer. Data in the colored bars correspond with the % of N recovery in the different N fates (N_2O and N_2 emissions, aboveground biomass (AGB), belowground biomass (BGB), soil at the different depths, and mineral N leaching). Vertical lines denote the standard error of the mean (n = 6, except for mineral N leaching, where n = 3).

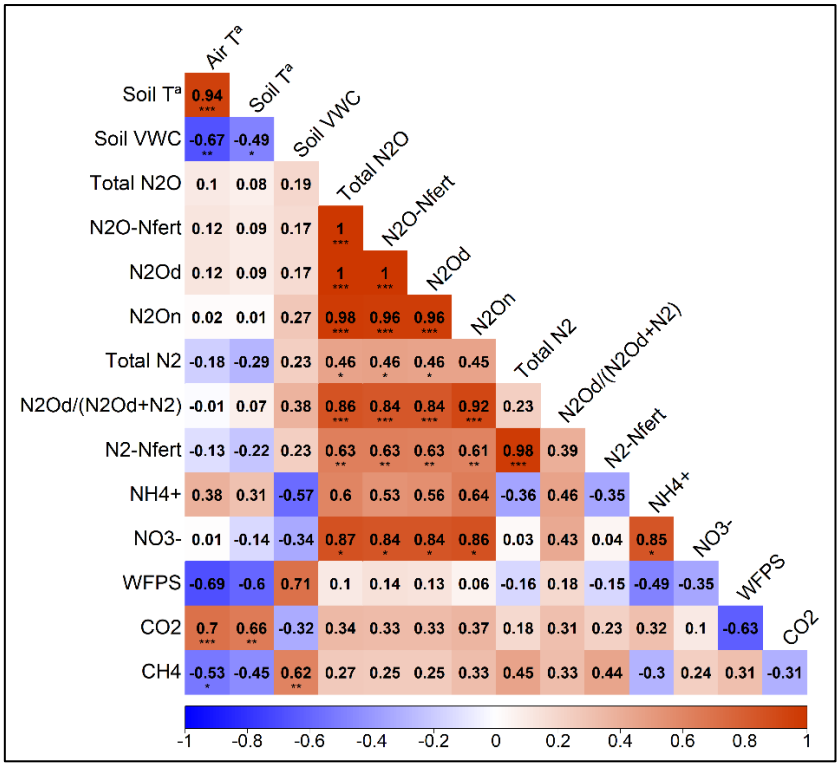

*Figure 4.33. Pearson correlation coefficients for the daily air and soil (at 10 cm depth) temperature, daily soil properties (VWC, WFPS, NH_4^+ and NO_3^-), daily total N_2O, N_2, CO_2 and CH_4 emissions, daily N_2O and N_2 emissions derived from the $K^{15}NO_3$ fertilizer (N_2O-N_{fert} and N_2-N_{fert}, respectively), and the daily denitrification ratio ($N_2Od/(N_2Od+N_2)$). Significance levels are represented by * (P < 0.05), ** (P < 0.01) and *** (P < 0.001).*

4.4.6. Discussion

4.4.6.1. N_2 and N_2O emissions in fertilized pre-alpine grasslands

This is one of the few experiments that provide information regarding direct N_2 emissions from ^{15}N-labeled fertilizer in pre-alpine grasslands (e.g., Dannenmann et al., 2024). Other studies have measured the N_2 losses in grasslands in Northern Ireland using the ^{15}NGF method (McGeough et al., 2012) or mountain grasslands soils using the Helium/Oxygen core method (Zistl-Schlingmann et al., 2019). In this experiment, after the application of 80 kg N ha^{-1} as $K^{15}NO_3$ together with 80 kg N ha^{-1} as $(NH_4)_2SO_4$ split in two applications, total measured N_2 emissions accounted for 2.1 ± 0.7 kg N ha^{-1}, with 1.1 ± 0.3 kg N ha^{-1} derived from the applied ^{15}N-labeled fertilizer (Table 4.27). This indicates that nearly half of the N_2 emissions were derived from sources other than ^{15}N−labeled KNO_3 (i.e., from endogenous soil mineral N or from the $(NH_4)_2SO_4$ fertilizer). Our measured N_2 emissions were lower than expected, considering the results by Dannenmann et al. (2024) under similar environmental conditions and also similar soil properties to those in the herein experiment (i.e., pre-alpine grassland in southern Germany with high-C and high-N soil content). Dannenmann et al. (2024) reported total N_2 emissions of approximately 3.8 kg N ha^{-1}, with a higher proportion derived from the fertilizer (3.0 kg N ha^{-1}) one month after the application of 97.2 kg N ha^{-1} of ^{15}N-labeled slurry to intact soil-plant mesocosms. Furthermore, Yankelzon et al. (2024) reported 10 kg N_2-N_{fert} losses one month after the application of 55 kg N ha^{-1} as double-labeled $^{15}NH_4{}^{15}NO_3$ in a wheat experiment conducted in the same region, but in a cropland soil with lower SOC content. In the latter study, fertilizer-derived N_2 emissions represented 62% of total N_2 losses. Considering the results of the present study together with the studies mentioned above, the addition of unlabeled NH_4^+ from fertilizers (both synthetic and organic manures) may have stimulated high microbial NH_4^+ oxidation, leading to denitrification of easily nitrified NH_4^+. This is supported by the low

soil NH_4^+ concentrations observed in this study, even two days after both fertilization events (Figure 4.26), and is also in accordance with Dannenmann et al. (2024), who reported a rapid decline in soil NH_4^+ to basal levels together with an increase in NO_3^- three days after slurry fertilization. Buchen et al. (2018) suggested the relevant impact of nitrifier denitrification and/or denitrification coupled with nitrification processes in grassland soils, based on the application of isotopocule methods. This is also supported by the high contribution (> 70%) of sources others than the ^{15}N-labeled KNO_3 to N_2O emissions during this experiment (Figure 4.28), and because N_2O_n represented more than one-third of total N_2O emissions (Figure 4.29 and Table 4.27). Furthermore, the higher $N_2O/(N_2O+N_2)$ ratio compared to the $N_2O_d/(N_2O_d+N_2)$ ratio (Table 4.27), also supports the contribution of nitrification processes.

The high WFPS values reported throughout experiment (64% – 80%) and the high soil NO_3^- concentrations after fertilization (Figure 4.26) may have favored denitrification conditions (Pilegaard, 2013). However, the measured total denitrification losses (i.e., $N_2O_d + N_2$) (Figure 4.32,Table 4.27) were lower than the 4.8% denitrification losses reported for grasslands in the global synthesis by Pan et al. (2022). This discrepancy may be particularly relevant because Pan et al. (2022) included a large number of acetylene-inhibition-based studies, which would systematically underestimate denitrification (Scheer et al., 2020). Dannenmann et al. (2024) also reported low denitrification losses (around 3.1% as N_2-N_{fert}), and the authors explained it because of a lack of easily available soil C essential for denitrification when measuring the soil DOC content. Furthermore, McGeough et al. (2012) observed higher N_2 fluxes in two of their seven experimental periods when cattle slurry –a source of labile C– was combined with NO_3^- compared to the application of NO_3^- with an inorganic NH_4^+ source. They also noted that the easily mineralizable C in the cattle slurry promoted N_2O emissions derived from NO_3^-. It is important to note that the ^{15}NGF method, used in the present study, only provides information about denitrification surface fluxes, without considering the storage and subsoil fluxes what

could lead to an underestimation of denitrification fluxes by 28% to 71% (Micucci et al., 2023; Well et al., 2019). This means that closing the chamber results in a rising concentration of ^{15}N-labeled molecules within the chamber headspace, causing surface flux to decrease over time while subsoil and storage fluxes increase (Micucci et al., 2023). Thus, the true N_2 losses may be higher than those reported in the present experiment due to the inherent underestimation associated with the ^{15}NGF method.

The low $N_2O_d/(N_2O_d+N_2)$ ratio reported when considering the cumulative N_2O_d and N_2 fluxes at the end of the experiment (0.10, Table 4.27) suggests that N_2 emissions dominated the end-products of denitrification. This ratio was lower than the mean 0.37 $N_2O/(N_2O+N_2)$ ratio reported by Pan et al. (2022) for grasslands. Furthermore, the $N_2O_d/(N_2O_d+N_2)$ ratio decreased as soil NO_3^- concentration decreased, with the highest $N_2O_d/(N_2O_d+N_2)$ values reported immediately after N fertilization (Figure 4.31). This pattern suggests that the high soil mineral N levels could limit the ability of soil microorganisms to completely denitrify soil NO_3^-. This aligns with general denitrification ecology, where high NO_3^- availability as an electron acceptor reduces the use of N_2O as an alternative electron acceptor (Butterbach-Bahl et al., 2013). In agreement, McGeough et al. (2012) reported higher N_2O fluxes and $N_2O/(N_2O+N_2)$ ratios when cattle slurry was combined with NO_3^- compared to the application of NO_3^- and an inorganic NH_4^+ source.

4.4.6.2. N balance

The 37.2% N recovery in plants reported in this experiment was higher than that reported by Zistl-Schlingmann et al. (2020a) (average recovery of 16% under intensive management) or lower than values observed by Dannenmann et al. (2024) and Schreiber et al. (2023) in similar grassland experiments (49% and 42%–47.5%, respectively). The plant N recovery in the present experiment may have been underestimated, as half of the fertilizer was applied in the second

fertilization, i.e., only 2 weeks before plant harvesting. The contribution of fertilizer N to AGB N (28%, Table 4.28) suggests that plants incorporated N from sources other than the KNO_3 fertilizer, such as NH_4^+−N from $(NH_4)_2SO_4$ fertilizer, atmospheric N deposition or biological N_2 fixation. The contribution of the fertilizer to the AGB was similar to the 30% reported by Dannenmann et al. (2024). However, opposed to the last study, the present experiment included the application of unlabeled fertilizer alongside ^{15}N−labeled KNO_3, which may have reduced the plant N recovery from the ^{15}N−labeled fertilizer.

The total soil N recovery from KNO_3 fertilizer (53.5%) was slightly higher than the 39% reported by Yankelzon et al. (2024) approximately 40 days after applying NH_4NO_3 as fertilizer. However, the recovery was double than those reported by Schreiber et al. (2023) 78 days after fertilizer application and by Dannenmann et al. (2024) one month after fertilizer application, both using $^{15}NH_4^+$ and ^{15}N-urea-labeled cattle slurry. Furthermore, most of the recovered soil N was found in the 5-15 cm and 15-40 cm layers, with only 10.7% recovered in the top 5 cm. These results contrast with those of Dannenmann et al. (2024), who found most soil N recovered in the 0-4 cm depth layer. These could be related to a relatively large irrigation together with the intense rainfall between the two fertilization events, that could have promoted N mobility to deeper soil layers. However, mineral N leaching losses accounted for only 0.3% of the applied KNO_3. Other studies in the same area have also reported low N leaching losses (i.e., 0.02% by Yankelzon et al. (2024) and 0.2% by Dannenmann et al. (2024)). Thus, the high soil N recovery and the low N leaching would suggest that microbial NO_3^- immobilization is leading to a stabilization in soil organic N, that could be facilitated by the high SOC content (Elrys et al., 2022). Some of the ^{15}N−labeled NO_3^- may have been transformed into NH_4^+ via DNRA (Rütting et al., 2011). However, Chen et al. (2015), in montane grassland soils with similar physicochemical properties, found that denitrification was more relevant than DNRA in

anaerobic laboratory incubations. Thus, under the conditions in this experiment, microbial NO_3^- immobilization could better explain the low N leaching and high soil N recovery.

As indicated above, part of the NO_3^- from the fertilizer may have been converted to NH_4^+ via DNRA. This NH_4^+ could then be volatilized as NH_3, potentially accounting for some of the unaccounted N losses of the system (Yankelzon et al., 2024). Another unaccounted N losses were NO emissions; however, these are assumed to be negligible, as previously confirmed under similar conditions (Zistl-Schlingmann et al., 2019). It is also important to note that N_2 emissions may have been underestimated, as previously discussed. Nevertheless, the overall percentage of N losses in the present study was considerably lower than in other studies conducted under Mediterranean conditions, where significant NH_3 volatilization losses (due to the basic soil pH and the widespread application of urea or slurries) or N leaching in irrigated crops can be expected (Gabriel et al., 2012; Guardia et al., 2021; Sanz-Cobena et al., 2014b).

CHAPTER 5

GENERAL DISCUSSION

5.1. Tillage intensity and crop residue management

Conservation agriculture plays a pivotal role in the development of sustainable agricultural systems in the current context of growing food demand and environmental change. Several studies and meta-analyses have reported that no-till practices generally reduce crop yields by 1.4% to 5.6% (Pittelkow et al., 2015a, 2015b; Sun et al., 2024). However, other studies have found no significant (Sun et al., 2024) or even positive (Fernández-Ortega et al., 2024) yield differences between conservation tillage and conventional tillage. Additionally, the meta-analysis of Pittelkow et al. (2015a) pointed out a 7.3% yield increase in rainfed agricultural systems and dry climates when no-till was combined with other conservation agriculture practices such as residue retention and crop rotation. Indeed, conservation tillage has greatest potential for yield improvement in regions prone to recurrent and prolonged droughts, such as the Mediterranean area (Morell et al., 2011a; Sun et al., 2024). This positive effect is likely due to improved water infiltration and higher soil moisture conservation, as reported by Lampurlanés et al. (2016).

Regarding GHGs sinks and sources, it is well known that the implementation of no tillage practices increases SOC content, with an average 23.7% increase according to Meng et al. (2024) because of the reduction of soil aggregates turnover, thus favoring the stabilization of SOC within soil aggregates (Bohoussou et al., 2022). These positive effects have also been reported in Mediterranean agroecosystems (Aguilera et al., 2013a), with SOC increases ranging from 11% to 15%, resulting in a C sequestration rate of 0.32 to 0.44 Mg C ha^{-1} yr^{-1}. However, tillage management has a marked influence on soil N_2O emissions consequence of the interaction between different factors such as soil density, water content, soil aeration, crop residues management and soil organic matter content, among others (Abalos et al., 2013; Y. Li et al., 2023a; Shakoor et al., 2021). According to Shakoor et al. (2024), no tillage reduces N_2O

emissions by 12% (by 18% in semiarid climatic areas) and 21% in China and United States croplands, respectively. Similarly, Meng et al. (2024) reported that reduced tillage and no-tillage practices reduce N_2O emissions by 12.3% and 14.3%, respectively. Studies under Mediterranean conditions have shown decreased (García-Marco et al., 2016) or similar (Guardia et al., 2016b) N_2O emission under no tillage compared to conventional tillage in one-year field experiments. The results from **Experiment 1** of this thesis indicate that soil tillage management did not significantly affect N_2O emissions in a rainfed barley crop under semiarid Mediterranean conditions. Similarly, a long-term experiment by Plaza-Bonilla et al. (2018) under semiarid Mediterranean conditions reported that cumulative N_2O emissions were generally comparable between no tillage compared and conventional tillage, although no tillage significantly mitigated the YSNE.

The agronomic and environmental performance of different tillage intensities is closely linked to crop residues management, including aspects such as removal or retention, quantity, quality, and incorporation depths. Straw return has been shown to have a positive effect on grain yield, with an average significant increase of 4.3% compared to no straw return, according to the meta-analysis by Zhang et al. (2024) for maize, rice, and wheat. However, this yield benefit was observed only when full straw residue (> 3,000 kg ha^{-1}) was returned to the soil, while partial straw return (< 3,000 kg ha^{-1}) had no significant effect, probably because complete straw return better enhances soil fertility and root development. These findings support the results from the unfertilized control area of **Experiment 2**, where maize grain yield was lower when crop residues were partially removed from the topsoil compared to when they were completely incorporated.

Regarding N_2O fluxes, the incorporation of crop residues into the soil has been shown to increase N_2O emissions by an average of 43% according to Abalos et al. (2022b). Furthermore, the recent meta-analysis by Meng et al. (2024) indicated that despite straw retention

significantly increased N_2O emissions (by 12.1%), this increase was mitigated when crop residues retention was combined with reduced tillage and no tillage. When crop residues are retained in the soil, the available C and N for soil microorganisms is increased, which can enhance denitrification and nitrification processes, potentially leading to increased N_2O emissions (Shakoor et al., 2021). However, the incorporation of mature residues —those with high lignin content and a C:N ratio > 30— can promote microbial biomass growth and increase inorganic N immobilization, thereby reducing N_2O emissions (Abalos et al., 2022b; Chen et al., 2013). Additionally, these residues may alter the DOC:NO_3^- ratio, favoring complete denitrification and shifting the N_2O:N_2 ratio towards greater N_2 production (Abalos et al., 2013). Before N synthetic fertilization in **Experiment 2**, N_2O emissions decreased when recalcitrant maize residues were retained in the topsoil, likely due to enhanced immobilization. However, after maize top-dressing fertilization, the opposite trend was observed, suggesting that N application was the variable that most conditioned the effect of crop residue incorporation on N_2O emissions. Supporting this, the recent study by Wei et al. (2024) concluded that the impact of straw retention on N_2O fluxes strongly depends on N fertilization and mineral N availability, with reductions in N_2O emissions under low-N conditions and increases under high-N conditions. They proposed that under low mineral N availability, straw may improve soil pore structure and aeration during "hot moment" events, reinforcing the immobilization effect. In contrast, under high N availability, the combination of straw and N substrate could promote denitrification in anoxic microsites. Given the limited number of field studies in Mediterranean agroecosystems, further research is needed to clarify these interactions under such conditions.

According to the meta-analysis by P. Li et al. (2023), straw input increased cumulative CO_2 emissions by an average of 24% compared to no straw input in upland fields, with a smaller increase observed under no tillage compared to conventional tillage. Regarding cumulative CH_4 emission, P. Li et al. (2023) found no significant differences in upland field studies when straw

was returned to the soil. Furthermore, when considering both upland and paddy soils, overall CH_4 emissions significantly decreased with higher input rate, longer input durations, under no-tillage conditions. Contrarily to these findings, the results of **Experiment 2** showed no significant differences in CO_2 and CH_4 emissions all over the experiment regardless of maize residue input.

The risk of N leaching is reduced by 9% -14% when crop residues are returned to the soil in upland fields (Zhijie Li et al., 2021; Wang et al., 2018). Another environmental risk that has not been evaluated in this thesis is the well-known problem of NH_3 volatilization, particularly in calcareous soils as those used in **Experiments 1 – 3**, when ureic or NH_4^+-N based fertilizers are applied (Recio et al., 2020; Sanz-Cobena et al., 2008). No-tillage practices reduce the adsorption capacity of NH_4^+ to soil colloids when crop residues are retained over the soil surface, thus increasing the NH_3 volatilization rates by 26% on average (Pan et al., 2016). This is consistent with recent findings by Guardia et al. (2024b) in a calcareous soil under Mediterranean conditions. To mitigate these losses while maintaining the benefits of conservation tillage, the use of urease inhibitors has been proposed as an effective strategy to reduce NH_3 volatilization and prevent pollution swapping (Guardia et al., 2021; Recio et al., 2020).

5.2. Cover crops in arable rotations

Cover cropping offers notable opportunities with regards to ecosystem services, such as weed and pathogen management, enhancement of biodiversity, as well as climate change adaptation (Kaye and Quemada, 2017; Muhammad et al., 2021). It also improves biological, physical, and chemical soil quality (Blanco-Canqui et al., 2011; Quintarelli et al., 2022). Furthermore, cover crops have been proposed as an alternative to bare fallow during the intercrop period, particularly for mitigating N leaching, with a reported 35% reduction in irrigated systems

according to Quemada et al. (2013), and for increasing SOC stocks (by 7% according to Peng et al. (2023)). Other documented benefits of cover cropping include their potential to enhance the phosphorous recycling by increasing its uptake by cash crops, and preventing nutrient loss via runoff (Yousefi et al., 2024).

However, the impact of cover crops on cash crop yields varies depending on several factors, including the species of both the cash and cover crop, soil properties, cash crop fertilizer management, and the duration of cover cropping phase (Peng et al., 2024; Van Eerd et al., 2023). According to the meta-analysis by Peng et al. (2024), cover cropping increased crop yields by an average of 3%, with improvements of up to 11% in rainfed drylands. The yield benefits were most pronounced when both legume and non-legume cover crop species were combined, reaching a 13% increase (Abdalla et al., 2019). However, in **Experiment 3** with irrigated maize, winter cover crops had no effect on maize yield, similar to the meta-analysis by Fan et al. (2021) in temperate areas. Other studies conducted under Mediterranean conditions have reported yield increases with legume cover crops but no effect with non-legume cover crops (Quemada et al., 2013), or even yield decreases with barley cover crops (Salmerón et al., 2011). The greater effect of legume cover crops may be due to the additional N provided through biological N fixation and N-rich residues.

Different results regarding how cover crops can affect N_2O emissions have been reported in several meta-analyses or reviews, with higher, lower or no effects depending on the cover crop species (legume or non-legume), their interaction with N fertilization, or the timing of measurement (during their growing period or after their incorporation as green manure) (Abdalla et al., 2019; Basche et al., 2014; Y. Li et al., 2023a; Muhammad et al., 2019). Field studies conducted under semiarid Mediterranean conditions have reported increased N_2O emissions with cover crops compared to bare fallow during the cover crops growing phase. This effect can be explained by the C supply from rhizodeposition from actively growing root

systems, which promotes denitrification (Guardia et al., 2016a; Sanz-Cobena et al., 2014a). This was supported by the results of **Experiment 2** of this thesis, with higher N_2O fluxes when high C:N ratio barley cover crop residues were incorporated into the soil, compared to bare fallow. This could also be influenced by denitrification occurring during hot moments after rewetting (Montoya et al., 2022), which were observed during **Experiment 2** (i.e., after cover crop termination), favored by the formation of anoxic environments when incorporating cereal C-rich residues. In contrast, in **Experiment 3**, cover cropping had no significant effect on cumulative N_2O emissions before maize fertilization (including both the cover crop growing phase and their incorporation into the soil), compared to bare fallow. Other studies under Mediterranean conditions using legume cover crops (vetch and pea) in cover crop-maize rotations reported higher N_2O emissions during the legume phase compared to control plots under bare fallow (Franco-Luesma et al., 2022; Sanz-Cobena et al., 2014a). A similar, but non-significant, trend was observed during the cover cropping period in **Experiment 3**. Furthermore, our results confirm the critical role of the cropping period (cover cropping, post-incorporation, cash cropping) when addressing the effects of cover crops on N_2O emissions. Overall, our findings suggest that cover cropping has a small effect on N_2O fluxes, thus questioning its adoption as an effective mitigation practice for direct N_2O emissions. However, when considering direct GHG emissions together with other components of the net CO_2 equivalent emissions balance (e.g., SOC stocks, operations and irrigation, upstream and downstream emissions or albedo change), results under Mediterranean conditions showed that cover cropping is a practice that could improve the agronomical and environmental sustainability of herbaceous cropping systems by reducing the net global warming potential while maintaining cash crop yields (Guardia et al., 2019).

In both **Experiments 2** and **3**, significant N_2O emission peaks were measured following the application of N fertilizer, as observed in other maize experiments under irrigated

Mediterranean conditions (Franco-Luesma et al., 2022; Guardia et al., 2016a). The increase in easily available mineral N after fertilization combined with high WFPS levels consequence of irrigation and elevated summer temperatures resulted in high soil N_2O emissions. These conditions could have favored denitrification processes (Butterbach-Bahl et al., 2013). It is important to note that the $^{15}N_2O$ analyses in **Experiment 3** revealed that NH_4^+−N oxidation-based processes (nitrification, nitrification coupled to denitrification, or nitrifier denitrification) were even more relevant than denitrification itself after maize top-dressing fertilization.

In both **Experiments 2** and **3**, respiration fluxes were higher with cover crops compared to bare fallow before maize fertilization, resulting in increased cumulative CO_2 emissions by the end of the cropping year. However, no differences were observed between cover crops and bare fallow after maize fertilization. This increase in CO_2 emissions was likely due to enhanced C inputs during the cover crop growing phase, which boosted the availability of C substrates, thereby stimulating microbial activity and soil respiration (Muhammad et al., 2021). Further studies on respiration fluxes associated with cover crops are needed to better understand their role as indicators of C cycling and their contribution to the net ecosystem C balance, together with CH_4 oxidation/emission. In line with findings by Guardia et al. (2016a) and Sanz-Cobena et al. (2014a), the soil in **Experiment 2** acted as a CH_4 sink, with no significant differences observed between cover crop treatments.

5.3. Synergies between agricultural practices to increase sustainability

As mentioned earlier, combining two or more conservation agriculture practices can result in higher crop yield increases and N_2O reductions compared to implementing a single practice (Meng et al., 2024; Pittelkow et al., 2015a). For example, integrating reduced tillage practices

with crop residue incorporation (instead of removal) has been shown to improve crop yields, particularly in dry years because of the conservation of soil moisture (Malhi and Lemke, 2007). Similarly, studies combining the practices of no tillage and cover cropping have reported environmental benefits compared to their individual implementation, such as reduced N_2O emissions (Fiorini et al., 2020). In other cases, while no significant effects on N_2O emissions or cash crop yields were observed, the combination reduced NO_3^- leaching (O'Brien et al., 2022).

Furthermore, Xuan Yang et al. (2024), in a 12-years field experiment, reported that recycling organic materials (via crop residue incorporation or manure application), adjusting the N fertilization rates via ISFM, and implementing water-saving irrigation techniques, reduced N leaching, NH_3 volatilization, and N_2O + NO + N_2 emissions by 47%, 11% and 29%, respectively, compared to conventional agricultural practices, all without compromising crop yields. One of the main differences between **Experiment 2** and **Experiment 3** of this thesis is that ISMF was performed in the former one, meanwhile the same synthetic N rate was applied in the latter. This difference may explain why no significant maize yield differences were reported between cover crops in **Experiment 3,** while in **Experiment 2** maize yield was slightly but significantly reduced (by 7%) under vetch compared to barley cover crops and bare fallow. These yield penalties with vetch highlight the challenge of optimizing integrated N management and accurately predicting N release from the decomposition of legume residues. Furthermore, higher cumulative N_2O emissions were reported in the legume-maize rotation at the end of **Experiment 3**, meanwhile no significant differences were found between cover crops and bare fallow when using ISFM in **Experiment 2**. This suggests that adjusting N fertilizer rates —considering the N supplied by legume cover crops and the soil mineral N levels before cash crop fertilization— can prevent increases in N_2O emissions when incorporating green manures in the annual rotation, as also reported by Abdalla et al. (2019), Franco-Luesma et al.

(2022), and Guardia et al. (2016a). In addition, Guardia et al. (2019) indicated that under ISFM, vetch had a greater mitigation potential than barley, emphasizing the significant role of upstream GHG emissions from synthetic N fertilizer production. Moreover, conventional fertilization in cover cropping systems may reduce the mitigation potential of legume cover crops compared to bare fallow and cereal cover crops. The authors concluded that combining cover cropping with ISFM is an effective agricultural practice for reducing the global warming potential of irrigated cropping systems in semiarid regions.

Another strategy that has been proposed to reduce N_2O emissions without compromising crop yields is the use of NIs (Xia et al., 2017), which have also been proven effective under Mediterranean conditions (Cayuela et al., 2017). The effectiveness of DMPSA was demonstrated in **Experiment 1** of this thesis, with a reduction of N_2O emissions before barley harvest under rainfed conditions. However, the effect on N_2O emissions and crop yields when NIs are combined with conservation agricultural practices has been less studied. In **Experiment 1**, the combination of no tillage and DMPSA application resulted in reduced cumulative N_2O emissions from ^{15}AN fertilizer. Although this combination did not result in significant crop yield increases, the mitigation of N_2O emissions makes NIs environmentally recommendable. This is further supported by the lower YSNE observed in no tillage compared to conventional tillage, and using enhanced fertilizes (DMPSA at barley top-dressing together with an urease inhibitor at basal fertilization) reported by Montoya et al. (2022) under similar environmental conditions and with similar soil physic-chemical properties than those in **Experiment 1**. Moreover, Corrochano-Monsalve et al. (2020) also reported positive results regarding N_2O emissions with the combination of no tillage and DMPSA under humid conditions in northern Spain. Regarding the effect of DMPSA on reducing N_2O emissions, results from **Experiment 1** align with findings by Guardia et al. (2018), showing that DMPSA inhibited N_2O emissions derived from both fertilizer-derived NH_4^+–N and NO_3^-–N. This suggests that DMPSA may also

exert a detrimental effect on denitrification rates (Barrena et al., 2017; Torralbo et al., 2017), thus possibly having a remarkable efficacy when combined with synthetic fertilizers based on various N forms (i.e., ureic–N, NH_4^+–N, NO_3^-–N).

5.4. Nitrous oxide emission factor

The N_2O EF was calculated in two field experiments with sprinkler-irrigated maize cropping systems under Mediterranean conditions (**Experiments 2** and **3**). The average EF (0.62%) in **Experiment 2** was twice as high as **Experiment 3** (0.3%). Even though both experiments were performed simultaneously in maize and using similar N fertilizer rates (between 170 – 220 kg N ha^{-1}), there were subtle differences between them (i.e., ISFM was used in **Experiment 2** but not in **Experiment 3**, in which AN was used instead of CAN). This discrepancy in EF values may be mainly attributed to differences in calculation methodologies: N difference and ^{15}N-tracing methods in **Experiment 2** and **3**, respectively. Indeed, considering the average cumulative N_2O emissions at the end of **Experiment 3** (160 mg N m^{-2}, Figure 4.19c) and the average N_2O emissions from the unfertilized control plots in **Experiment 2** (46.8 mg N m^{-2}, Table 4.12) (considering a 210 kg N ha^{-1} fertilization rate), the EF in **Experiment 3** would have raised to 0.54% using the N difference approach. Similarly, the average N_2O EF from the fertilizer applied at barley top-dressing in **Experiment 1** was 0.04% when the ^{15}N-tracing method is applied, rising to 0.5% using the N difference method (note that the crop received a previous fertilization event at seeding, and that the N_2O EF from the fertilizer considering the whole cropping cycle cannot be estimated). This suggests that the traditional EF estimation method may overestimate N_2O emissions compared to the ^{15}N-tracing approach. The recommended 0.5% EF for semiarid regions (IPCC, 2019b) and also the average 0.5% EF in Mediterranean regions (Cayuela et al., 2017) are higher than the EF calculated for **Experiments**

1 and **3** using the ^{15}N-tracing approach, but slightly lower than that for **Experiment 2** using the N difference approach.

For **Experiment 4**, the 0.1% EF (representing the N recovery as N_2O emissions from KNO_3 fertilizer) in pre-alpine grasslands was calculated based on a short period (one month after fertilization).

5.5. Main sources and processes leading to N_2O emissions

When considering the results of **Experiment 1** and **3**, both ^{15}AN and $A^{15}N$ contributed to N_2O emissions after fertilization. Despite the distinct environmental conditions in **Experiment 1** (rainfed barley in a dry year, resulting in WFPS values below 30% on most days after fertilization) and **Experiment 3** (irrigated maize with WFPS values ranging from 15% to 64% after maize irrigation), most N_2O emissions in both experiments were derived from fertilizer NH_4^+–N. This suggests that N_2O emissions were primarily related to NH_4^+ oxidation processes (e.g., nitrification, nitrifier denitrification, or coupled nitrification-denitrification) rather than denitrification (Butterbach-Bahl et al., 2013; Pilegaard, 2013). Our results are in accordance with those by Han et al. (2024), who reported higher N_2O emissions from nitrification compared to denitrification in croplands. They are also consistent with studies by Guardia et al. (2018) and Vallejo et al. (2014), which reported higher N_2O emissions derived from ^{15}AN fertilizer than from $A^{15}N$ fertilizer in Mediterranean cropping systems, even at WFPS values exceeding 70%. The significant contribution of nitrifying microbial populations to N_2O emissions in these cropping systems has also been reported by Montoya et al. (2022, 2018). According to Vallejo et al. (2014), under high soil moisture conditions (i.e., after irrigation or rainfall events), NH_4^+–N oxidation can occur in macropores where O_2 is available. The authors also suggested that N_2O emissions from fertilizer-derived NO_3^-–N under lower WFPS values may be related to denitrification processes occurring in anaerobic soil micro-sites. Therefore, the coexistence

of contrasting soil porosities likely facilitates the coupling of nitrification and denitrification processes in irrigated cropping systems, making it key driver of N_2O emissions. Montoya et al. (2022) also highlighted an increase in denitrifying soil microorganisms during rewetting events in the postharvest period of a rainfed cereal crop, leading to high N_2O emission peaks. This process, which was observed in **Experiment 1**, has been widely reported under Mediterranean conditions (Montoya et al., 2021b; Plaza-Bonilla et al., 2014) and requires attention for effective N_2O emissions mitigation strategies considering the entire cropping cycle (Guardia et al., 2024a).

When nitrification is the dominant microbiological process and most N_2O is emitted from NH_4^+−N, our results suggest that the use of NH_4^+−N-based fertilizers could increase N_2O emissions compared to NO_3^-−N-based fertilizers. Furthermore, the application of NH_4^+−N-based fertilizers have the risk of increasing NH_3 losses in calcareous soils, even though a right management during their application (i.e., incorporating the fertilizer instead of leaving it on the soil surface) can reduce this undesirable side-effect (Pan et al., 2016). However, the use of nitric fertilizers instead of NH_4^+−N-based fertilizers or urea is associated with a higher upstream C footprint related to their industrial production (Hoxha and Christensen, 2019) and may also increase NO_3^- leaching losses (Quemada et al., 2013). Thus, fertilizer application with a mixture of both sources (e.g., AN or CAN) could be an effective strategy to mitigate not only N_2O emissions but also other adverse effects, such as those discussed above. Furthermore, the effect of the mineral N source on N_2O emissions is highly dependent on climatic and soil conditions (Cowan et al., 2020; del Prado et al., 2006). For instance, Cowan et al. (2020) reported that urea application on temperate and C-rich grasslands resulted in a lower N_2O EF compared to AN or CAN, possibly due to the higher relevance of denitrification, whereas no differences were observed in arable crops. The authors suggested that this could be related to higher soil aeration in commonly tilled arable crop soils compared to grassland, being NO_3^- leaching potential, soil

pH and C/N substrates, well-known drivers for N_2O processes. Adjusting the fertilizer application timing to match the crop N demand is also necessary to ensure optimal plant N uptake, thereby avoiding N losses via denitrification or NO_3^- leaching (Rozas et al., 2004).

Grasslands frequently exhibit higher organic C levels, leading to a higher soil C:N ratio and higher soil moisture content due to greater precipitation compared to Mediterranean agricultural croplands. These edaphoclimatic conditions make denitrification the predominant source of soil N_2O emissions in grassland ecosystems (Ibraim et al., 2020; Müller et al., 2004b, 2002). In this context, the results obtained in **Experiment 4** of this thesis showed a higher contribution of denitrification during the peaks of N_2O emissions observed immediately after fertilization in pre-alpine grasslands (*hot moments*). This aligns with the meta-analysis by Han et al. (2024), which reported that N_2O emissions derived from denitrification were higher than those from nitrification in grassland experiments, though nitrification-related processes were also relevant (as observed in **Experiment 4** during N_2O *cold moments*). For instance, Buchen et al. (2018) suggested that nitrifier denitrification and/or denitrification coupled with nitrification are also relevant processes in grassland soils.

5.6. Fate of ^{15}N fertilizers

Techniques based on stable N isotopes (^{15}N enrichment or natural abundance) provide quantitatively accurate insights into N pool sizes and N transfer within the soil-plant-atmosphere system. For instance, studies based on ^{15}N natural abundance ($\delta^{15}N$) approaches have quantified the proportion of N derived from N_2 fixation (Manandhar et al., 2024), infer the extent of NH_3 volatilization based on variations in $\delta^{15}N$ signatures of substrates, and distinguish microbial pathways of N_2O formation in soils using isotopomer methods (Chalk et al., 2019). On the other hand, ^{15}N enrichment enables a more accurate quantification of N uptake from fertilizers (both organic or synthetic) and N recovery in plant and soil systems

(Ding et al., 2019; Guardia et al., 2018; Machado et al., 2021). In this thesis, the plant N recovery from fertilizer as well as the N from synthetic fertilizers recovered in the soil at the end of the cropping seasons were calculated using ^{15}N enrichment techniques (**Experiments 1, 3,** and **4,** Table 5.1). Furthermore, N recovery from maize residues applied in **Experiment 3** was also calculated.

Regarding the fate of ^{15}N-labeled maize residues, they were able to provide N in the next cash crop phase, with 7.7% of the N from the previous crop residues being recovered in the subsequent maize crop. This is consistent with the N recovery from maize residues reported by Mubarak et al. (2003) and Taveira et al. (2020). Thus, returning crop residues to the soil is beneficial not only for enhancing C sequestration and improving soil ecology but also for promoting efficient N recycling.

Regarding the fate of ^{15}N-labeled synthetic fertilizers, average plant N recovery in rainfed barley (**Experiment 1**) was 23%, regardless of tillage management or the use of DMPSA. Similarly, Giacomini et al. (2010) reported no differences in N recovery when comparing conventional tillage and minimum tillage, with an average 58% N recovered in wheat in a field study conducted in northern France. A review by Smith and Chalk (2020) found no significant differences in fertilizer N recovery between no tillage and conventional tillage in ^{15}N-tracing experiments, with an average plant N recovery of 37%. Taveira et al. (2020) also observed no differences in plant N recovery between tillage practices in soybean or maize crops. They suggested that the increased crop yield that can be observed under no tillage is likely related to the soil organic N pool or the indirect effects of organic matter on soil moisture, temperature, and plant growth conditions, as supported by Smith and Chalk (2020), rather than an increase in crop use of fertilizer-derived N. In their earlier work, Smith and Chalk (2018) also reported a 43% plant N recovery and 20-30% soil N recovery one year after synthetic fertilizer application.

The average plant N recovery in irrigated maize (**Experiment 3**) was higher with barley cover crops (42%) compared to bare fallow (26%). The immobilization of soil mineral N by the barley cover crop may have temporarily reduced NO_3^- leaching following maize fertilization, resulting in enhanced NO_3^- uptake form the fertilizer (Meng et al., 2021), thereby increasing plant N recovery with barley as the cover crop. In contrast, Gabriel and Quemada (2011) found no difference in N recovery in maize when comparing the use of vetch or barley compared to bare fallow in a three-year field experiment under similar climatic conditions, with average N recoveries ranging from 40% to 51%. Furthermore, in one of the experimental years, they reported higher maize N uptake with the vetch treatment compared to bare fallow, without an increase in crop ^{15}N recovery from the fertilizer, suggesting that reducing maize N fertilization should be recommended for the vetch treatment.

The average 22% soil N recovery in irrigated maize of **Experiment 3** was lower compared to the 36% soil N recovery in rainfed barley of **Experiment 1** (Table 5.1), which may be related to the lower N leaching losses commonly observed in rainfed compared to irrigated cropping systems (Maharjan et al., 2014). The higher soil recovery in rainfed barley could also be related to the lower crop recovery due to the drier conditions (Scordia et al., 2021) and the differences in NUE between winter cereals and maize (Song et al., 2022).

In **Experiments 1** and **3**, 41–45% of the applied N was unaccounted for (Table 5.1), which might be attributed to: 1) NH_3 volatilization due to NH_4^+ fertilization in calcareous soils, particularly when the fertilizer is not incorporated through irrigation or mechanically (e.g., **Experiment 1**); 2) N_2 emissions resulting from denitrification, especially under the water-saturated conditions of **Experiment 3**; and 3) NO_3^- leaching, likely higher under the irrigated conditions of **Experiment 3** compared to the rainfed conditions of **Experiment 1**.

In **Experiment 4**, plants recovered 37% of the ^{15}N-labeled fertilizer (Table 5.1), what represents less than 20% of the total N acquired by plants. This suggests that non-labeled NH_4^+−N applied fertilizer and other N sources, such as N_2 biological fixation, mineralization of soil organic N, and nitrification of soil endogenous N, significantly contributed to plant N uptake (Dannenmann et al., 2024; Zistl-Schlingmann et al., 2020a). Of the 54% soil N recovery (Table 5.1), only 10% was recovered in the top 5 cm of the soil layer. Given that NO_3^- leaching losses were low, the high N recovery in deeper layers may be attributed to microbial NO_3^- immobilization, which leads to the stabilization in soil organic N, favored by the high SOC content (Elrys et al., 2022). In **Experiment 4**, despite the favorable denitrification conditions due to high WFPS values, N_2 emissions and mineral N leaching accounted for only 1.4% and 0.3% of the applied KNO_3 fertilizer, respectively. Therefore, total N losses from the applied KNO_3 fertilizer, including unaccounted N, were relatively small compared to those reported in pre-alpine grassland experiments (Dannenmann et al., 2024; Schreiber et al., 2023). This is likely due to the use of cattle slurry in those studies, where NH_3 volatilization was a major N loss pathway.

Table 5.1 Average N recovery in plant and soil in Experiments 1, 3 and 4.

Experiment	Climate	Crop	Irrigation	Fertilizer	^{15}N−fertilizer rate (kg N ha^{-1})	N Recovery (%)		
						Unaccounted	Plant	Soil
1	Mediterranean semiarid	Barley	No	^{15}AN/A^{15}N	80	41	23	36
3	Mediterranean semiarid	Maize	Yes	^{15}AN/A^{15}N	210	45	33	22
4	Pre-alpine humid	Grassland	Yes	$K^{15}NO_3 + (NH_4)_2SO_4$	80	7	37	54

5.7. Testing of the hypotheses

To summarize whether the hypotheses proposed in the four experiments conducted in this thesis were supported, partially supported or not supported by the results, Table 5.2 presents a synthesis of the results obtained in the experiments that allow testing the hypotheses.

Table 5.2. Testing of the hypotheses.

Objective 1: To evaluate the effect of the combination of different tillage management (conventional tillage, T, or no tillage, NT) with the application of N fertilizer enhanced with DMPSA as nitrification inhibitor or without DMPSA on the biochemical processes responsible for N_2O emissions and on the N fate in a rainfed barley crop under Mediterranean conditions using a ^{15}N-labeled fertilizer.		
Hypotheses	**Testing**	**References and justification**
H1.1) DMPSA would mitigate N_2O emissions from nitrification of both exogenous and endogenous NH_4^+-N in T and, particularly, in NT.	Supported	Cumulative N_2O emissions from NH_4^+−N fertilizer and from soil endogenous N were lower with DMPSA application in the preharvest period, particularly in NT (Table 4.5). This suggests that DMPSA mitigates N_2O emissions from NH_4^+ oxidative processes, being nitrification the major NH_4^+ oxidative process (Butterbach-Bahl et al., 2013). Similar results were reported by Corrochano-Monsalve et al. (2020) and Guardia et al. (2018).
H1.2) Nitrification would be the main process affecting N_2O emissions, as commonly observed in calcareous and low soil organic matter content soils.	Supported	N_2O emissions derived from NH_4^+−N fertilizer were higher compared to those from NO_3^-−N fertilizer during barley growing phase (Table 4.5 and Figure 4.7). These results are in accordance with the review by Aguilera et al. (2013b).

Objective 2: To assess the combined effect of residual N from the previous crop and the residues management (higher residue input when left on the surface, or reduced input after partial removal and deep incorporation) with the integration of different cover crop species (vetch as a legume and barley as a cereal) compared to bare fallow on GHG emissions and cash crop (maize) yield under Mediterranean conditions.		
Hypotheses	**Testing**	**References and justification (when needed)**
H 2.1) Greater inputs of maize residue (high C:N ratio) may reduce N_2O emissions before maize fertilization in a subsequent campaign, due to immobilization, while also increasing N_2O emissions after synthetic N application, due to the release of N and particularly labile C for denitrifiers.	Supported	N_2O emissions were higher in –R compared to +R treatment before maize fertilization (P1 and P2) (Figure 4.11a-b), with opposite results after fertilization (P3) (Figure 4.11c). These results align with those reported in the meta-analyses by Abalos et al. (2022b), Chen et al. (2013), and Hu et al. (2019).
H 2.2) The legume cover crop would increase N_2O emissions due to its reduced effectiveness in terms of offsetting residual N and due to the mineral N input increase from the decomposition of their N-rich residues, which would increase yield-scaled N_2O losses in comparison to the cereal cover crop and bare fallow.	Not supported	There were no differences in N_2O emissions or YSNE between vetch and bare fallow throughout the different experimental periods and at the end of the experiment (Figure 4.11). • Low temperatures during winter caused low N_2O emissions during cover cropping phase (Ussiri and Lal, 2013). • Barley cover crop promoted denitrification during the highest N_2O emission pulse observed after soil rewetting (Zhijie Li et al., 2021). • N_2O emission peaks after N fertilization were the key drivers of annual N_2O losses masking the differences between cover crops, also attenuated through ISFM.
H 2.3) The residual N from the previous cropping season would increase N_2O emissions and drive the performance of cover crops compared to bare fallow, especially during the cover cropping phase.	Supported	Cumulative N_2O emissions before fertilization were lower in the unfertilized control area compared to the area receiving N fertilization the previous cropping season (Figure 4.10a). • Despite there were no significant differences in terms of soil mineral N between both areas, the legacy effect of the N applied in the previous cropping season would have influenced the N_2O emissions, especially at the beginning of the experiment.

Objective 3: To evaluate the combined effect of the incorporation of maize residues with two different cover crop species (barley and vetch) compared to bare fallow on the biochemical processes responsible for N_2O emissions and on the N fate of synthetic N applied in a maize crop under Mediterranean conditions using ^{15}N-labeled maize residues and a ^{15}N-labeled fertilizer.

Hypotheses	Testing	References and justification
H 3.1) The use of vetch as a legume cover crop and as green manure would increase N_2O emissions derived from both soil endogenous N and maize residues from the previous cropping system.	Not supported	Despite cumulative N_2O emissions being higher with vetch compared to barely (Figure 4.19c), there were no differences in N_2O_{15RES} and N_2O_{soil} between cover crops (Table 4.20 and Table 4.21). Possible reasons: • Slow mineralization of maize residues leading to low N_2O_{15RES} (Figure 4.21 and Figure 4.22). • Small differences in NO_3^- content at the end of P1 (cover crops growing phase) between fallow, vetch and barley (Figure 4.18b).
H 3.2) The incorporation of recalcitrant crop residues, such as those from maize stover, would be slowly mineralized, resulting in a limited contribution to N_2O emissions during the subsequent cropping year.	Supported	N_2O emissions derived from ^{15}N–enriched residues accounted for 5% (on average) of daily N_2O fluxes before maize fertilization (Figure 4.21) and up to 3% after fertilization (Figure 4.22). This suggests that high C:N ratio crop residues are slowly mineralized. Similar results were reported by Ferrari Machado et al. (2021).
H 3.3) Despite irrigated conditions, nitrification would be a relevant process influencing N_2O emissions, particularly when no C-rich cover crop residues are applied.	Partially supported	N_2O emissions derived from NH_4^+-N fertilizer were higher compared to those from NO_3^--fertilizer (Figure 4.22). No differences between cover crops or bare fallow were reported on N_2O emissions derived from the NH_4^+ or NO_3^- fertilizers (Table 4.21). • The WFPS was ca. 40% during maize irrigation, thus being favorable for NH_4^+-N oxidation based processes, including nitrification (Pilegaard, 2013). • Low organic C content and basic soil pH limits denitrification (Ussiri and Lal, 2013).

Objective 4: To quantify the N fate (soil, plant and leaching) and the N_2O and N_2 emissions in a pre-alpine grassland soil as well as the relative contribution of nitrification and denitrification processes on N gas fluxes using a ^{15}N-labeled fertilizer.

Hypotheses	Testing	References and justification
H 4.1) Denitrification rather than nitrification would be the dominant process contributing to N_2O emissions under high WFPS values.	Supported	N_2O emissions derived from denitrification represented more than two thirds of total N_2O emission (Table 4.27). These results are in accordance with the studies by Butterbach-Bahl et al. (2013) and Pilegaard (2013).
H 4.2) N_2 could be a major N loss pathway and predominantly explain the unrecovered N in the crop.	Partially supported	N_2 was the main gaseous N loss pathway, but only accounted for 1% of total NO_3^-–N applied (Figure 4.32), lower than the global average value reported by Pan et al. (2022). • Experimental conditions were not as favorable as expected to promote complete denitrification.

5.8. Synthesis of the thesis contribution, practical and research recommendations

This thesis contributes to a deeper understanding of N dynamics and N_2O emissions in Mediterranean croplands and pre-alpine grasslands, providing valuable insights for the stakeholders (particularly the agricultural sector), scientific community and policymakers who seek to design cost-effective strategies that enhance the sustainability of agroecosystems.

For the first time, the effectiveness of DMPSA combined with no tillage was evaluated in semi-arid Mediterranean agroecosystems, integrating ^{15}N isotopic tracing techniques to provide a more precise understanding of N_2O emission sources and N dynamics by determining the soil NH_4^+ and NO_3^- concentrations derived from the ^{15}N-labeled fertilizer for two weeks after fertilizer application and by calculating gross N transformation rates under field conditions (**Experiment 1**). Another novel aspect of this thesis is the evaluation of the interaction between maize residue inputs and cover crop type under Mediterranean climatic conditions, considering the legacy effect of previously applied N (**Experiment 2**). Furthermore, this research is the first to quantify the contribution of maize residue to N_2O emissions and N recovery within an annual cover crop–maize rotation in Mediterranean environments (**Experiment 3**). Additionally, this study provides valuable information regarding field N_2 emissions in pre-alpine grasslands and enhances the understanding of nitrification and denitrification contribution to N_2O emissions under non-Mediterranean conditions (**Experiment 4**).

Based on the experimental results, this study outlines practical recommendations for stakeholders and policymakers seeking to implement agricultural practices to mitigate N_2O emissions without compromising crop yields. A synthesis of these recommendations, along with key future research directions to further advance knowledge in this field, is presented in Table 5.3.

Table 5.3. Practical and research recommendations

Exp.	Crop	Agricultural practices	Recommendations for stakeholders/policymakers	Research recommendations
1	Rainfed barley	• Rapeseed residue incorporation • (Tillage/No tillage) • With/without DMPSA	• No tillage + DMPSA	• Longer experimental times that include climatic variations. • Agricultural practices that could mitigate summer rewetting events to reduce their impact on cumulative N_2O emissions. • Study the contribution of the different N_2O emission related processes under rainfed conditions in Mediterranean croplands measuring the N_2O isotopocules (^{15}N site preference, δO^{18}) and/or using ^{15}N tracing numerical models.
2	Irrigated maize	• Maize residue incorporation (higher/lower input) • Cover crops (vetch, barley, bare fallow) • ISFM	• Higher input of maize crop residues → no penalties in yield or increments in N_2O emissions; potential increases in C sequestration and water retention. • Use of cover crops instead of bare fallow → nutrient cycling, C stock, prevent soil erosion. • ISFM implementation → reduce C footprint (upstream emissions). Need to improve N rate dosing.	• Improve the prediction of N supply from cover crop residues with ISFM to prevent cash crop yield penalties. • Study the effect of cover crops on NH_3 emissions.

Exp.	Crop	Agricultural practices	Recommendations for stakeholders/policymakers	Research recommendations
3	Irrigated maize	• Maize residue incorporation • Cover crops (vetch, barley, bare fallow)	• Use of barley as cover crop → higher plant N recovery compared to and lower N_2O emissions than vetch. • Retain maize residues → low contribution to N_2O emissions and potential SOC increase. • Adjusting N fertilization rate via ISFM to mitigate N_2O emissions with vetch cover crop.	• Contribution of cover crops to direct N_2O emissions. • Study the contribution of the different N_2O emission related processes under irrigated conditions in Mediterranean croplands measuring the N_2O isotopocules (i.e., ^{15}N site preference, δO^{18}) and/or using ^{15}N tracing numerical models (e.g., Ntrace). • Use the ^{15}NGF method to quantify the denitrification losses (N_2O and N_2). • Use of over crop mixtures.
4	Grassland	• Conventional management	• Enhance crop N recovery and decrease the high soil N retention through grassland management. (cuts/year, density, mixtures with N-acquisitive species or cultivars) or fertilizer N management.	• Fungal/bacterial denitrification measuring the N_2O isotopocules (i.e., ^{15}N site preference, δO^{18}). • N_2 measurements under different experimental conditions. • NH_3 volatilization measurements.

During this research there has been found a series of knowledge gaps that should be addressed by future research.

I) Multiannual agronomic studies

The adoption of conservation agricultural practices, such as crop rotation, reduced or no-tillage systems, and cover cropping, can influence soil properties, N transformation rates, soil organic matter, or microbial communities. However, their effects may vary depending on whether they are assessed in short-term versus long-term studies (Berhane et al., 2020; Pittelkow et al., 2015b). Multiannual data could allow us to evaluate the variability on N_2O emissions and crop productivity in response to seasonal changes, varying weather conditions, soil moisture levels or different farming practices. Furthermore, organic amendments, including crop residues incorporation, are expected to have residual and/or additive effects through consecutive cropping cycles. Therefore, long-term studies are essential for comprehensively assess the sustainability of these practices and improve the accuracy of NUE and N_2O EFs estimations. This is essential for distinguishing long-term patterns from short-term anomalies, such as those caused by drought or unusually wet seasons, allowing the identification of consistent factors that influence N_2O emissions when implementing conservation agriculture practices beyond seasonal or annual variability.

II) Assessing management practices to mitigate N_2O pulse events

The N_2O hot moments after rewetting, particularly those occurring during summer and/or early autumn (postharvest period of winter crops), may account for the majority of N_2O emissions in rainfed cropping systems, as observed in Experiment 1. Therefore, it is necessary to assess whether different agricultural practices (e.g., tillage intensity, crop residue retention, or N management) could mitigate the N_2O emissions during these events. However, N_2O pulses following rewetting events are not only associated to agronomic management or fertilization

practices, but are also strongly influenced by microbial reactivation (Guardia et al., 2024a). In this context, it is necessary to i) enhance our understanding of the processes and drivers underlying these rewetting events and, ii) improve their quantification by developing protocols with higher temporal (i.e., automatic measuring chambers) and spatial resolution.

III) Assessing the contribution of cover crop residues to N_2O emissions

The incorporation of easily mineralizable cover crop residues, including both their aboveground and belowground biomass, is expected to stimulate N_2O emissions during the first weeks or months after their incorporation into the soil. Tracing experiments using ^{15}N–enriched cover crop residues (including legumes and non-legume species) could provide valuable insights into their specific contribution to N_2O emissions, allowing differentiation from emissions originated from soil, from cover crops mineralization, or from synthetic fertilizer applied to the cash crop. Furthermore, mixtures of legume and non-legume cover crops may combine the benefits of legumes (e.g., reduced synthetic N fertilizer requirements for the subsequent crop) with those of non-legumes (e.g., lower NO_3^- leaching), while also enhancing cash crop yields and microbial diversity (Drost et al., 2020; Elhakeem et al., 2021). However, there is limited information on their environmental and agronomic performance under field conditions, particularly in Mediterranean regions.

IV) Calculating gross N transformation rates

Understanding soil N transformation processes that regulate plant-available N and its potential losses from agricultural system is essential for mitigating N_2O emissions in agroecosystems. Performing ^{15}N-tracing experiments enable the use of numerical ^{15}N-tracing models (Müller et al., 2007, 2004a), which can provide detailed insights into how different N fertilization strategies (e.g., organic or synthetic fertilization, or the application of enhanced fertilizers) and agricultural management practices (e.g., tillage, crop residue incorporation, cover cropping)

influence N_2O consumption and production processes by calculating gross N transformation rates (e.g., N mineralization, NH_4^+ and NO_3^- immobilization, autotrophic and heterotrophic nitrification or DNRA) (Inselsbacher et al., 2013; Rütting et al., 2011). This knowledge can help to prevent N losses from agroecosystems and thus enhance crop yields. Most of these experiments have been conducted under controlled laboratory conditions, with only a few performed under field conditions and/or including plants (e.g., He et al., 2020; Loick et al., 2021), particularly in semiarid agroecosystems such as those in Mediterranean regions. Upscaling gross N transformation experiments to field settings and incorporating plant-soil interactions ―which play a crucial role in soil N cycling (L'Espérance et al., 2024)― will be a major challenge in future research on reactive N losses and crop N nutrition.

V) Discriminating between the different N_2O production and consumption processes

A better understanding of N_2O sources can be achieved through high-precision analytical techniques based on the natural abundance intramolecular distribution of ^{15}N within the N_2O molecule ($\delta^{15}N^{\alpha}$ and $\delta^{15}N^{\beta}$), what enables the calculation of the $\delta^{15}N$ site preference ($^{15}N^{SP}$, $\delta^{15}N$ difference in α site and β site of N_2O). Furthermore, the $^{15}N^{SP}$ together with the $\delta^{18}O$ in N_2O are considered robust tools to address N_2O and N_2 sources, distinguishing between bacterial denitrification, nitrifier nitrification, nitrifier denitrification and fungal denitrification (Zhijie Li et al., 2021; Toyoda et al., 2017). The different N_2O production pathways have their own range of isotopic signatures, as reported in several studies (Ibraim et al., 2019; Toyoda et al., 2017). Recently, these techniques have been used to discriminate the N_2O produced via nitrifier denitrification or DNRA (Xu et al., 2024), which has been identified as a relevant contributor to N_2O emissions under certain environmental and management conditions (e.g., acidic and fertile soils) but remains challenging to be differentiated from other N_2O production pathways.

VI) Quantification of N_2 losses

Although N_2 itself is environmentally benign and poses no risk to human health, its production during denitrification leads to economic losses by depleting the pool of available NO_3^-−N for crops, thereby reducing NUE (Pan et al., 2022). In Mediterranean agricultural systems, denitrification driven by high soil WFPS during irrigation or following rewetting events in rainfed systems may result in significant N_2 losses, yet these losses remain largely understudied. To our knowledge, the study by Guardia et al. (2018) is, to date, the only field experiment that has quantified N_2 losses under Mediterranean conditions, reporting an average emissions of 10 kg N ha^{-1} after the application of 180 kg N ha^{-1}. However, these findings were based on a two-week measurement period. Given that N_2 losses are closely related to N_2O emissions, assessing N_2 losses using the ^{15}NGF method (Friedl et al., 2020) could improve our understanding of the factors regulating the denitrification ratio (N_2O:N_2). This knowledge could help to develop management strategies to mitigate environmental impacts while improving NUE.

VII) Effect of agricultural practices on NH_3 volatilization

Ammonia volatilization from agricultural soils is a growing concern due to its adverse effects on human health (Wyer et al., 2022) and the environment, including soil acidification, eutrophication, and indirect N_2O emissions. Its volatilization, atmospheric transport, and subsequent deposition not only contribute to these environmental issues but also lead to economic losses by reducing NUE. Agricultural practices such as the incorporation of organic/synthetic fertilizers, the adequate choice of N sources, or the use of urease inhibitors, have been proven effective in mitigating NH_3 emissions (Guardia et al., 2021; Recio et al., 2020, 2018). However, limited information is available on NH_3 emissions in Mediterranean cropping systems, particularly using accurate quantification methods (Herrero et al., 2021), with regards to: i) the effect of cover crops, which may serve as a potential input of NH_4^+-N or

act as a physical barrier promoting volatilization; and ii) the role of irrigation management as a potential N incorporation pathway (e.g., through fertigation techniques).

CHAPTER 6

CONCLUSIONS

Based on the objectives described in Chapter 2, the following conclusions have been obtained:

1. During a dry season under Mediterranean conditions, DMPSA significantly mitigated N_2O emissions from both endogenous and exogenous N during the barley growing period. However, N_2O fluxes during barley cropping season were low, with most emissions driven by a postharvest rewetting peak. This suggests that although the use of DMPSA was effective during the cropping phase, the particular environmental conditions and N_2O emission pattern in rainfed Mediterranean crops may limit its potential for N_2O mitigation.

2. During a rainfed barley cropping season, combining DMPSA with no tillage improved crop development and plant N uptake while increasing N retention in the upper soil layers. This may reduce potential environmental impacts such as N leaching.

3. During a cover crop-maize rotation under Mediterranean conditions, the incorporation of high C:N ratio maize stover and the implementation of cover crops followed by their incorporation into the soil could be considered as potential N_2O hotspots under conditions favoring denitrification (e.g., following maize irrigation and after N fertilization).

4. The influence on N_2O emissions of the amount of maize residue input (i.e., higher N_2O emissions with lower maize residue input) was greater than that of cover cropping during the intercrop period. Neither of the two conservation agriculture practices (i.e., crop residue incorporation and cover cropping) had an effect on area-scaled or yield-scaled N_2O emissions when considering the entire cover crop-cash crop annual rotation.

5. Using vetch as a cover crop under ISFM can be an effective strategy to reduce direct and upstream emissions, but it requires a better quantification of the mineralized N which would be potentially available for the cash crop.

6. In both rainfed and irrigated systems under Mediterranean climate, NH_4^+ from fertilizer was the predominant source of N_2O emissions, suggesting that NH_4^+ oxidation-based processes

are relevant pathways for N_2O production in these environments. Furthermore, the contribution of soil endogenous N to N_2O emissions following synthetic N application should not be neglected. Maize residues had a low (< 5%) contribution to direct N_2O emissions during an annual cover crop-maize rotation.

7. Fertilizer N recovery in rainfed barley was not affected by tillage or DMPSA. However, cereal cover cropping increased plant N recovery in irrigated maize compared to bare fallow. Fertilizer–N recovery in plants was higher in irrigated maize (33%) compared to rainfed barley (23%). An average 41% and 45% of applied ^{15}N remained unaccounted for in rainfed barley and irrigated maize, respectively, suggesting potential losses via NH_3 volatilization, NO_3^- leaching, or N_2 emissions.

8. In the pre-alpine grassland experiment, N_2 was the primary gaseous N loss pathway (1.4% of the applied N fertilizer). Nearly half of the N_2 emissions originated from sources other than the ^{15}N-labeled fertilizer. Although N_2O emissions derived from denitrification accounted for 62% of total N_2O emissions, nitrification was the dominant process in the days with low N_2O fluxes. The recovery in crop and soil accounted for 37% and 54% of the synthetic ^{15}N applied, respectively.

9. Conservation agriculture practices such as no tillage, residue retention and incorporation, and the use of barley as a cover crop exhibited neutral to positive effects on N_2O emission mitigation, crop yield, and N recovery. Therefore, their implementation should be considered, particularly given their potential to enhance soil quality and reduce the carbon footprint.

En base a los objetivos propuestos en el Capítulo 2, se han obtenido las siguientes conclusiones:

1. En un cultivo de cebada en secano en clima Mediterráneo, el DMPSA mitigó significativamente las emisiones de N_2O procedentes del N endógeno del suelo y del fertilizante durante el periodo de cultivo de la cebada, durante el cual los flujos de N_2O fueron bajos, produciéndose los principales picos de emisión durante un evento de rehumectación del suelo en post-cosecha. Esto sugiere que, pese a que el DMPSA fue efectivo durante el periodo de cultivo, las particulares condiciones climáticas y el patrón de emisión de N_2O en cultivos de secano en climas Mediterráneos puede limitar su potencial para mitigar las emisiones de N_2O.
2. En un cultivo de cebada en secano, la combinación DMPSA y no laboreo mejoró el desarrollo del cultivo y la absorción de N por la planta y aumentó la retención de N en las capas superficiales del suelo. Esto puede reducir potenciales efectos medioambientales como el lixiviado de N.
3. En una rotación de cultivos cubierta y maíz en clima mediterráneo, la incorporación de residuos de maíz con alta relación C:N, y la implementación de cultivos cubierta seguido de su incorporación al suelo, podría considerarse como potencial "punto caliente" de emisión de N_2O bajo condiciones que favorezcan la desnitrificación (por ejemplo, tras el riego y la fertilización del maíz).
4. La influencia en las emisiones de N_2O de la cantidad de residuos de maíz incorporados en la capa arable del suelo (es decir, mayores emisiones de N_2O con una menor incorporación de rastrojos) fue mayor que el efecto de los cultivos cubierta durante el periodo intercultivo. Ninguna de esas dos prácticas de agricultura de conservación (manejo de residuos y cultivos cubierta) afectaron a las emisiones de N_2O por hectárea o escaladas al rendimiento al considerar la rotación anual completa (cultivo cubierta + cultivo principal).

5. El uso de veza como cultivo cubierta bajo un manejo integrado de la fertilización puede ser una estrategia efectiva para reducir las emisiones de N_2O directas y aguas arriba, pero requiere una mejor cuantificación del N mineralizado que podría estar disponible para el cultivo principal.

6. Tanto en cultivos de secano como de regadío en clima mediterráneo, el NH_4^+ del fertilizante fue la principal fuente de emisiones de N_2O, lo que sugiere que los procesos basados en la oxidación del NH_4^+ son vías relevantes para la producción de N_2O. Además, no se debería subestimar la contribución del N endógeno del suelo incluso tras la aplicación de fertilizantes sintéticos. Los residuos de maíz tuvieron una baja contribución (< 5%) a las emisiones directas de N_2O durante una rotación anual de cultivo cubierta–cultivo principal.

7. La recuperación de N procedente del fertilizante en la cebada no se vio afectada por el laboreo ni por el uso de DMPSA. Sin embargo, el uso de cereal como cultivo cubierta aumentó la recuperación del N del fertilizante aplicado al maíz (33%) en comparación con el barbecho (23%). De media, quedó sin contabilizar el 41% del ^{15}N aplicado en cebada y el 45% en maíz. Esto sugiere posibles pérdidas por volatilización de NH_3, lixiviación de NO_3^- o emisiones de N_2.

8. En el experimento en pastizales pre alpinos, el N_2 fue la principal vía de pérdida gaseosa de N (1,4% del N aplicado como fertilizante). Casi la mitad de las emisiones de N_2 procedieron de fuentes distintas al fertilizante marcado con ^{15}N. Aunque las emisiones de N_2O derivadas de la desnitrificación representaron el 62% del total de emisiones de N_2O, la nitrificación fue el proceso predominante en los días con bajos flujos de N_2O. La recuperación del N del fertilizante fue del 37% en el cultivo, permaneciendo el 54% en el suelo al final del ensayo.

9. Las prácticas de agricultura de conservación, como la siembra directa, la retención e incorporación de residuos en el suelo, y el uso de cebada como cultivo cubierta, mostraron

efectos neutros o positivos en la mitigación de emisiones de N_2O, en el rendimiento y en la recuperación de N por parte de los cultivos. Por lo tanto, su implementación debería considerarse, especialmente dado su potencial para además mejorar la calidad del suelo y reducir la huella de carbono.

REFERENCES

Abalos, D., Jeffery, S., Sanz-Cobena, A., Guardia, G., Vallejo, A., 2014. Meta-analysis of the effect of urease and nitrification inhibitors on crop productivity and nitrogen use efficiency. Agriculture, Ecosystems and Environment 189, 136–144. https://doi.org/10.1016/j.agee.2014.03.036

Abalos, D., Recous, S., Butterbach-Bahl, K., De Notaris, C., Rittl, T.F., Topp, C.F.E., Petersen, S.O., Hansen, S., Bleken, M.A., Rees, R.M., Olesen, J.E., 2022a. A review and meta-analysis of mitigation measures for nitrous oxide emissions from crop residues. Science of The Total Environment 828, 154388. https://doi.org/10.1016/j.scitotenv.2022.154388

Abalos, D., Rittl, T.F., Recous, S., Thiébeau, P., Topp, C.F.E., van Groenigen, K.J., Butterbach-Bahl, K., Thorman, R.E., Smith, K.E., Ahuja, I., Olesen, J.E., Bleken, M.A., Rees, R.M., Hansen, S., 2022b. Predicting field N2O emissions from crop residues based on their biochemical composition: A meta-analytical approach. Science of The Total Environment 812, 152532. https://doi.org/10.1016/j.scitotenv.2021.152532

Abalos, D., Sanz-Cobena, A., Andreu, G., Vallejo, A., 2017. Rainfall amount and distribution regulate DMPP effects on nitrous oxide emissions under semiarid Mediterranean conditions. Agriculture, Ecosystems and Environment 238, 36–45. https://doi.org/10.1016/j.agee.2016.02.003

Abalos, D., Sanz-Cobena, A., Garcia-Torres, L., van Groenigen, J.W., Vallejo, A., 2013. Role of maize stover incorporation on nitrogen oxide emissions in a non-irrigated Mediterranean barley field. Plant and Soil 364, 357–371. https://doi.org/10.1007/s11104-012-1367-4

Abdalla, K., Chivenge, P., Ciais, P., Chaplot, V., 2016. No-tillage lessens soil CO2 emissions the most under arid and sandy soil conditions: results from a meta-analysis. Biogeosciences 13, 3619–3633. https://doi.org/10.5194/bg-13-3619-2016

Abdalla, M., Hastings, A., Cheng, K., Yue, Q., Chadwick, D., Espenberg, M., Truu, J., Rees, R.M., Smith, P., 2019. A critical review of the impacts of cover crops on nitrogen leaching, net greenhouse gas balance and crop productivity. Global Change Biology 25, 2530–2543. https://doi.org/10.1111/gcb.14644

Aguilera, E., Lassaletta, L., Gattinger, A., Gimeno, B.S., 2013a. Managing soil carbon for climate change mitigation and adaptation in Mediterranean cropping systems: A meta-analysis. Agriculture, Ecosystems & Environment 168, 25–36. https://doi.org/10.1016/j.agee.2013.02.003

Aguilera, E., Lassaletta, L., Sanz-Cobena, A., Garnier, J., Vallejo, A., 2013b. The potential of organic fertilizers and water management to reduce N2O emissions in Mediterranean climate cropping systems. A review. Agriculture, Ecosystems and Environment 164, 32–52. https://doi.org/10.1016/j.agee.2012.09.006

Akiyama, H., Yan, X., Yagi, K., 2010. Evaluation of effectiveness of enhanced-efficiency fertilizers as mitigation options for N2O and NO emissions from agricultural soils: Meta-analysis. Global Change Biology 16, 1837–1846. https://doi.org/10.1111/j.1365-2486.2009.02031.x

Allende-Montalbán, R., Martín-Lammerding, D., del Mar Delgado, M., Porcel, M.A., Gabriel, J.L., 2022. Nitrate Leaching in Maize (Zea mays L.) and Wheat (Triticum aestivum L.) Irrigated Cropping Systems under Nitrification Inhibitor and/or Intercropping Effects. Agriculture 12, 478. https://doi.org/10.3390/agriculture12040478

AOAC, 2005. Official Methods of Analysis of AOAC INTERNATIONAL. Dumas method (990.03). 15 th edition. Washington D.C., USA.

Arcand, M.M., Congreves, K.A., 2020. Elucidating microbial carbon utilization and nitrous oxide dynamics with 13C-substrates and N2O isotopomers in contrasting horticultural soils. Applied Soil Ecology 147, 103401. https://doi.org/10.1016/j.apsoil.2019.103401

Aronson, E.L., Allison, S.D., Helliker, B.R., 2013. Environmental impacts on the diversity of methane-cycling microbes and their resultant function. Front. Microbiol. 4. https://doi.org/10.3389/fmicb.2013.00225

Aronson, E.L., Helliker, B.R., 2010. Methane flux in non-wetland soils in response to nitrogen addition: a meta-analysis. Ecology 91, 3242–3251. https://doi.org/10.1890/09-2185.1

Bai, X., Huang, Y., Ren, W., Coyne, M., Jacinthe, P.-A., Tao, B., Hui, D., Yang, J., Matocha, C., 2019. Responses of soil carbon sequestration to climate-smart agriculture practices: A meta-analysis. Global Change Biology 25, 2591–2606. https://doi.org/10.1111/gcb.14658

Barnard, R.L., Blazewicz, S.J., Firestone, M.K., 2020. Rewetting of soil: Revisiting the origin of soil CO2 emissions. Soil Biology and Biochemistry 147, 107819. https://doi.org/10.1016/j.soilbio.2020.107819

Barrat, H.A., Evans, J., Chadwick, D.R., Clark, I.M., Le Cocq, K., M. Cardenas, L., 2021. The impact of drought and rewetting on N2O emissions from soil in temperate and Mediterranean climates. European J Soil Science 72, 2504–2516. https://doi.org/10.1111/ejss.13015

Barrena, I., Menéndez, S., Correa-Galeote, D., Vega-Mas, I., Bedmar, E.J., González-Murua, C., Estavillo, J.M., 2017. Soil water content modulates the effect of the nitrification inhibitor 3,4-dimethylpyrazole phosphate (DMPP) on nitrifying and denitrifying bacteria. Geoderma 303, 1–8. https://doi.org/10.1016/j.geoderma.2017.04.022

Basche, A.D., Miguez, F.E., Kaspar, T.C., Castellano, M.J., 2014. Do cover crops increase or decrease nitrous oxide emissions? A meta-analysis. Journal of Soil and Water Conservation 69, 471–482. https://doi.org/10.2489/jswc.69.6.471

Beeckman, F., Motte, H., Beeckman, T., 2018. Nitrification in agricultural soils: impact, actors and mitigation. Current Opinion in Biotechnology 50, 166–173. https://doi.org/10.1016/j.copbio.2018.01.014

Bergstermann, A., Cárdenas, L., Bol, R., Gilliam, L., Goulding, K., Meijide, A., Scholefield, D., Vallejo, A., Well, R., 2011. Effect of antecedent soil moisture conditions on emissions and isotopologue distribution of N2O during denitrification. Soil Biology and Biochemistry 43, 240–250. https://doi.org/10.1016/j.soilbio.2010.10.003

Berhane, M., Xu, M., Liang, Z., Shi, J., Wei, G., Tian, X., 2020. Effects of long-term straw return on soil organic carbon storage and sequestration rate in North China upland crops: A meta-analysis. Glob Change Biol 26, 2686–2701. https://doi.org/10.1111/gcb.15018

Blanco-Canqui, H., Lal, R., 2009. Crop Residue Removal Impacts on Soil Productivity and Environmental Quality. Critical Reviews in Plant Sciences 28, 139–163. https://doi.org/10.1080/07352680902776507

Blanco-Canqui, H., Mikha, M.M., Presley, D.R., Claassen, M.M., 2011. Addition of Cover Crops Enhances No-Till Potential for Improving Soil Physical Properties. Soil Science Society of America Journal 75, 1471–1482. https://doi.org/10.2136/sssaj2010.0430

Bohoussou, Y.N., Kou, Y.-H., Yu, W.-B., Lin, B., Virk, A.L., Zhao, X., Dang, Y.P., Zhang, H.-L., 2022. Impacts of the components of conservation agriculture on soil organic carbon and total nitrogen storage: A global meta-analysis. Science of The Total Environment 842, 156822. https://doi.org/10.1016/j.scitotenv.2022.156822

Bolinder, M.A., Crotty, F., Elsen, A., Frac, M., Kismányoky, T., Lipiec, J., Tits, M., Tóth, Z., Kätterer, T., 2020. The effect of crop residues, cover crops, manures and nitrogen fertilization on soil organic carbon changes in agroecosystems: a synthesis of reviews.

Mitigation and Adaptation Strategies for Global Change 25, 929–952. https://doi.org/10.1007/s11027-020-09916-3

Bolleter, W.T., Bushman, C.J., Tidwell, P.W., 1961. Spectrophotometric Determination of Ammonia as Indophenol. Anal. Chem. 33, 592–594. https://doi.org/10.1021/ac60172a034

Bracken, C.J., Lanigan, G.J., Richards, K.G., Müller, C., Tracy, S.R., Grant, J., Krol, D.J., Sheridan, H., Lynch, M.B., Grace, C., Fritch, R., Murphy, P.N.C., 2021. Source partitioning using N2O isotopomers and soil WFPS to establish dominant N2O production pathways from different pasture sward compositions. Science of The Total Environment 781, 146515. https://doi.org/10.1016/j.scitotenv.2021.146515

Bremner, J.M., 1965. Isotope-Ratio Analysis of Nitrogen in Nitrogen-15 Tracer Investigations, in: Norman, A.G. (Ed.), Methods of Soil Analysis: Part 2 Chemical and Microbiological Properties. https://doi.org/10.2134/agronmonogr9.2.c35

Buchen, C., Lewicka-Szczebak, D., Flessa, H., Well, R., 2018. Estimating N2O processes during grassland renewal and grassland conversion to maize cropping using N2O isotopocules. Rapid Communications in Mass Spectrometry 32, 1053–1067. https://doi.org/10.1002/rcm.8132

Butterbach-Bahl, K., Baggs, E.M., Dannenmann, M., Kiese, R., Zechmeister-Boltenstern, S., 2013. Nitrous oxide emissions from soils: How well do we understand the processes and their controls? Philosophical Transactions of the Royal Society B: Biological Sciences 368, 20130122. https://doi.org/10.1098/rstb.2013.0122

Caranto, J.D., Lancaster, K.M., 2017. Nitric oxide is an obligate bacterial nitrification intermediate produced by hydroxylamine oxidoreductase. Proceedings of the National Academy of Sciences 114, 8217–8222. https://doi.org/10.1073/pnas.1704504114

Cárceles Rodríguez, B., Durán-Zuazo, V.H., Soriano Rodríguez, M., García-Tejero, I.F., Gálvez Ruiz, B., Cuadros Tavira, S., 2022. Conservation Agriculture as a Sustainable System for Soil Health: A Review. Soil Systems 6, 87. https://doi.org/10.3390/soilsystems6040087

Castellano-Hinojosa, A., González-López, J., Vallejo, A., Bedmar, E.J., 2020. Effect of urease and nitrification inhibitors on ammonia volatilization and abundance of N-cycling genes in an agricultural soil. Journal of Plant Nutrition and Soil Science 183, 99–109. https://doi.org/10.1002/jpln.201900038

Cayuela, M.L., Aguilera, E., Sanz-Cobena, A., Adams, D.C., Ábalos, D., Barton, L., Ryals, R., Silver, W.L., Alfaro, M.A., Pappa, V.A., Smith, P., Garnier, J., Billen, G., Bouwman, L., Bondeau, A., Lassaletta, L., 2017. Direct nitrous oxide emissions in Mediterranean climate cropping systems: Emission factors based on a meta-analysis of available measurement data. Agriculture, Ecosystems and Environment 238, 25–35. https://doi.org/10.1016/j.agee.2016.10.006

Chalk, P.M., Inácio, C.T., Chen, D., 2019. An overview of contemporary advances in the usage of 15N natural abundance (δ15N) as a tracer of agro-ecosystem N cycle processes that impact the environment. Agriculture, Ecosystems & Environment 283, 106570. https://doi.org/10.1016/j.agee.2019.106570

Charteris, A.F., Chadwick, D.R., Thorman, R.E., Vallejo, A., De Klein, C.A.M., Rochette, P., Cárdenas, L.M., 2020. Global Research Alliance N $_2$ O chamber methodology guidelines: Recommendations for deployment and accounting for sources of variability. J of Env Quality 49, 1092–1109. https://doi.org/10.1002/jeq2.20126

Chen, B., Liu, E., Tian, Q., Yan, C., Zhang, Y., 2014. Soil nitrogen dynamics and crop residues. A review. Agron. Sustain. Dev. 34, 429–442. https://doi.org/10.1007/s13593-014-0207-8

Chen, H., Li, X., Hu, F., Shi, W., 2013. Soil nitrous oxide emissions following crop residue addition: a meta-analysis. Global Change Biology 19, 2956–2964. https://doi.org/10.1111/gcb.12274

Chen, Z., Wang, C., Gschwendtner, S., Willibald, G., Unteregelsbacher, S., Lu, H., Kolar, A., Schloter, M., Butterbach-Bahl, K., Dannenmann, M., 2015. Relationships between denitrification gene expression, dissimilatory nitrate reduction to ammonium and nitrous oxide and dinitrogen production in montane grassland soils. Soil Biology and Biochemistry 87, 67–77. https://doi.org/10.1016/j.soilbio.2015.03.030

Chirinda, N., Olesen, J.E., Porter, J.R., Schjønning, P., 2010. Soil properties, crop production and greenhouse gas emissions from organic and inorganic fertilizer-based arable cropping systems. Agriculture, Ecosystems & Environment 139, 584–594. https://doi.org/10.1016/j.agee.2010.10.001

Christensen, S., Rousk, K., 2024. Global N2O emissions from our planet: Which fluxes are affected by man, and can we reduce these? iScience 27, 109042. https://doi.org/10.1016/j.isci.2024.109042

Congreves, K.A., Otchere, O., Ferland, D., Farzadfar, S., Williams, S., Arcand, M.M., 2021. Nitrogen Use Efficiency Definitions of Today and Tomorrow. Frontiers in Plant Science 12. https://doi.org/10.3389/fpls.2021.637108

Corrochano-Monsalve, M., González-Murua, C., Bozal-Leorri, A., Lezama, L., Artetxe, B., 2021. Mechanism of action of nitrification inhibitors based on dimethylpyrazole: A matter of chelation. Science of The Total Environment 752, 141885. https://doi.org/10.1016/j.scitotenv.2020.141885

Corrochano-Monsalve, M., Huérfano, X., Menéndez, S., Torralbo, F., Fuertes-Mendizábal, T., Estavillo, J.M., González-Murua, C., 2020. Relationship between tillage management and DMPSA nitrification inhibitor efficiency. Science of the Total Environment 718. https://doi.org/10.1016/j.scitotenv.2019.134748

Couto-Vázquez, A., González-Prieto, S.J., 2016. Fate of 15 N-fertilizers in the soil-plant system of a forage rotation under conservation and plough tillage. Soil and Tillage Research 161, 10–18. https://doi.org/10.1016/j.still.2016.02.011

Cowan, N., Carnell, E., Skiba, U., Dragosits, U., Drewer, J., Levy, P., 2020. Nitrous oxide emission factors of mineral fertilisers in the UK and Ireland: A Bayesian analysis of 20 years of experimental data. Environment International 135, 105366. https://doi.org/10.1016/j.envint.2019.105366

Cramer, W., Guiot, J., Fader, M., Garrabou, J., Gattuso, J.-P., Iglesias, A., Lange, M.A., Lionello, P., Llasat, M.C., Paz, S., Peñuelas, J., Snoussi, M., Toreti, A., Tsimplis, M.N., Xoplaki, E., 2018. Climate change and interconnected risks to sustainable development in the Mediterranean. Nature Clim Change 8, 972–980. https://doi.org/10.1038/s41558-018-0299-2

Cui, L., Li, D., Wu, Z., Xue, Y., Xiao, F., Zhang, L., Song, Y., Li, Y., Zheng, Y., Zhang, J., Cui, Y., 2021. Effects of Nitrification Inhibitors on Soil Nitrification and Ammonia Volatilization in Three Soils with Different pH. Agronomy 11, 1674. https://doi.org/10.3390/agronomy11081674

Daly, E.J., Hernandez-Ramirez, G., Congreves, K.A., Clough, T., Voigt, C., Harris, E., Ruser, R., 2024. Soil organic nitrogen priming to nitrous oxide: A synthesis. Soil Biology and Biochemistry 189, 109254. https://doi.org/10.1016/j.soilbio.2023.109254

Dannenmann, M., Bimüller, C., Gschwendtner, S., Leberecht, M., Tejedor, J., Bilela, S., Gasche, R., Hanewinkel, M., Baltensweiler, A., Kögel-Knabner, I., Polle, A., Schloter, M., Simon, J., Rennenberg, H., 2016. Climate Change Impairs Nitrogen Cycling in

European Beech Forests. PLoS ONE 11, e0158823. https://doi.org/10.1371/journal.pone.0158823

Dannenmann, M., Díaz-Pinés, E., Kitzler, B., Karhu, K., Tejedor, J., Ambus, P., Parra, A., Sánchez-Martin, L., Resco, V., Ramírez, D.A., Povoas-Guimaraes, L., Willibald, G., Gasche, R., Zechmeister-Boltenstern, S., Kraus, D., Castaldi, S., Vallejo, A., Rubio, A., Moreno, J.M., Butterbach-Bahl, K., 2018. Postfire nitrogen balance of Mediterranean shrublands: Direct combustion losses versus gaseous and leaching losses from the postfire soil mineral nitrogen flush. Global Change Biology 24, 4505–4520. https://doi.org/10.1111/gcb.14388

Dannenmann, M., Yankelzon, I., Wähling, S., Ramm, E., Schreiber, M., Ostler, U., Schlingmann, M., Stange, C.F., Kiese, R., Butterbach-Bahl, K., Friedl, J., Scheer, C., 2024. Fates of slurry-nitrogen applied to mountain grasslands: the importance of dinitrogen emissions versus plant N uptake. Biol Fertil Soils. https://doi.org/10.1007/s00374-024-01826-9

Davidson, E.A., Kanter, D., 2014. Inventories and scenarios of nitrous oxide emissions. Environ. Res. Lett. 9, 105012. https://doi.org/10.1088/1748-9326/9/10/105012

De Notaris, C., Abalos, D., Mikkelsen, M.H., Olesen, J.E., 2022. Potential for the adoption of measures to reduce N2O emissions from crop residues in Denmark. Science of The Total Environment 835, 155510. https://doi.org/10.1016/j.scitotenv.2022.155510

De Notaris, C., Mortensen, E.Ø., Sørensen, P., Olesen, J.E., Rasmussen, J., 2021. Cover crop mixtures including legumes can self-regulate to optimize N2 fixation while reducing nitrate leaching. Agriculture, Ecosystems & Environment 309, 107287. https://doi.org/10.1016/j.agee.2020.107287

De Notaris, C., Olesen, J.E., Sørensen, P., Rasmussen, J., 2020. Input and mineralization of carbon and nitrogen in soil from legume-based cover crops. Nutrient Cycling in Agroecosystems 116. https://doi.org/10.1007/s10705-019-10026-z

del Prado, A., Merino, P., Estavillo, J.M., Pinto, M., González-Murua, C., 2006. N2O and NO emissions from different N sources and under a range of soil water contents. Nutr Cycl Agroecosyst 74, 229–243. https://doi.org/10.1007/s10705-006-9001-6

Delgado, J.A., Del Grosso, S.J., Ogle, S.M., 2010. 15N isotopic crop residue cycling studies and modeling suggest that IPCC methodologies to assess residue contributions to N2O-N emissions should be reevaluated. Nutrient Cycling in Agroecosystems 86, 383–390. https://doi.org/10.1007/s10705-009-9300-9

Denk, T.R.A., Mohn, J., Decock, C., Lewicka-Szczebak, D., Harris, E., Butterbach-Bahl, K., Kiese, R., Wolf, B., 2017. The nitrogen cycle: A review of isotope effects and isotope modeling approaches. Soil Biology and Biochemistry 105, 121–137. https://doi.org/10.1016/j.soilbio.2016.11.015

Dimassi, B., Mary, B., Wylleman, R., Labreuche, J., Couture, D., Piraux, F., Cohan, J.-P., 2014. Long-term effect of contrasted tillage and crop management on soil carbon dynamics during 41 years. Agriculture, Ecosystems & Environment 188, 134–146. https://doi.org/10.1016/j.agee.2014.02.014

Ding, W., Li, S., He, P., Huang, S., 2019. Contribution and fate of maize residue- 15 N and urea- 15 N as affected by N fertilization regime. PLoS ONE 14, 1–17. https://doi.org/10.1371/journal.pone.0210176

Drinkwater, L.E., Janke, R.R., Rossoni-Longnecker, L., 2000. Effects of tillage intensity on nitrogen dynamics and productivity in legume-based grain systems. Plant and Soil 227, 99–113. https://doi.org/10.1023/A:1026569715168

Drost, S.M., Rutgers, M., Wouterse, M., de Boer, W., Bodelier, P.L.E., 2020. Decomposition of mixtures of cover crop residues increases microbial functional diversity. Geoderma 361, 114060. https://doi.org/10.1016/j.geoderma.2019.114060

Elhakeem, A., Bastiaans, L., Houben, S., Couwenberg, T., Makowski, D., van der Werf, W., 2021. Do cover crop mixtures give higher and more stable yields than pure stands? Field Crops Research 270, 108217. https://doi.org/10.1016/j.fcr.2021.108217

Elrys, A.S., Ali, A., Zhang, H., Cheng, Y., Zhang, J., Cai, Z., Müller, C., Chang, S.X., 2021. Patterns and drivers of global gross nitrogen mineralization in soils. Glob Change Biol 27, 5950–5962. https://doi.org/10.1111/gcb.15851

Elrys, A.S., Chen, Z., Wang, J., Uwiragiye, Y., Helmy, A.M., Desoky, E.M., Cheng, Y., Zhang, J., Cai, Z., Müller, C., 2022. Global patterns of soil gross immobilization of ammonium and nitrate in terrestrial ecosystems. Global Change Biology 1–17. https://doi.org/10.1111/gcb.16202

Erisman, J.W., Sutton, M.A., Galloway, J., Klimont, Z., Winiwarter, W., 2008. How a century of ammonia synthesis changed the world. Nature Geosci 1, 636–639. https://doi.org/10.1038/ngeo325

Fan, F., Van Der Werf, W., Makowski, D., Ram Lamichhane, J., Huang, W., Li, C., Zhang, C., Cong, W.-F., Zhang, F., 2021. Cover crops promote primary crop yield in China: A meta-regression of factors affecting yield gain. Field Crops Research 271, 108237. https://doi.org/10.1016/j.fcr.2021.108237

Farzadfar, S., Congreves, K.A., 2022. Background soil nitrogen regulates the contribution of cover crop-derived nitrogen into subsequent crop. Biol Fertil Soils 58, 871–881. https://doi.org/10.1007/s00374-022-01664-7

Fernandez Pulido, C.R., Rasmussen, J., Eriksen, J., Abalos, D., 2023. Cover crops for nitrogen loss reductions: functional groups, species identity and traits. Plant Soil. https://doi.org/10.1007/s11104-023-05895-x

Fernández-Ortega, J., Fanlo, R., Cantero-Martínez, C., 2024. Greenhouse gas emissions during alfalfa cultivation: How do soil management and crop fertilisation of preceding maize impact emissions? Field Crops Research 318, 109602. https://doi.org/10.1016/j.fcr.2024.109602

Ferrari Machado, P.V., Farrell, R.E., Bell, G., Taveira, C.J., Congreves, K.A., Voroney, R.P., Deen, W., Wagner-Riddle, C., 2021. Crop residues contribute minimally to spring-thaw nitrous oxide emissions under contrasting tillage and crop rotations. Soil Biology and Biochemistry 152, 108057. https://doi.org/10.1016/j.soilbio.2020.108057

Fiorini, A., Maris, S.C., Abalos, D., Amaducci, S., Tabaglio, V., 2020. Combining no-till with rye (Secale cereale L.) cover crop mitigates nitrous oxide emissions without decreasing yield. Soil and Tillage Research 196, 104442. https://doi.org/10.1016/j.still.2019.104442

Foster, P., Storelvmo, T., Armour, K., Collins, W., Dufresne, J.-L., Frame, D., Lunt, D.J., Mauritsen, T., Palmer, M.D., Watanabe, M., Wild, M., Zhang, H., 2021. The Earth's Energy Budget, Climate Feedbacks, and Climate Sensitivity, in: Climate Change 2021: The Physical Science Basis. Contribution of Working Group I to the Sixth Assessment Report of the Intergovernmental Panel on Climate Change. [Masson-Delmotte, V., P. Zhai, A. Pirani, S.L. Connors, C. Péan, S. Berger, N. Caud, Y. Chen, L. Goldfarb, M.I. Gomis, M. Huang, K. Leitzell, E. Lonnoy, J.B.R. Matthews, T.K. Maycock, T. Waterfield, O. Yelekçi, R. Yu, and B. Zhou (Eds.)]. Cambridge University Press, Cambridge, United Kingdom and New York, NY, USA, pp. 923-1054. doi: 10.1017/9781009157896.009.

Franco-Luesma, S., Lafuente, V., Alonso-Ayuso, M., Bielsa, A., Kouchami-Sardoo, I., Arrúe, J.L., Álvaro-Fuentes, J., 2022. Maize diversification and nitrogen fertilization effects on soil nitrous oxide emissions in irrigated mediterranean conditions. Front. Environ. Sci. 10, 914851. https://doi.org/10.3389/fenvs.2022.914851

Friedl, J., Cardenas, L.M., Clough, T.J., Dannenmann, M., Hu, C., Scheer, C., 2020. Measuring denitrification and the N2O:(N2O + N2) emission ratio from terrestrial soils. Current Opinion in Environmental Sustainability 47, 61–71. https://doi.org/10.1016/j.cosust.2020.08.006

Friedl, J., Warner, D., Wang, W., Rowlings, D.W., Grace, P.R., Scheer, C., 2023. Strategies for mitigating N2O and N2 emissions from an intensive sugarcane cropping system. Nutr Cycl Agroecosyst 125, 295–308. https://doi.org/10.1007/s10705-023-10262-4

Gabriel, J.L., Garrido, A., Quemada, M., 2013. Cover crops effect on farm benefits and nitrate leaching: Linking economic and environmental analysis. Agricultural Systems 121, 23–32. https://doi.org/10.1016/j.agsy.2013.06.004

Gabriel, J.L., Muñoz-Carpena, R., Quemada, M., 2012. The role of cover crops in irrigated systems: Water balance, nitrate leaching and soil mineral nitrogen accumulation. Agriculture, Ecosystems & Environment 155, 50–61. https://doi.org/10.1016/j.agee.2012.03.021

Gabriel, J.L., Quemada, M., 2011. Replacing bare fallow with cover crops in a maize cropping system: Yield, N uptake and fertiliser fate. European Journal of Agronomy 34, 133–143. https://doi.org/10.1016/j.eja.2010.11.006

Galloway, J.N., Aber, J.D., Erisman, J.W., Seitzinger, S.P., Howarth, R.W., Cowling, E.B., Cosby, B.J., 2003. The Nitrogen Cascade. BioScience 53, 341–356. https://doi.org/10.1641/0006-3568(2003)053[0341:TNC]2.0.CO;2

Garba, I.I., Bell, L.W., Williams, A., 2022. Cover crop legacy impacts on soil water and nitrogen dynamics, and on subsequent crop yields in drylands: a meta-analysis. Agronomy for Sustainable Development 42, 34. https://doi.org/10.1007/s13593-022-00760-0

García-Gómez, C., Babín, M., Obrador, A., Álvarez, J.M., Fernández, M.D., 2015. Integrating ecotoxicity and chemical approaches to compare the effects of ZnO nanoparticles, ZnO bulk, and ZnCl2 on plants and microorganisms in a natural soil. Environmental Science and Pollution Research 22, 16803–16813. https://doi.org/10.1007/s11356-015-4867-y

García-Marco, S., Ábalos, D., Espejo, R., Vallejo, A., Mariscal-Sancho, I., 2016. No tillage and liming reduce greenhouse gas emissions from poorly drained agricultural soils in Mediterranean regions. Science of the Total Environment 566–567, 512–520. https://doi.org/10.1016/j.scitotenv.2016.05.117

García-Marco, S., Ravella, S.R., Chadwick, D., Vallejo, A., Gregory, A.S., Cárdenas, L.M., 2014. Ranking factors affecting emissions of GHG from incubated agricultural soils. European Journal of Soil Science 65, 573–583. https://doi.org/10.1111/ejss.12143

García-Ruiz, J.M., López-Moreno, J.I., Vicente-Serrano, S.M., Lasanta–Martínez, T., Beguería, S., 2011. Mediterranean water resources in a global change scenario. Earth-Science Reviews 105, 121–139. https://doi.org/10.1016/j.earscirev.2011.01.006

Gardner, J.B., Drinkwater, L.E., 2009. The fate of nitrogen in grain cropping systems: A meta-analysis of 15N field experiments. Ecological Applications 19, 2167–2184. https://doi.org/10.1890/08-1122.1

Geens, E.L., Davies, G.P., Maggs, J.M., Barraclough, D., 1991. The use of mean pool abundances to interpret 15N tracer experiments. Plant and Soil 131, 97–105. https://doi.org/10.1007/BF00010424

Giacomini, S.J., Machet, J.M., Boizard, H., Recous, S., 2010. Dynamics and recovery of fertilizer 15N in soil and winter wheat crop under minimum versus conventional tillage. Soil and Tillage Research 108, 51–58. https://doi.org/10.1016/j.still.2010.03.005

Giorgi, F., 2006. Climate change hot-spots. Geophysical Research Letters 33. https://doi.org/10.1029/2006GL025734

Gomes, J., Brüggemann, N., Dick, D.P., Pedroso, G.M., Veloso, M., Bayer, C., 2019. Urea and legume residues as 15N-N2O sources in a subtropical soil. Soil Research 57, 287–293. https://doi.org/10.1071/SR18300

Gou, X., Reich, P.B., Qiu, L., Shao, M., Wei, G., Wang, J., Wei, X., 2023. Leguminous plants significantly increase soil nitrogen cycling across global climates and ecosystem types. Global Change Biology 29, 4028–4043. https://doi.org/10.1111/gcb.16742

Guardia, G., Abalos, D., García-Marco, S., Quemada, M., Alonso-Ayuso, M., Cárdenas, L.M., Dixon, E.R., Vallejo, A., 2016a. Effect of cover crops on greenhouse gas emissions in an irrigated field under integrated soil fertility management. Biogeosciences 13, 5245–5257. https://doi.org/10.5194/bg-13-5245-2016

Guardia, G., Aguilera, E., Vallejo, A., Álvaro-Fuentes, J., Cantero-Martínez, C., Sanz-Cobena, A., Barton, L., Volpi, I., Ibáñez, M.Á., 2024a. Contribution of the postharvest period to soil N2O emissions from arable Mediterranean crops. Journal of Cleaner Production 469, 143186. https://doi.org/10.1016/j.jclepro.2024.143186

Guardia, G., Aguilera, E., Vallejo, A., Sanz-Cobena, A., Alonso-Ayuso, M., Quemada, M., 2019. Effective climate change mitigation through cover cropping and integrated fertilization: A global warming potential assessment from a 10-year field experiment. Journal of Cleaner Production 241, 118307. https://doi.org/10.1016/j.jclepro.2019.118307

Guardia, G., Cangani, M.T., Andreu, G., Sanz-Cobena, A., García-Marco, S., Álvarez, J.M., Recio-Huetos, J., Vallejo, A., 2017a. Effect of inhibitors and fertigation strategies on GHG emissions, NO fluxes and yield in irrigated maize. Field Crops Research 204, 135–145. https://doi.org/10.1016/j.fcr.2017.01.009

Guardia, G., Cangani, M.T., Sanz-Cobena, A., Junior, J.L., Vallejo, A., 2017b. Management of pig manure to mitigate NO and yield-scaled N2O emissions in an irrigated Mediterranean crop. Agriculture, Ecosystems & Environment, Quantification and mitigation of greenhouse gas emissions in Mediterranean cropping systems 238, 55–66. https://doi.org/10.1016/j.agee.2016.09.022

Guardia, G., García-Gutiérrez, S., Rodríguez-Pérez, R., Recio, J., Vallejo, A., 2021. Increasing N use efficiency while decreasing gaseous N losses in a non-tilled wheat (Triticum aestivum L.) crop using a double inhibitor. Agriculture, Ecosystems and Environment 319. https://doi.org/10.1016/j.agee.2021.107546

Guardia, G., González-Murua, C., Fuertes-Mendizábal, T., Vallejo, A., 2020. The scarcity and distribution of rainfall drove the performance (i.e., mitigation of N oxide emissions, crop yield and quality) of calcium ammonium nitrate management in a wheat crop under rainfed semiarid conditions. Archives of Agronomy and Soil Science 66, 1827–1844. https://doi.org/10.1080/03650340.2019.1697805

Guardia, G., Monistrol-Arcas, A., Montoya, M., García-Gutiérrez, S., Abalos, D., Vallejo, A., 2023. Subsurface drip irrigation reduces CH4 emissions and ecosystem respiration compared to surface drip irrigation. Agricultural Water Management 285, 108380. https://doi.org/10.1016/j.agwat.2023.108380

Guardia, G., Sanz-Cobena, A., Ibáñez, M.Á., Recio, J., Vallejo, A., 2024b. Ammonia volatilization measured with the IHF method in a rainfed arable crop: Evaluation of

tillage intensity and the number of experimental replicates. Soil and Tillage Research 235, 105892. https://doi.org/10.1016/j.still.2023.105892

Guardia, G., Tellez-Rio, A., García-Marco, S., Martin-Lammerding, D., Tenorio, J.L., Ibáñez, M.Á., Vallejo, A., 2016b. Effect of tillage and crop (cereal versus legume) on greenhouse gas emissions and Global Warming Potential in a non-irrigated Mediterranean field. Agriculture, Ecosystems and Environment 221, 187–197. https://doi.org/10.1016/j.agee.2016.01.047

Guardia, G., Vallejo, A., Cárdenas, L.M., Dixon, E.R., García-Marco, S., 2018. Fate of 15N-labelled ammonium nitrate with or without the new nitrification inhibitor DMPSA in an irrigated maize crop. Soil Biology and Biochemistry 116, 193–202. https://doi.org/10.1016/j.soilbio.2017.10.013

Guenet, B., Gabrielle, B., Chenu, C., Arrouays, D., Balesdent, J., Bernoux, M., Bruni, E., Caliman, J.-P., Cardinael, R., Chen, S., Ciais, P., Desbois, D., Fouche, J., Frank, S., Henault, C., Lugato, E., Naipal, V., Nesme, T., Obersteiner, M., Pellerin, S., Powlson, D.S., Rasse, D.P., Rees, F., Soussana, J.-F., Su, Y., Tian, H., Valin, H., Zhou, F., 2021. Can N2O emissions offset the benefits from soil organic carbon storage? Global Change Biology 27, 237–256. https://doi.org/10.1111/gcb.15342

Guzman-Bustamante, I., Schulz, R., Müller, T., Ruser, R., 2022. Split N application and DMP based nitrification inhibitors mitigate N2O losses in a soil cropped with winter wheat. Nutr Cycl Agroecosyst 123, 119–135. https://doi.org/10.1007/s10705-022-10211-7

Haber, F., 1920. The synthesis of ammonia from its elements Nobel Lecture, June 2, 1920. Reson 7, 86–94. https://doi.org/10.1007/BF02836189

Hallin, S., Philippot, L., Löffler, F.E., Sanford, R.A., Jones, C.M., 2018. Genomics and Ecology of Novel N2O-Reducing Microorganisms. Trends in Microbiology 26, 43–55. https://doi.org/10.1016/j.tim.2017.07.003

Han, B., Yao, Y., Liu, B., Wang, Y., Su, X., Ma, L., Liu, D., Niu, S., Chen, X., Li, Z., 2024. Relative importance between nitrification and denitrification to N2O from a global perspective. Global Change Biology 30, e17082. https://doi.org/10.1111/gcb.17082

Harmsen, K., 2003. A comparison of the isotope-dilution and the difference method for estimating fertilizer nitrogen recovery fractions in crops. I. Plant uptake and loss of nitrogen. Netherlands Journal of Agricultural Science 50, 321–347. https://doi.org/10.1016/s1573-5214(03)80015-5

Hart, S.C., Stark, J.M., Davidson, E.A., Firestone, M.K., 1994. Nitrogen mineralization, immobilization, and nitrification, in: Weaver, R.W., Angle, S., Bottomley, P., Bezdicek, D., Smith, S., Tabatabai, A., Wollum, A. (Eds.), Methods of Soil Analysis: Part 2 Microbiological and Biochemical Properties. pp. 985–1018. https://doi.org/10.2136/sssabookser5.2.c42

Harty, M.A., McGeough, K.L., Carolan, R., Müller, C., Laughlin, R.J., Lanigan, G.J., Richards, K.G., Watson, C.J., 2017. Gross nitrogen transformations in grassland soil react differently to urea stabilisers under laboratory and field conditions. Soil Biology and Biochemistry 109, 23–34. https://doi.org/10.1016/j.soilbio.2017.01.025

Harvey, M.J., Sperlich, P., Clough, T.J., Kelliher, F.M., McGeough, K.L., Martin, R.J., Moss, R., 2020. Global Research Alliance N_2O chamber methodology guidelines: Recommendations for air sample collection, storage, and analysis. Journal of Environmental Quality 49, 1110–1125. https://doi.org/10.1002/jeq2.20129

He, X., Chi, Q., Cai, Z., Cheng, Y., Zhang, J., Müller, C., 2020. 15N tracing studies including plant N uptake processes provide new insights on gross N transformations in soil-plant systems. Soil Biology and Biochemistry 141, 107666. https://doi.org/10.1016/j.soilbio.2019.107666

Herrero, E., Sanz-Cobena, A., Guido, V., Guillén, M., Dauden, A., Rodríguez, R., Provolo, G., Quílez, D., 2021. Towards robust on-site ammonia emission measuring techniques based on inverse dispersion modeling. Agricultural and Forest Meteorology 307, 108517. https://doi.org/10.1016/j.agrformet.2021.108517

Ho, A., Reim, A., Kim, S.Y., Meima-Franke, M., Termorshuizen, A., de Boer, W., van der Putten, W.H., Bodelier, P.L.E., 2015. Unexpected stimulation of soil methane uptake as emergent property of agricultural soils following bio-based residue application. Global Change Biology 21, 3864–3879. https://doi.org/10.1111/gcb.12974

Hoxha, A., Christensen, B., 2019. The Carbon Footprint of Fertiliser Production: Regional Reference Values. International Fertiliser Society (IFS).

Hu, G., Liu, X., He, H., Zhang, W., Xie, H., Wu, Y., Cui, J., Sun, C., Zhang, X., 2015. Multi-seasonal nitrogen recoveries from crop residue in soil and crop in a temperate agro-ecosystem. PLoS ONE 10, 1–15. https://doi.org/10.1371/journal.pone.0133437

Hu, N., Chen, Q., Zhu, L., 2019. The Responses of Soil N2O Emissions to Residue Returning Systems: A Meta-Analysis. Sustainability 11, 748. https://doi.org/10.3390/su11030748

Hu, T., Sørensen, P., Margrethe, E., Chirinda, N., Sharif, B., Li, X., Olesen, J.E., 2018. Root biomass in cereals , catch crops and weeds can be reliably estimated without considering aboveground biomass. Agriculture , Ecosystems and Environment 251, 141–148. https://doi.org/10.1016/j.agee.2017.09.024

Huang, Y., Ren, W., Wang, L., Hui, D., Grove, J.H., Yang, X., Tao, B., Goff, B., 2018. Greenhouse gas emissions and crop yield in no-tillage systems: A meta-analysis. Agriculture, Ecosystems & Environment 268, 144–153. https://doi.org/10.1016/j.agee.2018.09.002

Huérfano, X., Fuertes-Mendizábal, T., Duñabeitia, M.K., González-Murua, C., Estavillo, J.M., Menéndez, S., 2015. Splitting the application of 3,4-dimethylpyrazole phosphate (DMPP): Influence on greenhouse gases emissions and wheat yield and quality under humid Mediterranean conditions. European Journal of Agronomy 64, 47–57. https://doi.org/10.1016/j.eja.2014.11.008

Huérfano, X., Fuertes-Mendizábal, T., Fernández-Diez, K., Estavillo, J.M., González-Murua, C., Menéndez, S., 2016. The new nitrification inhibitor 3, 4-dimethylpyrazole succinic (DMPSA) as an alternative to DMPP for reducing N2O emissions from wheat crops under humid Mediterranean conditions. European Journal of Agronomy 80, 78–87. https://doi.org/10.1016/j.eja.2016.07.001

Hütsch, B.W., Schubert, S., 2017. Harvest Index of Maize (Zea mays L.): Are There Possibilities for Improvement?, in: Advances in Agronomy. Elsevier, pp. 37–82. https://doi.org/10.1016/bs.agron.2017.07.004

Ibraim, E., Denk, T., Wolf, B., Barthel, M., Gasche, R., Wanek, W., Zhang, S., Kiese, R., Butterbach-Bahl, K., Eggleston, S., Emmenegger, L., Six, J., Mohn, J., 2020. Denitrification Is the Main Nitrous Oxide Source Process in Grassland Soils According to Quasi-Continuous Isotopocule Analysis and Biogeochemical Modeling. Global Biogeochemical Cycles 34, e2019GB006505. https://doi.org/10.1029/2019GB006505

Ibraim, E., Wolf, B., Harris, E., Gasche, R., Wei, J., Yu, L., Kiese, R., Eggleston, S., Butterbach-Bahl, K., Zeeman, M., Tuzson, B., Emmenegger, L., Six, J., Henne, S., Mohn, J., 2019. Attribution of N2O sources in a grassland soil with laser spectroscopy based isotopocule analysis. Biogeosciences 16, 3247–3266. https://doi.org/10.5194/bg-16-3247-2019

Ichir, L.L., Ismaili, M., Hofman, G., 2003. Recovery of 15N labeled wheat residue and residual effects of N fertilization in a wheat–wheat cropping system under Mediterranean

conditions. Nutrient Cycling in Agroecosystems 66, 201–207. https://doi.org/10.1023/A:1023976600760

Iglesias, A., Quiroga, S., Moneo, M., Garrote, L., 2012. From climate change impacts to the development of adaptation strategies: Challenges for agriculture in Europe. Climatic Change 112, 143–168. https://doi.org/10.1007/s10584-011-0344-x

Inselsbacher, E., Wanek, W., Strauss, J., Zechmeister-Boltenstern, S., Müller, C., 2013. A novel 15N tracer model reveals: Plant nitrate uptake governs nitrogen transformation rates in agricultural soils. Soil Biology and Biochemistry 57, 301–310. https://doi.org/10.1016/j.soilbio.2012.10.010

IPCC, 2022. Climate Change 2022: Mitigation of Climate Change. Working Group III Contribution to the IPCC Sixth Assessment Report. [P.R. Shukla, J. Skea, R. Slade, A. Al Khourdajie, R. van Diemen, D. McCollum, M. Pathak, S. Some, P. Vyas, R. Fradera, M. Belkacemi, A. Hasija, G. Lisboa, S. Luz, J. Malley, (eds.)]. Cambridge University Press, Cambridge, UK and New York, NY, USA. https://doi.org/10.1017/9781009157926

IPCC, 2021. Climate Change 2021: The Physical Science Basis. Contribution of Working Group I to the Sixth Assessment Report of the Intergovernmental Panel on Climate Change [Masson-Delmotte, V., P. Zhai, A. Pirani, S.L. Connors, C. Péan, S. Berger, N. Caud, Y. Chen, L. Goldfarb, M.I. Gomis, M. Huang, K. Leitzell, E. Lonnoy, J.B.R. Matthews, T.K. Maycock, T. Waterfield, O. Yelekçi, R. Yu, and B. Zhou (eds.)]. Cambridge University Press, Cambridge, United Kingdom and New York, NY, USA. https://doi.org/10.1017/9781009157896

IPCC, 2019a. Climate Change and Land: an IPCC special report on climate change, desertification, land degradation, sustainable land management, food security, and greenhouse gas fluxes in terrestrial ecosystems [P.R. Shukla, J. Skea, E. Calvo Buendia, V. Masson-Delmotte, H.-O. Pörtner, D. C. Roberts, P. Zhai, R. Slade, S. Connors, R. van Diemen, M. Ferrat, E. Haughey, S. Luz, S. Neogi, M. Pathak, J. Petzold, J. Portugal Pereira, P. Vyas, E. Huntley, K. Kissick, M. Belkacemi, J. Malley, (eds.)]. Cambridge University Press, Cambridge, UK and New York, NY, USA, 896 pp. http://doi.org/10.1017/9781009157988.

IPCC, 2019b. Refinement to the 2006 IPCC Guidelines for National Greenhouse Gas Inventories. In: Calvo Buendia, E., Tanabe, K., Kranjc, A., Baasansuren, J., Fukuda, M., Ngarize, S., Osako, A., Pyrozhenko, Y., Shermanau, P., Federici, S. (Eds.), Intergovernmental Panel on Climate Change (Switzerland).

Jensen, L.S., Salo, T., Palmason, F., Breland, T.A., Henriksen, T.M., Stenberg, B., Pedersen, A., Lundström, C., Esala, M., 2005. Influence of biochemical quality on C and N mineralisation from a broad variety of plant materials in soil. Plant Soil 273, 307–326. https://doi.org/10.1007/s11104-004-8128-y

Joffre, R., Rambal, S., 2001. Mediterranean Ecosystems, in: Encyclopedia of Life Sciences. Wiley. https://doi.org/10.1038/npg.els.0003196

Joshi, D.R., Sieverding, H.L., Xu, H., Kwon, H., Wang, M., Clay, S.A., Johnson, J.M., Thapa, R., Westhoff, S., Clay, D.E., 2023. A global meta-analysis of cover crop response on soil carbon storage within a corn production system. Agronomy Journal 1–15. https://doi.org/10.1002/agj2.21340

Kaye, J.P., Quemada, M., 2017. Using cover crops to mitigate and adapt to climate change. A review. Agronomy for Sustainable Development 37. https://doi.org/10.1007/s13593-016-0410-x

Kesenheimer, K., Pandeya, H.R., Müller, T., Buegger, F., Ruser, R., 2019. Nitrous oxide emissions after incorporation of winter oilseed rape (Brassica napus L.) residues under

two different tillage treatments. Journal of Plant Nutrition and Soil Science 182, 48–59. https://doi.org/10.1002/jpln.201700507

Kiese, R., Fersch, B., Baessler, C., Brosy, C., Butterbach-Bahl, K., Chwala, C., Dannenmann, M., Fu, J., Gasche, R., Grote, R., Jahn, C., Klatt, J., Kunstmann, H., Mauder, M., Rödiger, T., Smiatek, G., Soltani, M., Steinbrecher, R., Völksch, I., Werhahn, J., Wolf, B., Zeeman, M., Schmid, H. p., 2018. The TERENO Pre-Alpine Observatory: Integrating Meteorological, Hydrological, and Biogeochemical Measurements and Modeling. Vadose Zone Journal 17, 180060. https://doi.org/10.2136/vzj2018.03.0060

Kirkham, D., Bartholomew, W.V., 1954. Equations for Following Nutrient Transformations in Soil. Utilizing Tracer Data. Soil Science Society of America Journal 18, 33–34. https://doi.org/10.2136/sssaj1954.03615995001800010009x

Koba, K., Osaka, K., Tobari, Y., Toyoda, S., Ohte, N., Katsuyama, M., Suzuki, N., Itoh, M., Yamagishi, H., Kawasaki, M., Kim, S.J., Yoshida, N., Nakajima, T., 2009. Biogeochemistry of nitrous oxide in groundwater in a forested ecosystem elucidated by nitrous oxide isotopomer measurements. Geochimica et Cosmochimica Acta 73, 3115–3133. https://doi.org/10.1016/j.gca.2009.03.022

Kool, D.M., Dolfing, J., Wrage, N., Van Groenigen, J.W., 2011. Nitrifier denitrification as a distinct and significant source of nitrous oxide from soil. Soil Biology and Biochemistry 43, 174–178. https://doi.org/10.1016/j.soilbio.2010.09.030

Kuang, W., Wu, Y., Gao, X., Yin, M., Gui, D., Zeng, F., 2023. Soil profile N2O efflux from a cotton field in arid Northwestern China in response to irrigation and nitrogen management. Frontiers in Environmental Science 11.

Lal, R., 2003. Global Potential of Soil Carbon Sequestration to Mitigate the Greenhouse Effect. Critical Reviews in Plant Sciences 22, 151–184. https://doi.org/10.1080/713610854

Lampurlanés, J., Plaza-Bonilla, D., Álvaro-Fuentes, J., Cantero-Martínez, C., 2016. Long-term analysis of soil water conservation and crop yield under different tillage systems in Mediterranean rainfed conditions. Field Crops Research 189, 59–67. https://doi.org/10.1016/j.fcr.2016.02.010

Lashermes, G., Recous, S., Alavoine, G., Janz, B., Butterbach-Bahl, K., Ernfors, M., Laville, P., 2022. N2O emissions from decomposing crop residues are strongly linked to their initial soluble fraction and early C mineralization. Science of The Total Environment 806, 150883. https://doi.org/10.1016/j.scitotenv.2021.150883

Lassaletta, L., Billen, G., Grizzetti, B., Anglade, J., Garnier, J., 2014. 50 year trends in nitrogen use efficiency of world cropping systems: The relationship between yield and nitrogen input to cropland. Environmental Research Letters 9. https://doi.org/10.1088/1748-9326/9/10/105011

Lassaletta, L., Sanz-Cobena, A., Aguilera, E., Quemada, M., Billen, G., Bondeau, A., Cayuela, M.L., Cramer, W., Eekhout, J.P.C., Garnier, J., Grizzetti, B., Intrigliolo, D.S., Ruiz Ramos, M., Romero, E., Vallejo, A., Gimeno, B.S., 2021. Nitrogen dynamics in cropping systems under Mediterranean climate: a systemic analysis. Environ. Res. Lett. 16, 073002. https://doi.org/10.1088/1748-9326/ac002c

Le Mer, J., Roger, P., 2001. Production, oxidation, emission and consumption of methane by soils: A review. European Journal of Soil Biology 37, 25–50. https://doi.org/10.1016/S1164-5563(01)01067-6

L'Espérance, E., Bouyoucef, L.S., Dozois, J.A., Yergeau, E., 2024. Tipping the plant-microbe competition for nitrogen in agricultural soils. iScience 27, 110973. https://doi.org/10.1016/j.isci.2024.110973

Li, H., Wang, Lv, Peng, Y., Lv, S., Li, J., Yang, Z., Zhang, S., Abdo, A.I., Zhou, C., Wang, Linquan, 2023. Fate of fertilizer nitrogen from a winter wheat field under film mulching

and straw retention practices. Nutr Cycl Agroecosyst 125, 123–136. https://doi.org/10.1007/s10705-022-10217-1

Li, P., Zhang, A., Huang, S., Han, J., Jin, X., Shen, X., Hussain, Q., Wang, X., Zhou, J., Chen, Z., 2023. Optimizing Management Practices under Straw Regimes for Global Sustainable Agricultural Production. Agronomy 13, 710. https://doi.org/10.3390/agronomy13030710

Li, S., Sha, Z., Zhang, X., Lv, J., Chen, X., Yang, Q., 2023. Fertilizers inclusion with nitrification inhibitors alleviate soil CO2 emissions: a meta-analysis study. J Soils Sediments 23, 2011–2020. https://doi.org/10.1007/s11368-023-03464-4

Li, T., Zhang, W., Yin, J., Chadwick, D., Norse, D., Lu, Y., Liu, X., Chen, X., Zhang, F., Powlson, D., Dou, Z., 2018. Enhanced-efficiency fertilizers are not a panacea for resolving the nitrogen problem. Global Change Biology 24, e511–e521. https://doi.org/10.1111/gcb.13918

Li, X., Sørensen, P., Olesen, J.E., Petersen, S.O., 2016. Evidence for denitrification as main source of N2O emission from residue-amended soil. Soil Biology and Biochemistry 92, 153–160. https://doi.org/10.1016/j.soilbio.2015.10.008

Li, Y., Chen, J., Drury, C.F., Liebig, M., Johnson, J.M.F., Wang, Z., Feng, H., Abalos, D., 2023a. The role of conservation agriculture practices in mitigating N2O emissions: A meta-analysis. Agronomy for Sustainable Development 43, 63. https://doi.org/10.1007/s13593-023-00911-x

Li, Y., Ju, X., Wu, D., 2023b. Transient nitrite accumulation explains the variation of N2O emissions to N fertilization in upland agricultural soils. Soil Biology and Biochemistry 177, 108917. https://doi.org/10.1016/j.soilbio.2022.108917

Li, Zhijie, Reichel, R., Xu, Z., Vereecken, H., Brüggemann, N., 2021. Return of crop residues to arable land stimulates N2O emission but mitigates NO3− leaching: a meta-analysis. Agronomy for Sustainable Development 41, 66. https://doi.org/10.1007/s13593-021-00715-x

Li, Zhaolei, Zeng, Z., Song, Z., Wang, F., Tian, D., Mi, W., Huang, X., Wang, Jinsong, Song, L., Yang, Z., Wang, Jun, Feng, H., Jiang, L., Chen, Y., Luo, Y., Niu, S., 2021. Vital roles of soil microbes in driving terrestrial nitrogen immobilization. Global Change Biology 27, 1848–1858. https://doi.org/10.1111/gcb.15552

Liang, K., Wang, X., Du, Y., Li, G., Wei, Y., Liu, Y., Li, Z., Wei, X., 2022. Effect of Legume Green Manure on Yield Increases of Three Major Crops in China: A Meta-Analysis. Agronomy 12, 1753. https://doi.org/10.3390/agronomy12081753

Liang, L.L., Grantz, D.A., Jenerette, G.D., 2016. Multivariate regulation of soil CO2 and N2O pulse emissions from agricultural soils. Global Change Biology 22, 1286–1298. https://doi.org/10.1111/gcb.13130

Lim, J., Wehmeyer, H., Heffner, T., Aeppli, M., Gu, W., Kim, P.J., Horn, M.A., Ho, A., 2024. Resilience of aerobic methanotrophs in soils; spotlight on the methane sink under agriculture. FEMS Microbiology Ecology 100, fiae008. https://doi.org/10.1093/femsec/fiae008

Lionello, P., Scarascia, L., 2018. The relation between climate change in the Mediterranean region and global warming. Regional Environmental Change 18, 1481–1493. https://doi.org/10.1007/s10113-018-1290-1

Liu, S., Chi, Q., Cheng, Y., Zhu, B., Li, W., Zhang, X., Huang, Y., Müller, C., Cai, Z., Zhang, J., 2019. Importance of matching soil N transformations, crop N form preference, and climate to enhance crop yield and reducing N loss. Science of the Total Environment 657, 1265–1273. https://doi.org/10.1016/j.scitotenv.2018.12.100

Liu, S., Lin, F., Wu, S., Ji, C., Sun, Y., Jin, Y., Li, S., Li, Z., Zou, J., 2017. A meta-analysis of fertilizer-induced soil NO and combined NO+N2O emissions. Global Change Biology 23, 2520–2532. https://doi.org/10.1111/gcb.13485

Loick, N., Dixon, E., Matthews, G.P., Müller, C., Ciganda, V.S., López-Aizpún, M., Repullo, M.A., Cardenas, L.M., 2021. Application of a triple 15N tracing technique to elucidate N transformations in a UK grassland soil. Geoderma 385. https://doi.org/10.1016/j.geoderma.2020.114844

Macadam, X.M.B., Prado, A. del, Merino, P., Estavillo, J.M., Pinto, M., González-Murua, C., 2003. Dicyandiamide and 3,4-dimethyl pyrazole phosphate decrease N2O emissions from grassland but dicyandiamide produces deleterious effects in clover. Journal of Plant Physiology 160, 1517–1523. https://doi.org/10.1078/0176-1617-01006

Machado, P.V.F., Farrell, R.E., Deen, W., Voroney, R.P., Congreves, K.A., Wagner-Riddle, C., 2021. Contribution of crop residue, soil, and fertilizer nitrogen to nitrous oxide emissions varies with long-term crop rotation and tillage. Science of The Total Environment 767, 145107. https://doi.org/10.1016/j.scitotenv.2021.145107

Maharjan, B., Venterea, R.T., Rosen, C., 2014. Fertilizer and Irrigation Management Effects on Nitrous Oxide Emissions and Nitrate Leaching. Agronomy Journal 106, 703–714. https://doi.org/10.2134/agronj2013.0179

Malhi, S.S., Lemke, R., 2007. Tillage, crop residue and N fertilizer effects on crop yield, nutrient uptake, soil quality and nitrous oxide gas emissions in a second 4-yr rotation cycle. Soil and Tillage Research 96, 269–283. https://doi.org/10.1016/j.still.2007.06.011

Malhi, S.S., Lemke, R., Wang, Z.H., Chhabra, B.S., 2006. Tillage, nitrogen and crop residue effects on crop yield, nutrient uptake, soil quality, and greenhouse gas emissions. Soil and Tillage Research 90, 171–183. https://doi.org/10.1016/j.still.2005.09.001

Manandhar, S., Martinez, C., Menzies, N.W., Dalal, R.C., Bell, M., 2024. Comparison of natural abundance and enriched 15N methods to quantify nitrogen fertilizer recovery in maize under field conditions. Plant Soil. https://doi.org/10.1007/s11104-024-07088-6

Marsden, K.A., Marín-Martínez, A.J., Vallejo, A., Hill, P.W., Jones, D.L., Chadwick, D.R., 2016. The mobility of nitrification inhibitors under simulated ruminant urine deposition and rainfall: a comparison between DCD and DMPP. Biol Fertil Soils 52, 491–503. https://doi.org/10.1007/s00374-016-1092-x

Marsden, K.A., Scowen, M., Hill, P.W., Jones, D.L., Chadwick, D.R., 2015. Plant acquisition and metabolism of the synthetic nitrification inhibitor dicyandiamide and naturally-occurring guanidine from agricultural soils. Plant Soil 395, 201–214. https://doi.org/10.1007/s11104-015-2549-7

Martens, D.A., 2005. DENITRIFICATION, in: Hillel, D. (Ed.), Encyclopedia of Soils in the Environment. Elsevier, Oxford, pp. 378–382. https://doi.org/10.1016/B0-12-348530-4/00138-7

Martikainen, P.J., 2022. Heterotrophic nitrification – An eternal mystery in the nitrogen cycle. Soil Biology and Biochemistry 168, 108611. https://doi.org/10.1016/j.soilbio.2022.108611

Maucieri, C., Tolomio, M., McDaniel, M.D., Zhang, Y., Robatjazi, J., Borin, M., 2021. No-tillage effects on soil CH4 fluxes: A meta-analysis. Soil and Tillage Research 212, 105042. https://doi.org/10.1016/j.still.2021.105042

McGeough, K.L., Laughlin, R.J., Watson, C.J., Müller, C., Ernfors, M., Cahalan, E., Richards, K.G., 2012. The effect of cattle slurry in combination with nitrate and the nitrification inhibitor dicyandiamide on in situ nitrous oxide and dinitrogen emissions. Biogeosciences 9, 4909–4919. https://doi.org/10.5194/bg-9-4909-2012

McSwiney, C.P., Snapp, S.S., Gentry, L.E., 2010. Use of N immobilization to tighten the N cycle in conventional agroecosystems. Ecological Applications 20, 648–662. https://doi.org/10.1890/09-0077.1

Mei, K., Wang, Z., Huang, H., Zhang, C., Shang, X., Dahlgren, R.A., Zhang, M., Xia, F., 2018. Stimulation of N2O emission by conservation tillage management in agricultural lands: A meta-analysis. Soil and Tillage Research 182, 86–93. https://doi.org/10.1016/j.still.2018.05.006

Meng, X., Guo, Z., Yang, X., Su, W., Li, Z., Wu, X., Ahmad, I., Cai, T., Han, Q., 2021. Straw incorporation helps inhibit nitrogen leaching in maize season to increase yield and efficiency in the Loess Plateau of China. Soil and Tillage Research 211, 105006. https://doi.org/10.1016/j.still.2021.105006

Meng, X., Meng, F., Chen, P., Hou, D., Zheng, E., Xu, T., 2024. A meta-analysis of conservation tillage management effects on soil organic carbon sequestration and soil greenhouse gas flux. Science of The Total Environment 954, 176315. https://doi.org/10.1016/j.scitotenv.2024.176315

Micucci, G., Sgouridis, F., McNamara, N.P., Krause, S., Lynch, I., Roos, F., Well, R., Ullah, S., 2023. The 15N-Gas flux method for quantifying denitrification in soil: Current progress and future directions. Soil Biology and Biochemistry 184, 109108. https://doi.org/10.1016/j.soilbio.2023.109108

Minasny, B., Malone, B.P., McBratney, A.B., Angers, D.A., Arrouays, D., Chambers, A., Chaplot, V., Chen, Z.-S., Cheng, K., Das, B.S., Field, D.J., Gimona, A., Hedley, C.B., Hong, S.Y., Mandal, B., Marchant, B.P., Martin, M., McConkey, B.G., Mulder, V.L., O'Rourke, S., Richer-de-Forges, A.C., Odeh, I., Padarian, J., Paustian, K., Pan, G., Poggio, L., Savin, I., Stolbovoy, V., Stockmann, U., Sulaeman, Y., Tsui, C.-C., Vågen, T.-G., van Wesemael, B., Winowiecki, L., 2017. Soil carbon 4 per mille. Geoderma 292, 59–86. https://doi.org/10.1016/j.geoderma.2017.01.002

Ming, Y., Ningxi, G., Jiatong, Z., Zhanhan, H., Zixuan, C., Di, S., Hongtao, Z., 2024. Enhanced-efficiency nitrogen fertilizer provides a reliable option for mitigating global warming potential in agroecosystems worldwide. Science of The Total Environment 907, 168080. https://doi.org/10.1016/j.scitotenv.2023.168080

Miranda, K.M., Espey, M.G., Wink, D.A., 2001. A Rapid, Simple Spectrophotometric Method for Simultaneous Detection of Nitrate and Nitrite. Nitric Oxide 5, 62–71. https://doi.org/10.1006/niox.2000.0319

Monistrol, A., Vallejo, A., García-Gutiérrez, S., Hermoso-Peralo, R., Montoya, M., Atencia-Payares, L.K., Aguilera, E., Guardia, G., 2024. Interaction between burial depth and N source in drip-fertigated maize: Agronomic performance and correlation with spectral indices. Agricultural Water Management 301, 108951. https://doi.org/10.1016/j.agwat.2024.108951

Montoya, M., Castellano-Hinojosa, A., Vallejo, A., Álvarez, J.M., Bedmar, E.J., Recio, J., Guardia, G., 2018. Zinc fertilizers influence greenhouse gas emissions and nitrifying and denitrifying communities in a non-irrigated arable cropland. Geoderma 325, 208–217. https://doi.org/10.1016/j.geoderma.2018.03.035

Montoya, M., Guardia, G., Recio, J., Castellano-Hinojosa, A., Ginés, C., Bedmar, E.J., Álvarez, J.M., Vallejo, A., 2021a. Zinc-nitrogen co-fertilization influences N2O emissions and microbial communities in an irrigated maize field. Geoderma 383. https://doi.org/10.1016/j.geoderma.2020.114735

Montoya, M., Juhanson, J., Hallin, S., García-Gutiérrez, S., García-Marco, S., Vallejo, A., Recio, J., Guardia, G., 2022. Nitrous oxide emissions and microbial communities during the transition to conservation agriculture using N-enhanced efficiency fertilisers in a

semiarid climate. Soil Biology and Biochemistry 170, 108687. https://doi.org/10.1016/j.soilbio.2022.108687

Montoya, M., Vallejo, A., Corrochano-Monsalve, M., Aguilera, E., Sanz-Cobena, A., Ginés, C., González-Murua, C., Álvarez, J.M., Guardia, G., 2021b. Mitigation of yield-scaled nitrous oxide emissions and global warming potential in an oilseed rape crop through N source management. Journal of Environmental Management 288. https://doi.org/10.1016/j.jenvman.2021.112304

Morales, S.E., Jha, N., Saggar, S., 2015. Impact of urine and the application of the nitrification inhibitor DCD on microbial communities in dairy-grazed pasture soils. Soil Biology and Biochemistry 88, 344–353. https://doi.org/10.1016/j.soilbio.2015.06.009

Morell, F.J., Cantero-Martínez, C., Lampurlanés, J., Plaza-Bonilla, D., Álvaro-Fuentes, J., 2011a. Soil Carbon Dioxide Flux and Organic Carbon Content: Effects of Tillage and Nitrogen Fertilization. Soil Science Society of America Journal 75, 1874–1884. https://doi.org/10.2136/sssaj2011.0030

Morell, F.J., Lampurlanés, J., Álvaro-Fuentes, J., Cantero-Martínez, C., 2011b. Yield and water use efficiency of barley in a semiarid Mediterranean agroecosystem: Long-term effects of tillage and N fertilization. Soil and Tillage Research 117, 76–84. https://doi.org/10.1016/j.still.2011.09.002

Mubarak, A.R., Rosenani, A.B., Anuar, A.R., Siti Zauyah, D., 2003. Recovery of nitrogen from maize residue and inorganic fertilizer in a maize-groundnut rotation system in humid tropics of Malaysia. Communications in Soil Science and Plant Analysis 34, 2375–2394. https://doi.org/10.1081/CSS-120024774

Muhammad, I., Sainju, U.M., Zhao, F., Khan, A., Ghimire, R., Fu, X., Wang, J., 2019. Regulation of soil CO2 and N2O emissions by cover crops: A meta-analysis. Soil and Tillage Research 192, 103–112. https://doi.org/10.1016/j.still.2019.04.020

Muhammad, I., Wang, J., Sainju, U.M., Zhang, S., Zhao, F., Khan, A., 2021. Cover cropping enhances soil microbial biomass and affects microbial community structure: A meta-analysis. Geoderma 381, 114696. https://doi.org/10.1016/j.geoderma.2020.114696

Müller, C., Martin, M., Stevens, R.J., Laughlin, R.J., Kammann, C., Ottow, J.C.G., Jäger, H.-J., 2002. Processes leading to N2O emissions in grassland soil during freezing and thawing. Soil Biology and Biochemistry 34, 1325–1331. https://doi.org/10.1016/S0038-0717(02)00076-7

Müller, C., Rütting, T., Kattge, J., Laughlin, R.J., Stevens, R.J., 2007. Estimation of parameters in complex 15N tracing models by Monte Carlo sampling. Soil Biology and Biochemistry 39, 715–726. https://doi.org/10.1016/j.soilbio.2006.09.021

Müller, C., Stevens, R.J., Laughlin, R.J., 2004a. A 15N tracing model to analyse N transformations in old grassland soil. Soil Biology and Biochemistry 36, 619–632. https://doi.org/10.1016/j.soilbio.2003.12.006

Müller, C., Stevens, R.J., Laughlin, R.J., Jäger, H.-J., 2004b. Microbial processes and the site of N2O production in a temperate grassland soil. Soil Biology and Biochemistry 36, 453–461. https://doi.org/10.1016/j.soilbio.2003.08.027

Murphy, D.V., Recous, S., Stockdale, E.A., Fillery, I.R.P., Jensen, L.S., Hatch, D.J., Goulding, K.W.T., 2003. Gross nitrogen fluxes in soil: theory, measurement and application of 15N pool dilution techniques. Advances in Agronomy 79, 69–118. https://doi.org/10.1016/S0065-2113(02)79002-0

Nilahyane, A., Ghimire, R., Thapa, V.R., Sainju, U.M., 2020. Cover crop effects on soil carbon dioxide emissions in a semiarid cropping system. Agrosystems, Geosciences & Environment 3, e20012. https://doi.org/10.1002/agg2.20012

Nyabami, P., Maltais-Landry, G., Lin, Y., 2023. Nitrogen release dynamics of cover crop mixtures in a subtropical agroecosystem were rapid and species-specific. Plant and Soil. https://doi.org/10.1007/s11104-023-06183-4

O'Brien, P.L., Emmett, B.D., Malone, R.W., Nunes, M.R., Kovar, J.L., Kaspar, T.C., Moorman, T.B., Jaynes, D.B., Parkin, T.B., 2022. Nitrate losses and nitrous oxide emissions under contrasting tillage and cover crop management. Journal of Environmental Quality 51, 683–695. https://doi.org/10.1002/jeq2.20361

Pacholski, A., Berger, N., Bustamante, I., Ruser, R., Guardia, G., Mannheim, T., 2016. Effects of the novel nitrification inhibitor DMPSA on yield, mineral N dynamics and N2O emissions, in: Proceedings of the 2016 International Nitrogen Initiative Conference, "Solutions to Improve Nitrogen Use Efficiency for the World", 4 – 8 December 2016, Melbourne, Australia.

Palm, C., Blanco-Canqui, H., DeClerck, F., Gatere, L., Grace, P., 2014. Conservation agriculture and ecosystem services: An overview. Agriculture, Ecosystems & Environment 187, 87–105. https://doi.org/10.1016/j.agee.2013.10.010

Pan, B., Lam, S.K., Mosier, A., Luo, Y., Chen, D., 2016. Ammonia volatilization from synthetic fertilizers and its mitigation strategies: A global synthesis. Agriculture, Ecosystems & Environment 232, 283–289. https://doi.org/10.1016/j.agee.2016.08.019

Pan, B., Xia, L., Lam, S.K., Wang, E., Zhang, Y., Mosier, A., Chen, D., 2022. A global synthesis of soil denitrification: Driving factors and mitigation strategies. Agriculture, Ecosystems & Environment 327, 107850. https://doi.org/10.1016/j.agee.2021.107850

Pandey, C.B., Kumar, U., Kaviraj, M., Minick, K.J., Mishra, A.K., Singh, J.S., 2020. DNRA: A short-circuit in biological N-cycling to conserve nitrogen in terrestrial ecosystems. Science of The Total Environment 738, 139710. https://doi.org/10.1016/j.scitotenv.2020.139710

Paniagua, L.L., García-Martín, A., Moral, F.J., Rebollo, F.J., 2019. Aridity in the Iberian Peninsula (1960–2017): distribution, tendencies, and changes. Theor Appl Climatol 138, 811–830. https://doi.org/10.1007/s00704-019-02866-0

Patton, C.J., Kryskalla, J.R., 2011. Colorimetric determination of nitrate plus nitrite in water by enzymatic reduction, automated discrete analyzer methods (No. 5-B8), Techniques and Methods. U.S. Geological Survey. https://doi.org/10.3133/tm5B8

Peng, Y., Rieke, E.L., Chahal, I., Norris, C.E., Janovicek, K., Mitchell, J.P., Roozeboom, K.L., Hayden, Z.D., Strock, J.S., Machado, S., Sykes, V.R., Deen, B., Tavarez, O.B., Gamble, A.V., Scow, K.M., Brainard, D.C., Millar, N., Johnson, G.A., Schindelbeck, R.R., Kurtz, K.S.M., Van Es, H., Kumar, S., Van Eerd, L.L., 2023. Maximizing soil organic carbon stocks under cover cropping: insights from long-term agricultural experiments in North America. Agriculture, Ecosystems & Environment 356, 108599. https://doi.org/10.1016/j.agee.2023.108599

Peng, Y., Wang, L., Jacinthe, P.-A., Ren, W., 2024. Global synthesis of cover crop impacts on main crop yield. Field Crops Research 310, 109343. https://doi.org/10.1016/j.fcr.2024.109343

PerkinElmer, 2001. Techniques for Flow Injection Analysis in UV/Vis Spectroscopy. pp. 89–92.

Petersen, S.O., Nielsen, T.H., Frostegård, Å., Olesen, T., 1996. O2 uptake, C metabolism and denitrification associated with manure hot-spots. Soil Biology and Biochemistry 28, 341–349. https://doi.org/10.1016/0038-0717(95)00150-6

Pilegaard, K., 2013. Processes regulating nitric oxide emissions from soils. Philosophical Transactions of the Royal Society B: Biological Sciences 368, 20130126. https://doi.org/10.1098/rstb.2013.0126

Pinheiro, P.L., Recous, S., Dietrich, G., Weiler, D.A., Giovelli, R.L., Mezzalira, A.P., Giacomini, S.J., 2018. Straw removal reduces the mulch physical barrier and ammonia volatilization after urea application in sugarcane. Atmospheric Environment 194, 179–187. https://doi.org/10.1016/j.atmosenv.2018.09.031

Pittelkow, C.M., Liang, X., Linquist, B.A., van Groenigen, K.J., Lee, J., Lundy, M.E., van Gestel, N., Six, J., Venterea, R.T., van Kessel, C., 2015a. Productivity limits and potentials of the principles of conservation agriculture. Nature 517, 365–368. https://doi.org/10.1038/nature13809

Pittelkow, C.M., Linquist, B.A., Lundy, M.E., Liang, X., van Groenigen, K.J., Lee, J., van Gestel, N., Six, J., Venterea, R.T., van Kessel, C., 2015b. When does no-till yield more? A global meta-analysis. Field Crops Research 183, 156–168. https://doi.org/10.1016/j.fcr.2015.07.020

Plaza-Bonilla, D., Álvaro-Fuentes, J., Arrúe, J.L., Cantero-Martínez, C., 2014. Tillage and nitrogen fertilization effects on nitrous oxide yield-scaled emissions in a rainfed Mediterranean area. Agriculture, Ecosystems and Environment 189, 43–52. https://doi.org/10.1016/j.agee.2014.03.023

Plaza-Bonilla, D., Álvaro-Fuentes, J., Bareche, J., Pareja-Sánchez, E., Justes, É., Cantero-Martínez, C., 2018. No-tillage reduces long-term yield-scaled soil nitrous oxide emissions in rainfed Mediterranean agroecosystems: A field and modelling approach. Agriculture, Ecosystems & Environment 262, 36–47. https://doi.org/10.1016/j.agee.2018.04.007

Poeplau, C., Don, A., 2015. Carbon sequestration in agricultural soils via cultivation of cover crops – A meta-analysis. Agriculture, Ecosystems & Environment 200, 33–41. https://doi.org/10.1016/j.agee.2014.10.024

Powlson, D.S., Stirling, C.M., Jat, M.L., Gerard, B.G., Palm, C.A., Sanchez, P.A., Cassman, K.G., 2014. Limited potential of no-till agriculture for climate change mitigation. Nature Clim Change 4, 678–683. https://doi.org/10.1038/nclimate2292

Prather, M.J., Hsu, J., DeLuca, N.M., Jackman, C.H., Oman, L.D., Douglass, A.R., Fleming, E.L., Strahan, S.E., Steenrod, S.D., Søvde, O.A., Isaksen, I.S.A., Froidevaux, L., Funke, B., 2015. Measuring and modeling the lifetime of nitrous oxide including its variability. Journal of Geophysical Research. Atmospheres 120, 5693. https://doi.org/10.1002/2015JD023267

Priemé, A., Christensen, S., 2001. Natural perturbations, drying-wetting and freezing-thawing cycles, and the emission of nitrous oxide, carbon dioxide and methane from farmed organic soils. Soil Biology and Biochemistry 33, 2083–2091. https://doi.org/10.1016/S0038-0717(01)00140-7

Prosser, J.I., Hink, L., Gubry-Rangin, C., Nicol, G.W., 2020. Nitrous oxide production by ammonia oxidizers: Physiological diversity, niche differentiation and potential mitigation strategies. Global Change Biology 26, 103–118. https://doi.org/10.1111/gcb.14877

Qiao, C., Liu, L., Hu, S., Compton, J.E., Greaver, T.L., Li, Q., 2015. How inhibiting nitrification affects nitrogen cycle and reduces environmental impacts of anthropogenic nitrogen input. Global Change Biology 21, 1249–1257. https://doi.org/10.1111/gcb.12802

Quemada, M., Baranski, M., Nobel-de Lange, M.N.J., Vallejo, A., Cooper, J.M., 2013. Meta-analysis of strategies to control nitrate leaching in irrigated agricultural systems and their effects on crop yield. Agriculture, Ecosystems & Environment 174, 1–10. https://doi.org/10.1016/j.agee.2013.04.018

Quemada, M., Gabriel, J.L., 2016. Approaches for increasing nitrogen and water use efficiency simultaneously. Global Food Security 9, 29–35. https://doi.org/10.1016/j.gfs.2016.05.004

Quemada, M., Lassaletta, L., Jensen, L.S., Godinot, O., Brentrup, F., Buckley, C., Foray, S., Hvid, S.K., Oenema, J., Richards, K.G., Oenema, O., 2020. Exploring nitrogen indicators of farm performance among farm types across several European case studies. Agricultural Systems 177. https://doi.org/10.1016/j.agsy.2019.102689

Quintarelli, V., Radicetti, E., Allevato, E., Stazi, S.R., Haider, G., Abideen, Z., Bibi, S., Jamal, A., Mancinelli, R., 2022. Cover Crops for Sustainable Cropping Systems: A Review. Agriculture 12, 2076. https://doi.org/10.3390/agriculture12122076

Ravishankara, A., Daniel, J., Portman, R., 2009. Nitrous Oxide (N2O): The Dominant Ozone-Depleting Substance Emitted in the 21st Century. Science 326, 123–125. https://doi.org/10.1126/science.1176985

Real Decreto 1051/2022, de 27 de diciembre, por el que se establecen normas para la nutrición sostenible en los suelos agrarios. Boletín Oficial del Estado núm. 312. https://www.boe.es/eli/es/rd/2022/12/27/1051, n.d.

Recio, J., Álvarez, J.M., Rodríguez-Quijano, M., Vallejo, A., 2019. Nitrification inhibitor DMPSA mitigated N2O emission and promoted NO sink in rainfed wheat. Environmental Pollution 245, 199–207. https://doi.org/10.1016/j.envpol.2018.10.135

Recio, J., Montoya, M., Ginés, C., Sanz-Cobena, A., Vallejo, A., Alvarez, J.M., 2020. Joint mitigation of NH3 and N2O emissions by using two synthetic inhibitors in an irrigated cropping soil. Geoderma 373, 114423. https://doi.org/10.1016/j.geoderma.2020.114423

Recio, J., Vallejo, A., Le-Noë, J., Garnier, J., García-Marco, S., Álvarez, J.M., Sanz-Cobena, A., 2018. The effect of nitrification inhibitors on NH3 and N2O emissions in highly N fertilized irrigated Mediterranean cropping systems. Science of the Total Environment 636, 427–436. https://doi.org/10.1016/j.scitotenv.2018.04.294

Rehschuh, S., Fuchs, M., Tejedor, J., Schäfler-Schmid, A., Magh, R.-K., Burzlaff, T., Rennenberg, H., Dannenmann, M., 2019. Admixing Fir to European Beech Forests Improves the Soil Greenhouse Gas Balance. Forests 10, 213. https://doi.org/10.3390/f10030213

Ritchie, H., 2017. How many people does synthetic fertilizer feed? Our World in Data. https://ourworldindata.org/how-many-people-does-synthetic-fertilizer-feed

Rodriguez, C., Carlsson, G., Englund, J.-E., Flöhr, A., Pelzer, E., Jeuffroy, M.-H., Makowski, D., Jensen, E.S., 2020. Grain legume-cereal intercropping enhances the use of soil-derived and biologically fixed nitrogen in temperate agroecosystems. A meta-analysis. European Journal of Agronomy 118, 126077. https://doi.org/10.1016/j.eja.2020.126077

Roman-Perez, C.C., Hernandez-Ramirez, G., 2021. Sources and priming of nitrous oxide production across a range of moisture contents in a soil with high organic matter. Journal of Environmental Quality 50, 94–109. https://doi.org/10.1002/jeq2.20172

Rosa, L., Gabrielli, P., 2023. Achieving net-zero emissions in agriculture: a review. Environ. Res. Lett. 18, 063002. https://doi.org/10.1088/1748-9326/acd5e8

Rozas, H.R.S., Echeverría, H.E., Barbieri, P.A., 2004. Nitrogen Balance as Affected by Application Time and Nitrogen Fertilizer Rate in Irrigated No-Tillage Maize. Agronomy Journal 96, 1622–1631. https://doi.org/10.2134/agronj2004.1622

Rumpel, C., Amiraslani, F., Chenu, C., Garcia Cardenas, M., Kaonga, M., Koutika, L.-S., Ladha, J., Madari, B., Shirato, Y., Smith, P., Soudi, B., Soussana, J.-F., Whitehead, D., Wollenberg, E., 2020. The 4p1000 initiative: Opportunities, limitations and challenges for implementing soil organic carbon sequestration as a sustainable development strategy. Ambio 49, 350–360. https://doi.org/10.1007/s13280-019-01165-2

Ruppel, S., Jürgen, A., Graefe, J., Rühlmann, J., Peschke, H., 2006. Gross N transfer rates in field soils measured by dilution N-pool. Archives of Agronomy and Soil Science 52, 377–388. https://doi.org/10.1080/03650340600849357

Rütting, T., Boeckx, P., Müller, C., Klemedtsson, L., 2011. Assessment of the importance of dissimilatory nitrate reduction to ammonium for the terrestrial nitrogen cycle. Biogeosciences 8, 1779–1791. https://doi.org/10.5194/bg-8-1779-2011

Salmerón, M., Isla, R., Cavero, J., 2011. Effect of winter cover crop species and planting methods on maize yield and N availability under irrigated Mediterranean conditions. Field Crops Research 123, 89–99. https://doi.org/10.1016/j.fcr.2011.05.006

Sang, J., Lakshani, M.M.T., Chamindu Deepagoda, T.K.K., Shen, Y., Li, Y., 2022. Drying and rewetting cycles increased soil carbon dioxide rather than nitrous oxide emissions: A meta-analysis. Journal of Environmental Management 324, 116391. https://doi.org/10.1016/j.jenvman.2022.116391

Sanz-Cobena, A., García-Marco, S., Quemada, M., Gabriel, J.L., Almendros, P., Vallejo, A., 2014a. Do cover crops enhance N2O, CO2 or CH4 emissions from soil in Mediterranean arable systems? Science of the Total Environment 466–467, 164–174. https://doi.org/10.1016/j.scitotenv.2013.07.023

Sanz-Cobena, A., Lassaletta, L., Aguilera, E., Prado, A. del, Garnier, J., Billen, G., Iglesias, A., Sánchez, B., Guardia, G., Abalos, D., Plaza-Bonilla, D., Puigdueta-Bartolomé, I., Moral, R., Galán, E., Arriaga, H., Merino, P., Infante-Amate, J., Meijide, A., Pardo, G., Álvaro-Fuentes, J., Gilsanz, C., Báez, D., Doltra, J., González-Ubierna, S., Cayuela, M.L., Menéndez, S., Díaz-Pinés, E., Le-Noë, J., Quemada, M., Estellés, F., Calvet, S., van Grinsven, H.J.M., Westhoek, H., Sanz, M.J., Gimeno, B.S., Vallejo, A., Smith, P., 2017. Strategies for greenhouse gas emissions mitigation in Mediterranean agriculture: A review. Agriculture, Ecosystems and Environment 238, 5–24. https://doi.org/10.1016/j.agee.2016.09.038

Sanz-Cobena, A., Lassaletta, L., Estellés, F., Del Prado, A., Guardia, G., Abalos, D., Aguilera, E., Pardo, G., Vallejo, A., Sutton, M.A., Garnier, J., Billen, G., 2014b. Yield-scaled mitigation of ammonia emission from N fertilization: the Spanish case. Environmental Research Letters 9, 125005. https://doi.org/10.1088/1748-9326/9/12/125005

Sanz-Cobena, A., Misselbrook, T.H., Arce, A., Mingot, J.I., Diez, J.A., Vallejo, A., 2008. An inhibitor of urease activity effectively reduces ammonia emissions from soil treated with urea under Mediterranean conditions. Agriculture, Ecosystems & Environment 126, 243–249. https://doi.org/10.1016/j.agee.2008.02.001

Sarkodie-Addo, J., Lee, H.C., Baggs, E.M., 2003. Nitrous oxide emissions after application of inorganic fertilizer and incorporation of green manure residues. Soil Use and Management 19, 331–339. https://doi.org/10.1111/j.1475-2743.2003.tb00323.x

Scheer, C., Fuchs, K., Pelster, D.E., Butterbach-Bahl, K., 2020. Estimating global terrestrial denitrification from measured N2O:(N2O + N2) product ratios. Current Opinion in Environmental Sustainability, Climate Change, Reactive Nitrogen, Food Security and Sustainable Agriculture 47, 72–80. https://doi.org/10.1016/j.cosust.2020.07.005

Scheer, C., Rowlings, D.W., Firrel, M., Deuter, P., Morris, S., Grace, P.R., 2014. Impact of nitrification inhibitor (DMPP) on soil nitrous oxide emissions from an intensive broccoli production system in sub-tropical Australia. Soil Biology and Biochemistry 77, 243–251. https://doi.org/10.1016/j.soilbio.2014.07.006

Scheer, C., Rütting, T., 2023. Use of 15N tracers to study nitrogen flows in agro-ecosystems: transformation, losses and plant uptake. Nutr Cycl Agroecosyst 125, 89–93. https://doi.org/10.1007/s10705-023-10269-x

Schleusner, P., Lammirato, C., Tierling, J., Lebender, U., Rütting, T., 2018. Primed N $_2$ O emission from native soil nitrogen: A ^{15} N-tracing laboratory experiment. J. Plant Nutr. Soil Sci. 181, 621–627. https://doi.org/10.1002/jpln.201700312

Schreiber, M., Bazaios, E., Ströbel, B., Wolf, B., Ostler, U., Gasche, R., Schlingmann, M., Kiese, R., Dannenmann, M., 2023. Impacts of slurry acidification and injection on fertilizer nitrogen fates in grassland. Nutr Cycl Agroecosyst 125, 171–186. https://doi.org/10.1007/s10705-022-10239-9

Scordia, D., Cosentino, S.L., Mantineo, M., Testa, G., Patanè, C., 2021. Nitrogen Balance in a Sweet Sorghum Crop in a Mediterranean Environment. Agronomy 11, 1292. https://doi.org/10.3390/agronomy11071292

Sha, Z., Ma, X., Wang, J., Lv, T., Li, Q., Misselbrook, T., Liu, X., 2020. Effect of N stabilizers on fertilizer-N fate in the soil-crop system: A meta-analysis. Agriculture, Ecosystems and Environment 290. https://doi.org/10.1016/j.agee.2019.106763

Shaaban, M., 2024. Microbial pathways of nitrous oxide emissions and mitigation approaches in drylands. Journal of Environmental Management 354, 120393. https://doi.org/10.1016/j.jenvman.2024.120393

Shah, F., Wu, W., 2019. Soil and Crop Management Strategies to Ensure Higher Crop Productivity within Sustainable Environments. Sustainability 11, 1485. https://doi.org/10.3390/su11051485

Shakoor, A., Pendall, E., Arif, M.S., Farooq, T.H., Iqbal, S., Shahzad, S.M., 2024. Does no-till crop management mitigate gaseous emissions and reduce yield disparities: An empirical US-China evaluation. Science of The Total Environment 917, 170310. https://doi.org/10.1016/j.scitotenv.2024.170310

Shakoor, A., Shahbaz, M., Farooq, T.H., Sahar, N.E., Shahzad, S.M., Altaf, M.M., Ashraf, M., 2021. A global meta-analysis of greenhouse gases emission and crop yield under no-tillage as compared to conventional tillage. Science of The Total Environment 750, 142299. https://doi.org/10.1016/j.scitotenv.2020.142299

Shan, J., Yan, X., 2013. Effects of crop residue returning on nitrous oxide emissions in agricultural soils. Atmospheric Environment 71, 170–175. https://doi.org/10.1016/j.atmosenv.2013.02.009

Shukla, P.N., Pandey, K.D., Mishra, V.K., 2013. Environmental Determinants of Soil Methane Oxidation and Methanotrophs. Critical Reviews in Environmental Science and Technology 43, 1945–2011. https://doi.org/10.1080/10643389.2012.672053

Smith, C.J., Chalk, P.M., 2020. The role of 15N in tracing N dynamics in agro-ecosystems under alternative systems of tillage management: A review. Soil and Tillage Research 197, 104496. https://doi.org/10.1016/j.still.2019.104496

Smith, C.J., Chalk, P.M., 2018. The residual value of fertiliser N in crop sequences: An appraisal of 60 years of research using 15N tracer. Field Crops Research 217, 66–74. https://doi.org/10.1016/j.fcr.2017.12.006

Smith, M.S., Zimmerman, K., 1981. Nitrous Oxide Production by Nondenitrifying Soil Nitrate Reducers. Soil Science Society of America Journal 45, 865–871. https://doi.org/10.2136/sssaj1981.03615995004500050008x

Snyder, C.S., Bruulsema, T.W., Jensen, T.L., Fixen, P.E., 2009. Review of greenhouse gas emissions from crop production systems and fertilizer management effects. Agriculture, Ecosystems & Environment 133, 247–266. https://doi.org/10.1016/j.agee.2009.04.021

Soil Survey Staff, 2014. Keys to Soil Taxonomy, 12th ed. Change 327–328.

Song, D., Jiang, R., Fan, D., Zou, G., Du, L., Wei, D., Guo, X., He, W., 2022. Evaluation of Nitrogen Fertilizer Fates and Related Environmental Risks for Main Cereals in China's Croplands from 2004 to 2018. Plants 11, 2507. https://doi.org/10.3390/plants11192507

Soon, Y.K., Arshad, M.A., 2005. Tillage and liming effects on crop and labile soil nitrogen in an acid soil. Soil and Tillage Research 80, 23–33. https://doi.org/10.1016/j.still.2004.02.017

Spott, O., Russow, R., Apelt, B., Stange, C.F., 2006. A 15N-aided artificial atmosphere gas flow technique for online determination of soil N2 release using the zeolite Köstrolith SX6®. Rapid Communications in Mass Spectrometry 20, 3267–3274. https://doi.org/10.1002/rcm.2722

Spott, O., Russow, R., Stange, C.F., 2011. Formation of hybrid N2O and hybrid N2 due to codenitrification: First review of a barely considered process of microbially mediated N-nitrosation. Soil Biology and Biochemistry 43, 1995–2011. https://doi.org/10.1016/j.soilbio.2011.06.014

Stevens, R.J., Laughlin, R.J., 2001. Lowering the detection limit for dinitrogen using the enrichment of nitrous oxide. Soil Biology and Biochemistry 33, 1287–1289. https://doi.org/10.1016/S0038-0717(01)00036-0

Sullivan, D., Andrews, N., Sullivan, C., Brewer, L., 2019. OSU Organic Fertilizer & Cover Crop Calculator: Predicting Plant-available Nitrogen.

Sun, J., Niu, W., Du, Y., Ma, L., Huang, S., Mu, F., Zhang, Q., Li, G., Zhu, J., Siddique, K.H.M., 2024. Regionally adapted conservation tillage reduces the risk of crop yield losses: A global meta-analysis. Soil and Tillage Research 244, 106265. https://doi.org/10.1016/j.still.2024.106265

Sutton, M.A., Bleeker, A., Howard, C.M., Bekunda, M., Grizzetti, B., De Vries, W., Van Grinsven, H.J.M., Abrol, Y.P., Adhya, T.K., Billen, G., Davidson, E.A., Datta, A., Diaz, R., Erisman, J.W., Oenema, O., Palm, C., Raghuram, N., Reis, S., Scholz, R.W., Sims, T., Westhoek, H., Zhang, F.S., with contributions from Ayyappan S., Bouwman A.F., Bustamante M., Fowler D., Galloway J.N., Gavito M.E., Garnier J., Greenwood S., Hellums D.T., Holland M., Hoysall C., Jaramillo V.J., Klimont Z., Ometto J.P., Pathak, H., Plocq Fichelet V., Powlson D., Ramakrishna K., Roy A., Sanders K., Sharma C.,, Singh B., Singh U., Yan X.Y. & Zhang Y, 2013. Our nutrient world: the challenge to produce more food and energy with less pollution. Global Overview of Nutrient Management. Centre for Ecology & Hydrology on behalf of the Global Partnership on Nutrient Management (GPNM) and the International Nitrogen Initiative (INI).

Taveira, C.J., Farrell, R.E., Wagner-Riddle, C., Machado, P.V.F., Deen, B., Congreves, K.A., 2020. Tracing crop residue N into subsequent crops: Insight from long-term crop rotations that vary in diversity. Field Crops Research 255, 107904. https://doi.org/10.1016/j.fcr.2020.107904

Thapa, R., Mirsky, S.B., Tully, K.L., 2018. Cover Crops Reduce Nitrate Leaching in Agroecosystems: A Global Meta-Analysis. Journal of Environmental Quality 47, 1400–1411. https://doi.org/10.2134/jeq2018.03.0107

Thilakarathna, S.K., Hernandez-Ramirez, G., 2021. How does management legacy, nitrogen addition, and nitrification inhibition affect soil organic matter priming and nitrous oxide production? J. environ. qual. 50, 78–93. https://doi.org/10.1002/jeq2.20168

Tian, H., Xu, R., Canadell, J.G., Thompson, R.L., Winiwarter, W., Suntharalingam, P., Davidson, E.A., Ciais, P., Jackson, R.B., Janssens-Maenhout, G., Prather, M.J., Regnier, P., Pan, N., Pan, S., Peters, G.P., Shi, H., Tubiello, F.N., Zaehle, S., Zhou, F., Arneth, A., Battaglia, G., Berthet, S., Bopp, L., Bouwman, A.F., Buitenhuis, E.T., Chang, J., Chipperfield, M.P., Dangal, S.R.S., Dlugokencky, E., Elkins, J.W., Eyre, B.D., Fu, B., Hall, B., Ito, A., Joos, F., Krummel, P.B., Landolfi, A., Laruelle, G.G., Lauerwald, R., Li, W., Lienert, S., Maavara, T., MacLeod, M., Millet, D.B., Olin, S., Patra, P.K., Prinn, R.G., Raymond, P.A., Ruiz, D.J., Van Der Werf, G.R., Vuichard, N., Wang, J., Weiss,

R.F., Wells, K.C., Wilson, C., Yang, J., Yao, Y., 2020. A comprehensive quantification of global nitrous oxide sources and sinks. Nature 586, 248–256. https://doi.org/10.1038/s41586-020-2780-0

Tonitto, C., David, M.B., Drinkwater, L.E., 2006. Replacing bare fallows with cover crops in fertilizer-intensive cropping systems: A meta-analysis of crop yield and N dynamics. Agriculture, Ecosystems & Environment 112, 58–72. https://doi.org/10.1016/j.agee.2005.07.003

Torralbo, F., Menéndez, S., Barrena, I., Estavillo, J.M., Marino, D., González-Murua, C., 2017. Dimethyl pyrazol-based nitrification inhibitors effect on nitrifying and denitrifying bacteria to mitigate N2O emission. Sci Rep 7, 13810. https://doi.org/10.1038/s41598-017-14225-y

Toyoda, S., Yoshida, N., Koba, K., 2017. Isotopocule analysis of biologically produced nitrous oxide in various environments. Mass Spectrometry Reviews 36, 135–160. https://doi.org/10.1002/mas.21459

Tufail, M.A., Naeem, A., Arif, M.S., Farooq, T.H., Shahzad, S.M., Dar, A.A., Albasher, G., Shakoor, A., 2022. Unraveling the efficacy of nitrification inhibitors (DCD and DMPP) in reducing nitrogen gases emissions across agroecosystems: A three-decade global data synthesis (1993–2021). Fuel 324, 124725. https://doi.org/10.1016/j.fuel.2022.124725

Turmel, M.-S., Speratti, A., Baudron, F., Verhulst, N., Govaerts, B., 2015. Crop residue management and soil health: A systems analysis. Agricultural Systems 134, 6–16. https://doi.org/10.1016/j.agsy.2014.05.009

United Nations, 2022. United Nations, Department of Economic and Social Affairs, Population Division (2022). World Population Prospects 2022, Online Edition, World Population Prospects 2022, Online Edition. United Nations, Department of Economic and Social Affairs, Population Division (2022).

Unkovich, M., Jamieson, N., Monaghan, R., Barraclough, D., 1998. Nitrogen mineralisation and plant nitrogen acquisition in a nitrogen-limited calcereous grassland. Environmental and Experimental Botany 40, 209–219. https://doi.org/10.1016/S0098-8472(98)00038-0

Urra, J., Mijangos, I., Lanzén, A., Lloveras, J., Garbisu, C., 2018. Effects of corn stover management on soil quality. European Journal of Soil Biology 88, 57–64. https://doi.org/10.1016/j.ejsobi.2018.06.005

Ussiri, D., Lal, R., 2013. Soil Emission of Nitrous Oxide and its Mitigation. Springer Science & Business Media.

Vallejo, A., Meijide, A., Boeckx, P., Arce, A., García-torres, L., Aguado, P.L., Sanchez-martin, L., 2014. Nitrous oxide and methane emissions from a surface drip-irrigated system combined with fertilizer management. European Journal of Soil Science 65, 386–395. https://doi.org/10.1111/ejss.12140

Van Eerd, L.L., Chahal, I., Peng, Y., Awrey, J.C., 2023. Influence of cover crops at the four spheres: A review of ecosystem services, potential barriers, and future directions for North America. Science of The Total Environment 858, 159990. https://doi.org/10.1016/j.scitotenv.2022.159990

Venterea, R.T., 2007. Nitrite-driven nitrous oxide production under aerobic soil conditions: kinetics and biochemical controls. Global Change Biology 13, 1798–1809. https://doi.org/10.1111/j.1365-2486.2007.01389.x

Venterea, R.T., Petersen, S.O., Klein, C.A.M., Pedersen, A.R., Noble, A.D.L., Rees, R.M., Gamble, J.D., Parkin, T.B., 2020. Global Research Alliance N_2O chamber methodology guidelines: Flux calculations. Journal of Environmental Quality 49, 1141–1155. https://doi.org/10.1002/jeq2.20118

Volpi, I., Laville, P., Bonari, E., di Nasso, N.N. o, Bosco, S., 2017. Improving the management of mineral fertilizers for nitrous oxide mitigation: The effect of nitrogen fertilizer type, urease and nitrification inhibitors in two different textured soils. Geoderma 307, 181–188. https://doi.org/10.1016/j.geoderma.2017.08.018

Wang, M., Pendall, E., Fang, C., Li, B., Nie, M., 2018. A global perspective on agroecosystem nitrogen cycles after returning crop residue. Agriculture, Ecosystems & Environment 266, 49–54. https://doi.org/10.1016/j.agee.2018.07.019

Wang, R., Hu, Y., Wang, Y., Ali, S., Liu, Q., Guo, S., 2019. Nitrogen application increases soil respiration but decreases temperature sensitivity: Combined effects of crop and soil properties in a semiarid agroecosystem. Geoderma 353, 320–330. https://doi.org/10.1016/j.geoderma.2019.07.019

Wang, S., Luo, S., Yue, S., Li, S., 2016. Fate of 15N fertilizer under different nitrogen split applications to plastic mulched maize in semiarid farmland. Nutrient Cycling in Agroecosystems 105, 129–140. https://doi.org/10.1007/s10705-016-9780-3

Wang, Y., Saikawa, E., Avramov, A., Hill, N.S., 2022. Agricultural Greenhouse Gas Fluxes Under Different Cover Crop Systems. Frontiers in Climate 3, 742320. https://doi.org/10.3389/fclim.2021.742320

Wang, Z.-H., Li, S.-X., 2019. Chapter Three - Nitrate N loss by leaching and surface runoff in agricultural land: A global issue (a review), in: Sparks, D.L. (Ed.), Advances in Agronomy. Academic Press, pp. 159–217. https://doi.org/10.1016/bs.agron.2019.01.007

Wegner, B.R., Chalise, K.S., Singh, S., Lai, L., Abagandura, G.O., Kumar, S., Osborne, S.L., Lehman, R.M., Jagadamma, S., 2018. Response of Soil Surface Greenhouse Gas Fluxes to Crop Residue Removal and Cover Crops under a Corn–Soybean Rotation. Journal of Environmental Quality 47, 1146–1154. https://doi.org/10.2134/jeq2018.03.0093

Wei, H., Li, Y., Zhu, K., Ju, X., Wu, D., 2024. The divergent role of straw return in soil O2 dynamics elucidates its confounding effect on soil N2O emission. Soil Biology and Biochemistry 199, 109620. https://doi.org/10.1016/j.soilbio.2024.109620

Wei, H., Song, X., Liu, Y., Wang, R., Zheng, X., Butterbach-Bahl, K., Venterea, R.T., Wu, D., Ju, X., 2023. In situ 15N-N2O site preference and O2 concentration dynamics disclose the complexity of N2O production processes in agricultural soil. Global Change Biology 29, 4910–4923. https://doi.org/10.1111/gcb.16753

Wei, J., Ibraim, E., Brüggemann, N., Vereecken, H., Mohn, J., 2019. First real-time isotopic characterisation of N2O from chemodenitrification. Geochimica et Cosmochimica Acta 267, 17–32. https://doi.org/10.1016/j.gca.2019.09.018

Well, R., Maier, M., Lewicka-Szczebak, D., Köster, J.-R., Ruoss, N., 2019. Underestimation of denitrification rates from field application of the ^{15}N gas flux method and its correction by gas diffusion modelling. Biogeosciences 16, 2233–2246. https://doi.org/10.5194/bg-16-2233-2019

WMO, 2024. World Meteorological Organization Greenhouse Gas Bulletin [WWW Document]. URL https://library.wmo.int/idurl/4/69057

Wrage, N., Velthof, G.L., Van Beusichem, M.L., Oenema, O., 2001. Role of nitrifier denitrification in the production of nitrous oxide. Soil Biology and Biochemistry 33, 1723–1732. https://doi.org/10.1016/S0038-0717(01)00096-7

Wrage-Mönnig, N., Horn, M.A., Well, R., Müller, C., Velthof, G., Oenema, O., 2018. The role of nitrifier denitrification in the production of nitrous oxide revisited. Soil Biology and Biochemistry 123, A3–A16. https://doi.org/10.1016/j.soilbio.2018.03.020

Wu, J., Cheng, X., Xing, W., Liu, G., 2022. Soil-atmosphere exchange of CH4 in response to nitrogen addition in diverse upland and wetland ecosystems: A meta-analysis. Soil Biology and Biochemistry 164, 108467. https://doi.org/10.1016/j.soilbio.2021.108467

Wyer, K.E., Kelleghan, D.B., Blanes-Vidal, V., Schauberger, G., Curran, T.P., 2022. Ammonia emissions from agriculture and their contribution to fine particulate matter: A review of implications for human health. Journal of Environmental Management 323, 116285. https://doi.org/10.1016/j.jenvman.2022.116285

Xia, L., Lam, S.K., Chen, D., Wang, J., Tang, Q., Yan, X., 2017. Can knowledge-based N management produce more staple grain with lower greenhouse gas emission and reactive nitrogen pollution? A meta-analysis. Glob Change Biol 23, 1917–1925. https://doi.org/10.1111/gcb.13455

Xiao, H., Shi, Z., Li, Z., Wang, L., Chen, J., Wang, J., 2020. Responses of soil respiration and its temperature sensitivity to nitrogen addition: A meta-analysis in China. Applied Soil Ecology 150, 103484. https://doi.org/10.1016/j.apsoil.2019.103484

Xu, C., Han, X., Ru, S., Cardenas, L., Rees, R.M., Wu, D., Wu, W., Meng, F., 2019. Crop straw incorporation interacts with N fertilizer on N 2 O emissions in an intensively cropped farmland. Geoderma 341, 129–137. https://doi.org/10.1016/j.geoderma.2019.01.014

Xu, Z., Hattori, S., Masuda, Y., Toyoda, S., Koba, K., Yu, P., Yoshida, N., Du, Z.-J., Senoo, K., 2024. Unprecedented N2O production by nitrate-ammonifying Geobacteraceae with distinctive N2O isotopocule signatures. mBio 15, e02540-24. https://doi.org/10.1128/mbio.02540-24

Yan, M., Pan, G., Lavallee, J.M., Conant, R.T., 2020. Rethinking sources of nitrogen to cereal crops. Global Change Biology 26, 191–199. https://doi.org/10.1111/gcb.14908

Yang, M., Fang, Y., Sun, D., Shi, Y., 2016. Efficiency of two nitrification inhibitors (dicyandiamide and 3, 4-dimethypyrazole phosphate) on soil nitrogen transformations and plant productivity: A meta-analysis. Scientific Reports 6, 1–10. https://doi.org/10.1038/srep22075

Yang, Xuan, Bol, R., Xia, L., Xu, C., Yuan, N., Xu, X., Wu, W., Meng, F., 2024. Integrated farming optimization ensures high-yield crop production with decreased nitrogen leaching and improved soil fertility: The findings from a 12-year experimental study. Field Crops Research 318, 109572. https://doi.org/10.1016/j.fcr.2024.109572

Yang, Xiaolin, Xiong, J., Du, T., Ju, X., Gan, Y., Li, S., Xia, L., Shen, Y., Pacenka, S., Steenhuis, T.S., Siddique, K.H.M., Kang, S., Butterbach-Bahl, K., 2024. Diversifying crop rotation increases food production, reduces net greenhouse gas emissions and improves soil health. Nat Commun 15, 198. https://doi.org/10.1038/s41467-023-44464-9

Yankelzon, I., Schilling, L., Butterbach-Bahl, K., Gasche, R., Han, J., Hartl, L., Kepp, J., Matson, A., Ostler, U., Scheer, C., Schneider, K., Tenspolde, A., Well, R., Wolf, B., Wrage-Moennig, N., Dannenmann, M., 2024. Lysimeter-based full fertilizer 15N balances corroborate direct dinitrogen emission measurements using the 15N gas flow method. Biol Fertil Soils. https://doi.org/10.1007/s00374-024-01801-4

Yin, M., Gao, X., Kuang, W., Zhang, Y., 2023. Meta-analysis of the effect of nitrification inhibitors on the abundance and community structure of N2O-related functional genes in agricultural soils. Science of The Total Environment 865, 161215. https://doi.org/10.1016/j.scitotenv.2022.161215

Yousefi, M., Dray, A., Ghazoul, J., 2024. Assessing the effectiveness of cover crops on ecosystem services: a review of the benefits, challenges, and trade-offs. International Journal of Agricultural Sustainability 22, 2335106. https://doi.org/10.1080/14735903.2024.2335106

Zhang, R., Yu, H., Zhang, W., Li, W., Su, H., Wu, S., Xu, Q., Li, Y., Yao, H., 2024. Straw return enhances grain yield and quality of three main crops: evidence from a meta-analysis. Front. Plant Sci. 15, 1433220. https://doi.org/10.3389/fpls.2024.1433220

Zhu, G., Ju, X., Zhang, J., Müller, C., Rees, R.M., Thorman, R.E., Sylvester-Bradley, R., 2019. Effects of the nitrification inhibitor DMPP (3,4-dimethylpyrazole phosphate) on gross N transformation rates and N2O emissions. Biology and Fertility of Soils 55, 603–615. https://doi.org/10.1007/s00374-019-01375-6

Zhu, X., Burger, M., Doane, T.A., Horwath, W.R., 2013. Ammonia oxidation pathways and nitrifier denitrification are significant sources of N2O and NO under low oxygen availability. Proceedings of the National Academy of Sciences 110, 6328–6333. https://doi.org/10.1073/pnas.1219993110

Zhu, X., Di, D., Ma, M., Shi, W., 2019. Stable Isotopes in Greenhouse Gases from Soil: A Review of Theory and Application. Atmosphere 10, 377. https://doi.org/10.3390/atmos10070377

Zistl-Schlingmann, M., Feng, J., Kiese, R., Stephan, R., Zuazo, P., Willibald, G., Wang, C., Butterbach-Bahl, K., Dannenmann, M., 2019. Dinitrogen emissions: an overlooked key component of the N balance of montane grasslands. Biogeochemistry 143, 15–30. https://doi.org/10.1007/s10533-019-00547-8

Zistl-Schlingmann, M., Kwatcho Kengdo, S., Kiese, R., Dannenmann, M., 2020a. Management Intensity Controls Nitrogen-Use-Efficiency and Flows in Grasslands—A 15N Tracing Experiment. Agronomy 10, 606. https://doi.org/10.3390/agronomy10040606

Zistl-Schlingmann, M., Kwatcho-kengdo, S., Schreiber, M., Berauer, B., Kiese, R., Dannenmann, M., 2020b. Nitrogen use efficiency of different slurry management in the pre- alpine grassland region – a 15N tracing experiment.